INL/EXT-20-28987
Revision 1

# Examination of Legacy Metallic Fuel Pins (U-10Zr) Tested in FFTF

W. J. Carmack, D. L. Porter,
D. G. Cummings, H. J. M. Chichester,
S.L. Hayes — INL

D. W. Wootan — PNNL

April 2013
Rev. 1 May 2020


The INL is a U.S. Department of Energy National Laboratory operated by Battelle Energy Alliance

INL/EXT-20-28987-R.1

# Examination of Legacy Metallic Fuel Pins (U-10Zr) Tested in FFTF

**W. J. Carmack, D. L. Porter,**
**D. G. Cummings, H. J. M. Chichester,**
**S.L. Hayes – INL**

**D. W. Wootan* – PNNL**

**April 2013**
**Rev.1 – May 2020**

**Idaho National Laboratory**
**Idaho Falls, Idaho 83415**

***Pacific Northwest National Laboratory**

**http://www.inl.gov**

**Prepared for the**
**U.S. Department of Energy**
**National Nuclear Security Administration**
**Under DOE Idaho Operations Office**
**Contract DE-AC07-05ID14517**

INTENTIONALLY BLANK

# SUMMARY

The MFF series of metallic fuel (U-10wt%Zr) tests performed in the Fast Fuel Test Facility (FFTF) were the beginning tests to qualify the fuel as a driver fuel for FFTF. They all performed very well, to relatively high burnup and with no pin breaches. Tests MFF-3 and MFF-5 were chosen to be destructively examined because they were run at high peak cladding temperatures, 643 and 649°C respectively, and to modest to high burnup (138 and 101 MWd/kgM respectively). They were the only sodium fast reactor (SFR) metallic tests, with long (91.4 cm) fuel columns and clad in HT9, to be operated at these high temperatures.

Extensive operating condition reconstruction was performed to accompany the examination, providing detailed operating conditions axially along the pins. In addition, detailed ORIGEN calculations provided fuel burnup along the pin length. These calculations and detailed cross-section metallography allowed a PhD dissertation to be performed where the fuel/cladding chemical interaction (FCCI) was modeled using Fickian and Soret Effect driven diffusion of rare earth fission products to the cladding surface and interact with the cladding.

The examination of the MFF-3 and MFF-5 pins included neutron radiography, axial profilometry including pin bow and length measurements, precision gamma scanning, plenum gas puncturing to measure fission gas release, detailed chemical/isotopic analyses of fuel samples to confirm burnup calculations, and metallography of pin cross-sections, including micro-hardness measurements of fuel and cladding.

The exams produced several interesting findings:

1. The axial fuel growth was very small, only 1.7 and 3.6% for MFF-3 and -5, respectively. Compare those values to the earlier FFTF test where U-10Zr fuel swelled axially ~7%. Comparing design and operating conditions the high operating temperature of the MFF-3 and -5 tests are suspected as the potential cause. This is an important finding for prediction of future SFR fuel pin designs.
2. The axial profilometry of the more highly dosed MFF-3 pin ($19 \times 10^{22}$ n/cm$^2$, E>0.1 MeV) showed a pronounced double peak, one at the top of the fuel column and the other a little below peak flux location on the fuel column. MOX pins have previously shown this behavior with HT9 cladding. It may be due to a peaking in thermal creep at the top due to high cladding temperature and some wall thinning due to FCCI, and a peaking of the irradiation creep further down the fuel column due to high neutron exposure. Fuel pin length measurements indicated there may also be cladding swelling, but there was too much apparent growth in the MFF-5 pins to be accounted for with the small diameter increases. Cladding density would be needed to confirm.
3. The calculated and measured fuel burnups were very consistent.
4. The fission gas release value was low (61%) for MFF-3 compared with other tests results, including MFF-5 (79%), although only one pin from each test was measured.
5. Metallography and other exams were consistent with the results from other tests, including the large database collected from tests performed on shorter pins in the Experimental Breeder Reactor II.

Future work could include further study of gas release using other MFF pins, including the colder operating pins from MFF-2 and/or MFF-6. Likewise the axial fuel growth could be further examined for links to operating temperature by producing neutron radiographs of pins from MFF-2 and MFF-6.

INTENTIONALLY BLANK

## AKNOWLEDGEMENTS

The authors would like to thank all of those who made these experiments possible, including the skilled craftsmen in INL's Fuel Manufacturing Facility (FMF) – fuel slug fabrication; those at the Hanford Westinghouse Hanford Company (WHC) who fabricated the fuel pins and experiment assemblies; Ron Baker, who led the effort to qualify U-10Zr metallic fuel for use in FFTF, supported by Jim Dittmer (fabrication), 'MFF' experimenter Al Pitner and others as well as the WHC analysts whose calculations guided reactor placement and flow to produce the right operating conditions, and provided the safety analysis to provide a basis to allow the experiments be irradiated. Jim Corrigan led this team of analysts which included A. E. Bridges and others.

The authors would also like to thank all those who performed expert characterization of the as-irradiated pins in the Hot Fuel Examination Facility and the Analytical Laboratory at the INL's Materials and Fuels Complex. HFEF engineers Glen Papaioannou, Paul Lind, Katelyn Wachs and David Sell from HFEF are especially to be thanked.

INTENTIONALLY BLANK

# CONTENTS

# FIGURES

# TABLES

# ACRONYMS

| | |
|---|---|
| BOC | beginning of cycle |
| BOL | beginning-of-life |
| EBLM | element bow and length machine |
| EBR-II | Experimental Breeder Reactor-II |
| ECP | element contact profilometry |
| EFPD | effective full power day(s) |
| ELP | element laser profilometry |
| EOC | end of cycle |
| EOL | end-of-life |
| EPMA | electron probe microanalysis |
| FCCI | fuel/cladding chemical interaction |
| FCRD | Fuel Cycle Research and Development |
| FCMI | Fuel/cladding mechanical interaction |
| FMF | Fuel Manufacturing Facility |
| FFTF | Fast Flux Test Facility |
| GASR | gas assay sample and recharge system |
| HEU | highly enriched uranium |
| HFEF | Hot Fuel Examination Facility |
| IFR | Integral Fast Reactor |
| INL | Idaho National Laboratory |
| MOX | mixed oxide (fuel) |
| NADB | nuclear analysis database |
| PNNL | Pacific Northwest National Laboratory |
| RDR | Reload Design Report |
| RFR | relative fission rate |
| SFR | sodium fast reactor |
| TFR | total fission rate |
| WHC | Westinghouse Hanford Company |

INTENTIONALLY BLANK

# Examination of Legacy Metallic Fuel Pins (U-10Zr) Tested in FFTF

## 1. INTRODUCTION

In the 1980s and early 1990s there was a resurgence of interest in using metallic fuel in sodium-cooled fast reactors. It was shown to provide economic and simplicity benefits in initial fabrication and also in reprocessing as well as reactor safety benefits, resulting in the Integral Fast Reactor program.[1] These were reviewed in a recent article on the fast reactor fuels tests performed in the United States.[2] Most all of the testing was performed in the Experimental Breeder Reactor-II (EBR-II), especially involving the ternary fuel alloy U-xPu-10Zr. Only one such test of ternary fuel, named IFR-1, was performed in the Fast Flux Test Facility (FFTF) reactor, to show behavior of prototypic length fuel pins. [3]

Another important set of full (prototypic)-length 169-pin experiments, using U-10Zr metallic fuel clad with ferritic/martensitic HT9 stainless steel, were also performed in the FFTF reactor. They were part of a test series, named the 'MFF' experiments, designed to qualify this fuel, named the 'Series III.b' design, for general use as driver fuel in the FFTF.[4] Seven of the planned tests were conducted, their operating conditions summarized in Table 1.

Table 1. MFF fuel tests conducted in the FFTF.

| Test | Peak Linear Power (kW/m) | Peak Clad Temperature (°C) | Test Duration (EFPD) | Peak Burnup (MWd/KgM) | Fast (E>0.1MeV) Fluence $10^{22}$ n/cm$^2$ |
|---|---|---|---|---|---|
| MFF-1 | 42.7 | 577 | 250 | 38 | 5.6 |
| MFF-1A | 43.0 | 577 | 685 | 95 | 17.3 |
| MFF-2 | 54.1 | 618 | 853 | 143 | 19.9 |
| MFF-3 | 59.1 | 643 | 726 | 138 | 19.2 |
| MFF-4 | 56.8 | 618 | 726 | 135 | 19.0 |
| MFF-5 | 55.8 | 649 | 503 | 101 | 14.0 |
| MFF-6 | 55.8 | 588 | 503 | 95 | 12.8 |

The tests were supposed to bracket the potential operating conditions if used as an FFTF driver fuel, so some of the test were operated with elevated peak cladding temperatures. These were MFF-3 and MFF-5. In fact these two tests operated with HT9 cladding temperatures hotter than all but one of the EBR-II tests (X447),[5] and at the shut-down of the FFTF were never planned to be examined. The current Fuel Cycle Research and Development (FCRD) program recognized their potential worth and some pins were set aside at the time the others were being conditioned as used fuel.

The purpose of this report is to detail the post-irradiation examination of several fuel pins from the MFF-3 and MFF-5 experiments.

# 2. MFF-3 AND MFF-5 DESIGN AND OPERATING CONDITIONS

## 2.1 Design

An outline the design of fuel pins used in the MFF-3 and MFF-5 tests is shown in Table 2. MFF-5 also had a shorter Inconel reflector below the fuel slugs, requiring modifying subassembly internal characteristics to axially center the fuel in the FFTF core.

Table 2. MFF-3 and MFF-5 fuel pin design characteristics.

| | MFF-3 | MFF-5 |
|---|---|---|
| Fuel Slug | | |
| diameter (mm) | 4.98 | 4.98 |
| length (cm) | 91.4 | 91.4 |
| composition | U-10Zr | U-10Zr |
| density (g/cm$^3$) | 15.8 | 15.8 |
| mass slug (g) | 281.3 | 281.3 |
| wt% U | 90 | 90 |
| mass U (g) | 253.2 | 253.2 |
| $^{235}$U enrichment (%) | 32.4 | 31.0 |
| mass $^{235}$U (g) | 82.05 | 78.5 |
| mass $^{238}$U (g) | 171.1 | 174.7 |
| wt% Zr | 10 | 10 |
| mass Zr (g) | 28.1 | 28.1 |
| Axial Reflector | | |
| material | Inconel | Inconel |
| number | 1 | 1 |
| diameter (mm) | 4.81 | 4.81 |
| length (cm) | 16.5 | 6.4 |
| Cladding | | |
| OD (mm) | 6.86 | 6.86 |
| thickness (mm) | 0.559 | 0.559 |
| Wire wrap diameter/pitch (mm/cm) | 1.35/15.24 | 1.35/22.86 |
| material | HT-9 | HT-9 |
| Other Characteristics | | |
| sodium fill above fuel (cm) | 2.54 | 2.54 |
| Total Pin Length (cm) | 238 | 237 |
| smeared density, % | 75.2 | 75.2 |
| gas plenum volume (cm$^3$ @ 25°C) | 28.9 | 31.5 |

## 2.2 Operating Conditions

When it was decided that examination of MFF-3 and -5 pins would be done, the as-run conditions for the two assemblies and for each fuel pin were calculated. The calculations were performed at the Pacific Northwest National Laboratory (PNNL). Assembly conditions were modified cycle-by-cycle as influenced by reactor power and the changes to the core loading (influences of neighboring assemblies). From these, sodium temperatures associated with the two assemblies could be calculated. Finally detailed pin-by-pin conditions could be calculated.

Details of the analysis can be found elsewhere.[6] The following summarizes the calculated operating conditions and calculation methods.

### 2.2.1 Assembly Burnup Calculations

Previous burnup calculations for FFTF assemblies used in Core Reload Design Reports were based on two dimensional methods. Burnup calculations for this study for MFF-3 and MFF-5 were accomplished with a sequence of three-dimensional calculations to provide more accurate axial treatment. Starting with a beginning of cycle (BOC) nuclear analysis database (NADB), completion of this sequence results in an end of cycle (EOC) NADB. The EOC NADB is updated to give an NADB for the beginning of the next cycle by accounting for decay of $^{241}$Pu between cycles and manually updating the NADB loading file to include the core loading changes.

The burnup calculations were based on actual core loadings and irradiation histories, not predicted or planned values. Also, data presented in tables and figures in this section were based on three-dimensional (3D) models, whereas the Reload Design Report (RDR) calculations were based on 2D models, with approximate 3D axial factors applied when needed.

The flux calculations that were part of the burnup calculation sequence were made with the control rod bank positioned at nominally the cycle averaged position. Sometimes for short cycles these calculations were the source of BOC flux and power distributions used in generating the data. For the other cycles, separate runs for the BOC were made. In all cases where EOC data were reported, separate runs were made.

After all the runs to generate the required flux and power distributions were completed, six post-processing runs were made for the BOC or EOC of each cycle reported to generate the data tables. Data generated for MFF-3 and MFF-5 include:

- Assembly fission powers, fast neutron fluxes ( > 0.1 MeV), total fluxes
- Radial spatial distributions of fast flux and fission power by pin
- Axial power, total flux, and fast flux distributions
- Fast flux at the duct walls
- Burnup dependent material compositions for six axial segments.

MFF-3 was inserted into the FFTF core at the beginning of Cycle 10C and was irradiated for 726.2 effective full-power days (EFPD) and MFF-5 was inserted for the beginning of Cycle 11B-1 and was irradiated for 503 EFPD. Figure 1 and Figure 2 show the FFTF core loadings for the cycles in which the tests were inserted. The initial operating conditions for each of the two subassemblies are listed in Table 3.

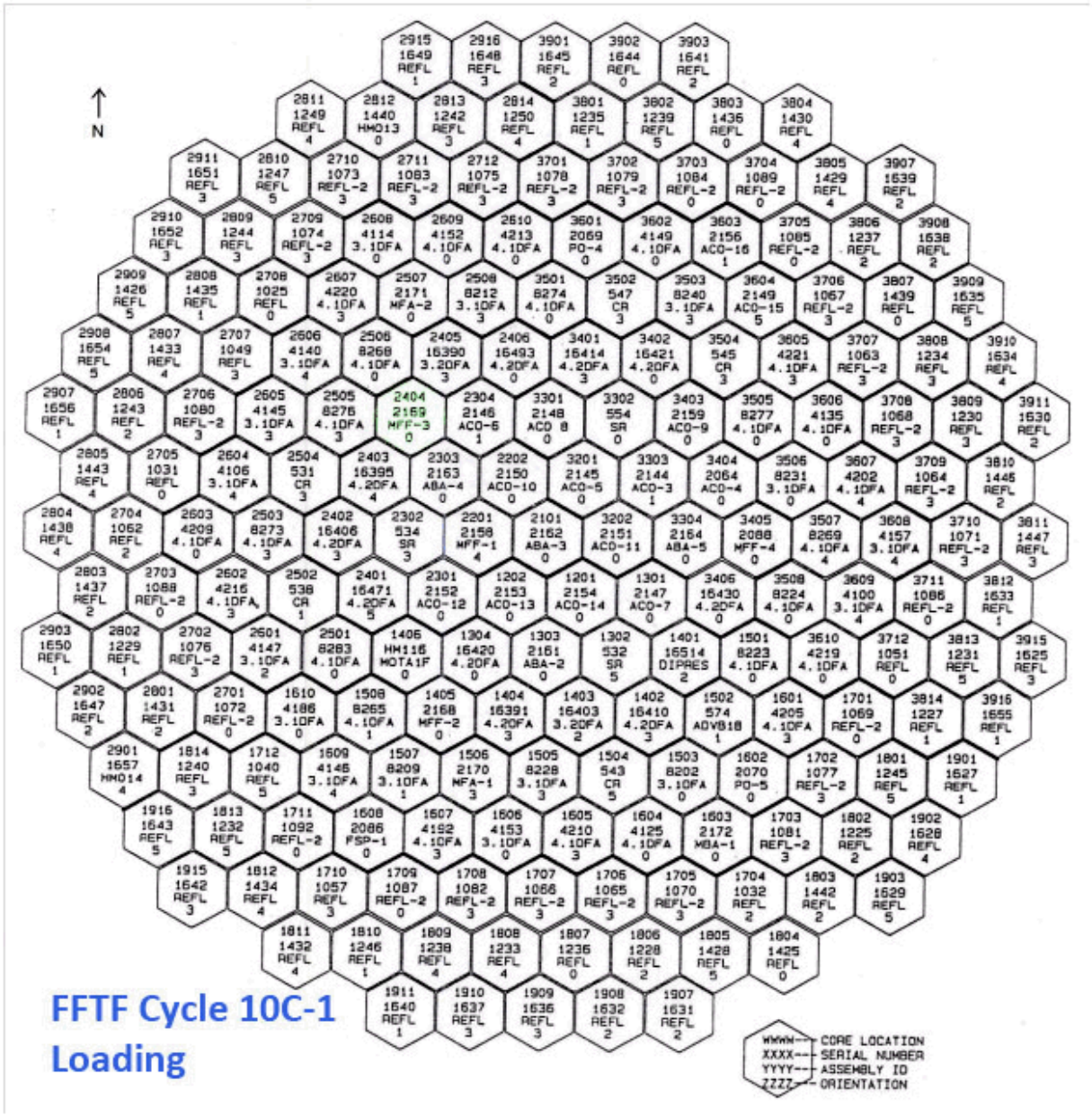


Figure 1. FFTF Core Loading for Cycle 10C-1; MFF-3 highlighted in green.

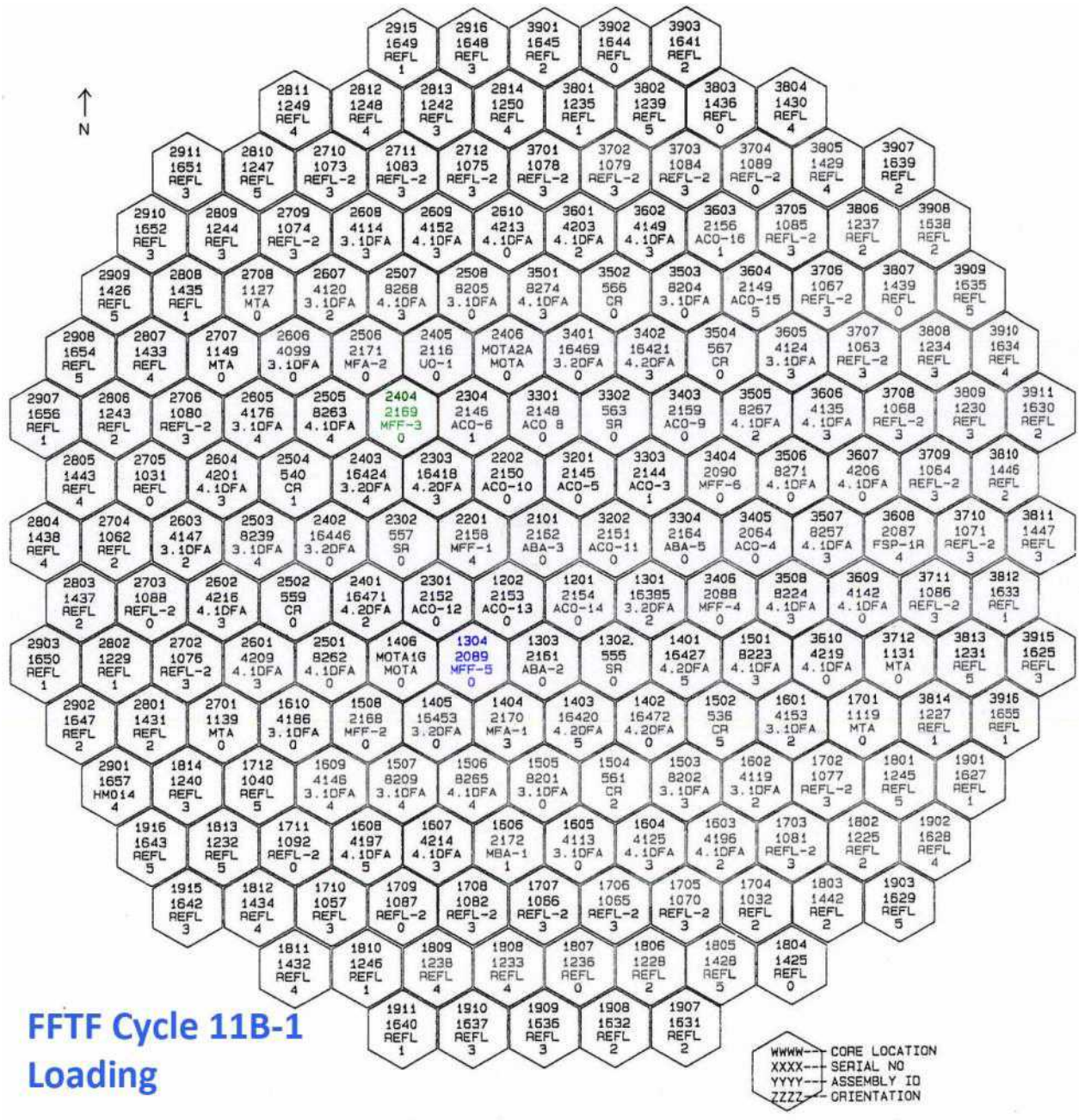


Figure 2. FFTF Core Loading for Cycle 11B-1; MFF-3 highlighted in green; MFF-5 highlighted in blue.

Table 3. MFF-3 and MFF-5 initial assembly conditions.

| Test | Test Start | Core Position | S/A Outlet T (°C) | Sodium Flow Rate ($m^3$/hr) | S/A Power (MW) |
|---|---|---|---|---|---|
| MFF-3 | 10C (BOC)* | 2404 | 580 | 110 | 7.94 |
| MFF-5 | 11B-1 (BOC) | 1304 | 564 | 108 | 7.55 |

*10C (BOC) = FFTF Cycle 10C at the Beginning of Cycle.

The assembly conditions were tracked cycle-by cycle, calculating the following conditions for the beginning and end of cycle (BOC and EOC).

- Fission Power Generated in MFF-3, MFF-5 and Neighboring Assemblies
- Assembly Averaged Fast and Total Flux for MFF-3 and MF3-5
- Axial Distribution of Total Flux, Fast Flux and Power in MFF-3
- Axial Distribution of Total Flux, Fast Flux and Power in MFF-5
- Fission Power Distribution by Pin in MFF-3
- Fission Power Distribution by Pin in MFF-5
- Fast Flux Distribution by Pin in MFF-3
- Fast Flux Distribution by Pin in MFF-5
- MFF-3 and MFF-5 Duct Wall Flux Greater than 0.1 MeV
- Fission Fractions by Isotope in MFF-3 and MFF-5.

The MFF-3 and -5 compositions were compiled for the end of each cycle.

The ratio of the axial assembly power to the average is shown for in Figure 3 for MFF-3(BOL); similar profiles would be expected for MFF-5 and at other points in the irradiation history of each.

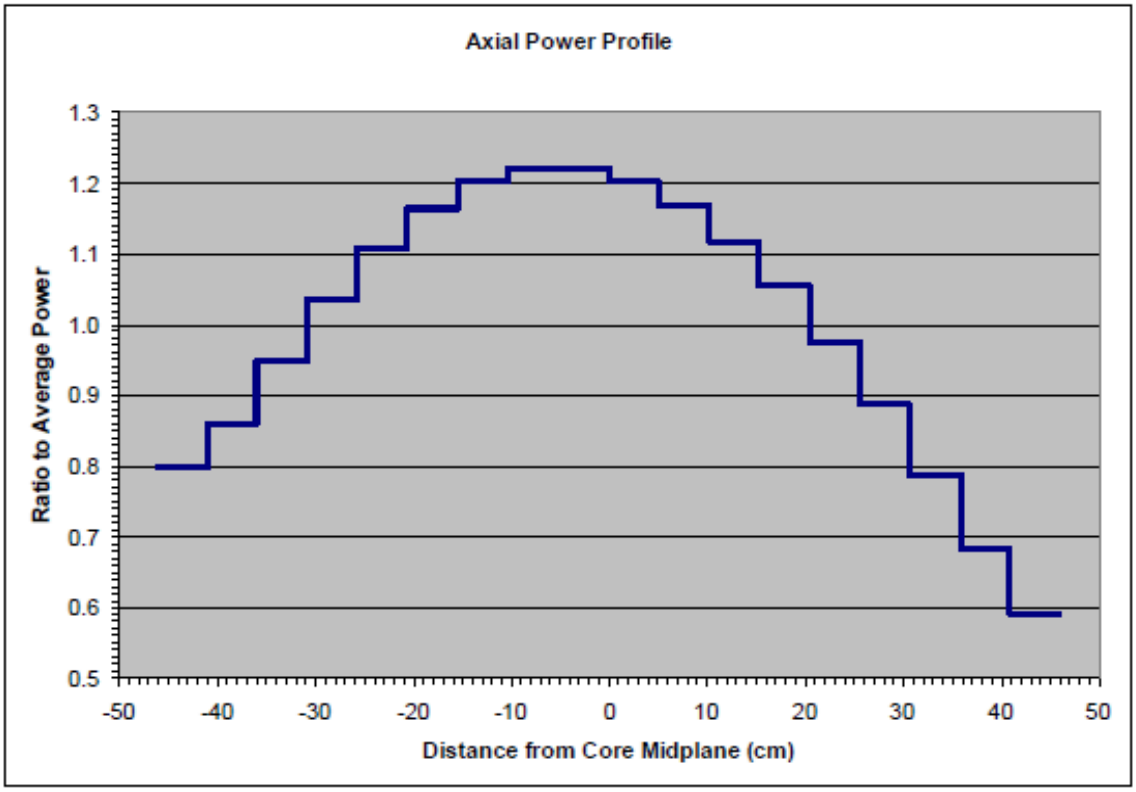


Figure 3. Ratio of axial assembly power to average (from Ref. 6).

#### 2.2.1.1 Assembly Fission Rates

First, the assembly-averaged fission rate, $FR_i$, (fissions/sec per $cm^3$) for each of the seven fissionable isotopes, i, was computed (approximately) using the equation:

$$FR_i = N_i \sum_{g=1}^{G} \sigma_{i,g}\theta_g$$

*where*

$N_i$ = the average atom density (atoms per barn-cm) of isotope i in MFF-3 or MFF-5 at a particular point in time,

$\sigma_{i,g}$ = the fission cross section of isotope i in energy group g,

$\theta_g$ = the average neutron flux (neutrons/cm2-sec) in MFF-3 or MFF-5 at a particular point in time, and

G = the number of neutron energy groups (12)

Next, the total fission rate, FRT, averaged over an assembly was computed as the sum of the seven values of RFi computed using the equation above. Then the relative fission rate of each of the seven fissionable isotopes, RFRi, was computed as:

$$RFR_i = FR_i/FR_T$$

The equation used for computing the $FR_i$ values is an approximation (except for BOL conditions) because of the axial variation in the buildup or depletion on the isotopes. Thus, the $FR_T$ was not used to obtain the total fission rates listed in the tables. However, the $RFR_i$ values tabulated are reasonably accurate because most of the effect of axial burnup variation is divided out in obtaining the relative values.

The total fission rate, TFR, (fissions/sec) in an assembly (MFF-3 or MFF-5) was computed from the adjusted fission power, P, (MW) produced in the assembly using the equation:

$$TFR = P \times C/FE$$

*where*

C = the factor for converting power in MW to units of MeV/sec

C = $6.24146 \times 10^{18}$ MeV per MW-sec, and

FE = fission energy (212 MeV/fission)

Burnup-dependent material compositions for MFF-3 and MFF-5 were calculated at the end of each cycle. The burnup-dependent compositions for the fuel were computed using the three dimensional diffusion theory and burnup codes 3DBF and BURN3D.[7] The fuel was subdivided into six axial regions to properly account for the effect that the axial flux distribution has on the fuel depletion rate. The composition data included fuel, fission products and stainless steel components.

## 2.2.2 Sodium Temperatures

### *2.2.2.1 Methods*

The calculation of sodium temperatures with the SUPERENERGY code based on two dimensional diffusion theory methods[8] with generic axial flux and power profiles from 3-D calculations was a normal part of the core reload design process. The results of these calculations were reported in core reload design and operating reports for Cycles 10C through 12B.

There were two sources of sodium temperature analyses for MFF-3 and MFF-5. The output files of SUPERENERGY temperature calculations that were previously part of the core reload design process for Cycles 11A through 12B were located, and the outlet temperatures and subchannel temperatures for MFF-3 and MFF-5 for these cycles were obtained from these files. No SUPERENERGY output files were available for Cycle 10C. Therefore, the full calculational sequence was performed to generate the temperature distributions for BOC 10C-1 and EOC 10C-3 for MFF-3 and MFF-5.

Data provided for MFF-3 and MFF-5 for each BOC and EOC include:

- Assembly outlet temperatures
- Sodium subchannel temperatures at three axial elevations corresponding to the top of the fuel column, the top of the upper axial reflector in driver fuel pins, and the top of the fuel pin bundle.

The SUPERENERGY code is a subchannel code that was designed specifically for hexagon shaped, wire wrapped pin bundles and was used to calculate the FFTF core assembly mixed-mean outlet temperatures, the assembly subchannel temperatures of all core assemblies, the core assembly duct wall temperatures, and the temperature of the reflector assembly coolant channels. The assembly mixed mean outlet temperatures was used as a basis for comparison to the FFTF above-core instrumentation data and to show that the core loading plans are in compliance with FFTF technical specifications prior to reactor operation. Figure 4 and Figure 5 show the calculated assembly power at the beginning and/or end of each reactor cycle /subcycle for MFF-3 and MFF-5, respectively, as well as the assembly outlet temperatures calculated and measured by the above-core instrumentation. Some points were not calculated due to the short cycle run times. Note that the horizontal scale is not linear in time as FFTF cycle length varied.

The relatively steady decrease in assembly power as the fuel burns out is seen for MFF-3 and for MFF-5 is more influenced by changes in the influence of neighboring assemblies. The comparison of the calculated vs. measured assembly outlet temperature has been used to assess the axial fuel growth of the metallic fuel as the calculation models do not account for a drop in linear power density due to axial fuel swelling.[9] The outlet temperatures measured become lower than expected. However, these two figures show that for MFF-3 and MFF-5 this was not the case. This will be further discussed subsequently in this report when the axial growth data is presented.

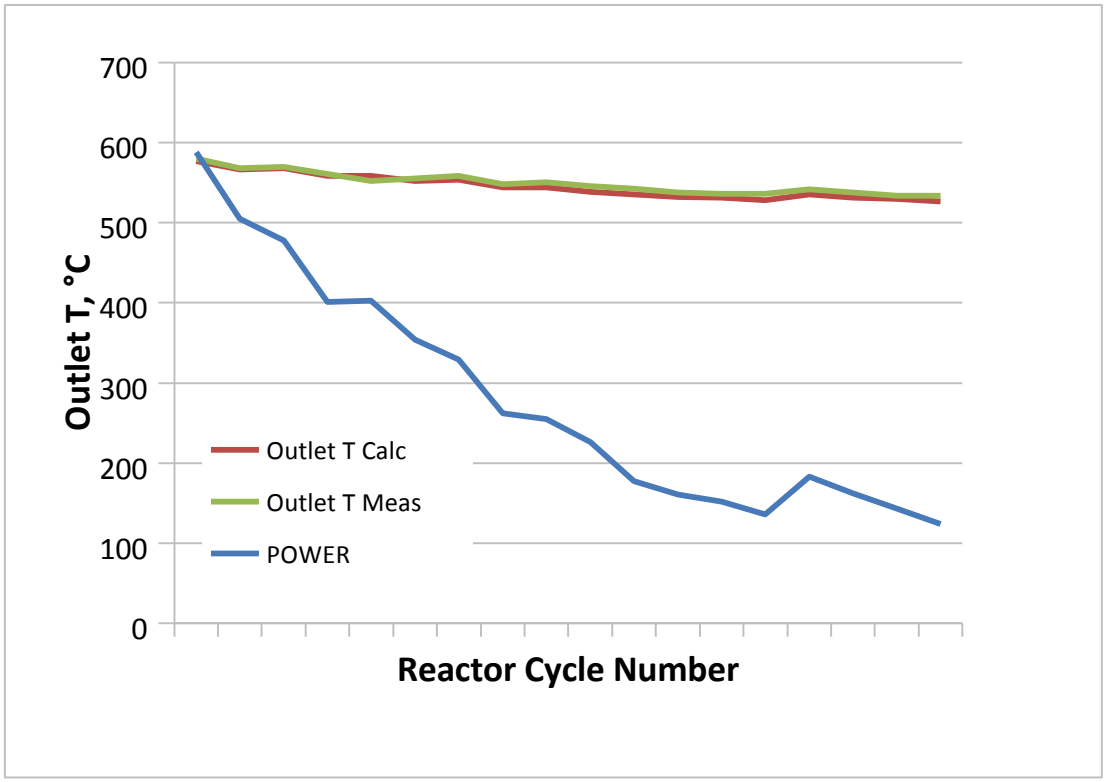


Figure 4. MFF-3 Assembly power and outlet temperature (calculated and measured) at beginning (B) and/or end (E) of reactor cycle.

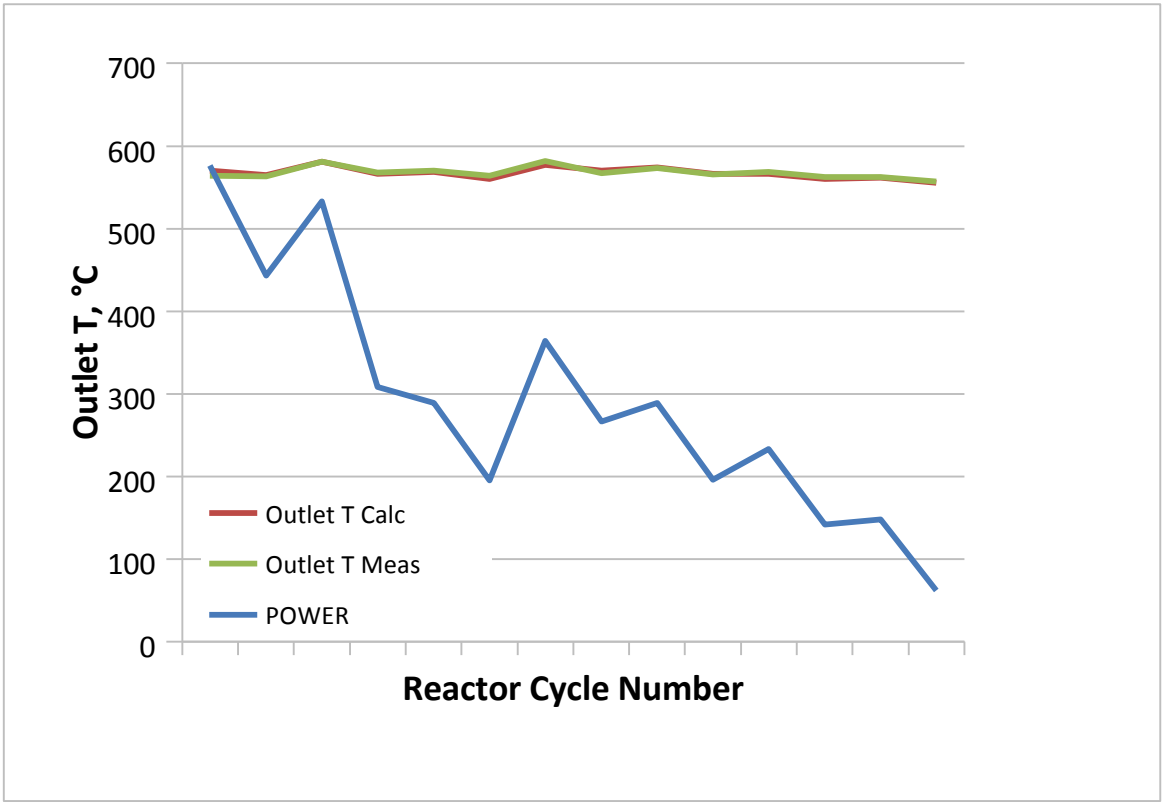

Figure 5. MFF-5 Assembly power and outlet temperature (calculated and measured) at beginning (B) and/or end (E) of reactor cycle.

The subchannel temperatures are used in design analyses of test pins, post-irradiation data correlation of test pins, and for lifetime analyses of driver fuel pins. The duct wall temperatures are used in the structural analyses of the individual assemblies and of the core restraint system. The flow field is described in terms of two correlated parameters, a subchannel mixing parameter and a swirl flow parameter. These two parameters, along with the energy equation and a subchannel flow split model, can completely describe the temperature field in a pin bundle without the use of momentum and continuity. The mixing parameters and flow split correlations are based on extensive experimental test data.

The subchannel temperatures were calculated for MFF-3 and MFF-5 in all subchannels of the fuel bundle and at each cycle, except again for very short cycles. These could then be used to choose, for example, the hottest operating pins in the bundle.

### 2.2.3 Detailed Pin Calculations

#### *2.2.3.1 Methods*

Details of the pin burnup calculation methods can be found elsewhere.6 Data for specific pins in MFF-3 and MFF-5 during their residence in the FFTF core and for decay times following discharge were generated based on three-dimensional calculations of detailed irradiation conditions for these pins to help analysts and designers in evaluating these fuel tests. This information would then allow a more detailed interpretation of test results and development of performance correlations and/or models for metallic fuel assemblies.

Obtaining radionuclide inventories involved:

1. Compiling pin information
    a. Pins selected in each test assembly for detailed burnup calculations
    b. Irradiation history (irradiation and decay times) of each assembly
    c. Initial as-built compositions of the selected fuel pins
    d. Decay times selected following end of irradiation
2. Generating total flux and effective one-group reaction cross sections for each irradiation cycle for each axial layer of each pin in each assembly.
3. Using the as-built pin compositions along with pin-segment-specific fluxes and cross sections by cycle to generate radionuclide inventories for each fuel pin axial segment at the beginning and end of each irradiation cycle and selected decay times following discharge, accounting for isotope buildup, depletion and radioactive decay.

The length of the fuel column in the three dimensional flux calculations was 92.28 cm, with 18 axial layers in the fuel region, corresponding to layers 12 through 29 in the 3DBF flux model. Individual calculations of pin segments were made using the average flux and cross sections over each of the axial layers, providing eighteen fuel pin segments per pin. Thus, each detailed pin burnup calculation corresponds to a 5.127 cm long segment of a fuel pin. Data provided for MFF-3 and MFF-5 for the beginning and end of each operating cycle include neutron flux, cross sections, and burnup dependent compositions for 18 axial pin segments for selected fuel pins.

This information was then used in the SAFE[10] thermal hydraulic model to calculate axial fuel and cladding temperatures for select pins.

#### 2.2.3.2 Selected Pins

Nine pins from MFF-3 and ten pins from MFF-5 were selected by INL for detailed burnup calculations. The locations of the selected pins in MFF-3 and MFF-5 are shown in Figure 6 and Figure 7, respectively.

```
Strip layer
1    193001 193072 193073 193002 193074 193075 193003 193004

2                          193065 193066 193067 193068 193069 193070 193071 193005 193006
                                                                                  (1)
3                       193057 193058 193007 193059 193060 193061 193008 193062 193063 193064

4                   193049 193050 193051 193052 193009 193010 193053 193054 193055 193056 193011
                                                 (9)                   (2)
5              193012 193043 193013 193044 193014 193015 193016 193045 193018 193046 193047 193048
                                                (7) (5)
6         193122 193123 193124 193125 193126 193127 193019 193020 193128 193129 193130 193021 193131
                                                (8) (6)      (3)
7    193109 193110 193111 193112 193022 193113 193114 193115 193116 193117 193118 193119 193120 193121
                                                      (4)
8 193023 193099 193100 193024 193101 193102 193103 193025 193104 193105 193026 193106 193107 193108 193027 X
                                                                                                  0° Index Notch
9    193086 193087 193088 193089 193090 193091 193092 193093 193094 193095 193096 193097 193028 193098

10        193076 193029 193077 193078 193079 193030 193080 193081 193082 193083 193031 193084 193085

11             193163 193164 193165 193032 193166 193167 193168 193169 193033 193170 193171 193035

12                 193036 193154 193155 193156 193157 193037 193158 193159 193160 193161 193162

13                      193145 193146 193147 193148 193149 193150 193151 193152 193038 193153

14                           193137 193138 193039 193139 193140 193141 193142 193143 193144

15                                193040 193132 193133 193134 193041 193135 193136 193042


    (x) = pin number for pin composition calculations
```

Figure 6. Pin loading of the MFF-3 assembly. The location of the assembly index notch in shown, as are the pins selected for composition calculation (in red).

```
Strip layer
1                          195007 195043 195044 195008 195045 195046 195047 195009

2                          195035 195036 195005 195037 195038 195039 195006 195041 195042

3                       195024 195025 195026 195027 195028 195030 195031 195032 195033 195034

4                    195017 195018 195001 195019 195020 195002 195021 195022 195003 195023 195004

5                195069 195106 195107 195108 195109 195110 195111 195112 195113 195114 195115 195116
                                                      (7)
6           195096 195097 195098 195099 195066 195100 195101 195102 195067 195103 195104 195068 195105
                                                 (8) (4)       (1)
7      195093 195016 195094 195095 195058 195059 195060 195061 195062 195063 195064 195065 195091 195092
                                        (10) (9)      (5) (2)
8 195010 195048 195049 195050 195011 195051 195052 195012 195053 195054 195013 195055 195056 195057 195015 X
                                                                                                  0° Index Notch
                                                 (6) (3)
9      195142 195143 195144 195145 195146 195147 195148 195149 195150 195151 195152 195153 195082 195154

10          195132 195079 195133 195134 195135 195080 195081 195136 195137 195138 195139 195140 195141

11               195126 195127 195073 195128 195074 195075 195076 195129 195077 195130 195131 195078

12                    195070 195117 195118 195119 195071 195072 195121 195122 195123 195124 195125

13                       195185 195186 195187 195188 195189 195190 195191 195090 195192 195193

14                            195087 195088 195159 195089 195160 195181 195182 195183 195184

15                                195083 195084 195155 195156 195085 195157 195158 195086
(x) = pin number for pin composition calculations
```

Figure 7. Pin loading of the MFF-5 assembly. The location of the assembly index notch in shown, as are the pins selected for composition calculation (in red).

#### 2.2.3.3 Selected Pin Total Flux

The effective one-group neutron flux for each cycle and each of 18 axial layers of each pin was calculated by running the HEDPIN code for each of the 18 layers of the fuel column in the 3DBF flux file for each cycle. These fluxes were generated from the same 3DBF flux files with the mid-cycle control rod elevations that were used in the assembly cycle burn calculations that created the nuclear analysis database files (NADBs) for each cycle.6

#### 2.2.3.4 Cross Sections for Axial Segments

For each of the pin segment total flux values, effective one group fission and capture reaction cross sections for $^{235}U$, $^{238}U$, $^{239}Pu$, $^{240}Pu$, and $^{241}Pu$ were generated for each pin segment for each cycle. This was done by running the HEDPIN code on the same 3DBF flux files for each cycle, but this time multiplying the multi-group flux by the metallic fuel test multi-group cross sections to calculate reaction rates instead of total flux, and using the HEDPIN interpolating fit to obtain the values for each pin segment. The effective one group reaction cross sections were then obtained by dividing the reaction rates by the total flux. These pin-segment-cycle-dependent cross sections were substituted into the FFTF metallic fuel specific ORIGEN2 cross section library for each ORIGEN2 calculation.

The ORIGEN2 input files for each pin segment were constructed using the total flux values as constant over each cycle, with actual irradiation times and decay times between each cycle. Nuclide inventories for each pin segment were calculated, which included the beginning and end of each operating cycle and twelve decay times extending out to the year 2040 following the end of irradiation.

#### 2.2.3.5 Calculation of Pin Powers

The peak linear power for each assembly can be calculated by multiplying the assembly fission power, a factor accounting for the difference in the power deposited in the pin (fuel and cladding) and the fission power, and the radial and axial peaking factors. The pin energy deposition for the U-10Zr metallic fuel pins differs from the standard mixed $U/PuO_2$ fuel pins in FFTF because the $^{235}U$ enriched pins release less energy per fission than pins driven by $^{239}Pu$ fission and have a different composition with internal sodium and zirconium. The slightly different pin energy deposition rates for the metallic fuel pins were included in the calculated peak pin powers.

The total heat distribution for the FFTF core (including nonfueled components) is obtained by combining the local direct fission heat production with other nuclear heat sources, such as gamma ray absorption, charged particle reactions, and neutron scattering recoils. The energy produced from all of these sources is combined and adjusted so that the total is properly normalized for a recoverable heat energy of 291 MW at full power for Cycles 9 through 12 (previously 400MW for Cycles 1 through 8).

Pin fission power can be calculated as

$$PP_F = AP_F * R/N$$

*where*

$PP_F$ = pin fission power

$AP_F$ = assembly fission power

N = number of pins = 169

R = ratio of particular pin power to assembly average pin power = assembly map of radial pin power distribution normalized to assembly average of 1.0.

Pin deposited power can be calculated as

$$PP_D = PP_F * D$$

*where*

$PP_D$ = pin deposited power

D = ratio of power deposited in pin (fuel and cladding) to fission power generated in pin.

Power in each of the eighteen axial pin segments can then be obtained by multiplying the pin powers by the axial power profile (which has been normalized to an axial average of 1.0) and dividing by 18.

The pin segment power can be converted to linear powers at specific axial elevations by dividing by the fuel segment height (5.127 cm in the model).

#### 2.2.3.6 Individual Pin Thermal Operating Conditions

Normalized pin power distributions were calculated using the HEDPIN computer program based on interpolating the fission powers from the calculational mesh to the pin positions. The pin power distributions and subchannel coolant temperatures were used to determine fuel pin temperature and power profiles using the SAFE[10] computer code.

Two pins were identified for detailed temperature and axial power distribution analysis and full non-destructive and destructive post-irradiation examination. The pins with serial number 193045 (a 4th row pin) from the MFF-3 assembly and serial number 195011 (a 4th row pin) from the MFF-5 assembly appeared to have experienced high power and hence high temperature operation, nearly peak for the assembly. Because of the orientation of the assemblies during their irradiation history, some of the 4th row pins tend to be the highest power pins and hence the highest temperature pins in the assembly over the life of the assembly. Figure 8 and Figure 9, provide a cycle-to-cycle history of the peak pin power and the peak inner cladding temperature for Pin 193045 from MFF-3, respectively. Figure 10 shows the axial linear power profile and axial temperature profiles for Pin 193045 from MFF-3.

Figure 11 and Figure 12 provide a cycle-to-cycle history of the peak pin power and the peak inner cladding temperature for Pin 195011 from MFF-5, respectively. Figure 13 shows the axial linear power profile and axial temperature profiles for Pin 195011 from MFF-5.

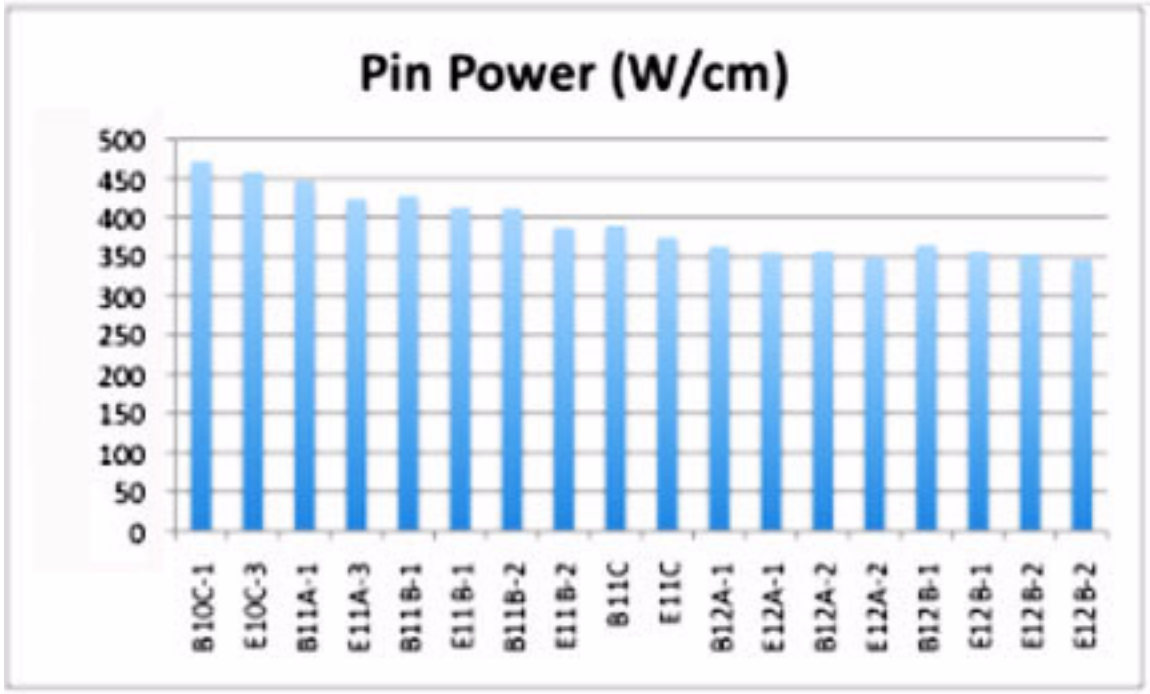


Figure 8. MFF-3, Pin Number 193045, pin power as a function of FFTF cycle number.

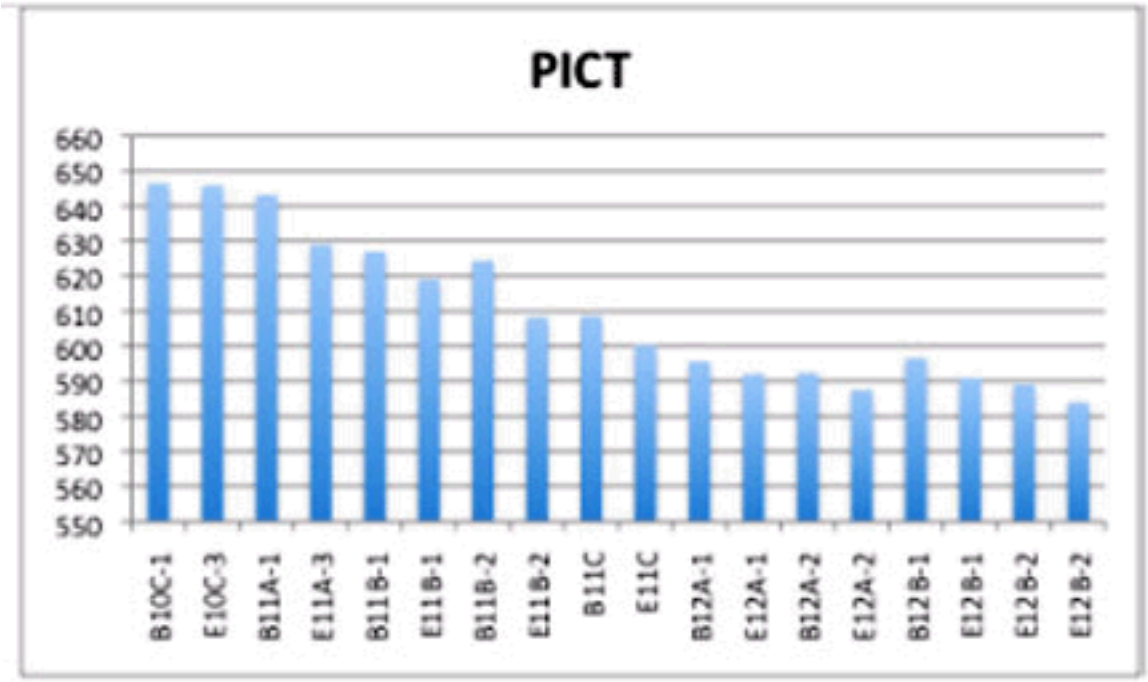


Figure 9. MFF-3, Pin Number 193045 peak inner cladding temperature, in °C, as a function of FFTF cycle number.

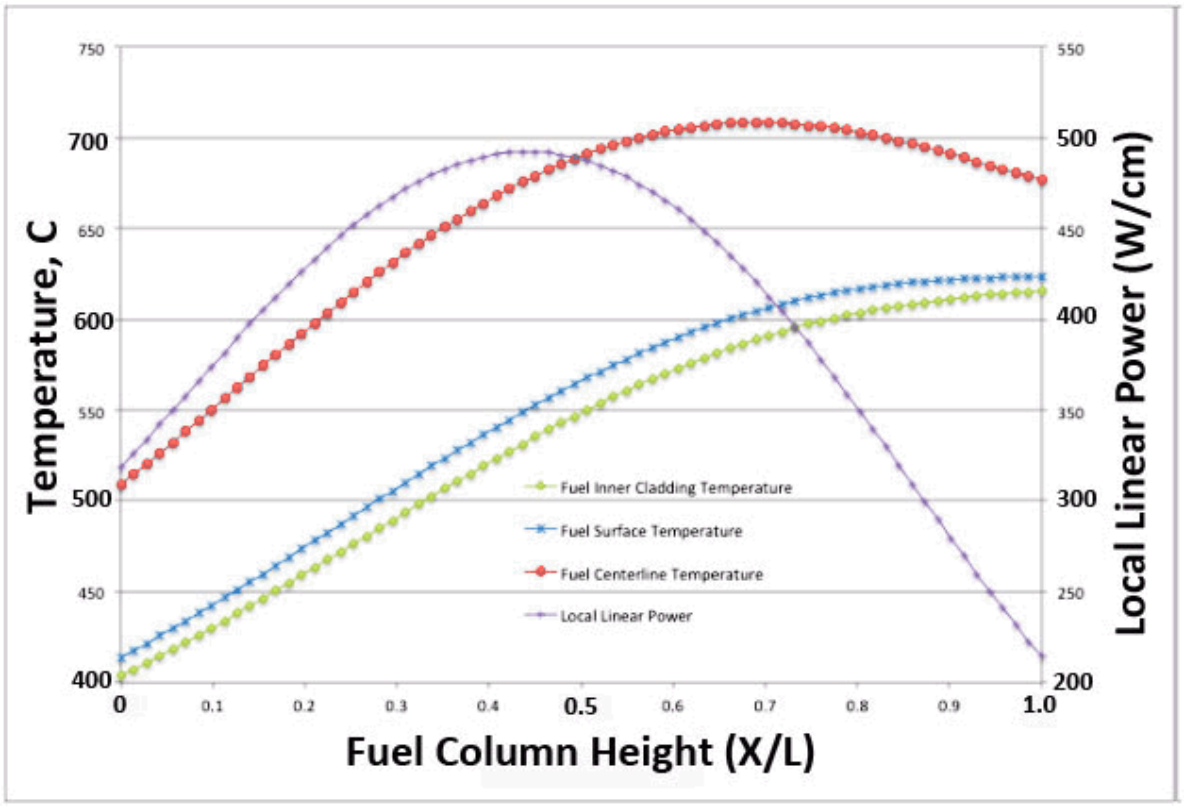


Figure 10. MFF-3, Pin Number 193045 inner cladding, fuel centerline and fuel surface temperatures, as well as pin power as a function of axial position on the pin. Values are averaged over the total EFPDs.

Note that the fuel temperatures peak below the top of the fuel column as the pin power drops off, but the cladding temperature peaks at the top of the fuel column, influenced by the steady increase in the coolant temperature.

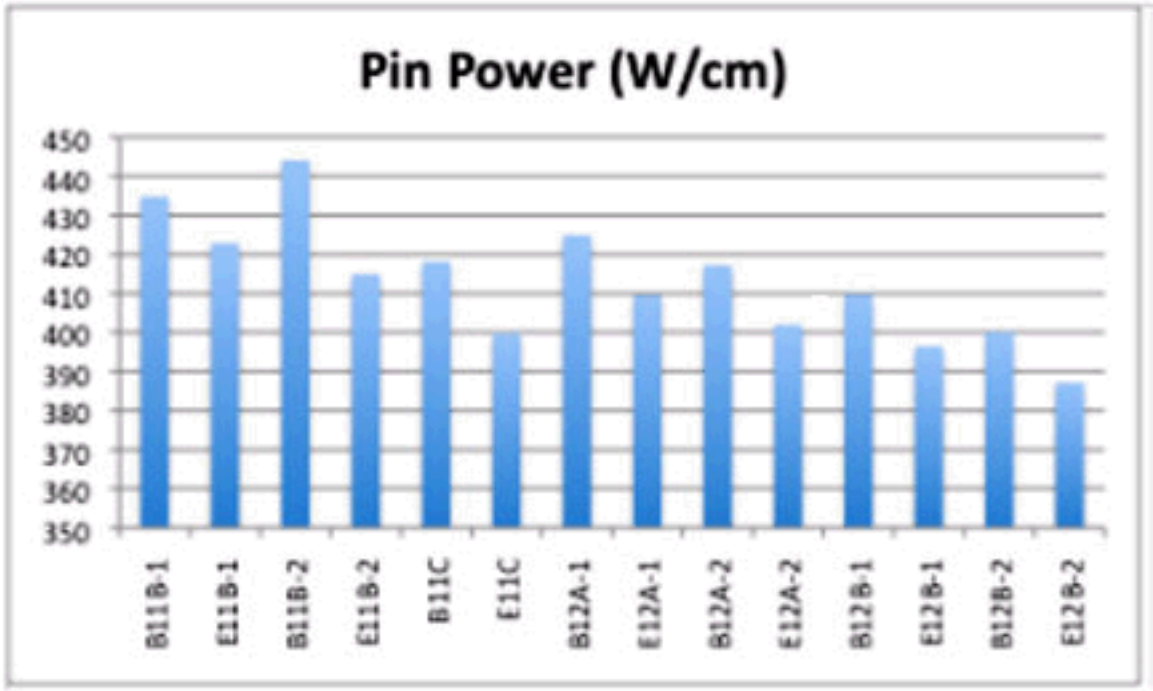


Figure 11. MFF-5, Pin Number 195011, pin power as a function of FFTF cycle number.

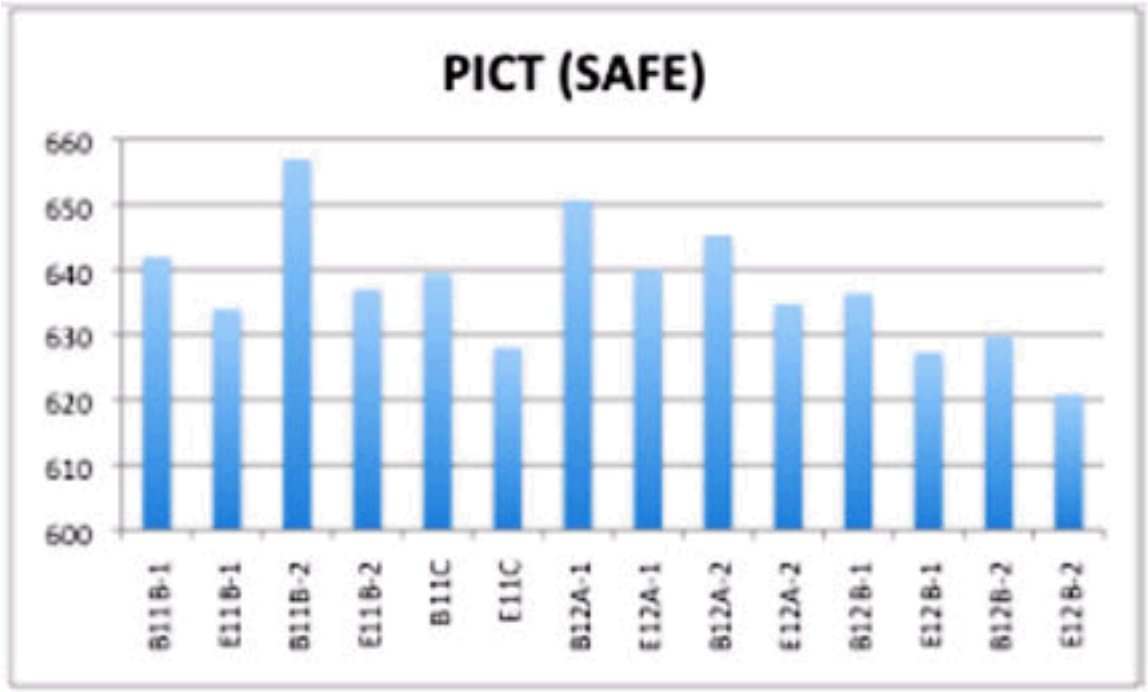


Figure 12. MFF-5, Pin Number 195011 peak inner cladding temperature, in °C, as a function of FFTF cycle number.

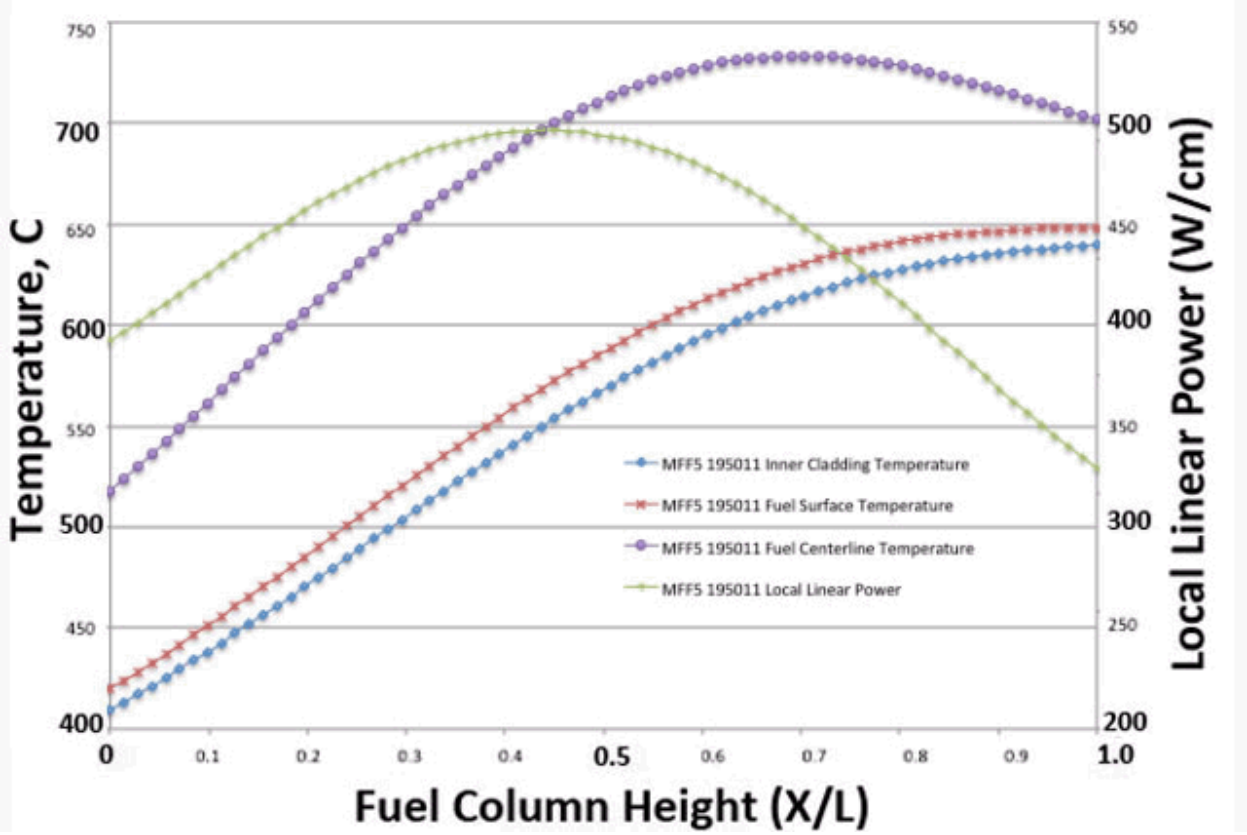


Figure 13. MFF-5, Pin Number 195011, inner cladding, fuel centerline and fuel surface temperatures, as well as pin power as a function of axial position on the pin. Values are averaged over the total EFPDs.

#### *2.2.3.7 ORIGEN Calculation*

Appendix A contains a large table, Table A-1(a-m), showing the results of ORIGEN-based composition calculations for a single pin, 195011,where isotopic fuel (heavy metal) and fission product compositions were calculated for every two-inch segment of the 36-inch fuel column. The compositions were calculated for both pins that were destructively characterized, one from MFF-3 and one from MFF-5. These results are used subsequently in this report to compare burnup/depletion calculations with analytical chemistry measurements. The compositions were also useful in computing the expected radiation fields around samples from the fuel pins, allowing work to be planned to minimize personnel exposures.

## 3. POST-IRRADIATION EXAMINATIONS

Table 4 shows the MFF-3 and MFF-5 pin numbers and the examinations performed on each of them. The table shows which pins were examined by neutron radiography, visual, precision gamma scanning, bow and length measurements, element spiral contact profilometry (ESP), element linear contact profilometry (ECP), plenum gas chemical analysis and pressure measurements (GASR), metallography and microhardness.

Table 4. Post-irradiation examination listing.

| Assembly: Fuel Pin Number | Examinations | | | | | | | |
|---|---|---|---|---|---|---|---|---|
| | Neutron Radiography | Visual | Gamma Scans | ECP | ESP | GASR | Burnup Analysis | Metallography |

| | | | | | | | | |
|---|---|---|---|---|---|---|---|---|
| MFF-3: 193020 | X | X | X | | X | | | |
| MFF-3: 193025 | X | X | X | | X | | | |
| MFF-3: 193045 | X | X | X | X | | X | X | X |
| MFF-3: 193062 | X | X | X | | X | | | |
| | | | | | | | | |
| MFF-5: 195011 | X | X | X | X | | X | X | X |
| MFF-5: 195012 | X | X | X | | X | | | |
| MFF-5: 195051 | X | X | X | | X | | | |
| MFF-5: 195052 | X | X | X | | X | | | |

## 3.1 Neutron Radiography

Four irradiated metallic fuel pins in each of MFF-3 and MFF-5 were radiographed using indium foil neutron detectors (epithermal neutrons) and dysprosium foil detectors (thermal neutrons). The activated foils were then used to transfer images to film. The films were ~43 cm long requiring six shots to cover the entire pin length of 240 cm.

The epithermal neutrons provide for weaker contrast because of the neutrons being of higher energy, but do allow greater penetration of the fuel. Appendix B shows the pins that received detailed examinations (highlighted in Table 4). Note that the images shown in Appendix B have been 'stitched together' from the component radiographs over the length of the pin. The larger digitized radiograph files have been archived as have the original radiographs/films. Also note that there is a slight 'double image' created by aperture misalignment in the neutron beam port.

The spacer wires can be seen in the images, shown wrapped around the cladding in all but the images of 193045 and 195011, the pins that were eventually destructively examined. The wires had been removed to allow these destructive exams.

The axial growth of the fuel slugs was measured using the neutron radiography as shown in Figure 14. A precision graduated (to 0.02 inches or 0.51 mm) scale was placed next to the fuel during radiography and used to measure the fuel column length. The relative fuel column length changes are indicated and are compared to a representative radiograph from U-10Zr fuel previously irradiated in FFTF, in assembly IFR-1. Note that the fuel in IFR-1 showed significantly greater axial growth. The IFR-1 data is much more similar to the experience gathered through EBR-II testing.[11] The IFR-1 peak cladding temperature (BOL) was 610°C

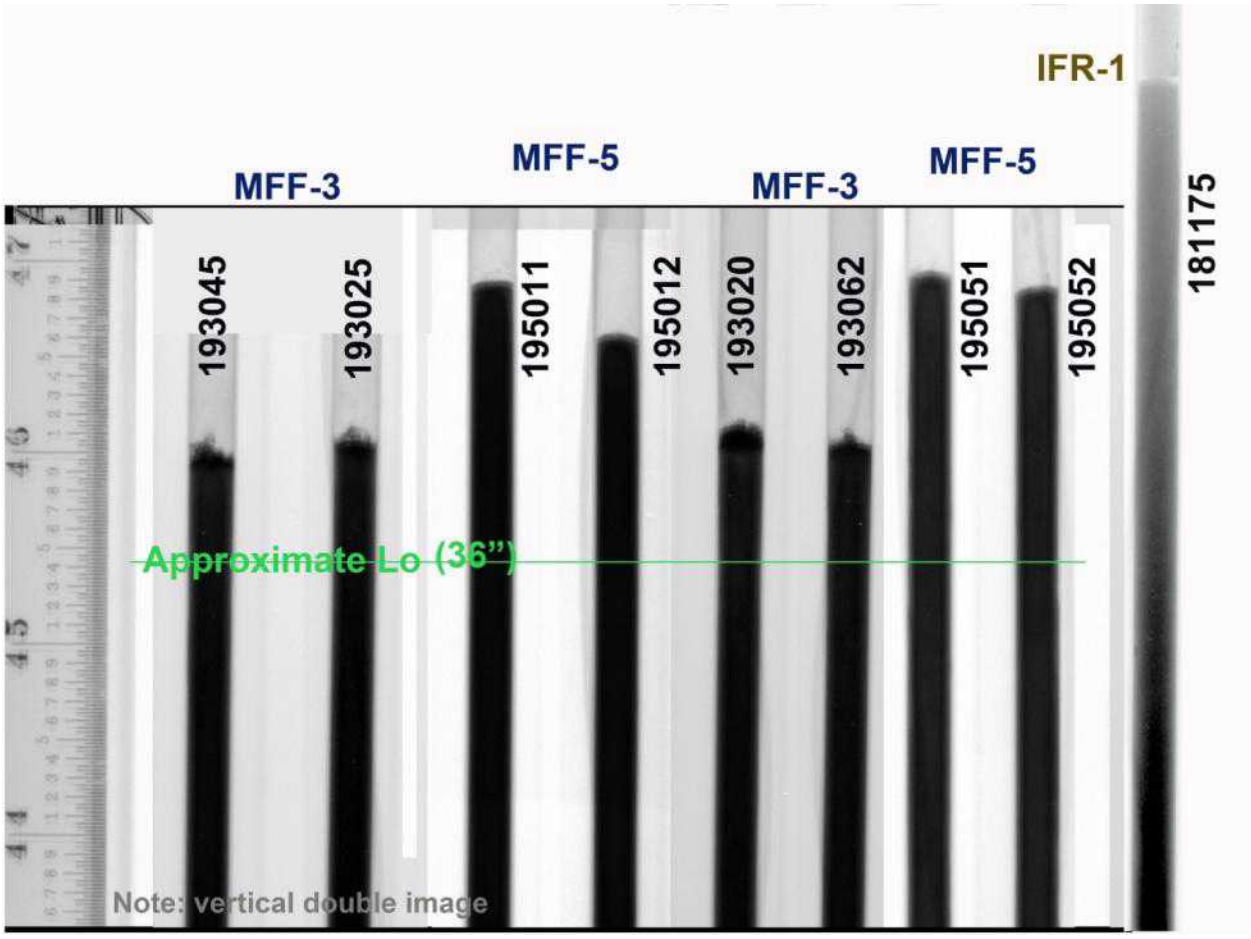


Figure 14. Neutron radiography of the tops of the fuel columns of two MFF-3 and two MFF-5 pins, showing the low axial growth compared to a typical IFR-1 pin (36 in. = 91.4 cm, the initial fuel column length).

The measured fuel growth is shown in Table 5; the as-fabricated lengths are assumed from the specification (91.44 cm) as none were measured prior to irradiation. Note that the axial growth is much less than expected from other testing.

The axial fuel column growth due to swelling is an important measurement in that most all of the other data related to the 33.4-cm fuel column length of EBR-II experimental pins. There was a question as to whether cladding contact due to radial swelling would then restrain further axial growth. In addition, the aspect ratio is much larger for the FFTF fuel, creating more axial stress from the weight of the slug at the bottom of the fuel column. The fact that the IFR-1 was only slightly less than EBR-II testing data, however, indicates that there is another factor involved in creating these low axial growth observations. One theory is that the very high fuel temperatures, combined with the long fuel column/large aspect ratio, creates the low axial growth as fuel creep forces material to flow in the opposite direction to the growth. Note, however that the axial growth in the EBR-II test X447, where the fuel operated as hot as the fuel operated in the MFF-3 and MFF-5 tests, the expansion was 5-9 % with an average of 7 %, much like the colder IFR-1 test.[12]

Table 5. Axial growth of active fuel column as determined by neutron radiography.

| | MFF-3 | | | | MFF-5 | | | |
|---|---|---|---|---|---|---|---|---|
| Pin No. | 193045 | 193025 | 193020 | 193062 | 195011 | 195012 | 195051 | 195052 |

| $\Delta L/L_o$, % | 1.5 | 1.6 | 1.8 | 1.6 | 3.7 | 3.0 | 3.9 | 3.8 |
|---|---|---|---|---|---|---|---|---|
| Avg., % | 1.6 | | | | 3.6 | | | |

FFTF assemblies were each monitored for outlet temperature. As mentioned previously, it was noted that the assembly outlet temperature of the MFF-2 assembly was exhibiting a decline in outlet temperature that was larger than could be explained by depletion of fissile material content.9 A graphical representation of this is shown in Figure 15.[13] A similar phenomenon was seen in the outlet temperatures of the IFR-1 assembly.

Recall that Figure 4 and Figure 5 did not show an underprediction of the outlet temperature decline. This may be because the axial fuel growth was so small; the expansion of the fuel column of the U-10Zr fuel in the IFR-1 assembly was ~7%, at least twice that of MFF-3 and MFF-5.3. The MFF-2 axial expansion is to be measured to test this theory.

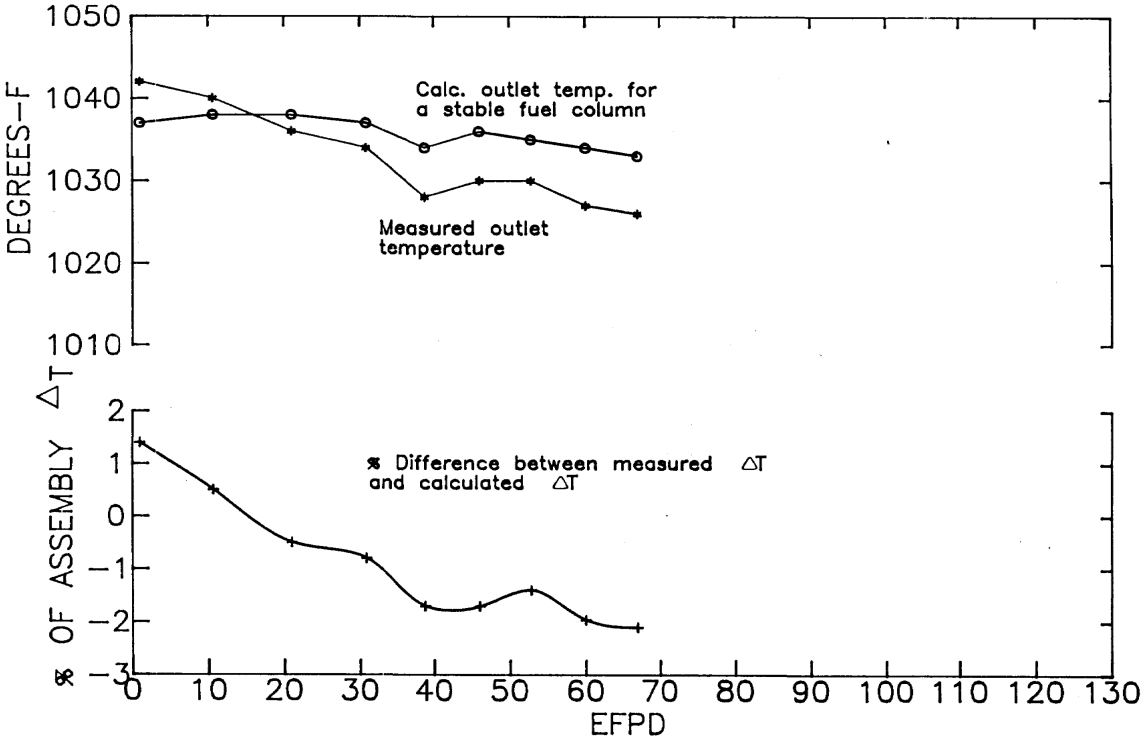


Figure 15. Assembly MFF-2 outlet temperatures; cycle 10B (from Ref. 13).

## 3.2 Gamma Scanning

Eight pins, four from MFF-3 and four from MFF-5, were scanned axially for gamma radiation. Parameters used were a slit width of 2.54 mm, step size of 2.54 mm and a live time of 240s. The isotopes scanned were Cs-134, Co-60 and Eu-154. These were the only long-lived fission and activation products which could reliably be scanned. The Co-60 marks the stainless steel (HT-9) hardware locations, the Cs-134 represents the very mobile fission products, and the Eu-154 was the only rare earth fission product remaining which could be scanned. There were no relatively immobile fission products remaining to assess were the fuel was located. The gross activity (all isotopes) was also recorded.

Figure 16 and Figure 17 show typical gamma scan traces for an MFF-3 pin (193045) and an MFF-5 pin (195011) respectively. The Co-60 traces show where the activated stainless steel (HT-9) from the fuel

jacket and end plugs are located and especially the Inconel reflector. The Cs-134 is peaked in the typical region just above the fuel where Cs gets trapped in the bond sodium that forms a molten plug above the fuel column. Some of these plugs can be forced by build-up of fission gas upwards in the plenum although there are no obvious spikes in Cs shown here.

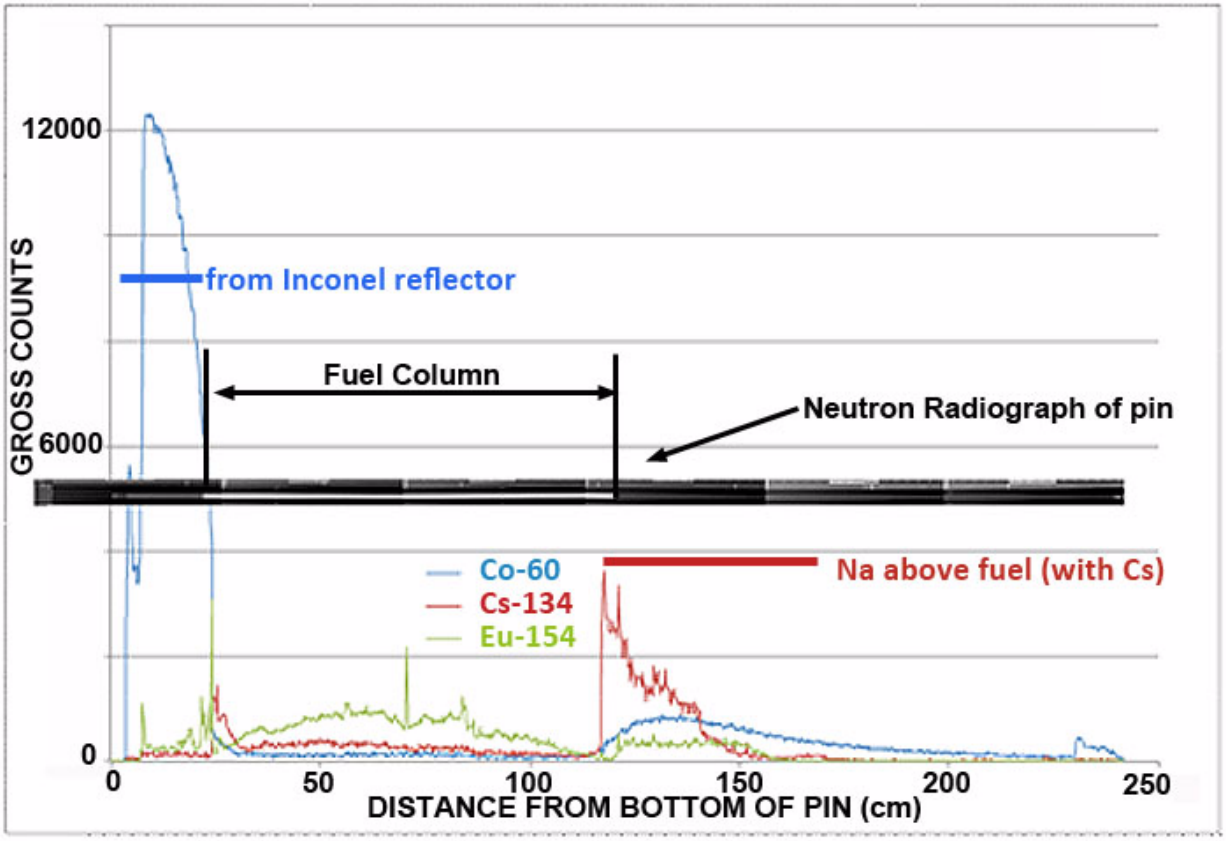


Figure 16. Gamma scan traces for Pin 193045 from MFF-3. Neutron radiograph is superimposed.

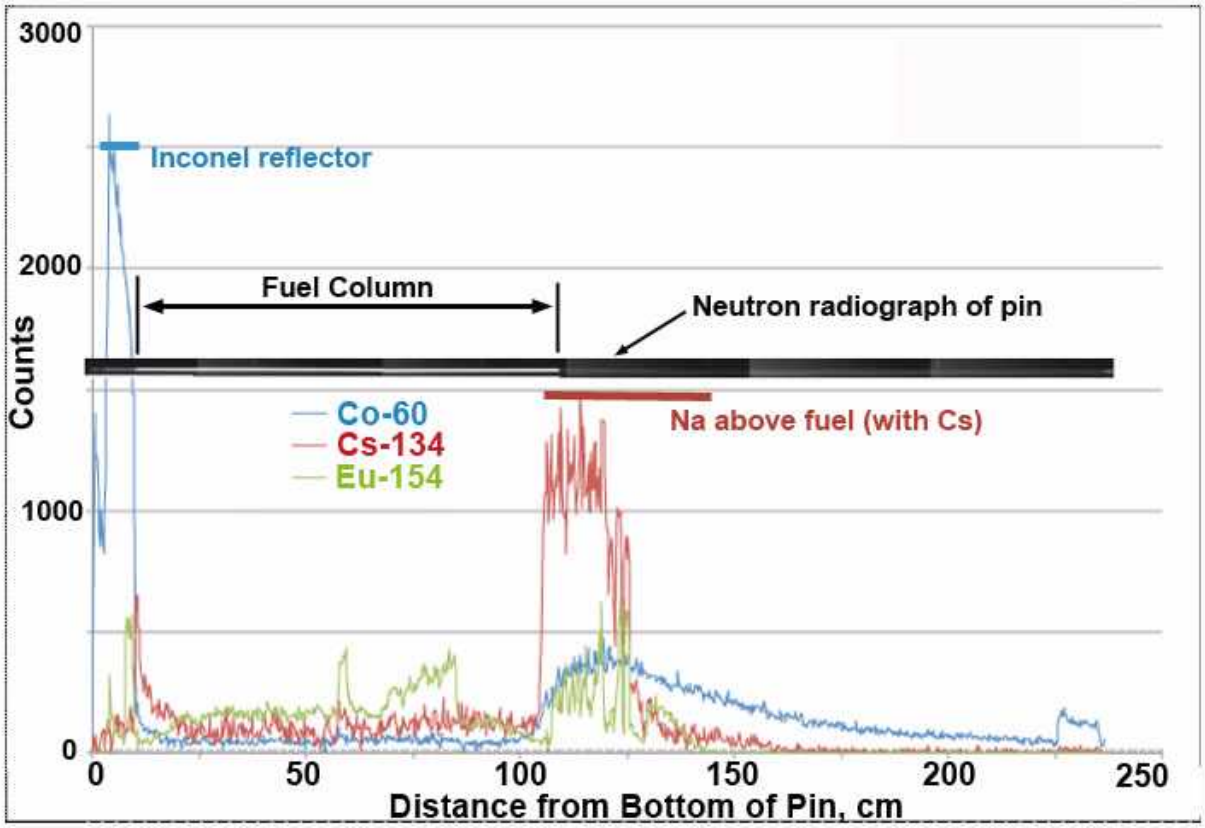


Figure 17. Gamma scan traces for Pin 195011 from MFF-5. Neutron radiograph is superimposed.

All of the gamma scan results are plotted in figures in Appendix C.

## 3.3 Bow and Length

The bow-and-length measurement maps the free-hanging position of the fuel rod tangent along the axial length of the specimen. The element bow and length machine (EBLM) has two orthogonal bars, each holding a light source and photo detector. The bars traverse a 12 × 12-in. area in the X-Y plane, centered on the system examination center. The bow data is reported as coordinates on a two-dimensional grid at discreet axial positions, and total length is determined by summing the individual chord lengths. Figure 18 shows the coordinate reference frame used to record measurements for bow and length. The complete set of data has been archived but is not presented here.

The length measurement uncertainty is ±381 µm (0.015 in.). The bow uncertainty is ±510 µm (0.020 in.) The uncertainty of the azimuthal orientation is ±3.0°, and the uncertainty of axial position is ±250 µm (0.010 in.).

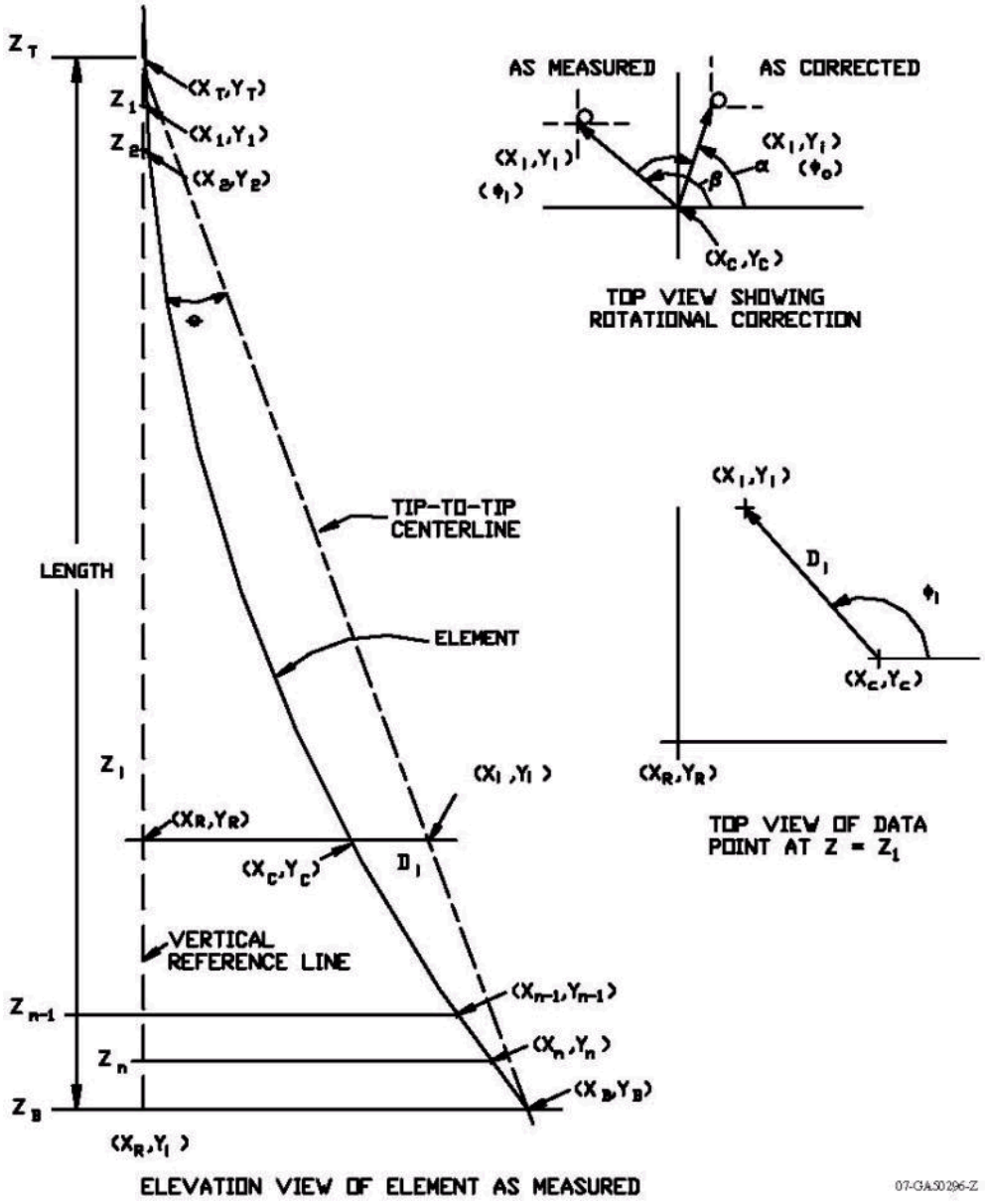


Figure 18. Sketch for the reference frame and measurement coordinates used to record bow and length data.

The pin length was measured two ways. The first was directly noting the Z travel during profilometry, called ‘hanging length’, shown as ‘LENGTH’ in the drawing. Secondly, the true length is extracted from the Z-data along with the bow coordinate data. The results are shown in Table 6.

Table 6. ‘Hanging’ lengths of pins before and after irradiation.

| Pin | As-built Length, cm | Hanging Length, cm | Growth, cm |
|---|---|---|---|
| 193025 | 238.11 | 238.57 | 0.46 |
| 193025 | 238.11 | 238.59 | 0.48 |
| 193020 | 238.11 | 238.68 | 0.57 |
| 193062 | 238.12 | 239.18 | 1.06 |
| 193062 | 238.12 | 239.27 | 1.15 |
| 195051 | 237.11 | 237.86 | 0.75 |
| 195012 | 237.11 | 237.60 | 0.49 |
| 195012 | 237.11 | 237.60 | 0.49 |
| 195052 | 237.11 | 238.03 | 0.92 |
| 195052 | 237.11 | 238.03 | 0.92 |

## 3.4 Element Spiral Contact Profilometer (ESP)

The diameter profiles for six pins (three MFF-3, three MFF-5) were measured using spiral profilometry, measuring the pin diameter as a function of pin elevation. This allowed the diameter measurements without removal of the spacer wire. The results are shown in Figure 19 through Figure 24.

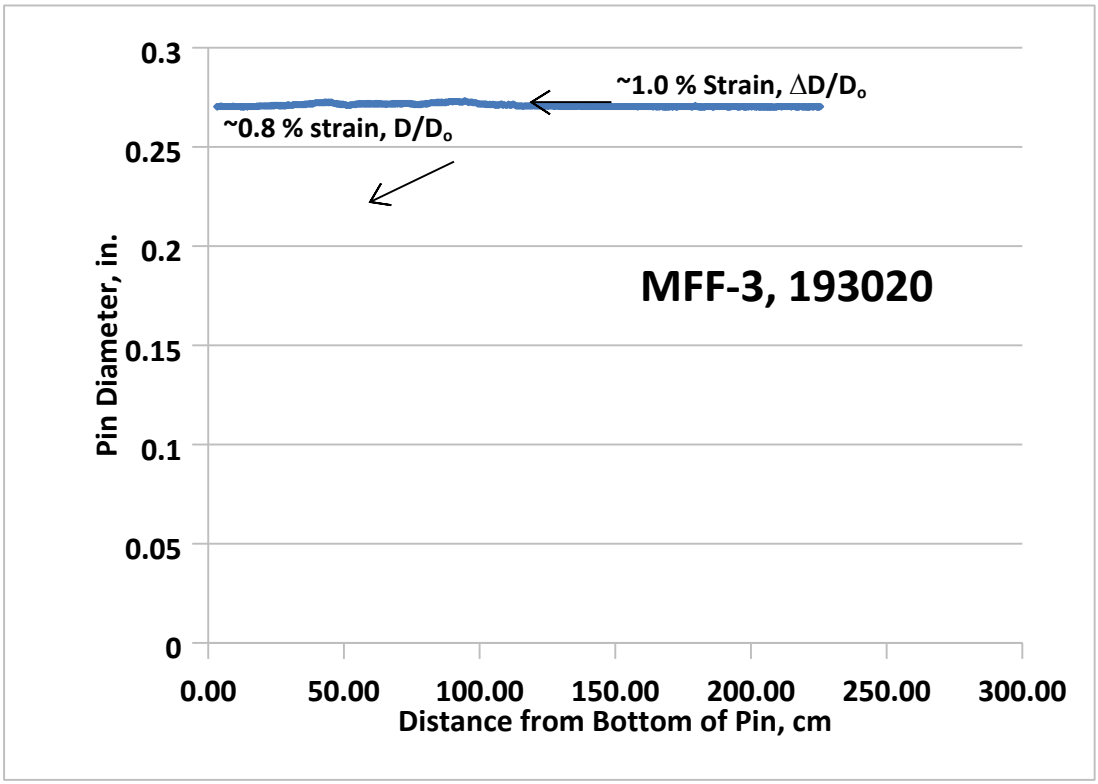


Figure 19. Spiral contact profilometry for MFF-3 Pin 193020.

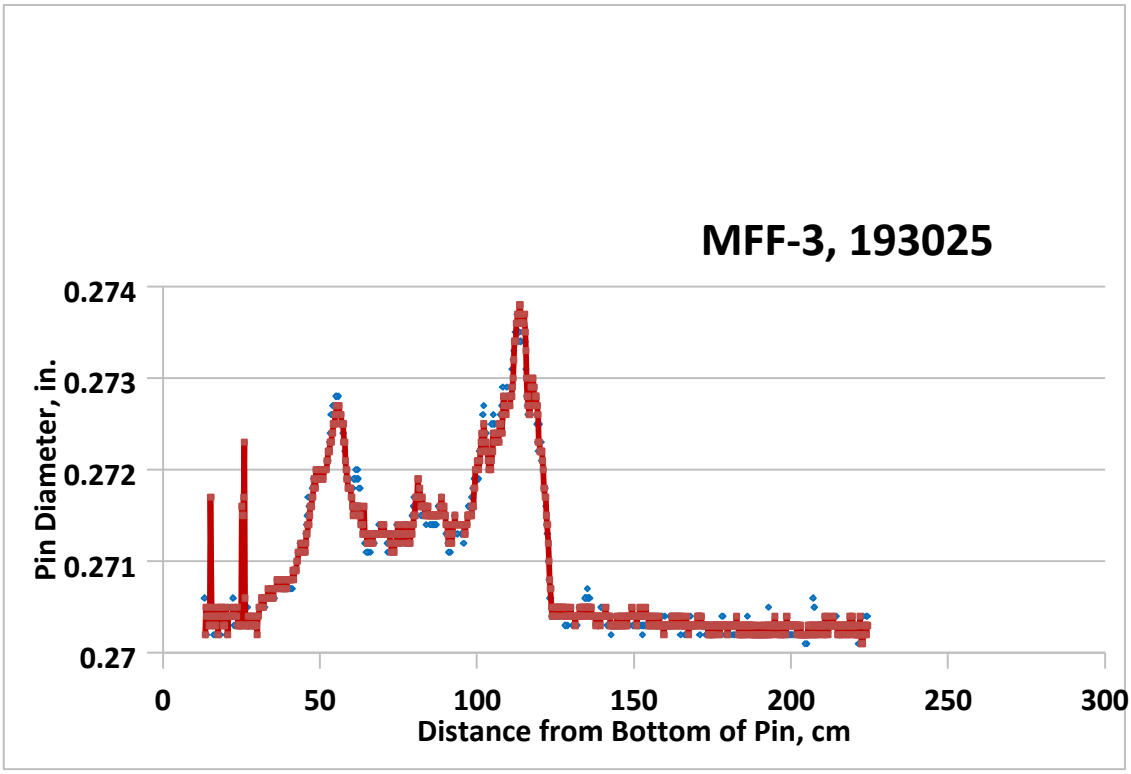


Figure 20. Spiral contact profilometry for MFF-3 Pin 193025.

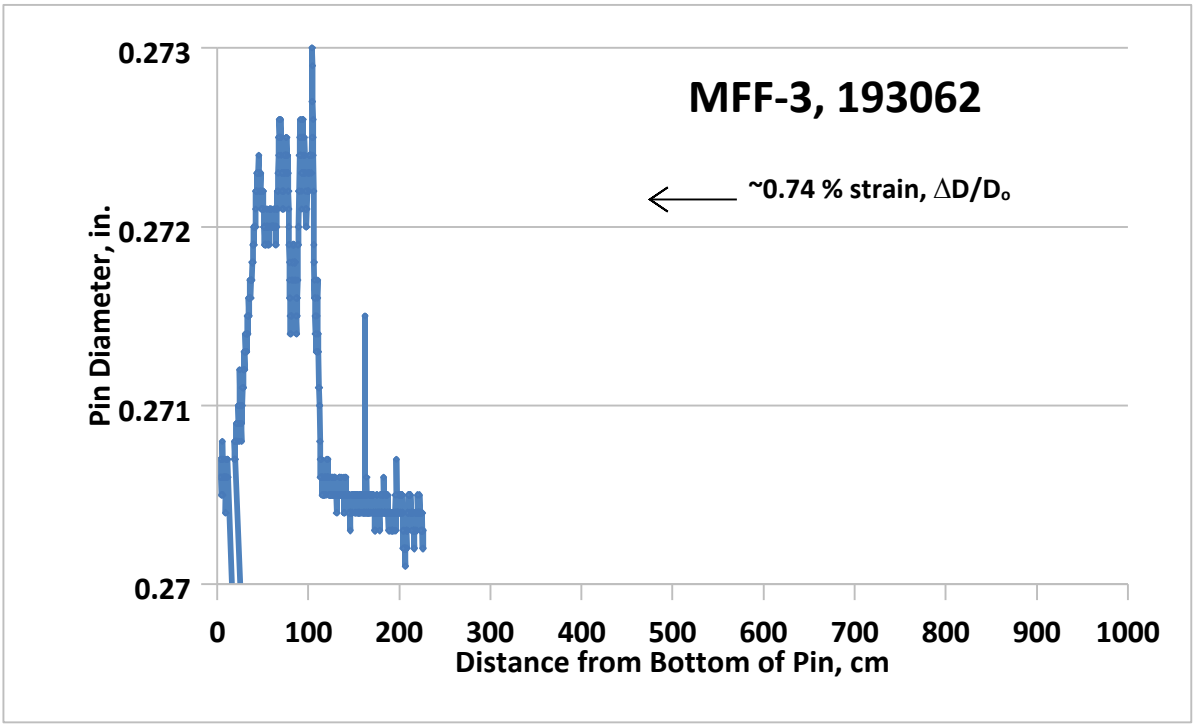


Figure 21. Spiral contact profilometry for MFF-3 Pin 193062.

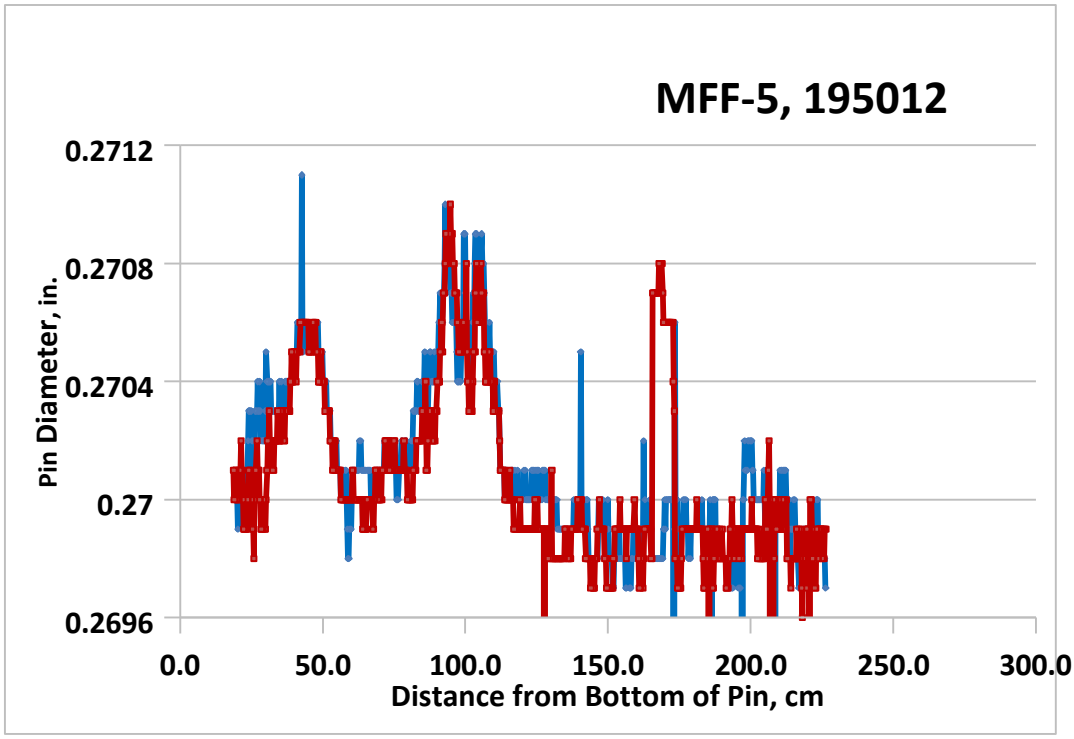


Figure 22. Spiral contact profilometry for MFF-5 Pin 195012.

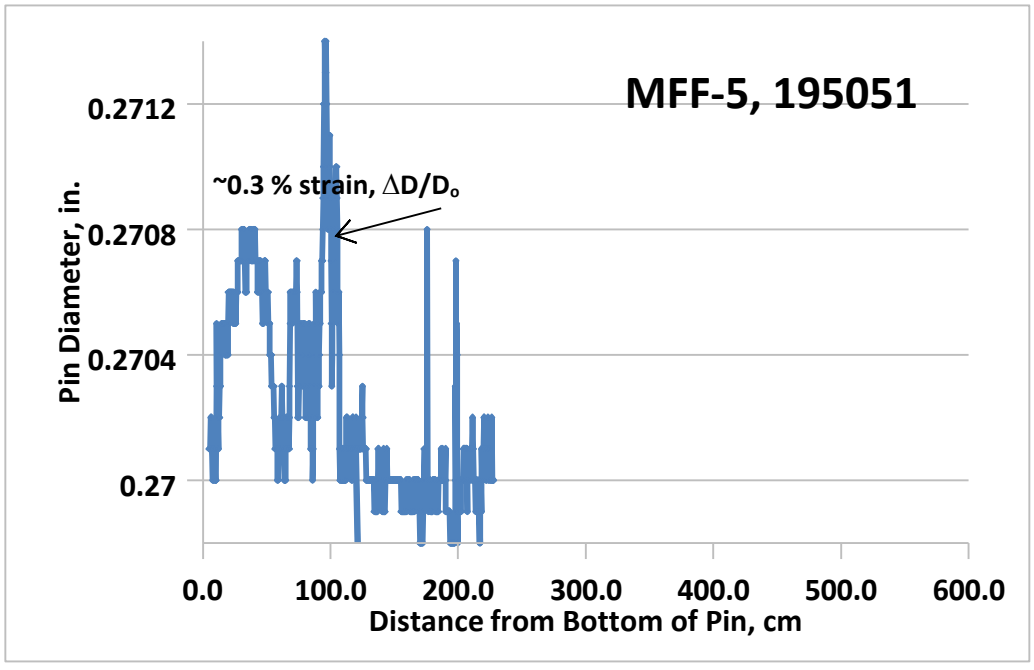


Figure 23. Spiral contact profilometry for MFF-5 Pin 195051.

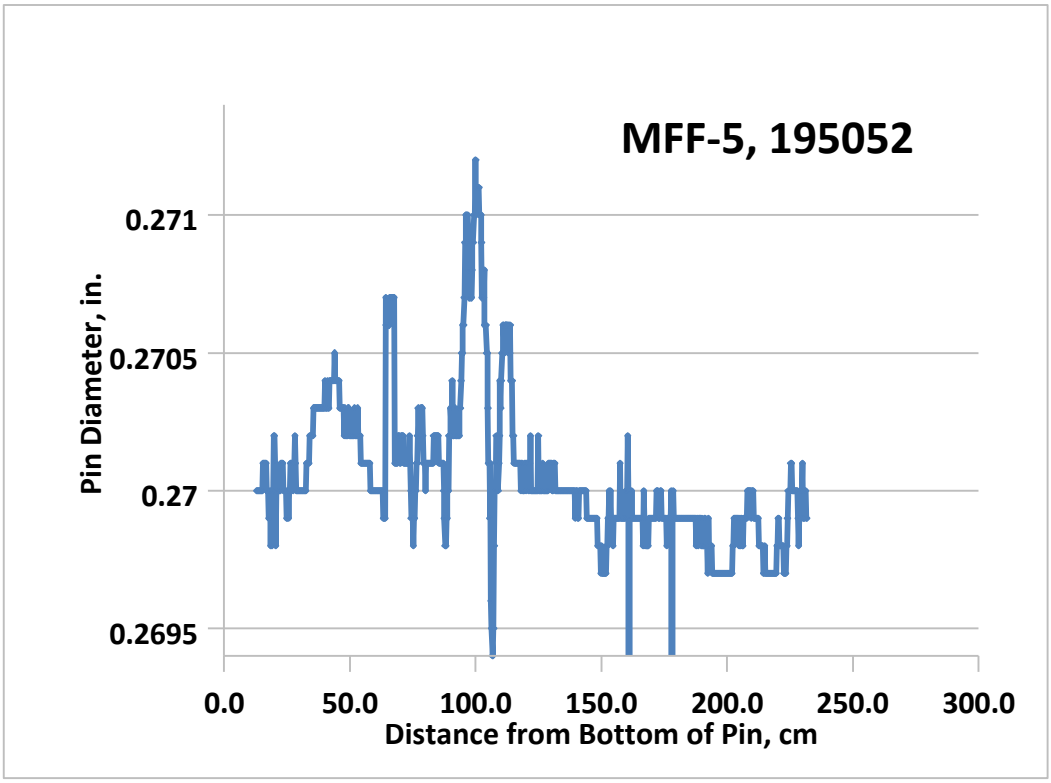


Figure 24. Spiral contact profilometry for MFF-5 Pin 195052.

## 3.5 Element Linear Contact Profilometer (ECP)

The two pins that were to be destructively examined were examined using linear contact profilometry where the pin diameter is measured as a function of axial position. The wire wrap is removed and the pin diameter is recorded as a function of elevation at a constant circumferential location. The pin is then rotated and a profile recorded every 45° until the pin has been rotated 135°. This allows interpretation of bulges to one side, detection of ovality and even relative direction of ovality, showing approximate locations of minor and major elliptical axes.

The scans were taken ~13 cm from the bottom of the pin to ~4 cm from the top. The 13-cm location will be used in the graphical representations of the data as the '0' elevation.

**NOTE:** *For MFF-3, the bottom end plug is 3.4 cm from its tip to where it joins the cladding; the end plug insert into the cladding is 0.64 cm long; the internal axial reflector is 16.5 cm long. For MFF-5, the bottom end plug is 2.9 cm from its tip to where it joins the cladding; the end plug insert into the cladding is 0.64 cm long; the internal axial reflector is 6.4 cm. So, the bottom of the fuel column starts at 7 cm on the MFF-3, 193045 graph, and at -3.1 cm on the MFF-5, 195011 graph.*

Figure 25 and Figure 26 show the linear contact profilometry traces for Pins 193015 (MFF-3) and 195011 (MFF-5), respectively. As stated above the '0' position is actually 1.5 cm from the base of the pin. The entire scans are not shown as the plenum shows little or no strain.

The MFF-3 pin shows peak strain of 1.2-1.3% with a 'double peak' behavior, one peak occurring near core midplane (highest neutron fluence) and one nearing the top of the fuel column (peak cladding temperature). These perhaps represent peaks in irradiation-induced creep and thermal creep. Figure 26 shows that the MFF-5 pin has only about one-third of the diameter strain that the MFF-3 pin demonstrated, the centerline strain even less than that.

Regular undulations are usually an indication of an elliptical cross section. This is sometimes due to handling and sometimes created when the pins expand together and contact along a pinch point where the wire wraps align along a grid, and the cladding is compressed, forming the minor axis of the ellipse on the cladding cross section, usually at places of maximum strain. At 90° the bulge corresponding to the major axis of the ellipse is developed. Therefore, the peaks and valleys align for those 90° apart, and valleys and peaks are aligned. See for example in Figure 25 the red (45°) and green (135°) at ~45 cm elevation. Another place of potential elliptical shape is just into the plenum at ~110 cm elevation.

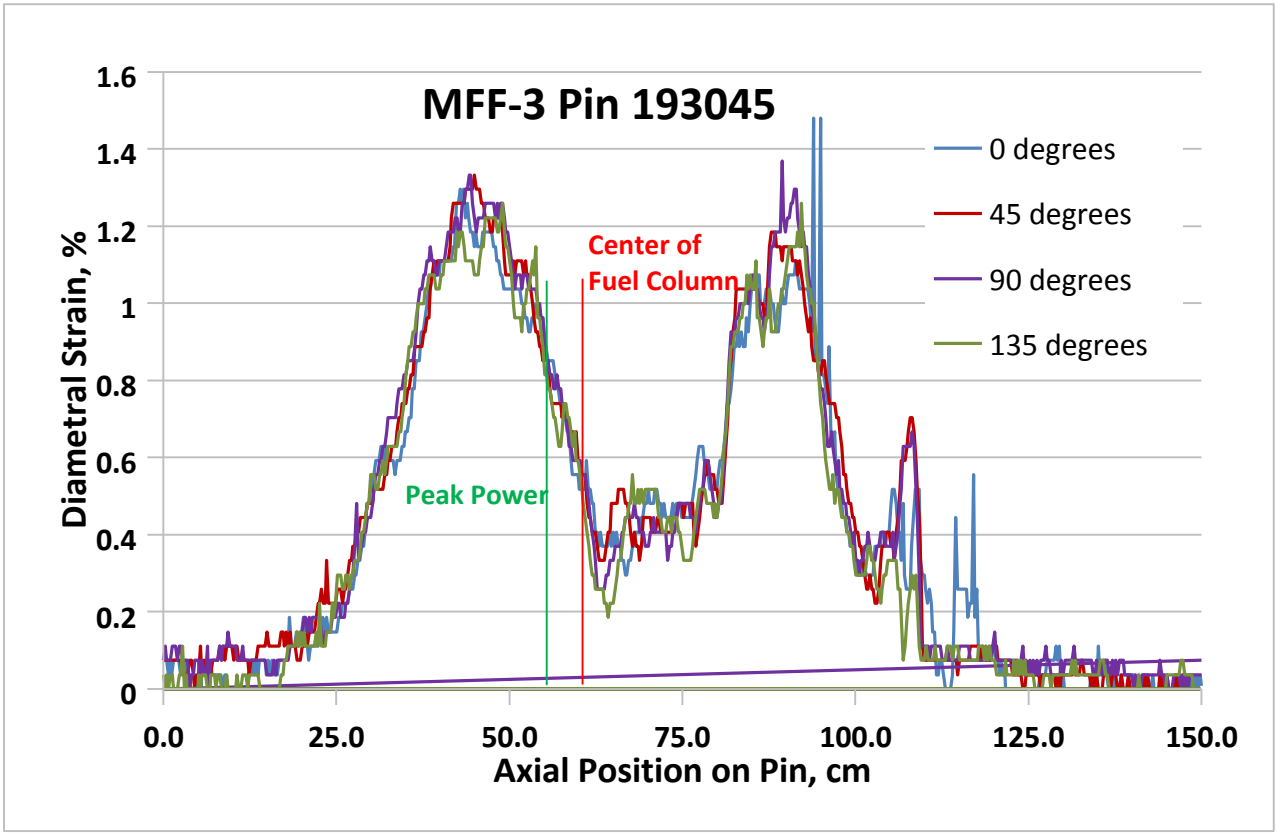


Figure 25. Linear contact profilometry of Pin 193045. Four scans shown as pin is rotated 45°between scans. Much of the plenum is not shown to emphasize the fuel column.

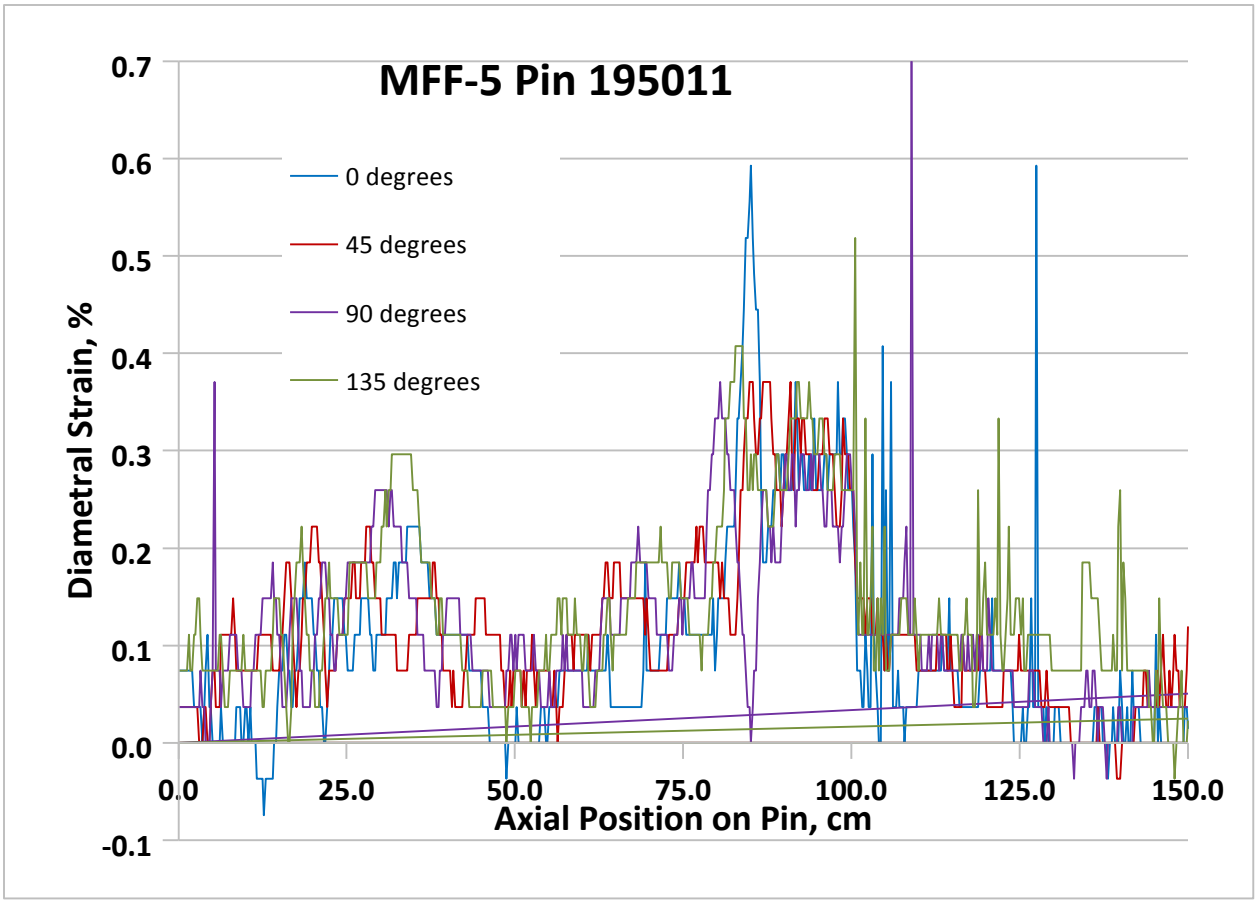


Figure 26. Linear contact profilometry of Pin 195011. Four scans are shown as pin is rotated 45°between scans. Much of the plenum is not shown to emphasize the fuel column.

The fuel pin with fission gas pressure behaves much like a balanced biaxial tension pressure vessel. This means that deviatoric stresses are only found in the radial and circumferential directions. An internal pressure can cause no permanent axial strain (no axial creep). So, fuel pin length changes can only occur by void swelling of the cladding, or if other stresses are introduced. Assuming the former, fuel pin length changes could be used to estimate the amount of swelling involved in the diameter increases just shown.

If the 'hanging' lengths were used (Table 6), then the diameter increase (0.7-1.2%) in the MFF-3 tubing could be explained by swelling if the length change was only spread over the lower area of diameter growth. It is assumed the operating temperature is too high for swelling to occur in the upper diameter peak. The lower peak has a width at half maximum of ~ 20 cm; the smallest pin growth is ~ 0.5 cm or 2.5%. This implies too much swelling. The peak strains in the MFF-5 pins are much less, but the apparent length change is as great for MFF-5 pins. Immersion density measurements on the cladding will be required to assess if any void swelling has occurred.

## 3.6 Plenum Gas Pressure and Composition (GASR Analysis)

The gas assay sample and recharge system (GASR) provides the ability to puncture cylindrical capsules or fuel elements in their plenum regions to measure the free volume and pressure and to gather a sample for gas composition and isotopic analyses. With the sampling head secured to the fuel pin cladding, a laser penetrates the cladding wall under the sampling head. The sampler is positioned on the gas plenum region of the fuel pin and when punctured the fission gas in the plenum is released to the GASR system. It is collected into a known volume and the pressure is measured. This provides a measure

of the total gas in the plenum. A gas sample is taken to measure composition using a gas mass spectrometer. Finally, the fuel pin plenum is backfilled to measure its volume, and this provides a way to calculate the gas pressure that existed in the fuel plenum.

Table 7 provides a predicted amount of fission gas produced during irradiation. It also shows plenum volumes and the pressure and moles of fission gas collected during GASR testing. Based upon these numbers, the final row of the table shows the percentage of gas released. The measured pressure has been corrected to account for the fact that the original was filled with gas at atmospheric pressure; the gas composition was used to provide the best estimate for that correction (92-93% of the gas was Xe+Kr). This changed the release percentage downwards by about 5 percentage points.

Note that the two U-10Zr pins punctured from the IFR-1 experiment showed gas release of 69 and 73%, so in comparison the MFF-3 data looks lower and the MFF-5 looks slightly higher, but in the same range. It appears that a larger data set is required to relate design or operating parameters to gas release.

Table 8 shows the gas composition of two of those pins. Table 9 shows the isotopic ratios of that gas.

Table 7. Fission gas pressure and volume measured for IFR-1 fuel pins.

| Test Number | MFF-3 | MFF-5 |
|---|---|---|
| Pin Number | 193045 | 195011 |
| Fuel Type | U-10Zr | U-10Zr |
| Avg Fission density, $10^{21}/cm^3$ | 4.3 | 3.1 |
| Peak BU (a/o) | 13.8 | 10.1 |
| Avg BU (a/o) | 10.85 | 7.61 |
| Fuel Mass, g * | 281.3 | 281.3 |
| Fuel Volume ($cm^3$) * | 17.8 | 17.8 |
| Moles of HM burned | 0.116 | 0.081 |
| F.G. generated (moles) | 0.0314 | 0.0233 |
| Plenum Pressure (psi) #^ | 296.6 | 253.2 |
| Plenum Volume ($cm^3$) # | 21.7 | 24.8 |
| Moles Gas in plenum | 0.0190 | 0.0184 |
| Fission Gas Release, % | 56 | 74 |

* Design; # measured (GASR ; ^ corrected for original plenum volume.

The plenum volumes used and listed in the table are those measured during the GASR procedure by back-filling the sampled volume. Those design volumes listed in Table 2 are 28.9 $cm^3$ and 31.5 $cm^3$ for MFF-3 and MFF-5, respectively. The smaller measured volumes are to be expected because when the fuel swells it displaces bond sodium in the original annulus between fuel OD and cladding ID. The porosity in the fuel makes up the extra volume.

The porosity in the fuel is either ‘closed’ or ‘open,’ the open porosity can theoretically be connected to the plenum but may contain bond sodium or fission gas. Of course the gas in open porosity, if released during puncturing and creating open plenum volume, would be included in the measured plenum volume and the open volume sampled on refilling, providing an accurate measure of gas release. If gas is trapped in this open porosity then the plenum volume would be underestimated using the measured volume and the amount of released gas underestimated. As a worse case, if the plenum volume were assumed to be

the as-built volume (no closed porosity) then the volumes would be equal to those design volumes listed above and the gas release would be calculated as 75% and 86% for MFF-3 and MFF-5 respectively. This of course would be an overestimate because there is gas trapped in closed porosity. The point is that there may be some small underestimation in calculating the gas release. This correction has never been applied to previous data so for comparisons this should be ignored.

Table 8. Fission gas composition of the MFF-3 and MFF-5 pins punctured for analysis.

| Assembly/Pin No.: | MFF-3/193045 | MFF-5/195011 |
|---|---|---|
| Gas Composition | Mol% | |
| Hydrogen | 0.02 | 0.03 |
| Helium | 7.54 | 6.60 |
| Nitrogen | 0.01 | 0.01 |
| Oxygen | 0.00 | 0.00 |
| Argon | 0.04 | 0.04 |
| Carbon dioxide | 0.02 | 0.04 |
| Krypton | 13.10 | 13.10 |
| Xenon | 78.90 | 79.90 |

Table 9. Isotopic ratios of the fission gas of the MFF-3 and MFF-5 fuel pins.

| Pin Number: | | 193045 | 195011 |
|---|---|---|---|
| Element | Isotope Ratio | | |
| Xenon | 124/132 | 0.001 | 0.002 |
| | 126/132 | 0.001 | 0.001 |
| | 128/132 | 0.004 | 0.005 |
| | 129/132 | 0.014 | 0.017 |
| | 130/132 | 0.005 | 0.007 |
| | 131/132 | 0.658 | 0.632 |
| | 134/132 | 1.631 | 1.601 |
| | 136/132 | 1.334 | 1.311 |
| Krypton | 78/84 | 0.002 | 0.015 |
| | 80/84 | 0.006 | 0.004 |
| | 82/84 | 0.020 | 0.014 |
| | 83/84 | 0.510 | 0.512 |
| | 85/84 | 0.066 | 0.064 |
| | 86/84 | 1.723 | 1.764 |

## 3.7 Optical Metallography

The two pins selected for destructive examination were sectioned according to the diagram shown in

Figure 27. Rough section cuts were indexed to the bottom of the fuel pin (tip of spade) and are dimensioned in inches in the drawings. The detailed section cuts were referenced from the bottom of the fuel pin or from the bottom of the lower rough cut.

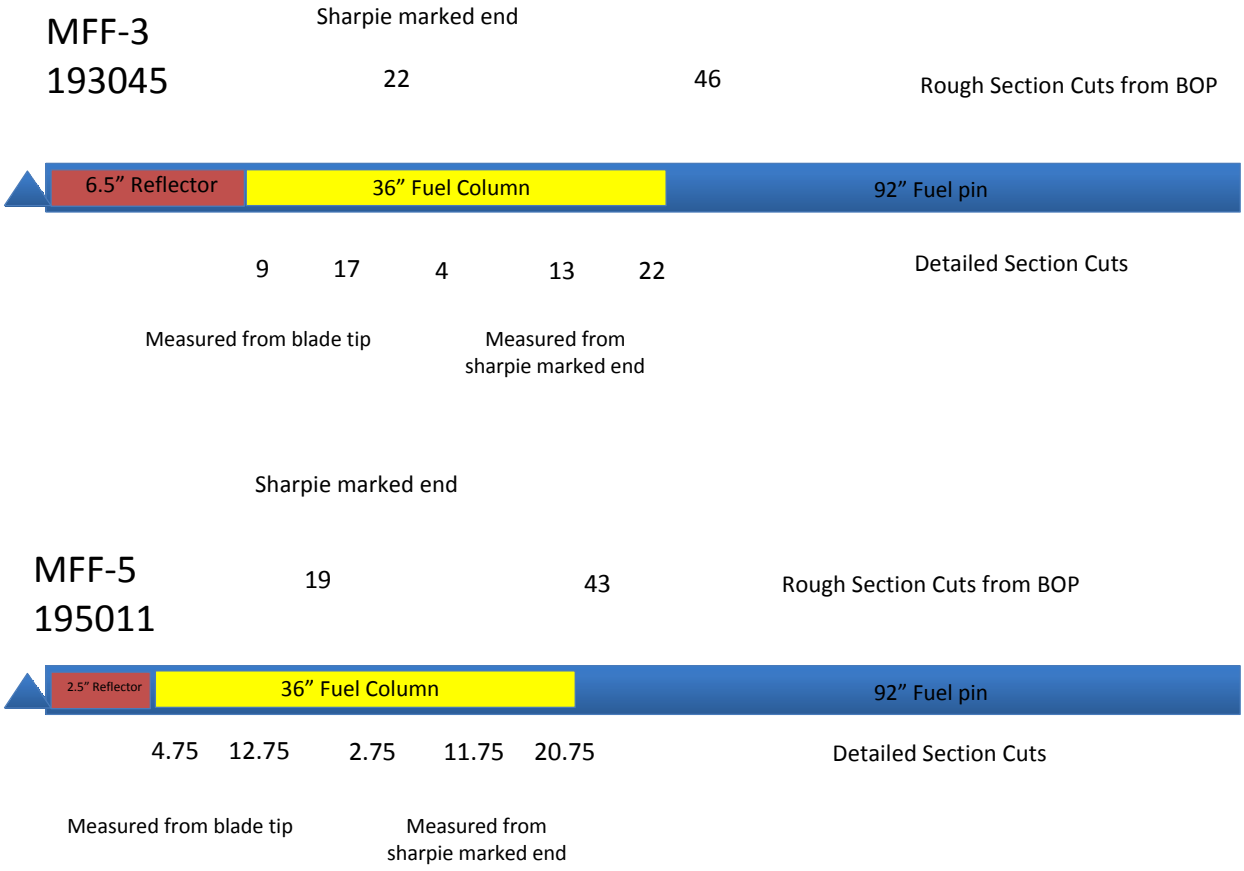


Figure 27. Sectioning diagram for Pins 193045 and 195011. The detailed cuts show where metallography and burnup samples were taken. Location dimensions are in inches.

The cuts resulted in samples for metallography and chemistry being taken at X/L (of the fuel column) 0.03, 0.25, 0.48, 0.74 and 0.98 for Pin 193045 and 0.03, 0.24, 0.48, 0.72 and 0.96 for Pin 195011. For simplicity we will compare like sections here and call them X/L = 0.0, 0.25, 0.5, 0.75 and 1.0. Figure 28 and Figure 29 show the relative positions of each section on the MFF-3 and MFF-5 pins along with the time averaged operating conditions.

Table 10 and Table 11 also show the fuel operating conditions.

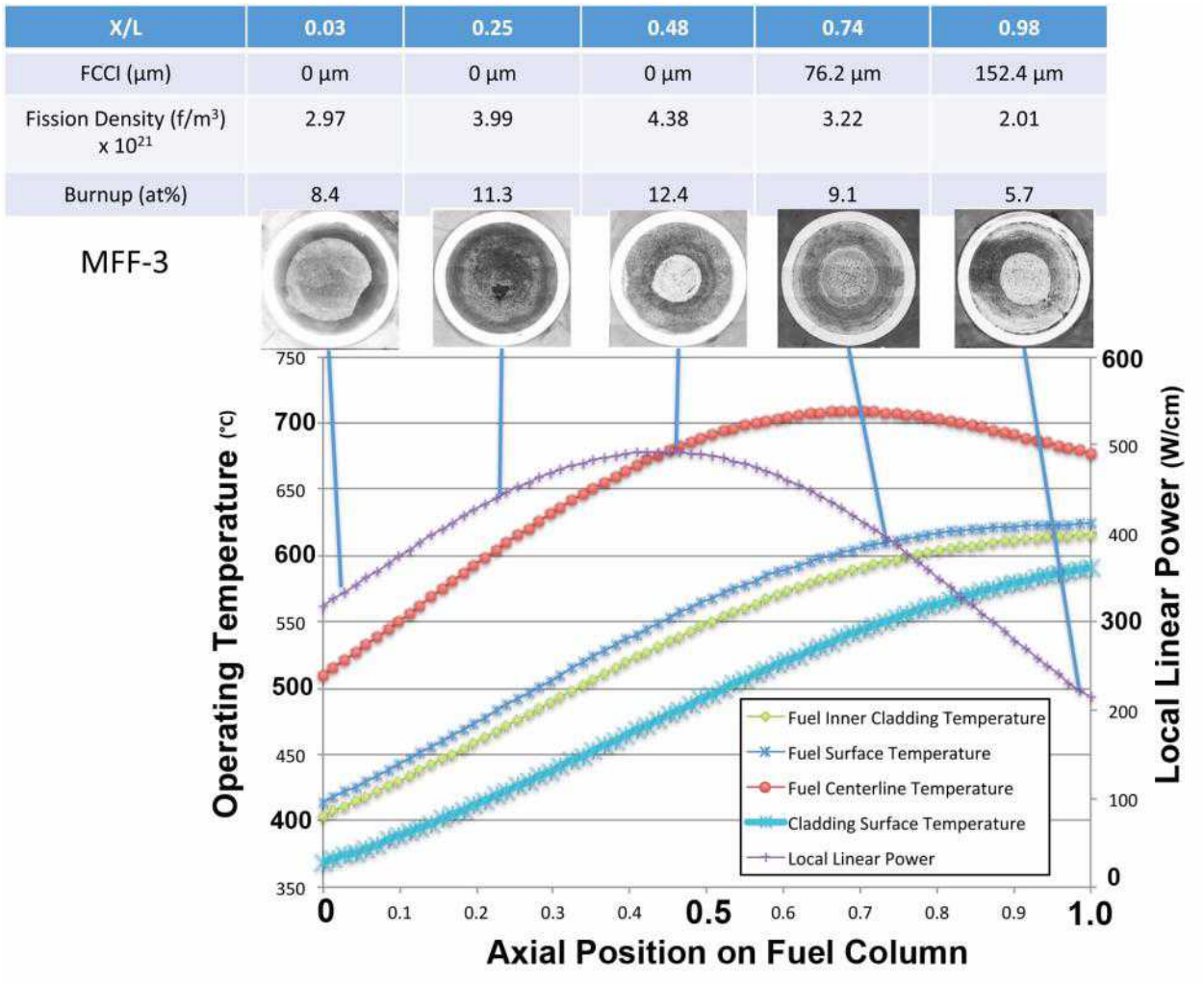


Figure 28. Metallography summary for MFF-3 Pin 193045 showing axial location and operating conditions. Operating conditions are time averaged.

| X/L | 0.03 | 0.24 | 0.48 | 0.72 | 0.96 |
|---|---|---|---|---|---|
| FCCI (µm) | 0 µm | 0 µm | 0 µm | 50.8 | 25.4 |
| sion Density (f/m$^3$) x 10$^{21}$ | 2.37 | 3.15 | 3.46 | 2.86 | 1.70 |
| Burnup (at%) | 6.7 | 8.9 | 9.8 | 8.1 | 4.8 |

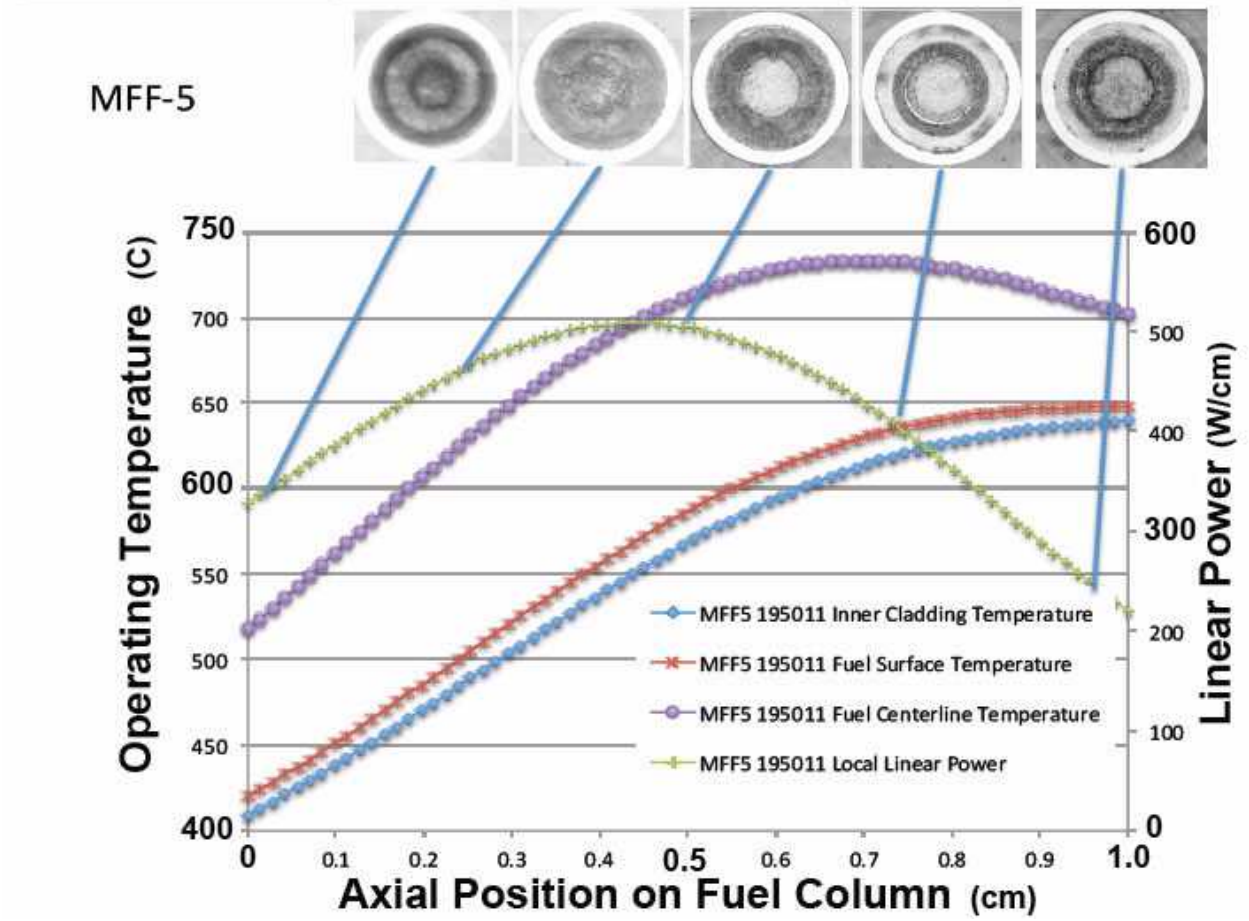


Figure 29. Metallography summary for MFF-5 Pin 195011 showing axial location and operating conditions. Operating conditions are time averaged.

Table 10. MFF-3 (193045) metallographic section operating conditions.

| Axial Location (X/L) | Peak Linear Power (W/cm) | Time Averaged Peak Cladding T (°C) | Time Averaged Peak Fuel Centerline T (°C) | HM Burnup (at.%) |
|---|---|---|---|---|
| 0.03 | 334 | 413 | 527 | 8.5 |
| 0.24 | 446 | 475 | 619 | 11.3 |
| 0.48 | 489 | 550 | 700 | 12.4 |
| 0.72 | 359 | 604 | 712 | 9.1 |
| 0.96 | 223 | 615 | 682 | 5.7 |

Table 11. MFF-5 (195011) metallographic section operating conditions.

| Axial Location (X/L) | Peak Linear Power (W/cm) | Time Averaged Peak Cladding T (°C) | Time Averaged Peak Fuel Centerline T (°C) | HM Burnup (at.%) |
|---|---|---|---|---|
| 0.03 | 345 | 414 | 532 | 6.7 |
| 0.24 | 461 | 480 | 628 | 8.9 |
| 0.48 | 507 | 556 | 712 | 9.8 |
| 0.72 | 417 | 612 | 738 | 8.1 |
| 0.96 | 249 | 635 | 709 | 4.8 |

## 3.7.1 MFF-3 Metallography

### *3.7.1.1 X/L = 0.03*

The X/L = 0 is the position at the bottom of the active fuel column, where the active fuel column and the lower Inconel reflector meet. The metallographic cross-section at X/L = 0.03 is taken just above this in the fuel. It represents the location with the lowest operating temperatures sectioned just above this in the fuel. It is the position that operates at the lowest temperatures.

Figure 30 shows a metallographic cross-section of MFF-3 Pin193045 taken at the 0.03 X/L location (2.7 cm up from the bottom of the fuel column). Three are some voids/fission gas bubbles apparent in the central region of the fuel and the large dark areas next to the cladding are void space created by fuel pull-out during the metallographic preparation process. The fuel would be swollen radially enough to contact the cladding but at the low cladding temperatures may not have been bonded to the cladding through FCCI.

There is no evidence of radial zone appearance; none would have been expected. The light dots may be second-phase precipitates (silicides, oxides, carbides) often seen is as-cast fuel and likely very stable in the irradiated fuel, or debris from polishing. This photo was ‘stitched’ together from a number of smaller photos to provide a high-resolution image across the entire surface.

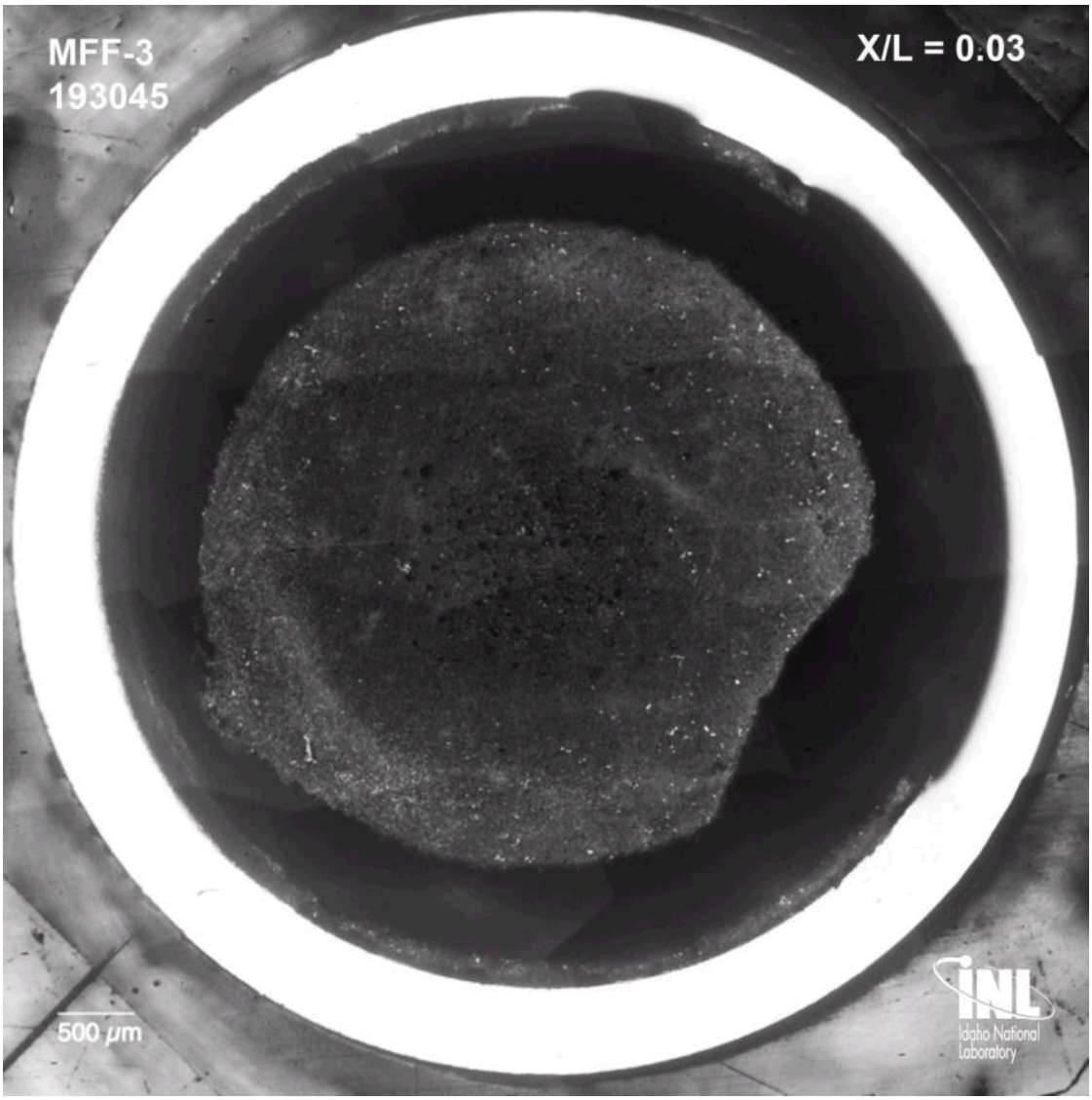


Figure 30. Metallographic section of MFF-3 Pin 193045 at the X/L = 0.03 axial location.

#### *3.7.1.2 X/L = 0.25*

The section at 0.25 X/L is also not complicated. Voids/gas bubbles are evident in the photograph (Figure 31). The large dark area near the center is just a fuel pull-out area created during the metallographic preparation process. Likewise, the best interpretation for the dark areas around the exterior of the fuel, next to the inside surface of the cladding, is also pull-out. The fuel is fully swollen out to the cladding at this level of burnup (11.3 at.%). The small, aligned dots at some locations on the cladding are indent marks from the hardness testing. The results of this are discussed subsequently in this report. Again there is no evidence of radial zones in the appearance of this section.

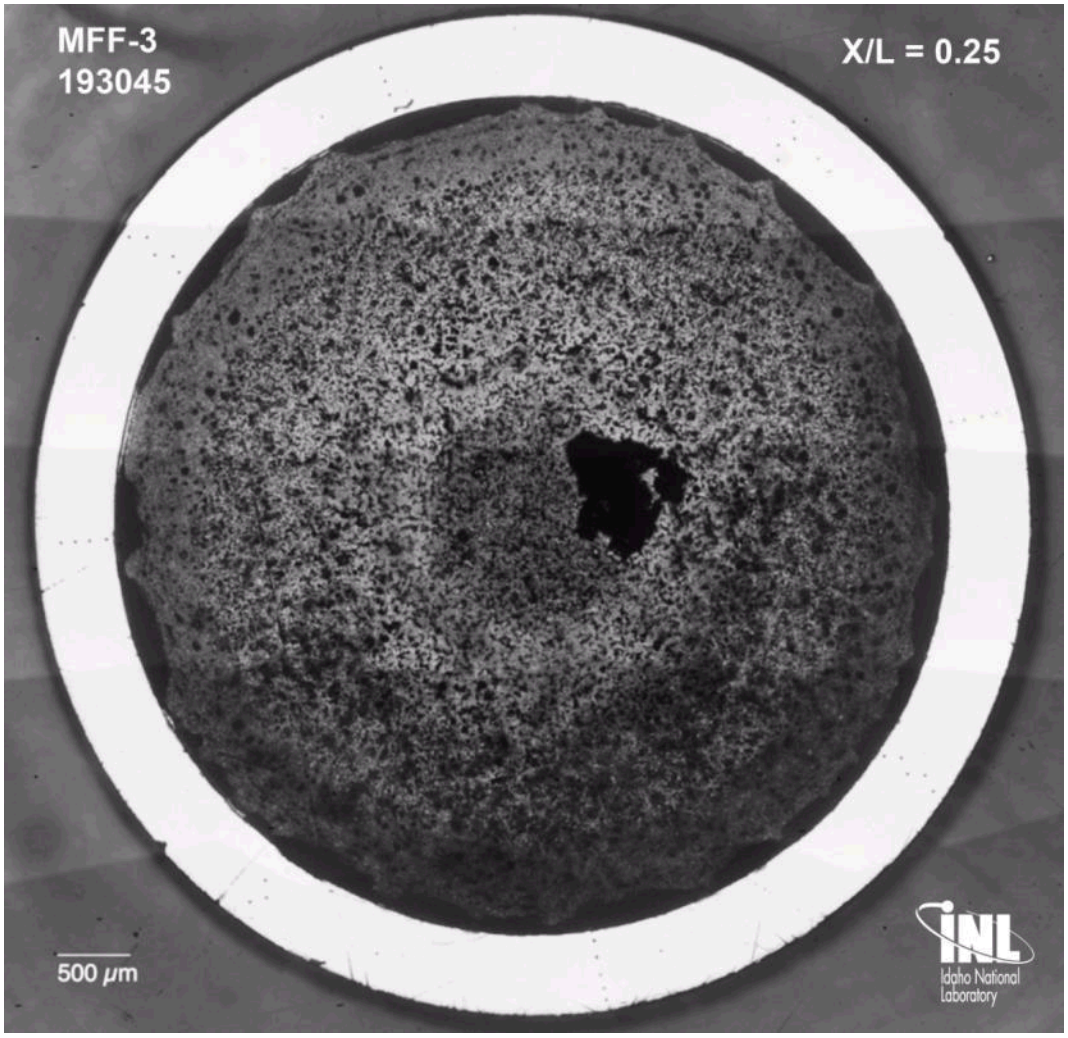


Figure 31. Metallographic section of MFF-3 Pin 193045 at the X/L = 0.24 axial location.

#### *3.7.1.3 X/L = 0.49*

The X/L location of 0.49 shows the first evidence of radial zones. These are formed at points where radially phase fields are crossed thermally (during fuel operation). It requires crossing into the β+γ phase field, which exists according to stable phase equilibria at T ≥662°C, in approaching the fuel center.[14] A portion of the U-Zr phase diagram taken from Reference 14 is shown in Figure 32 to help with the explanation. Hofman et al.'s model[14] is built around a three-zone model. All three might be present in some of the images from hotter regions (axial) of the fuel but are not obvious – a two-zone structure is more plausible. In the three-zone model the central zone is the γ or $\gamma_1 + \gamma_2$ phase field. Zr is rejected from the β+γ phase field into the central zone. In their model, ostensibly because of slow diffusion in the α+δ phase field zone, there is no Zr migration out of the outer, α+δ radial zone. The first boundary, approaching the center from the cladding, is the α+δ/β+γ phase field boundary. In Figure 33 the boundary between the dark and light colored area would therefore represent the boundary at 662°C. To form the third, inner zone a fuel temperature regime >692°C is required.

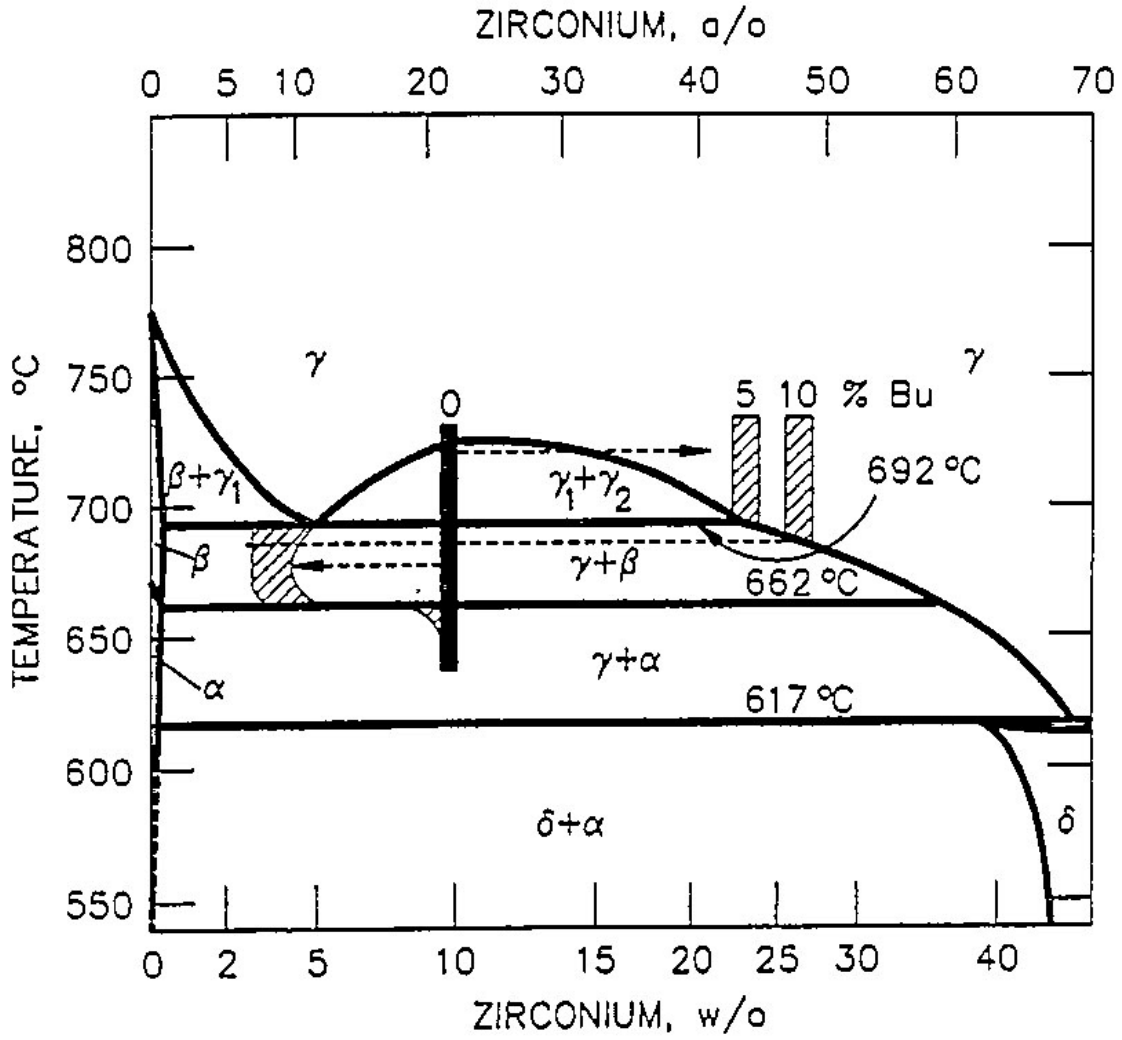


Figure 32. Portion of the U-Zr phase diagram important to U-Zr zone formation (from Ref. 13).

In this case the image appears to represent only the two cooler zones which would indicate that Zr has migrated out of the β+γ phase field in the center of the fuel pin to the α+δ phase field outer zone. The δ, or $UZr_2$ phase is not thermodynamically modeled in their paper and perhaps the phase is relatively stable, compared to the γ phase, and that as the Zr migrates to the cooler zone further $UZr_2$ is precipitated. The two-zone structure has frequently been observed in U-Pu-Zr fuels.[15] Of course further analysis, such as by electron microprobe (EPMA), would be required to show the Zr concentration profile, to prove that Zr has migrated radially outward, or to uncover the presence of a third, central zone.

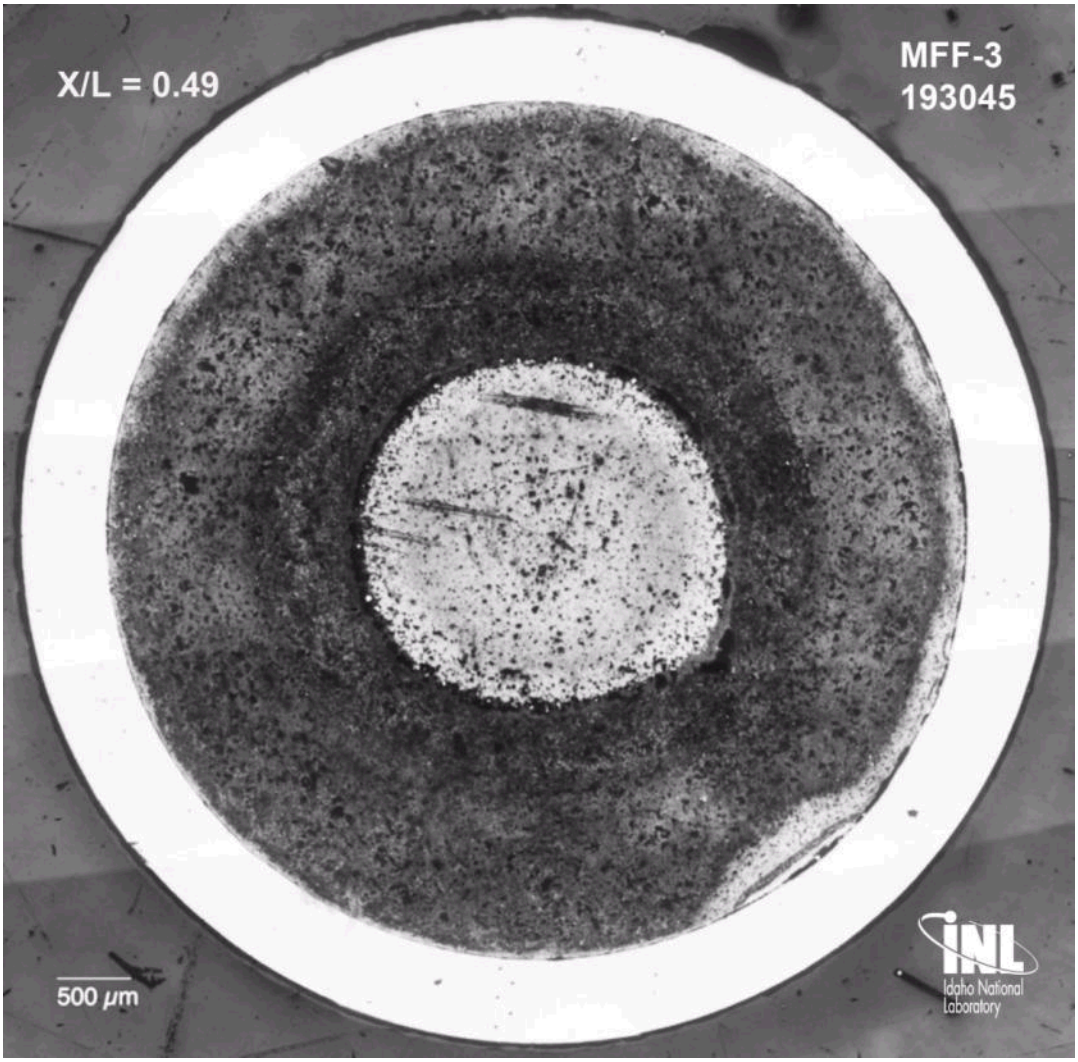


Figure 33. Metallographic section of MFF-3 Pin 193045 at the X/L = 0.49 axial location.

#### *3.7.1.4 X/L = 0.74*

Note that the central volume is largest at this location. Testing the assumption that this fits the β+γ phase field (T >662°C) the time-averaged fuel centerline temperature (Figure 10) would predict that this metallographic section would have the largest central zone. The image perhaps indicates a third zone in the center where the gas bubbles are larger, but again EPMA may be required to prove its presence. Also, there may have been a third zone when the fuel was swelling early in life, but as the fuel cooled due to U depletion it reverted to γ+β.

There is evidence of fuel/cladding interaction (see light-colored areas in the fuel at the top, 12 o'clock position); most of the interaction area is in the fuel where cladding components (especially Fe) have diffused into the fuel. There is some cladding thickness reduction in those areas. This FCCI is very non-uniform around the circumference of the fuel, as is usually observed in this fuel/cladding combination. The typical FCCI zone formed in the cladding by rare earth fission products diffusing into the cladding is not apparent in Figure 34.

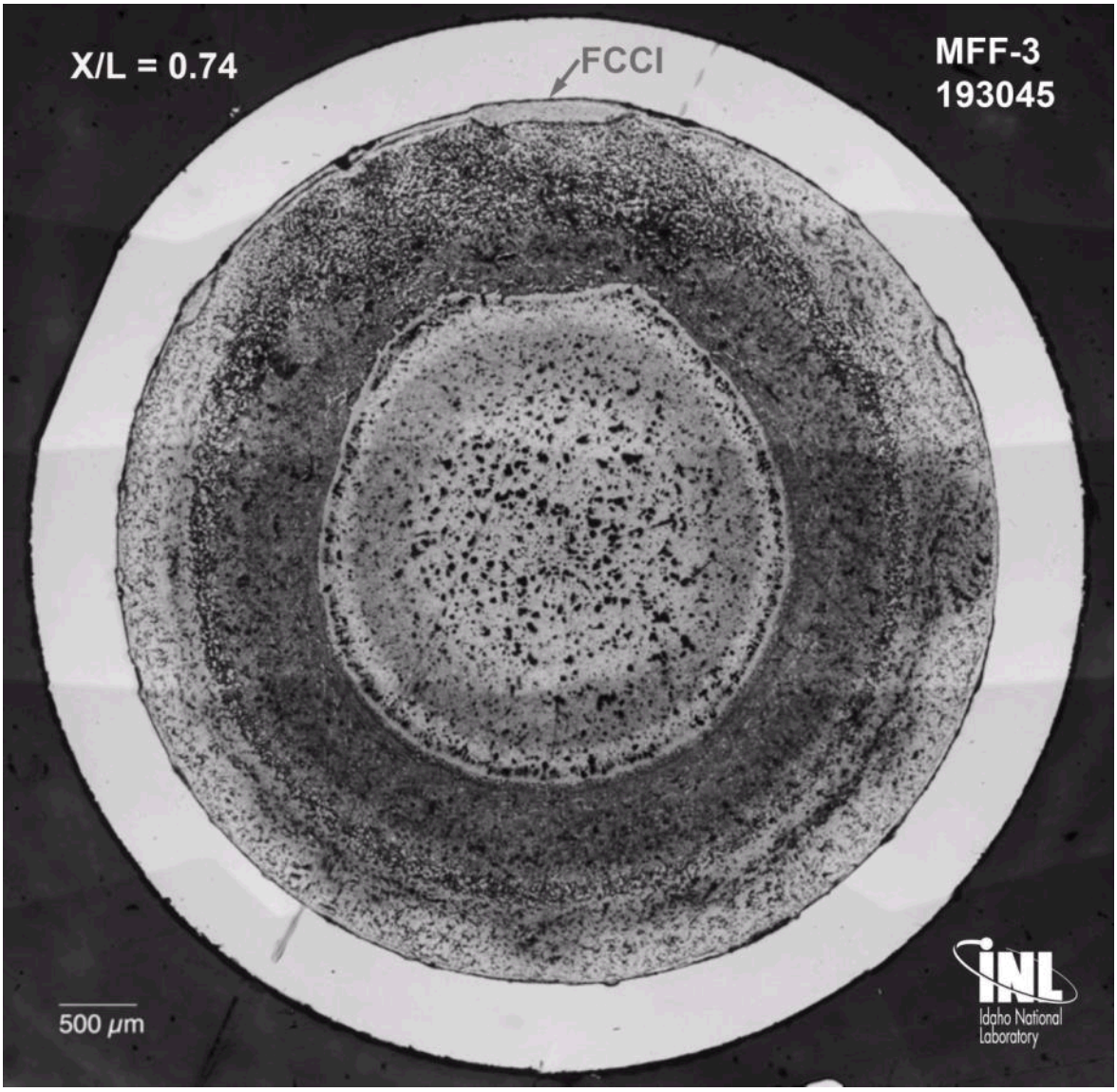


Figure 34. Metallographic section of MFF-3 Pin 193045 at the X/L = 0.74 axial location.

#### *3.7.1.5 X/L = 0.98*

The overall appearance, as shown in Figure 35, is that of a two-zone structure. The light-colored central volume therefore represents one that operated in the β+γ phase field which exists according to stable phase equilibria at T >662°C. The time-averaged fuel centerline temperature at this elevation see (Figure 10) is above 662°C. Compared to the 0.74 X/L location the fuel temperatures here are lower and hence the smaller central volume.

Figure 10 would predict that the fuel center be about the same temperature (averaged) as the X/L = 0.49 location but at lower power, so the temperature gradient is not as large from the center to the outside surface at X/L = 0.98. Hence a slightly larger central zone may be expected and this zone does appear slightly larger than that in Figure 33.

The fuel/cladding interaction was measured to be largest in this location, and does appear to be far more uniform around the circumference than at the other location. There is some staining on the surface of the cladding which should be ignored.

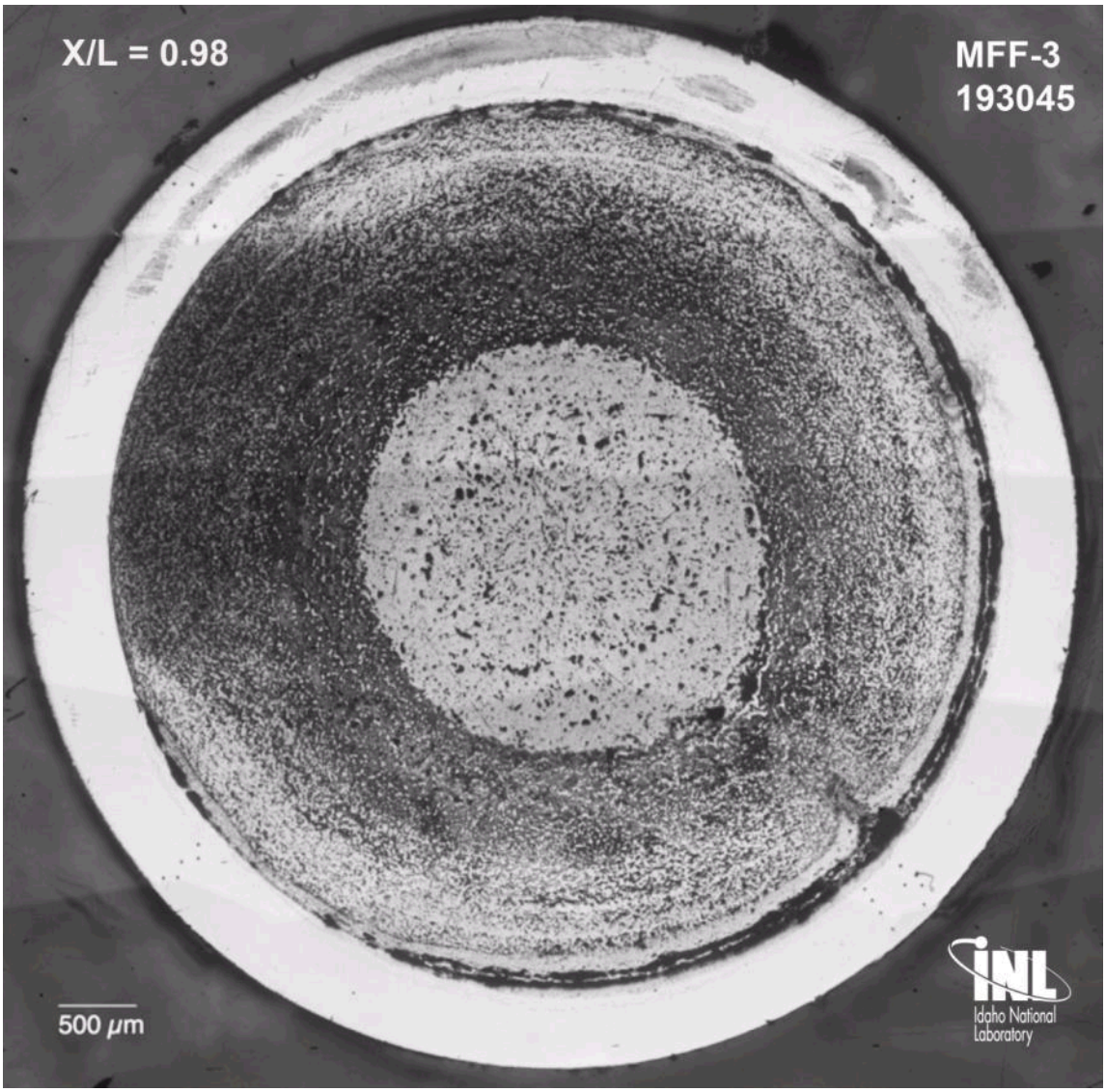


Figure 35. Metallographic section of MFF-3 Pin 193045 at the X/L = 0.98 axial location.

An enlargement of a portion of the image shown in Figure 35 is shown in Figure 36. It shows the FCCI region of maximum depth. This layer has the appearance of a typical FCCI zone where rare earth fission products have diffused into the cladding.[16]

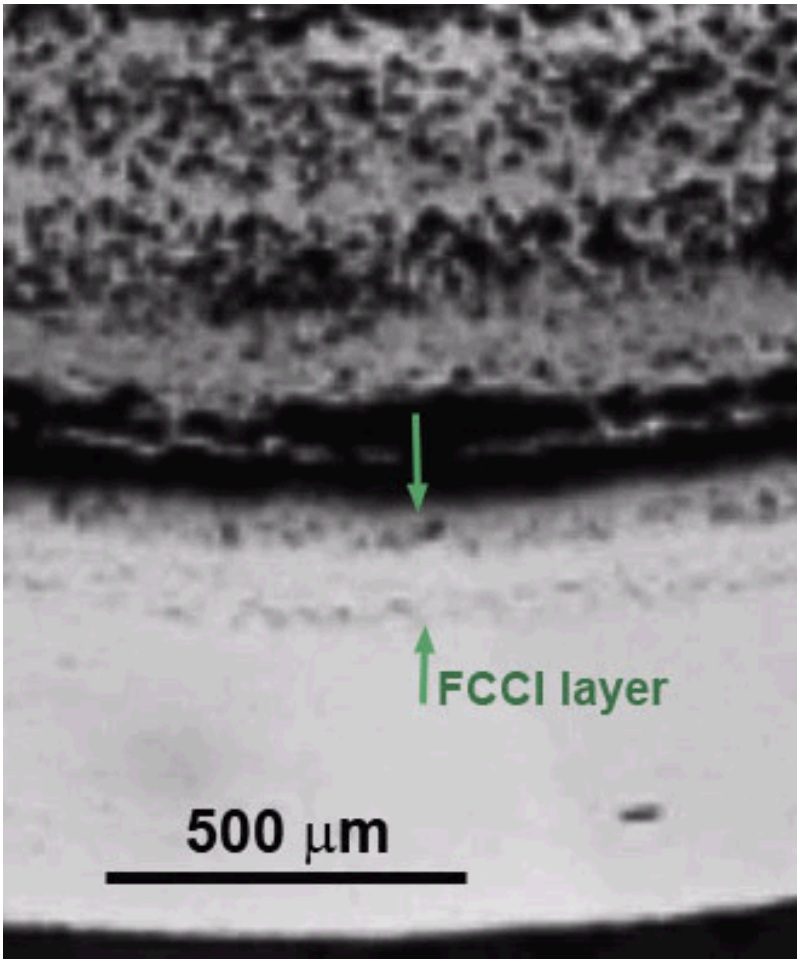


Figure 36. Area of fuel/cladding chemical interaction (FCCI) in the X/L = 0.98 cross-section of Pin 193045.

### 3.7.2 MFF-5 Metallography

The following images show as-polished cross-sections of MFF-5 Pin 195011. Operating conditions of the fuel pin at these locations were given in Table 11.

#### *3.7.2.1 X/L = 0.03*

Figure 37 shows the same appearance as the lower section of the MFF-3 pin, including a large fraction of fuel pull-out near the outer diameter of the fuel slug. It shows no evidence of zone formation as would be expected by its operating temperatures, nor does it show any evidence of FCCI.

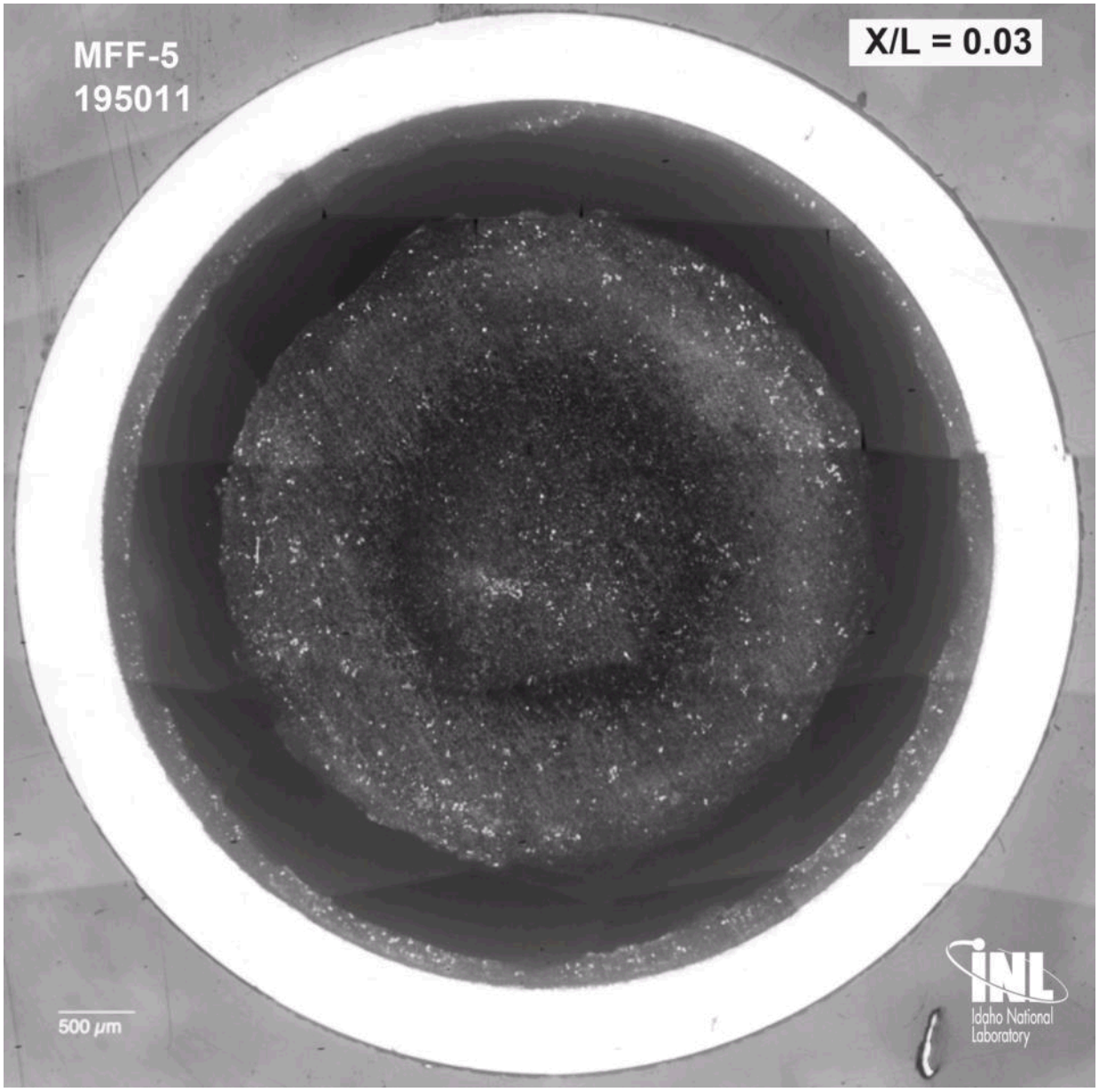


Figure 37. Metallographic section of MFF-5 Pin 195011 at the X/L = 0.03 axial location.

#### *3.7.2.2 X/L = 0.24*

As with the previous section at X/L = 0.03 this section at X/L/ = 0.24, Figure 38, looks to have the same features as that of the MFF-3 pin at X/L/ = 0.25. There is no zone formation or obvious FCCI.

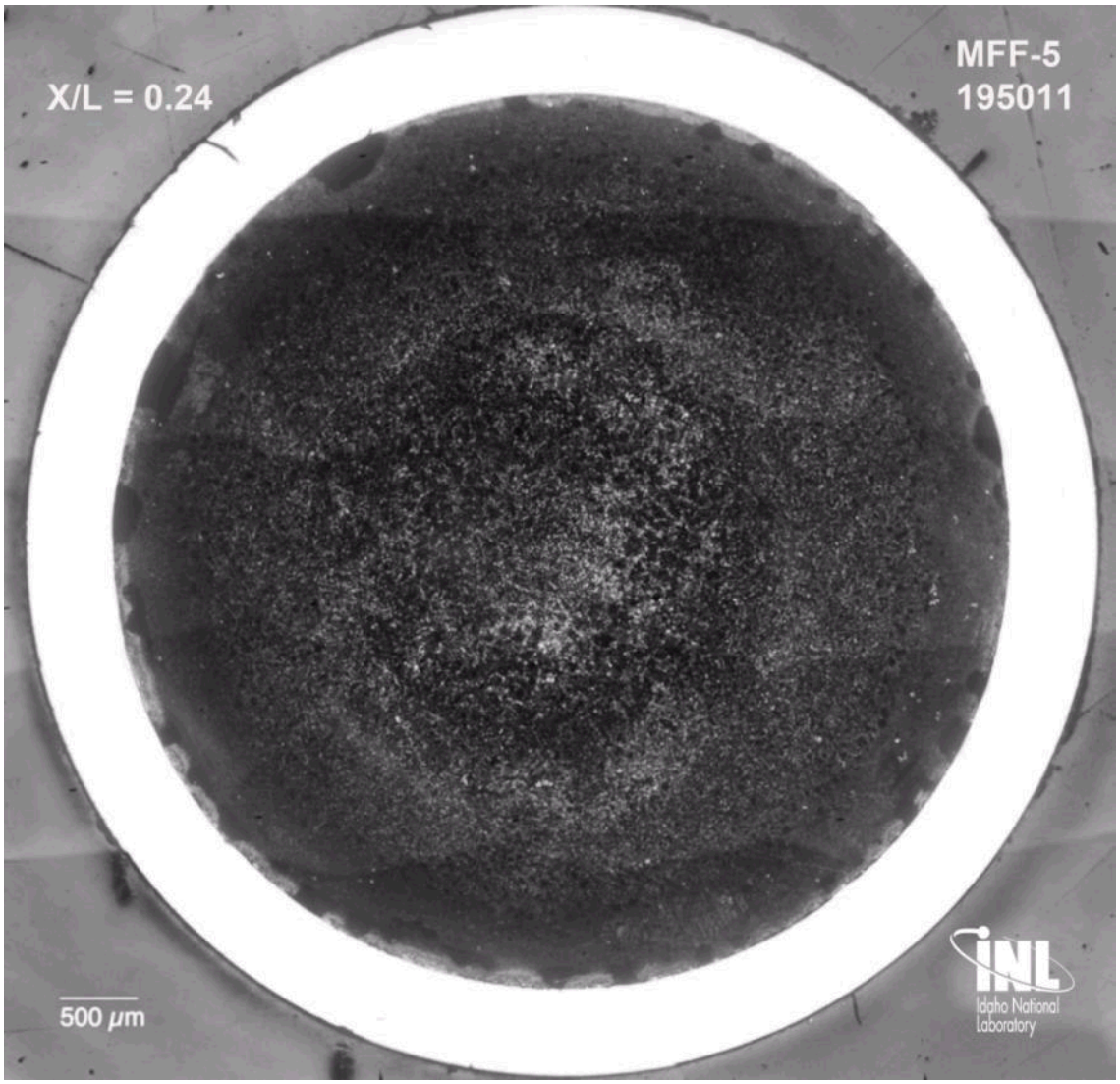


Figure 38. Metallographic section of MFF-5 Pin 195011 at the X/L = 0.24 axial location.

#### *3.7.2.3 X/L = 0.48*

Figure 39 shows the polished section at X/L = 0.48. It displays a typical two-zone structure. There are areas around the circumference of the cladding inner diameter that indicate that there may be some fuel/cladding chemical interaction. The apparent FCCI however may be artifacts from polishing. The as-polished surface appearances are discussed here. In the subsequent section of this report (Cladding Metallography and FCCI) the appearance of the etched cladding, cladding microhardness results, and depth of FCCI are discussed.

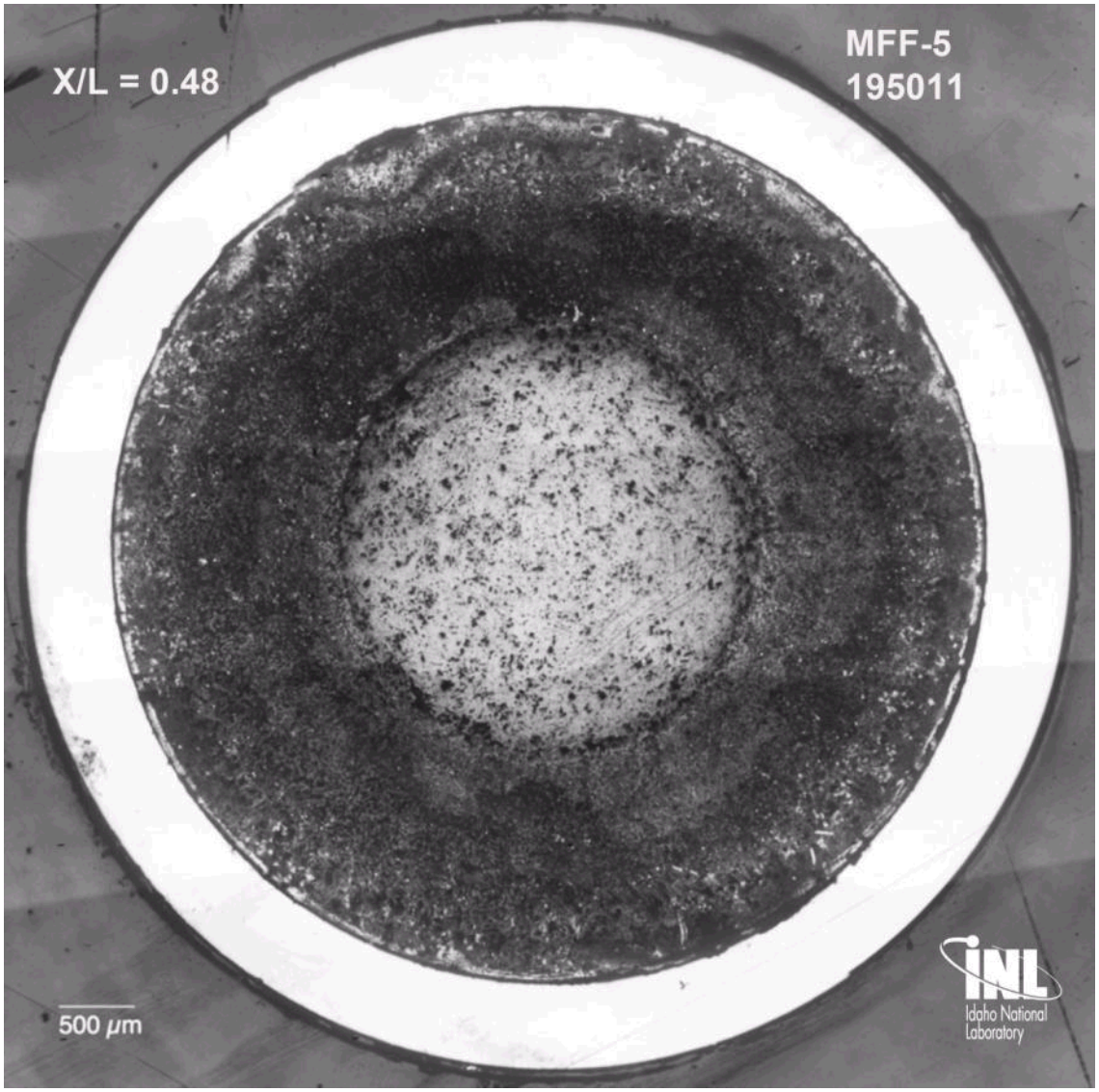

Figure 39. Metallographic section of MFF-5 Pin 195011 at the X/L = 0.48 axial location.

#### *3.7.2.4 X/L = 0.72*

The metallographic section of pin 195011 at X/L = 0.72 shows the first indications of the three-zone structure (Figure 40). This would imply that the Zr concentration in the outer zone had changed very little, perhaps increasing slightly, the banding at mid-radius representing the second zone would be very reduced in Zr concentration, and the central zone enriched in Zr. The mid-radius zone however usually polishes very well and appears lighter in color; it appears dark in color here. Near end of life the operating temperature of the fuel center may have reduced enough so that it was operating less than 692°C, or whatever the non-equilibrium temperature is representing the [β+γ]-to-[ $\gamma_1+\gamma_2$] phase field boundary.

One question is why the MFF-5 pin may have shown a three-zone structure when the MFF-3 pin did not. The MFF-5 assembly did not operate to as high a burnup as MFF-3, resulting in a significantly higher operating temperature when time averaged. Figure 28 and Figure 29 show these values. The latter stages of MFF-3 Pin 193045 operation had considerably lower fuel temperatures due to the fissile depletion. Note that Pin 193045 had latter stage (last three cycles) peak linear power of about 350 W/cm while MFF-5 Pin 195011 ranges from 385 W/cm to 415 W/cm.

A comparison of Table 10 with Table 11 also shows the operating temperature differences on average. The fact that the average and end-of-life fuel centerline temperatures are expected to have been higher in MFF-5 means that microstructures may reflect this, reflecting a significant central zone operating for an extended time at T > 692°C. As the U was depleted and the pin power diminished, the mid-radius zone retreated towards the center and eventually consumed it, leaving gas bubble morphologies reminiscent of the previous zone structure.

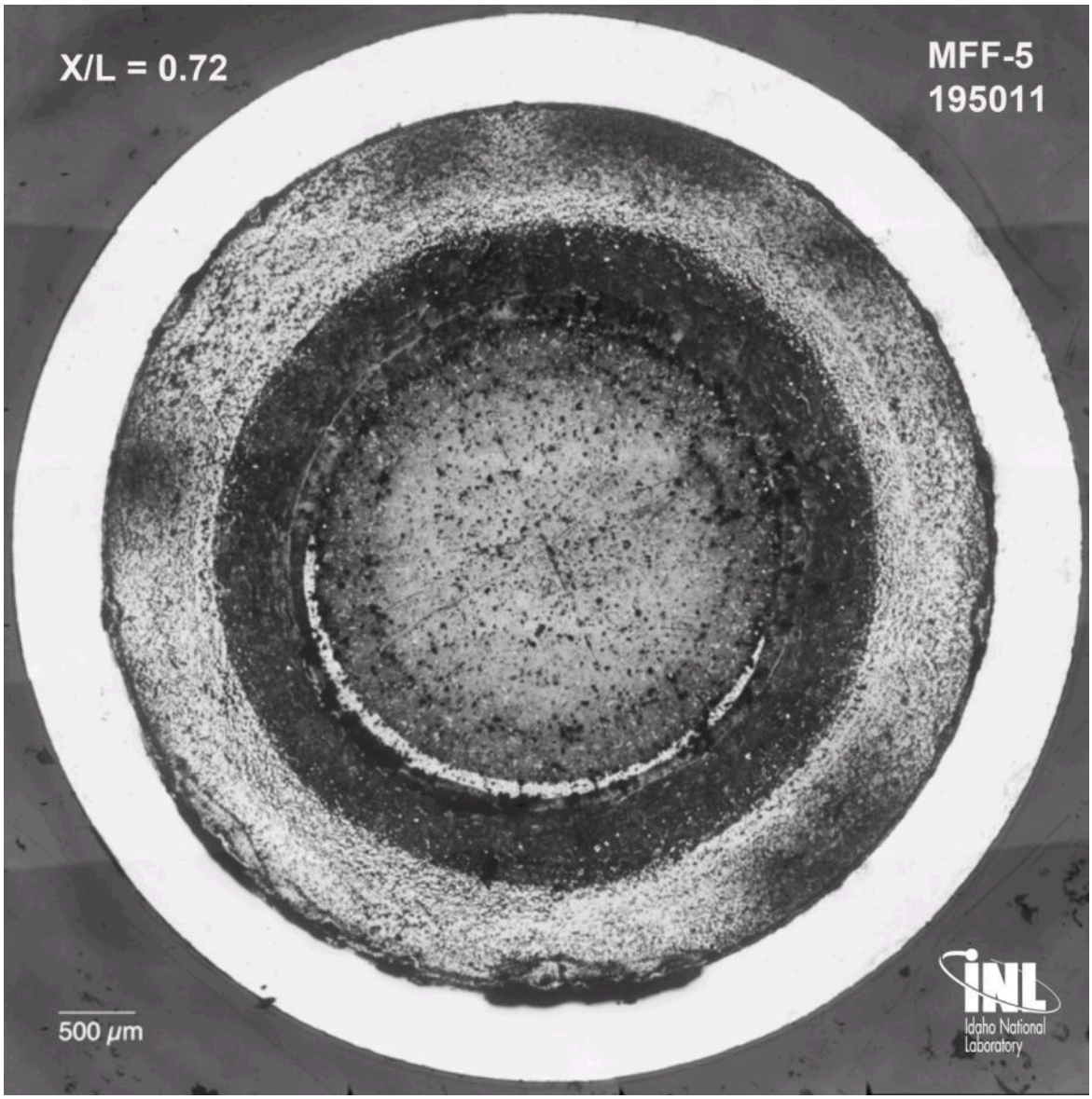


Figure 40. Metallographic section of MFF-5 Pin 195011 at the X/L = 0.74 axial location.

#### *3.7.2.5 X/L = 0.96*

The appearance of the cross-section at X/L = 0.96 (Figure 41) looks something like that shown in the image of the X/L = 0.76 section. It has what now looks like a two-zone structure but the outer zone looks as though it may have been two zones at some time. Of course only a radial analysis of the Zr concentration will help prove or disprove this hypothesis, which may be important to fully benchmark a model for Zr redistribution. The importance of this model is in predicting the melting temperatures of the various zones as they are affected by Zr concentration.

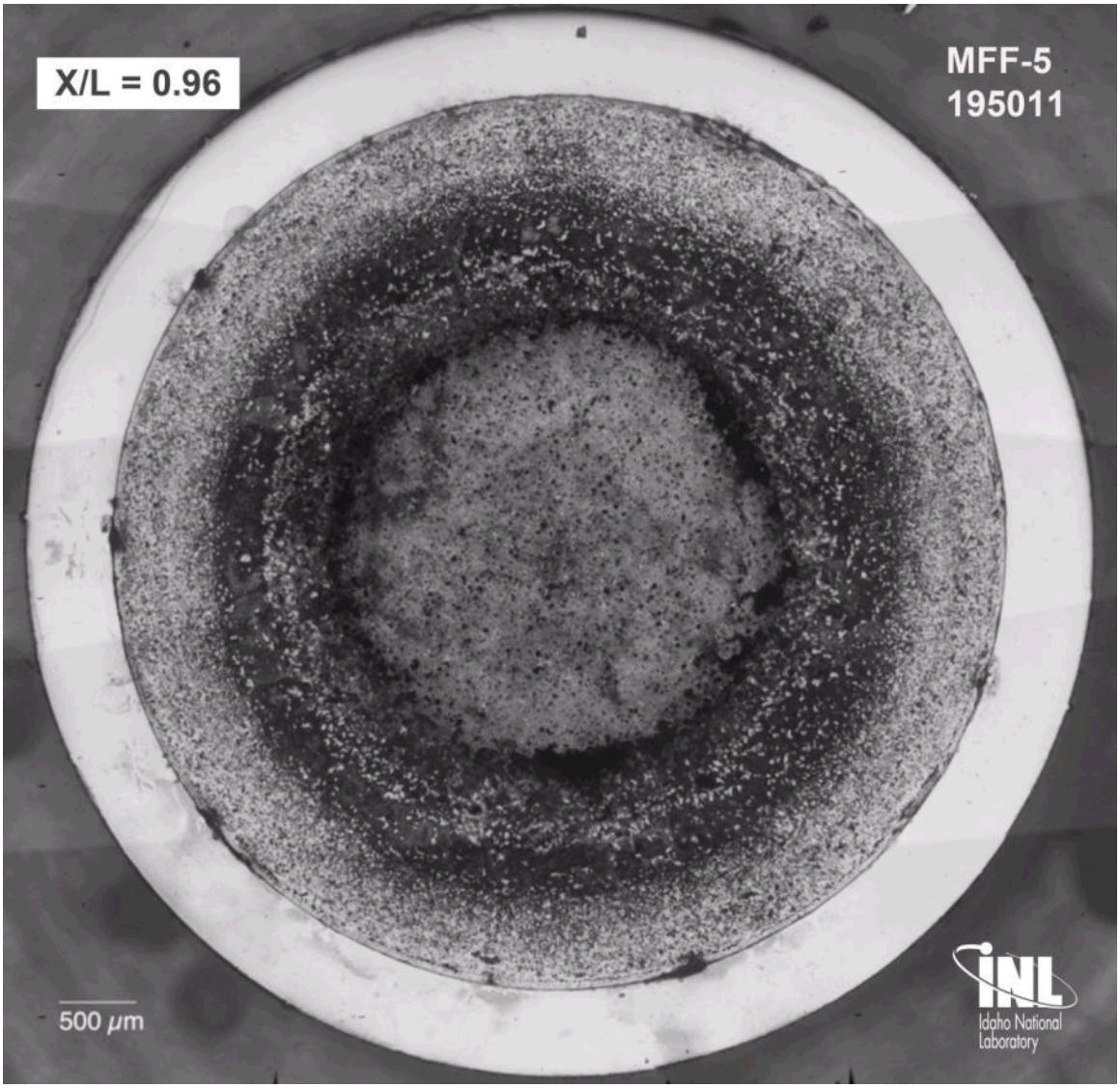


Figure 41. Metallographic section of MFF-5 Pin 195011 at the X/L = 0.96 axial location.

### 3.7.3 Cladding Metallography and Fuel/cladding Chemical Interaction (FCCI)

Fuel/cladding interaction can take several forms in regards to metallic fuel and HT9 cladding. The interdiffusion of rare earth fission products and cladding components is considered the most important as it produces a diffusion layer in the cladding that is brittle and considered cladding wastage, and sometimes contains low melting compounds. This FCCI effect in the MFF pins has been analyzed in considerable depth and modeled as part of a Ph.D. dissertation[17] and will be summarized later in this section.

A second effect is that the small carbides created in the cladding during tempering of the steel can dissolve and be transported into the fuel, effectively decarburizing the cladding. Figure 42 shows the results of this phenomenon where a U-Pu-Zr piece of fuel was sandwiched with HT9 cladding and heated to 705°C for 300 hr.[18] The HT9 has been decarburized to a depth of about 620 microns. Note that the now ferritic decarburized region also shows grain growth and is very soft (hardness indents are large). This same effect has been observed in HT9 cladding on metallic fuel so hardness testing and cladding etching will be used to examine for this effect in the MFF pins.

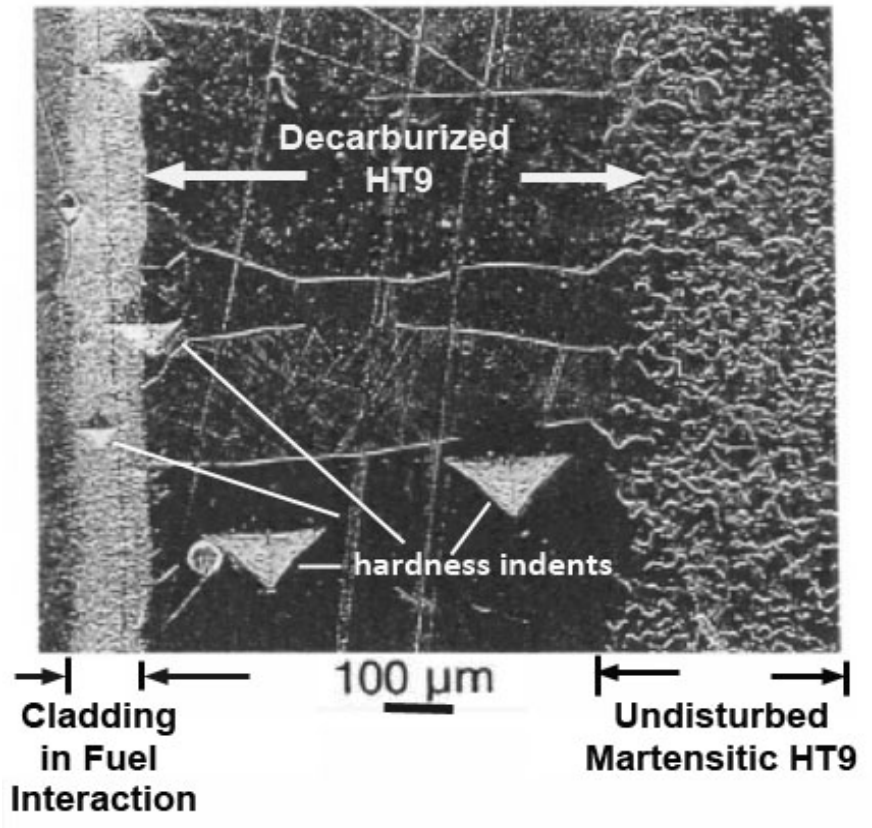


Figure 42. Polished and etched surface cut across diffusion couple of U-Pu-Zr fuel and HT9 cladding. 705°C for 300 hr. Large hardness indents show soft, decarburized area of large-grain ferrite in the HT9.

Figure 43 and Figure 44 graphically show some of the microhardness measurements taken on the HT9 cladding surfaces in the metallography samples of Pins 193045 and 195011. The data plotted include individual measurements taken closest to the OD of the cladding and closest to the fuel (cladding ID) at each 90° rotation around the circumference of the cladding. The average of those for each axial location is also shown.

Note that the hardness in general decreases going up the fuel pin OD, and are lower for the measurements taken closest to the cladding ID. This likely reflects the cladding temperature and an over-tempering phenomenon, counteracted only by some radiation hardening. The latter is reflected by the slight increase in hardness at core center (X/L = 0.5). None of these hardness measurements reflect softening from carbon loss or hardening from rare earth fission product diffusion into the cladding although a few such measurements were made that reflect these phenomena.

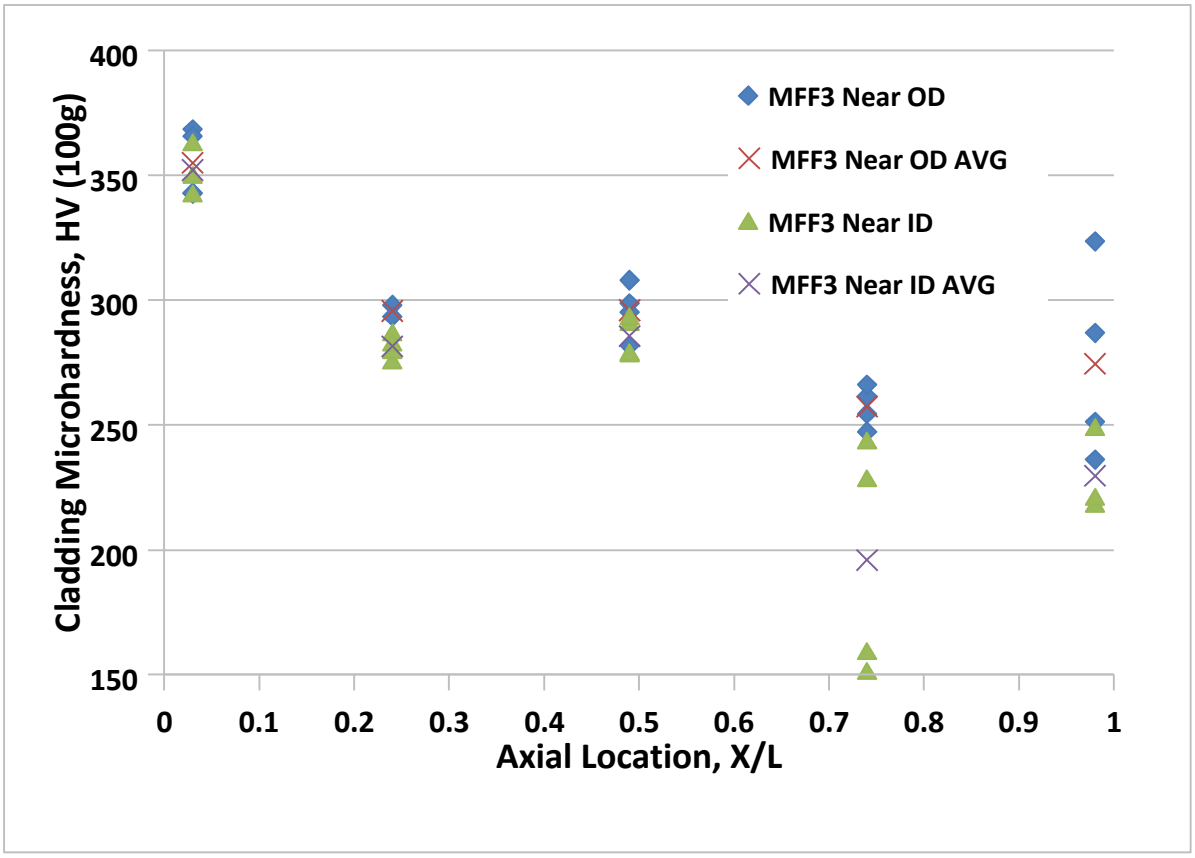


Figure 43. MFF-3 Pin 193045 HT9 cladding microhardness as a function of axial location.

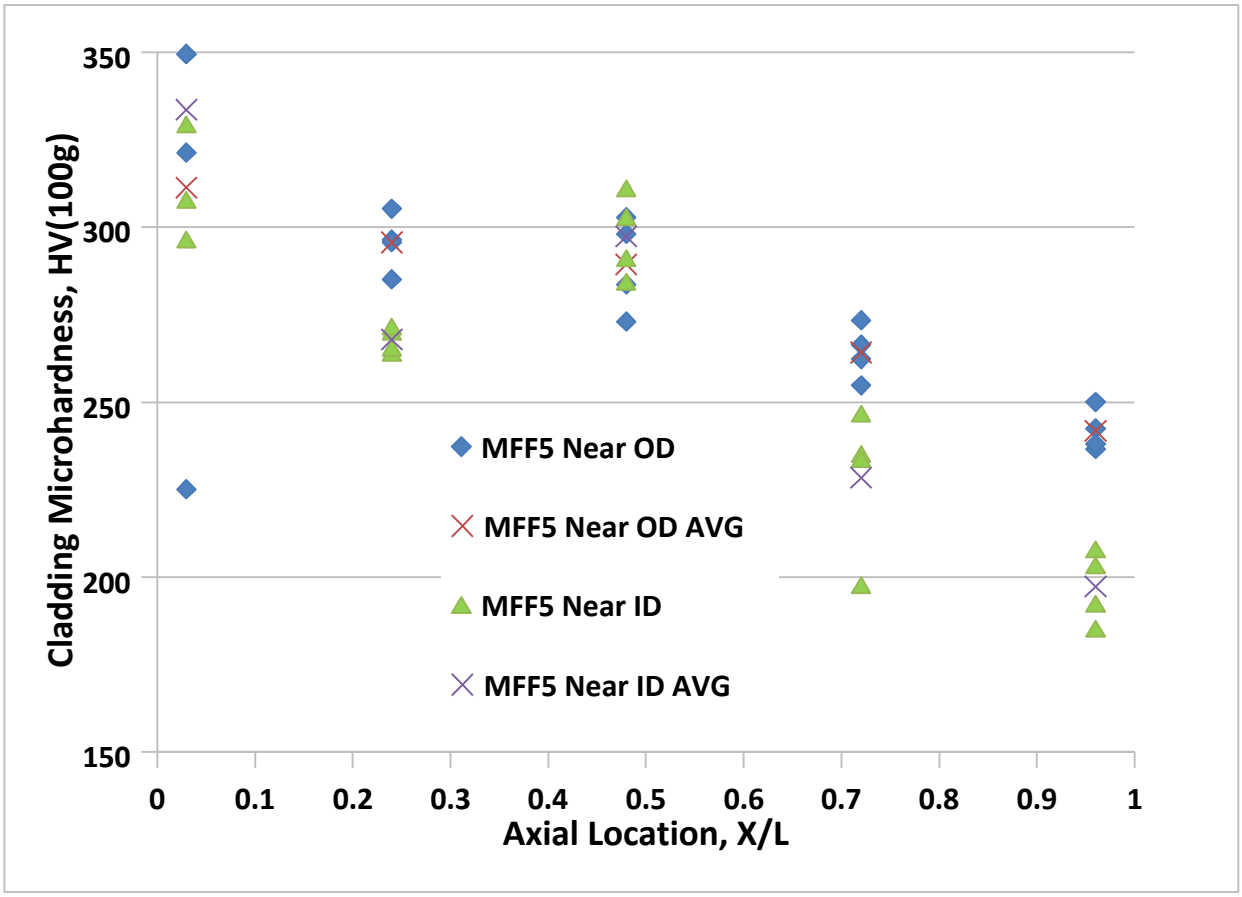


Figure 44. MFF-5 Pin 195011 HT9 cladding microhardness as a function of axial location.

The measured peak FCCI values were shown in Figure 28 and Figure 29, and the FCCI maximum depth along with time-averaged inner clad temperature and fuel centerline temperature are shown in Table 12. The values predicted by the model developed by Carmack are also shown.[17] These values represent only the rare earth fission product interaction with the cladding. The MFF-5 pin shows a peak interaction between the middle and top of the fuel column, the same behavior as seen in an earlier FFTF experiment (IFR-1) and attributed to the effect of higher driving force (temperature gradient) in moving rare earths to the cladding surface. The MFF-3 pin shows a peak near the top of the fuel column. Note that both MFF-3 and MFF-5 operated at significantly higher cladding temperatures than did IFR-1.

As mentioned previously Reference 17 presents a treatise on the FCCI of these pins, and others from an experiment, X447, run in EBR-II. All were experiments which were run with very high peak cladding temperatures and therefore presented the most FCCI. A model was developed based upon the diffusion of rare earth fission products through the fuel induced by both Fickian (concentration gradient) and Soret (thermal gradient) effects and a subsequent reaction of these fission products with the cladding. The model predicted the FCCI layer growth, if not the exact magnitude of the temperature dependence, as seen in the sample graphical representation for MFF-5 Pin 195011, in Figure 45.

Table 12. Fuel/cladding interaction layer depth as a function of axial position.

| S/A, Pin | $X/L_0$ | Burnup (at%) | Measured Max Depth (μm) | Predicted FCCI (μm) | Time Ave. Fuel Centerline T (°C) | Time Ave. Inner Clad T (°C) |
|---|---|---|---|---|---|---|

| | | | | | | |
|---|---|---|---|---|---|---|
| MFF5 195011 | 0.03 | 6.7 | 0 | 0 | 532 | 414 |
| | 0.24 | 8.9 | 0 | 0 | 628 | 480 |
| | 0.48 | 9.8 | 0 | 20 | 712 | 556 |
| | 0.72 | 8.1 | 50.8 | 149 | 736 | 612 |
| | 0.96 | 4.8 | 25.4 | 84 | 709 | 635 |
| MFF3 193045 | 0.03 | 8.4 | 0 | 0 | 527 | 413 |
| | 0.25 | 11.3 | 0 | 0 | 619 | 475 |
| | 0.49 | 12.4 | 0 | 27 | 700 | 550 |
| | 0.74 | 9.1 | 76.2 | 138 | 712 | 604 |
| | 0.98 | 5.7 | 152.4 | 70 | 682 | 615 |

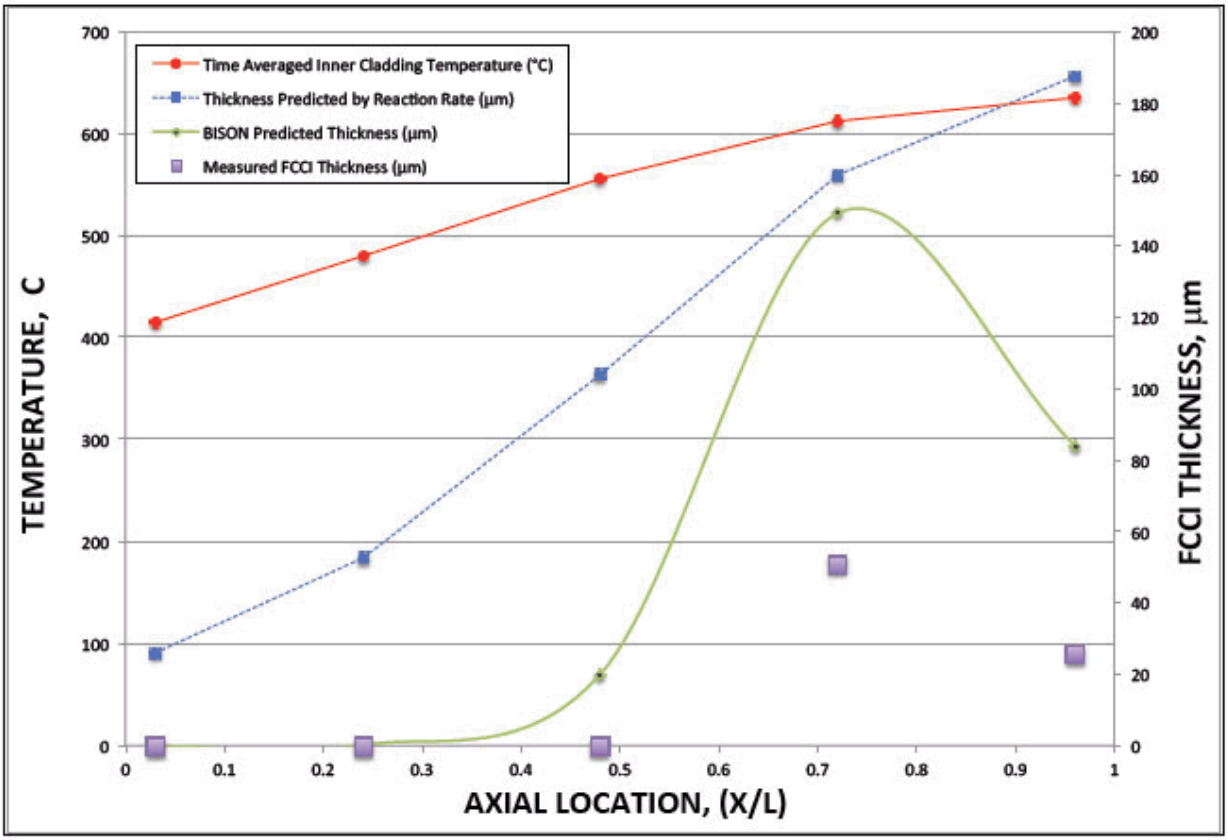


Figure 45. Fuel/cladding Chemical Interaction (FCCI) in MFF-5 Pin 195011. Shown are measured peak FCCI, predicted FCCI, and both time-averaged inner clad and fuel centerline temperatures.[17]

## 3.8 Fuel Chemistry and Burnup

A review of the as-run reactor physics calculations has already been presented earlier in this report. These calculations culminated with ORIGEN results as a function of axial position for the two fuel pins destructively examined, 193045 and 195011.These results are listed in Appendix A, Tables A-1 and A-2, of this report.

Sections of the fuel pins taken near the axial locations used for metallography were taken and sent to the Analytical Laboratory for chemical and isotopic analysis. In this section we will review the results of these analyses with emphasis on how well the chemical analysis results matched with those calculated.

The fuel pin sections were dissolved and the fuel (HM plus Zr) estimated by: (1) Measuring the Zr content and assuming the HM/Zr ratio to get the HM and total fuel mass, or (2) Measuring the cladding component concentrations (Fe, Cr, Mo), then using the cladding mass to estimate the fuel mass that would go with that length of cladding. These were only estimates as there were potential problems with oxidation of the fuel (oxidized U would not dissolve properly). However, the estimates could be used to test the accuracy in seeing how closely masses matched between the two estimation methods (cladding and Zr) – they matched fairly well (within ten percent of one another).

All pertinent isotopes were measured including, $^{233}$U, $^{234}$U, $^{235}$U, $^{236}$U, $^{238}$U, $^{237}$Np, $^{239}$Pu, $^{240}$Pu, $^{241}$m/Z, $^{242}$m/Z, and fission products $^{85}$Rb, $^{86}$Sr,$^{87}$Rb,$^{88}$Sr,$^{89}$Y, $^{99}$Tc,$^{101}$Ru, $^{102}$Ru,$^{103}$Rh, $^{104}$Ru, $^{105}$Pd,$^{106}$Pd, $^{107}$Pd, $^{108}$Pd,$^{109}$Ag,$^{110}$Pd,$^{111}$Cd,$^{112}$Cd,$^{114}$Cd,$^{116}$Cd,$^{133}$Cs,$^{135}$Cs,$^{136}$Ba,$^{137}$m/Z,$^{138}$Ba,$^{139}$La,$^{140}$Ce,$^{141}$Pr,$^{142}$Ce,$^{143}$Nd,$^{144}$Nd,$^{145}$ Nd,$^{146}$Nd,$^{147}$Sm, $^{148}$m/Z,$^{149}$Sm,$^{150}$Nd,$^{152}$Sm, and $^{154}$Sm.

'$^{xxx}$m/Z' means of the isotopic mass 'xxx' and for all atomic species with that isotopic mass, such as $^{139}$Nd and $^{139}$Sm, combined, or $^{241}$Am and $^{241}$Pu, combined. For these analyses they could not be differentiated without an additional separation process which was not done.

The fission product concentrations and their expected fission yields were then used to calculate the fuel burnup. Using those with long half-lives and those that can be easily differentiated from the other isotopes, the 'best' indicators of burnup for a fast neutron spectrum were chosen. Table 13 shows the burnups calculated for each of nine isotopes or isotope combinations. The final column is an average of the nine predicted burnups. Figure 46 shows these plotted for the two pins analyzed, one from MFF-3 and one from MFF-5. Also plotted are burnups calculated from the ORIGEN calculations (see Appendix A) summing the heavy metals for each two-inch (5.1 cm) fuel section and computing $[(HM_{as\text{-}built} - HM_{ORIGEN})/ HM_{as\text{-}built}]$. The calculated and measured burnups are in general agreement.

Figure 47 shows the ORIGEN predicted $^{99}$Tc concentrations compared to the measured values. The comparison between the two is very good.

Table 13. Summary fuel burnups (heavy metal) computed from measured isotopic concentration measurements for isotopes thought to be most reliable for burnup determination.

| Pin | X/L | BU, $^{139}$La | BU, $^{140}$Ce | BU, $^{141}$Pr | BU, $^{142}$Ce | BU, $^{143}$Nd |
|---|---|---|---|---|---|---|
| MFF-3: 193045 | 0.04 | 9.14 | 8.80 | 8.84 | 8.91 | 8.58 |
| 193045 | 0.25 | 12.04 | 12.03 | 11.69 | 11.87 | 11.39 |
| 193045 | 0.50 | 13.04 | 13.15 | 12.64 | 12.96 | 12.20 |
| 193045 | 0.75 | 10.26 | 10.40 | 9.82 | 10.08 | 9.63 |
| 193045 | 0.96 | 9.20 | 8.20 | 9.17 | 8.11 | 8.50 |
| MFF-5: 195011 | 0.04 | 6.77 | 6.35 | 6.48 | 6.59 | 6.34 |
| 195011 | 0.25 | 9.11 | 8.97 | 8.81 | 8.88 | 8.56 |
| 195011 | 0.50 | 9.38 | 9.69 | 9.35 | 9.43 | 9.27 |
| 195011 | 0.75 | 7.93 | 8.01 | 7.72 | 7.82 | 7.53 |
| 195011 | 0.96 | 5.46 | 5.38 | 5.17 | 5.31 | 5.07 |

| Pin | X/L | BU, $^{144}$Nd | BU, $^{143}$Nd+$^{144}$Nd | BU, $^{145}$Nd+$^{146}$Nd | BU, $^{99}$Tc | BU, Avg |
|---|---|---|---|---|---|---|
| MFF-3: 193045 | 0.04 | | | | | |

| | | | | | | |
|---|---|---|---|---|---|---|
| | | 8.84 | | | | |
| 193045 | 0.25 | 11.67 | 11.53 | 11.75 | 11.59 | 11.7 |
| 193045 | 0.50 | 12.72 | 12.45 | 12.70 | 12.59 | 12.7 |
| 193045 | 0.75 | 9.84 | 9.73 | 9.89 | 10.74 | 10.0 |
| 193045 | 0.96 | 8.53 | 8.51 | 8.62 | 6.89 | 8.4 |
| MFF-5: 195011 | 0.04 | 6.50 | 6.42 | 6.56 | 6.47 | 6.0 |
| 195011 | 0.25 | 8.70 | 8.62 | 8.78 | 8.67 | 8.8 |
| 195011 | 0.50 | 9.31 | 9.29 | 9.54 | 9.34 | 9.4 |
| 195011 | 0.75 | 7.69 | 7.60 | 7.69 | 8.03 | 7.8 |
| 195011 | 0.96 | 5.15 | 5.11 | 5.12 | 5.00 | 5.2 |

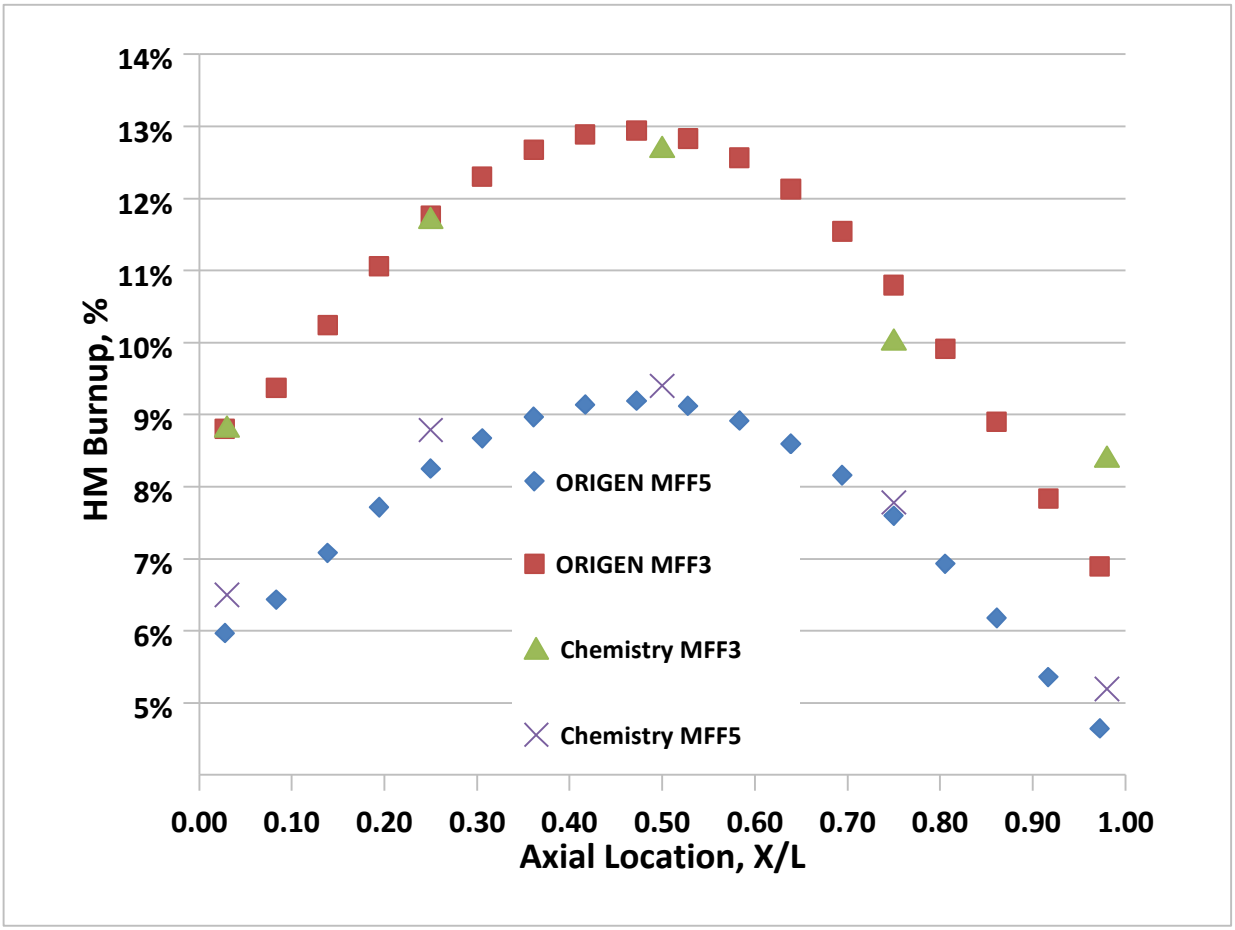


Figure 46. Heavy metal burnup as a function of axial location as calculated (ORIGEN) and measured (average of isotopic analyses). MFF-3 Pin 193045 and MFF-5 Pin 195011 are represented.

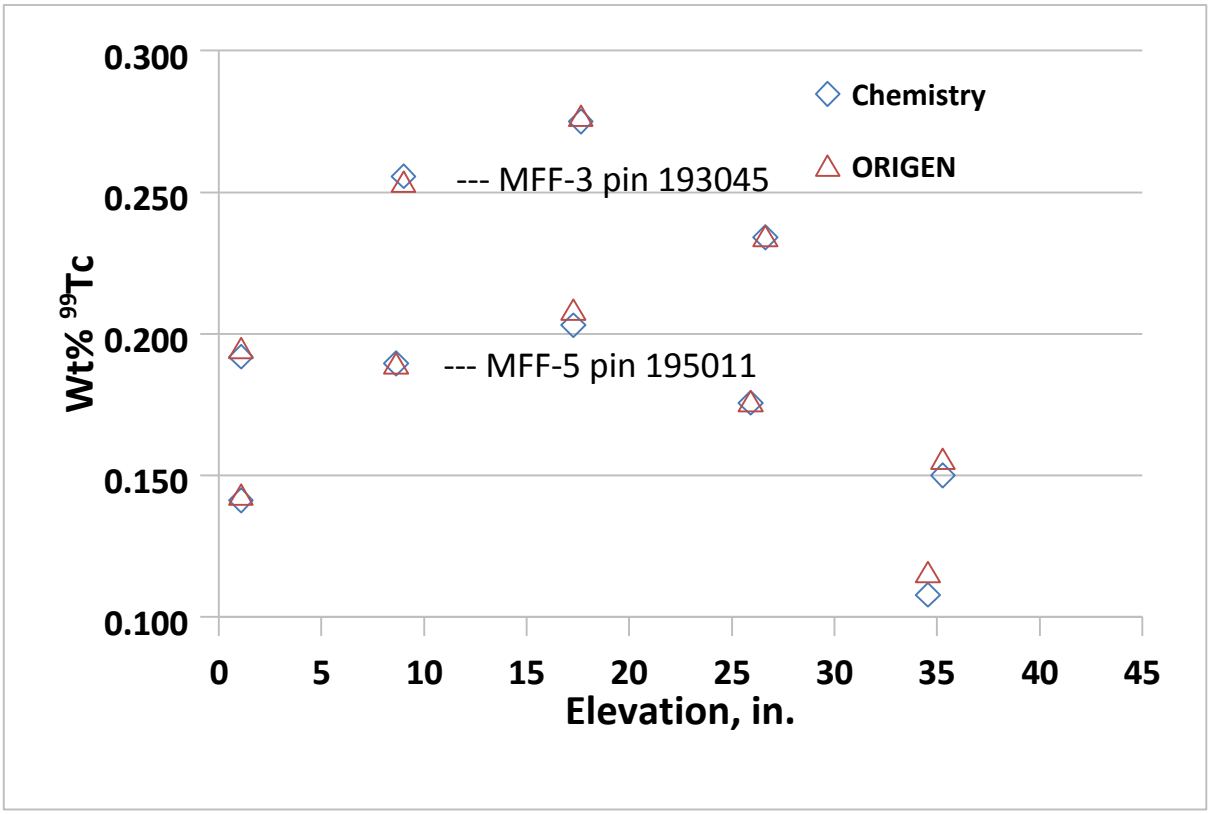


Figure 47. Tc-99 content after irradiation as a function of axial location as calculated (ORIGEN) and measured (Analytical Laboratory). MFF-3 Pin 193045 and MFF-5 Pin 195011 are represented.

# 4. CONCLUSIONS

1. Metallic fuel pins (U-10Zr/ HT9 cladding) from high-temperature FFTF driver fuel qualification tests MFF-3 and MFF-5 were examined using neutron radiography (axial expansion); gamma scanning; plenum gas pressure, volume, and composition; linear and spiral profilometry (cladding diameter); optical metallography and microhardness; isotopic and chemical analysis of fuel segments.
2. A full as-run neutronics analysis was completed tracking cycle-by-cycle the sodium and pin-by-pin cladding and fuel temperatures, fuel burnup and neutron exposure (fluence), and all of these as a function of axial position along the fuel pin pins. Assembly outlet temperature was also calculated as a function of reactor cycle.
3. The fuel in these experiments showed axial fuel growth less than observed in previous experiments, with the measured MFF-3 pins averaging 1.6% and MFF-5 pins 3.6% expansion. Previous tests showed averages of 7-9% expansion. While there are some indications as to the cause for this, namely the elevated fuel temperature in these tests, measurements of pins from two other FFTF assemblies may be done to help to discover the reason for this unexpected behavior.
4. The fission gas release was measured only for one pin from MFF-3 and one from MFF-5. The MFF-3 pin showed a gas release of only 61% which is low compared to other fuel tests, including MFF-5 which showed a release of 79%, more like other tests, including IFR-1, another FFTF test.
5. Chemical/isotopic analyses of cross-sections of one fuel each from MFF-3 and MFF-5 correlated very well with ORIGEN calculations produced covering the axial length of the fuel column.
6. The cladding diameters as a function of axial position showed two peaks, especially in the MFF-3

pins which were operated to higher neutron exposures. The peaks occurred at the top of the fuel column and slightly below the position of peak neutron flux, a little below the fuel column geometric center. The pin length showed little or no growth, indicating most of the strain should be related to creep. Therefore the two peaks may be related to irradiation creep (near the peak flux position) and thermal creep (at the top of the fuel column due to higher cladding temperature and FCCI clad wall thinning).

7. Axial growth of the pins was measured to estimate how much swelling may be present. There was enough apparent growth to explain the large diameter peak in the MFF-3 pin axial profile, but too much axial growth when compare to the smaller diameter increases in the MFF-5 pins. Immersion density of cladding would be required to address this issue.
8. Other pin performance characteristics looked very much like that exhibited by the fuel tests previously performed in EBR-II, on much shorter pins.

# 5. REFERENCES

INTENTIONALLY BLANK

# Appendix A

# Fuel Pin ORIGEN Calculation

# Appendix A

# Fuel Pin ORIGEN Calculation

The following Tables, A-1a through A-1m show an example of the results of a final isotopic prediction for one of the MFF-5 fuel pins, in this case Pin 195011, the MFF-5 pin that was destructively examined. The tables show the calculated elemental and isotopic compositions of eighteen 2-inch segments of the ~36-inch fuel column, assuming no axial growth. Note that they are normalized to a mass of 14.2 grams (heavy metal [HM] plus fission products [FP] – original Zr content not included) for each fuel segment. The individual isotopic compositions were decayed from the time of reactor shutdown to remove the assembly until 3/11/2011, the time when the examinations were being done.

This ORIGEN-based information was used to calculate HM burnup and compare these numbers with those calculated from the analytical chemistry results. The numbers were also helpful in estimating the expected activity of a given sample of the fuel, thereby allowing adequate preparation to minimize the exposure of laboratory personnel.

Tables A-2a through A-2m represent similar calculations for MFF-3 Pin 193045.

Table A-1a. Composition (grams) in 2-inch fuel segment: ORIGEN calculation results for Pin195011, decayed to 3/11/2011.

| Position: | 1 | 3 | 5 | 7 | 9 | 11 | 13 | 15 | 17 | 19 | 21 | 23 | 25 | 27 | 29 | 31 | 33 | 35 |
|---|---|---|---|---|---|---|---|---|---|---|---|---|---|---|---|---|---|---|
| HE 4 | 4.01E-06 | 4.41E-06 | 5.09E-06 | 5.81E-06 | 6.49E-06 | 7.07E-06 | 7.50E-06 | 7.76E-06 | 7.84E-06 | 7.72E-06 | 7.42E-06 | 6.96E-06 | 6.36E-06 | 5.66E-06 | 4.90E-06 | 4.12E-06 | 3.41E-06 | 2.89E-06 |
| TH230 | 0.00E+00 | 0.00E+00 | 0.00E+00 | 4.93E-08 | 5.26E-08 | 5.51E-08 | 5.69E-08 | 5.80E-08 | 5.83E-08 | 5.79E-08 | 5.67E-08 | 5.48E-08 | 5.22E-08 | 4.89E-08 | 0.00E+00 | 0.00E+00 | 0.00E+00 | 0.00E+00 |
| TH232 | 1.35E-07 | 1.31E-07 | 1.38E-07 | 1.46E-07 | 1.53E-07 | 1.59E-07 | 1.63E-07 | 1.66E-07 | 1.66E-07 | 1.65E-07 | 1.62E-07 | 1.58E-07 | 1.51E-07 | 1.43E-07 | 1.33E-07 | 1.22E-07 | 1.12E-07 | 1.08E-07 |
| PA231 | 7.05E-08 | 6.94E-08 | 6.74E-08 | 6.55E-08 | 6.38E-08 | 6.25E-08 | 6.16E-08 | 6.10E-08 | 6.09E-08 | 6.11E-08 | 6.17E-08 | 6.27E-08 | 6.41E-08 | 6.59E-08 | 6.80E-08 | 7.04E-08 | 7.30E-08 | 7.50E-08 |
| U233 | 1.44E-06 | 1.62E-06 | 1.76E-06 | 1.87E-06 | 1.95E-06 | 2.02E-06 | 2.06E-06 | 2.08E-06 | 2.09E-06 | 2.08E-06 | 2.06E-06 | 2.01E-06 | 1.95E-06 | 1.86E-06 | 1.75E-06 | 1.61E-06 | 1.44E-06 | 1.23E-06 |
| U234 | 6.69E-04 | 7.73E-04 | 8.69E-04 | 9.55E-04 | 1.03E-03 | 1.08E-03 | 1.13E-03 | 1.15E-03 | 1.16E-03 | 1.15E-03 | 1.12E-03 | 1.08E-03 | 1.02E-03 | 9.45E-04 | 8.60E-04 | 7.64E-04 | 6.58E-04 | 5.44E-04 |
| U235 | 3.29E+00 | 3.26E+00 | 3.17E+00 | 3.08E+00 | 3.01E+00 | 2.95E+00 | 2.90E+00 | 2.88E+00 | 2.87E+00 | 2.88E+00 | 2.91E+00 | 2.96E+00 | 3.02E+00 | 3.10E+00 | 3.20E+00 | 3.31E+00 | 3.42E+00 | 3.51E+00 |
| U236 | 2.31E-01 | 2.24E-01 | 2.35E-01 | 2.49E-01 | 2.61E-01 | 2.71E-01 | 2.78E-01 | 2.83E-01 | 2.84E-01 | 2.82E-01 | 2.77E-01 | 2.69E-01 | 2.58E-01 | 2.44E-01 | 2.27E-01 | 2.09E-01 | 1.91E-01 | 1.85E-01 |
| U237 | 1.68E-12 | 1.48E-12 | 1.72E-12 | 2.10E-12 | 2.50E-12 | 2.86E-12 | 3.15E-12 | 3.33E-12 | 3.38E-12 | 3.30E-12 | 3.09E-12 | 2.78E-12 | 2.38E-12 | 1.95E-12 | 1.52E-12 | 1.14E-12 | 8.55E-13 | 7.90E-13 |
| U238 | 9.43E+00 | 9.40E+00 | 9.37E+00 | 9.33E+00 | 9.30E+00 | 9.28E+00 | 9.26E+00 | 9.25E+00 | 9.25E+00 | 9.25E+00 | 9.26E+00 | 9.28E+00 | 9.31E+00 | 9.34E+00 | 9.38E+00 | 9.42E+00 | 9.46E+00 | 9.50E+00 |
| NP236 | 0.00E+00 | 0.00E+00 | 1.38E-07 | 1.72E-07 | 2.05E-07 | 2.33E-07 | 2.55E-07 | 2.68E-07 | 2.72E-07 | 2.66E-07 | 2.52E-07 | 2.29E-07 | 2.00E-07 | 1.67E-07 | 1.32E-07 | 0.00E+00 | 0.00E+00 | 0.00E+00 |
| NP237 | 9.04E-03 | 1.01E-02 | 1.17E-02 | 1.33E-02 | 1.48E-02 | 1.60E-02 | 1.69E-02 | 1.74E-02 | 1.76E-02 | 1.73E-02 | 1.67E-02 | 1.58E-02 | 1.45E-02 | 1.30E-02 | 1.13E-02 | 9.51E-03 | 7.75E-03 | 6.29E-03 |
| PU238 | 4.49E-04 | 5.80E-04 | 7.49E-04 | 9.28E-04 | 1.10E-03 | 1.25E-03 | 1.36E-03 | 1.43E-03 | 1.45E-03 | 1.42E-03 | 1.34E-03 | 1.22E-03 | 1.07E-03 | 8.97E-04 | 7.16E-04 | 5.41E-04 | 3.83E-04 | 2.58E-04 |
| PU239 | 2.52E-01 | 2.59E-01 | 2.76E-01 | 2.94E-01 | 3.10E-01 | 3.22E-01 | 3.31E-01 | 3.37E-01 | 3.38E-01 | 3.36E-01 | 3.30E-01 | 3.20E-01 | 3.06E-01 | 2.89E-01 | 2.68E-01 | 2.45E-01 | 2.21E-01 | 2.04E-01 |
| PU240 | 7.64E-03 | 7.03E-03 | 7.78E-03 | 8.87E-03 | 9.94E-03 | 1.09E-02 | 1.16E-02 | 1.20E-02 | 1.22E-02 | 1.19E-02 | 1.14E-02 | 1.07E-02 | 9.62E-03 | 8.44E-03 | 7.17E-03 | 5.91E-03 | 4.89E-03 | 4.63E-03 |
| PU241 | 5.43E-05 | 4.77E-05 | 5.57E-05 | 6.79E-05 | 8.08E-05 | 9.25E-05 | 1.02E-04 | 1.08E-04 | 1.09E-04 | 1.07E-04 | 9.98E-05 | 8.96E-05 | 7.68E-05 | 6.30E-05 | 4.92E-05 | 3.68E-05 | 2.76E-05 | 2.55E-05 |
| PU242 | 1.60E-06 | 1.36E-06 | 1.68E-06 | 2.21E-06 | 2.81E-06 | 3.39E-06 | 3.87E-06 | 4.17E-06 | 4.26E-06 | 4.11E-06 | 3.76E-06 | 3.24E-06 | 2.62E-06 | 2.00E-06 | 1.43E-06 | 9.57E-07 | 6.46E-07 | 5.74E-07 |
| AM241 | 8.29E-05 | 7.28E-05 | 8.49E-05 | 1.04E-04 | 1.23E-04 | 1.41E-04 | 1.55E-04 | 1.64E-04 | 1.67E-04 | 1.62E-04 | 1.52E-04 | 1.37E-04 | 1.17E-04 | 9.60E-05 | 7.50E-05 | 5.60E-05 | 4.21E-05 | 3.89E-05 |
| CM242 | 0.00E+00 | 0.00E+00 | 0.00E+00 | 0.00E+00 | 1.45E-10 | 1.74E-10 | 1.98E-10 | 2.13E-10 | 2.17E-10 | 2.10E-10 | 1.93E-10 | 1.67E-10 | 0.0E+00 | 0.0E+00 | 0.00E+00 | 0.00E+00 | 0.00E+00 | 0.00E+00 |
| SUM HM isotpes | 1.32E+01 | 1.32E+01 | 1.31E+01 | 1.30E+01 | 1.29E+01 | 1.28E+01 | 1.28E+01 | 1.28E+01 | 1.28E+01 | 1.28E+01 | 1.28E+01 | 1.29E+01 | 1.29E+01 | 1.30E+01 | 1.31E+01 | 1.32E+01 | 1.33E+01 | 1.34E+01 |

Position=Segment location (midpoint of 2-in. segment) from bottom of fuel (BOF); sample wgt. 14.2g.

Table A-1b. Composition (grams) in 2-inch fuel segment: ORIGEN calculation results for Pin195011, decayed to 3/11/2011.

| 6 | 1 | 3 | 5 | 7 | 9 | 11 | 13 | 15 | 17 | 19 | 21 | 23 | 25 | 27 | 29 | 31 | 33 | 35 |
|---|---|---|---|---|---|---|---|---|---|---|---|---|---|---|---|---|---|---|
| HE | 4.01E-06 | 4.41E-06 | 5.09E-06 | 5.81E-06 | 6.49E-06 | 7.07E-06 | 7.50E-06 | 7.76E-06 | 7.84E-06 | 7.72E-06 | 7.42E-06 | 6.96E-06 | 6.36E-06 | 5.66E-06 | 4.90E-06 | 4.12E-06 | 3.41E-06 | 2.89E-06 |
| TH | 1.72E-07 | 1.73E-07 | 1.85E-07 | 1.97E-07 | 2.08E-07 | 2.17E-07 | 2.23E-07 | 2.27E-07 | 2.28E-07 | 2.26E-07 | 2.22E-07 | 2.15E-07 | 2.05E-07 | 1.94E-07 | 1.80E-07 | 1.64E-07 | 1.48E-07 | 1.38E-07 |
| PA | 7.08E-08 | 6.97E-08 | 6.78E-08 | 6.59E-08 | 6.43E-08 | 6.31E-08 | 6.22E-08 | 6.16E-08 | 6.15E-08 | 6.17E-08 | 6.23E-08 | 6.33E-08 | 6.46E-08 | 6.63E-08 | 6.84E-08 | 7.07E-08 | 7.32E-08 | 7.52E-08 |
| U | 1.30E+01 | 1.29E+01 | 1.28E+01 | 1.27E+01 | 1.26E+01 | 1.25E+01 | 1.24E+01 | 1.24E+01 | 1.24E+01 | 1.24E+01 | 1.25E+01 | 1.25E+01 | 1.26E+01 | 1.27E+01 | 1.28E+01 | 1.29E+01 | 1.31E+01 | 1.32E+01 |
| NP | 9.04E-03 | 1.01E-02 | 1.17E-02 | 1.33E-02 | 1.48E-02 | 1.60E-02 | 1.69E-02 | 1.74E-02 | 1.76E-02 | 1.73E-02 | 1.67E-02 | 1.58E-02 | 1.45E-02 | 1.30E-02 | 1.13E-02 | 9.51E-03 | 7.75E-03 | 6.29E-03 |
| PU | 2.60E-01 | 2.66E-01 | 2.84E-01 | 3.04E-01 | 3.21E-01 | 3.35E-01 | 3.45E-01 | 3.50E-01 | 3.52E-01 | 3.49E-01 | 3.43E-01 | 3.32E-01 | 3.17E-01 | 2.98E-01 | 2.76E-01 | 2.51E-01 | 2.27E-01 | 2.09E-01 |
| AM | 8.29E-05 | 7.28E-05 | 8.49E-05 | 1.04E-04 | 1.23E-04 | 1.41E-04 | 1.55E-04 | 1.64E-04 | 1.67E-04 | 1.62E-04 | 1.52E-04 | 1.37E-04 | 1.17E-04 | 9.61E-05 | 7.51E-05 | 5.60E-05 | 4.21E-05 | 3.89E-05 |
| CM | 0.00E+00 | 0.00E+00 | 0.00E+00 | 0.00E+00 | 1.48E-09 | 1.91E-09 | 2.28E-09 | 2.52E-09 | 2.59E-09 | 2.48E-09 | 2.20E-09 | 1.81E-09 | 1.38E-09 | 0.00E+00 | 0.00E+00 | 0.00E+00 | 0.00E+00 | 0.00E+00 |
| SUM HM elements | 1.32E+01 | 1.32E+01 | 1.31E+01 | 1.30E+01 | 1.29E+01 | 1.28E+01 | 1.28E+01 | 1.28E+01 | 1.28E+01 | 1.28E+01 | 1.28E+01 | 1.29E+01 | 1.29E+01 | 1.30E+01 | 1.31E+01 | 1.32E+01 | 1.33E+01 | 1.34E+01 |
| H 3 | 7.93E-07 | 8.48E-07 | 9.25E-07 | 9.98E-07 | 1.06E-06 | 1.11E-06 | 1.14E-06 | 1.16E-06 | 1.17E-06 | 1.16E-06 | 1.14E-06 | 1.10E-06 | 1.05E-06 | 9.85E-07 | 9.07E-07 | 8.19E-07 | 7.24E-07 | 6.40E-07 |
| LI 6 | 1.18E-08 | 1.26E-08 | 1.37E-08 | 1.47E-08 | 1.56E-08 | 1.62E-08 | 1.67E-08 | 1.70E-08 | 1.71E-08 | 1.70E-08 | 1.66E-08 | 1.61E-08 | 1.54E-08 | 1.45E-08 | 1.34E-08 | 1.21E-08 | 1.08E-08 | 9.58E-09 |
| GE 72 | 1.78E-06 | 1.94E-06 | 2.13E-06 | 2.30E-06 | 2.44E-06 | 2.56E-06 | 2.64E-06 | 2.69E-06 | 2.70E-06 | 2.68E-06 | 2.62E-06 | 2.54E-06 | 2.42E-06 | 2.27E-06 | 2.09E-06 | 1.88E-06 | 1.65E-06 | 1.44E-06 |
| GE 73 | 4.48E-06 | 4.81E-06 | 5.25E-06 | 5.65E-06 | 5.99E-06 | 6.25E-06 | 6.44E-06 | 6.55E-06 | 6.58E-06 | 6.53E-06 | 6.41E-06 | 6.21E-06 | 5.93E-06 | 5.58E-06 | 5.15E-06 | 4.66E-06 | 4.12E-06 | 3.63E-06 |
| GE 74 | 8.91E-06 | 9.55E-06 | 1.04E-05 | 1.13E-05 | 1.20E-05 | 1.25E-05 | 1.29E-05 | 1.31E-05 | 1.32E-05 | 1.31E-05 | 1.28E-05 | 1.24E-05 | 1.18E-05 | 1.11E-05 | 1.02E-05 | 9.23E-06 | 8.15E-06 | 7.18E-06 |
| AS 75 | 1.51E-05 | 1.61E-05 | 1.75E-05 | 1.88E-05 | 2.00E-05 | 2.08E-05 | 2.15E-05 | 2.18E-05 | 2.19E-05 | 2.18E-05 | 2.14E-05 | 2.07E-05 | 1.98E-05 | 1.86E-05 | 1.72E-05 | 1.56E-05 | 1.38E-05 | 1.22E-05 |
| GE 76 | 3.51E-05 | 3.74E-05 | 4.07E-05 | 4.39E-05 | 4.65E-05 | 4.86E-05 | 5.01E-05 | 5.10E-05 | 5.12E-05 | 5.09E-05 | 4.99E-05 | 4.83E-05 | 4.61E-05 | 4.33E-05 | 3.99E-05 | 3.61E-05 | 3.20E-05 | 2.84E-05 |
| SE 76 | 2.77E-07 | 3.42E-07 | 4.20E-07 | 4.97E-07 | 5.67E-07 | 6.26E-07 | 6.69E-07 | 6.95E-07 | 7.02E-07 | 6.91E-07 | 6.62E-07 | 6.16E-07 | 5.57E-07 | 4.85E-07 | 4.07E-07 | 3.26E-07 | 2.47E-07 | 1.80E-07 |
| SE 77 | 6.99E-05 | 7.41E-05 | 8.04E-05 | 8.63E-05 | 9.14E-05 | 9.54E-05 | 9.82E-05 | 9.98E-05 | 1.00E-04 | 9.96E-05 | 9.77E-05 | 9.47E-05 | 9.05E-05 | 8.52E-05 | 7.88E-05 | 7.14E-05 | 6.35E-05 | 5.66E-05 |
| SE 78 | 1.42E-04 | 1.51E-04 | 1.64E-04 | 1.76E-04 | 1.87E-04 | 1.96E-04 | 2.02E-04 | 2.05E-04 | 2.06E-04 | 2.05E-04 | 2.01E-04 | 1.94E-04 | 1.85E-04 | 1.74E-04 | 1.61E-04 | 1.45E-04 | 1.29E-04 | 1.14E-04 |
| SE 79 | 2.16E-04 | 2.30E-04 | 2.51E-04 | 2.71E-04 | 2.88E-04 | 3.01E-04 | 3.10E-04 | 3.16E-04 | 3.17E-04 | 3.15E-04 | 3.09E-04 | 2.99E-04 | 2.85E-04 | 2.67E-04 | 2.47E-04 | 2.23E-04 | 1.97E-04 | 1.74E-04 |

| | | | | | | | | | | | | | | | | | | |
|---|---|---|---|---|---|---|---|---|---|---|---|---|---|---|---|---|---|---|
| BR 79 | 4.62E-08 | 4.94E-08 | 5.39E-08 | 5.81E-08 | 6.17E-08 | 6.45E-08 | 6.65E-08 | 6.76E-08 | 6.80E-08 | 6.75E-08 | 6.61E-08 | 6.40E-08 | 6.10E-08 | 5.73E-08 | 5.28E-08 | 4.77E-08 | 4.22E-08 | 3.72E-08 |
| SE 80 | 4.63E-04 | 4.91E-04 | 5.34E-04 | 5.75E-04 | 6.10E-04 | 6.37E-04 | 6.56E-04 | 6.67E-04 | 6.70E-04 | 6.66E-04 | 6.53E-04 | 6.32E-04 | 6.04E-04 | 5.67E-04 | 5.24E-04 | 4.74E-04 | 4.20E-04 | 3.74E-04 |
| BR 81 | 7.36E-04 | 7.82E-04 | 8.49E-04 | 9.12E-04 | 9.65E-04 | 1.01E-03 | 1.04E-03 | 1.05E-03 | 1.06E-03 | 1.05E-03 | 1.03E-03 | 9.99E-04 | 9.56E-04 | 9.00E-04 | 8.32E-04 | 7.55E-04 | 6.71E-04 | 5.97E-04 |
| SE 82 | 1.07E-03 | 1.14E-03 | 1.24E-03 | 1.34E-03 | 1.42E-03 | 1.49E-03 | 1.53E-03 | 1.56E-03 | 1.56E-03 | 1.55E-03 | 1.52E-03 | 1.47E-03 | 1.41E-03 | 1.32E-03 | 1.22E-03 | 1.10E-03 | 9.76E-04 | 8.64E-04 |

Position=Segment location (midpoint of 2-in. segment) from bottom of fuel (BOF); 2-in of fuel ~14.2g.

Table A-1c. Composition (grams) in 2-inch fuel segment: ORIGEN calculation results for Pin195011, decayed to 3/11/2011.

| Position: | 1 | 3 | 5 | 7 | 9 | 11 | 13 | 15 | 17 | 19 | 21 | 23 | 25 | 27 | 29 | 31 | 33 | 35 |
|---|---|---|---|---|---|---|---|---|---|---|---|---|---|---|---|---|---|---|
| KR 82 | 1.70E-05 | 2.07E-05 | 2.53E-05 | 2.99E-05 | 3.40E-05 | 3.74E-05 | 4.00E-05 | 4.15E-05 | 4.19E-05 | 4.13E-05 | 3.95E-05 | 3.69E-05 | 3.34E-05 | 2.92E-05 | 2.45E-05 | 1.97E-05 | 1.51E-05 | 1.11E-05 |
| KR 83 | 1.84E-03 | 1.95E-03 | 2.12E-03 | 2.27E-03 | 2.41E-03 | 2.51E-03 | 2.58E-03 | 2.63E-03 | 2.64E-03 | 2.62E-03 | 2.57E-03 | 2.49E-03 | 2.38E-03 | 2.24E-03 | 2.08E-03 | 1.88E-03 | 1.68E-03 | 1.49E-03 |
| KR 84 | 3.54E-03 | 3.78E-03 | 4.12E-03 | 4.44E-03 | 4.72E-03 | 4.94E-03 | 5.09E-03 | 5.18E-03 | 5.21E-03 | 5.17E-03 | 5.07E-03 | 4.90E-03 | 4.67E-03 | 4.38E-03 | 4.04E-03 | 3.64E-03 | 3.22E-03 | 2.85E-03 |
| KR 85 | 2.49E-04 | 2.65E-04 | 2.89E-04 | 3.11E-04 | 3.30E-04 | 3.45E-04 | 3.56E-04 | 3.62E-04 | 3.64E-04 | 3.61E-04 | 3.54E-04 | 3.43E-04 | 3.27E-04 | 3.07E-04 | 2.83E-04 | 2.56E-04 | 2.27E-04 | 2.01E-04 |
| RB 85 | 3.99E-03 | 4.23E-03 | 4.59E-03 | 4.94E-03 | 5.24E-03 | 5.47E-03 | 5.63E-03 | 5.73E-03 | 5.76E-03 | 5.72E-03 | 5.61E-03 | 5.43E-03 | 5.19E-03 | 4.88E-03 | 4.50E-03 | 4.08E-03 | 3.62E-03 | 3.23E-03 |
| KR 86 | 6.60E-03 | 7.01E-03 | 7.62E-03 | 8.21E-03 | 8.70E-03 | 9.09E-03 | 9.37E-03 | 9.53E-03 | 9.58E-03 | 9.51E-03 | 9.32E-03 | 9.02E-03 | 8.62E-03 | 8.10E-03 | 7.47E-03 | 6.76E-03 | 5.99E-03 | 5.33E-03 |
| RB 86 | 0.00E+00 | 0.00E+00 | 0.00E+00 | 0.00E+00 | 0.00E+00 | 0.00E+00 | 0.00E+00 | 0.00E+00 | 0.00E+00 | 0.00E+00 | 0.00E+00 | 0.00E+00 | 0.00E+00 | 0.00E+00 | 0.00E+00 | 0.00E+00 | 0.00E+00 | 0.00E+00 |
| SR 86 | 3.72E-05 | 4.56E-05 | 5.58E-05 | 6.61E-05 | 7.54E-05 | 8.32E-05 | 8.89E-05 | 9.24E-05 | 9.34E-05 | 9.19E-05 | 8.80E-05 | 8.19E-05 | 7.40E-05 | 6.45E-05 | 5.41E-05 | 4.33E-05 | 3.30E-05 | 2.42E-05 |
| RB 87 | 8.40E-03 | 8.92E-03 | 9.70E-03 | 1.04E-02 | 1.11E-02 | 1.16E-02 | 1.19E-02 | 1.21E-02 | 1.22E-02 | 1.21E-02 | 1.19E-02 | 1.15E-02 | 1.10E-02 | 1.03E-02 | 9.51E-03 | 8.60E-03 | 7.63E-03 | 6.79E-03 |
| SR 87 | 1.75E-07 | 2.15E-07 | 2.69E-07 | 3.28E-07 | 3.84E-07 | 4.33E-07 | 4.71E-07 | 4.94E-07 | 5.01E-07 | 4.91E-07 | 4.65E-07 | 4.25E-07 | 3.75E-07 | 3.19E-07 | 2.60E-07 | 2.04E-07 | 1.55E-07 | 1.17E-07 |
| SR 88 | 1.24E-02 | 1.31E-02 | 1.43E-02 | 1.54E-02 | 1.63E-02 | 1.70E-02 | 1.75E-02 | 1.78E-02 | 1.79E-02 | 1.78E-02 | 1.74E-02 | 1.69E-02 | 1.61E-02 | 1.52E-02 | 1.40E-02 | 1.27E-02 | 1.12E-02 | 9.99E-03 |
| SR 89 | 1.37E-42 | 1.37E-42 | 1.50E-42 | 1.62E-42 | 1.75E-42 | 1.75E-42 | 1.87E-42 | 1.87E-42 | 1.87E-42 | 1.87E-42 | 1.87E-42 | 1.75E-42 | 1.75E-42 | 1.62E-42 | 1.50E-42 | 1.37E-42 | 1.25E-42 | 1.12E-42 |
| Y 89 | 1.56E-02 | 1.66E-02 | 1.80E-02 | 1.94E-02 | 2.06E-02 | 2.15E-02 | 2.21E-02 | 2.25E-02 | 2.26E-02 | 2.24E-02 | 2.20E-02 | 2.13E-02 | 2.04E-02 | 1.91E-02 | 1.77E-02 | 1.60E-02 | 1.42E-02 | 1.26E-02 |
| SR 90 | 1.17E-02 | 1.24E-02 | 1.35E-02 | 1.45E-02 | 1.54E-02 | 1.61E-02 | 1.65E-02 | 1.68E-02 | 1.69E-02 | 1.68E-02 | 1.65E-02 | 1.59E-02 | 1.52E-02 | 1.43E-02 | 1.32E-02 | 1.19E-02 | 1.06E-02 | 9.44E-03 |
| Y 90 | 2.93E-06 | 3.11E-06 | 3.38E-06 | 3.63E-06 | 3.85E-06 | 4.02E-06 | 4.15E-06 | 4.22E-06 | 4.24E-06 | 4.21E-06 | 4.13E-06 | 3.99E-06 | 3.81E-06 | 3.59E-06 | 3.31E-06 | 3.00E-06 | 2.66E-06 | 2.37E-06 |
| ZR 90 | 7.37E-03 | 7.82E-03 | 8.50E-03 | 9.15E-03 | 9.70E-03 | 1.01E-02 | 1.05E-02 | 1.06E-02 | 1.07E-02 | 1.06E-02 | 1.04E-02 | 1.01E-02 | 9.60E-03 | 9.02E-03 | 8.32E-03 | 7.53E-03 | 6.68E-03 | 5.95E-03 |
| Y 91 | 4.34E-37 | 4.62E-37 | 4.99E-37 | 5.33E-37 | 5.61E-37 | 5.82E-37 | 5.98E-37 | 6.06E-37 | 6.09E-37 | 6.06E-37 | 5.97E-37 | 5.82E-37 | 5.60E-37 | 5.31E-37 | 4.95E-37 | 4.53E-37 | 4.06E-37 | 3.63E-37 |
| ZR 91 | 1.98E-02 | 2.10E-02 | 2.28E-02 | 2.46E-02 | 2.60E-02 | 2.72E-02 | 2.80E-02 | 2.85E-02 | 2.86E-02 | 2.84E-02 | 2.79E-02 | 2.70E-02 | 2.58E-02 | 2.42E-02 | 2.24E-02 | 2.02E-02 | 1.80E-02 | 1.60E-02 |
| ZR 92 | 2.09E-02 | 2.22E-02 | 2.41E-02 | 2.60E-02 | 2.76E-02 | 2.88E-02 | 2.97E-02 | 3.02E-02 | 3.04E-02 | 3.02E-02 | 2.96E-02 | 2.86E-02 | 2.73E-02 | 2.56E-02 | 2.37E-02 | 2.14E-02 | 1.89E-02 | 1.68E-02 |
| ZR 93 | 2.29E-02 | 2.44E-02 | 2.65E-02 | 2.86E-02 | 3.03E-02 | 3.17E-02 | 3.27E-02 | 3.32E-02 | 3.34E-02 | 3.32E-02 | 3.25E-02 | 3.15E-02 | 3.00E-02 | 2.82E-02 | 2.60E-02 | 2.35E-02 | 2.08E-02 | 1.85E-02 |
| KR 83 | 1.84E-03 | 1.95E-03 | 2.12E-03 | 2.27E-03 | 2.41E-03 | 2.51E-03 | 2.58E-03 | 2.63E-03 | 2.64E-03 | 2.62E-03 | 2.57E-03 | 2.49E-03 | 2.38E-03 | 2.24E-03 | 2.08E-03 | 1.88E-03 | 1.68E-03 | 1.49E-03 |
| KR 84 | 3.54E-03 | 3.78E-03 | 4.12E-03 | 4.44E-03 | 4.72E-03 | 4.94E-03 | 5.09E-03 | 5.18E-03 | 5.21E-03 | 5.17E-03 | 5.07E-03 | 4.90E-03 | 4.67E-03 | 4.38E-03 | 4.04E-03 | 3.64E-03 | 3.22E-03 | 2.85E-03 |
| KR 85 | 2.49E-04 | 2.65E-04 | 2.89E-04 | 3.11E-04 | 3.30E-04 | 3.45E-04 | 3.56E-04 | 3.62E-04 | 3.64E-04 | 3.61E-04 | 3.54E-04 | 3.43E-04 | 3.27E-04 | 3.07E-04 | 2.83E-04 | 2.56E-04 | 2.27E-04 | 2.01E-04 |
| RB 85 | 3.99E-03 | 4.23E-03 | 4.59E-03 | 4.94E-03 | 5.24E-03 | 5.47E-03 | 5.63E-03 | 5.73E-03 | 5.76E-03 | 5.72E-03 | 5.61E-03 | 5.43E-03 | 5.19E-03 | 4.88E-03 | 4.50E-03 | 4.08E-03 | 3.62E-03 | 3.23E-03 |

Position=Segment location (midpoint of 2-in. segment) from bottom of fuel (BOF); 2 in. of fuel ~14.2g.

Table A-1d. Composition (grams) in 2-inch fuel segment: ORIGEN calculation results for Pin195011, decayed to 3/11/2011.

| Position: | 1 | 3 | 5 | 7 | 9 | 11 | 13 | 15 | 17 | 19 | 21 | 23 | 25 | 27 | 29 | 31 | 33 | 35 |
|---|---|---|---|---|---|---|---|---|---|---|---|---|---|---|---|---|---|---|
| KR 86 | 6.60E-03 | 7.01E-03 | 7.62E-03 | 8.21E-03 | 8.70E-03 | 9.09E-03 | 9.37E-03 | 9.53E-03 | 9.58E-03 | 9.51E-03 | 9.32E-03 | 9.02E-03 | 8.62E-03 | 8.10E-03 | 7.47E-03 | 6.76E-03 | 5.99E-03 | 5.33E-03 |
| RB 86 | 0.00E+00 | 0.00E+00 | 0.00E+00 | 0.00E+00 | 0.00E+00 | 0.00E+00 | 0.00E+00 | 0.00E+00 | 0.00E+00 | 0.00E+00 | 0.00E+00 | 0.00E+00 | 0.00E+00 | 0.00E+00 | 0.00E+00 | 0.00E+00 | 0.00E+00 | 0.00E+00 |
| SR 86 | 3.72E-05 | 4.56E-05 | 5.58E-05 | 6.61E-05 | 7.54E-05 | 8.32E-05 | 8.89E-05 | 9.24E-05 | 9.34E-05 | 9.19E-05 | 8.80E-05 | 8.19E-05 | 7.40E-05 | 6.45E-05 | 5.41E-05 | 4.33E-05 | 3.30E-05 | 2.42E-05 |
| RB 87 | 8.40E-03 | 8.92E-03 | 9.70E-03 | 1.04E-02 | 1.11E-02 | 1.16E-02 | 1.19E-02 | 1.21E-02 | 1.22E-02 | 1.21E-02 | 1.19E-02 | 1.15E-02 | 1.10E-02 | 1.03E-02 | 9.51E-03 | 8.60E-03 | 7.63E-03 | 6.79E-03 |
| SR 87 | 1.75E-07 | 2.15E-07 | 2.69E-07 | 3.28E-07 | 3.84E-07 | 4.33E-07 | 4.71E-07 | 4.94E-07 | 5.01E-07 | 4.91E-07 | 4.65E-07 | 4.25E-07 | 3.75E-07 | 3.19E-07 | 2.60E-07 | 2.04E-07 | 1.55E-07 | 1.17E-07 |
| SR 88 | 1.24E-02 | 1.31E-02 | 1.43E-02 | 1.54E-02 | 1.63E-02 | 1.70E-02 | 1.75E-02 | 1.78E-02 | 1.79E-02 | 1.78E-02 | 1.74E-02 | 1.69E-02 | 1.61E-02 | 1.52E-02 | 1.40E-02 | 1.27E-02 | 1.12E-02 | 9.99E-03 |
| SR 89 | 1.37E-42 | 1.37E-42 | 1.50E-42 | 1.62E-42 | 1.75E-42 | 1.75E-42 | 1.87E-42 | 1.87E-42 | 1.87E-42 | 1.87E-42 | 1.87E-42 | 1.75E-42 | 1.75E-42 | 1.62E-42 | 1.50E-42 | 1.37E-42 | 1.25E-42 | 1.12E-42 |
| Y 89 | 1.56E-02 | 1.66E-02 | 1.80E-02 | 1.94E-02 | 2.06E-02 | 2.15E-02 | 2.21E-02 | 2.25E-02 | 2.26E-02 | 2.24E-02 | 2.20E-02 | 2.13E-02 | 2.04E-02 | 1.91E-02 | 1.77E-02 | 1.60E-02 | 1.42E-02 | 1.26E-02 |
| SR 90 | 1.17E-02 | 1.24E-02 | 1.35E-02 | 1.45E-02 | 1.54E-02 | 1.61E-02 | 1.65E-02 | 1.68E-02 | 1.69E-02 | 1.68E-02 | 1.65E-02 | 1.59E-02 | 1.52E-02 | 1.43E-02 | 1.32E-02 | 1.19E-02 | 1.06E-02 | 9.44E-03 |
| Y 90 | 2.93E-06 | 3.11E-06 | 3.38E-06 | 3.63E-06 | 3.85E-06 | 4.02E-06 | 4.15E-06 | 4.22E-06 | 4.24E-06 | 4.21E-06 | 4.13E-06 | 3.99E-06 | 3.81E-06 | 3.59E-06 | 3.31E-06 | 3.00E-06 | 2.66E-06 | 2.37E-06 |
| ZR 90 | 7.37E-03 | 7.82E-03 | 8.50E-03 | 9.15E-03 | 9.70E-03 | 1.01E-02 | 1.05E-02 | 1.06E-02 | 1.07E-02 | 1.06E-02 | 1.04E-02 | 1.01E-02 | 9.60E-03 | 9.02E-03 | 8.32E-03 | 7.53E-03 | 6.68E-03 | 5.95E-03 |
| Y 91 | 4.34E-37 | 4.62E-37 | 4.99E-37 | 5.33E-37 | 5.61E-37 | 5.82E-37 | 5.98E-37 | 6.06E-37 | 6.09E-37 | 6.06E-37 | 5.97E-37 | 5.82E-37 | 5.60E-37 | 5.31E-37 | 4.95E-37 | 4.53E-37 | 4.06E-37 | 3.63E-37 |
| ZR 91 | 1.98E-02 | 2.10E-02 | 2.28E-02 | 2.46E-02 | 2.60E-02 | 2.72E-02 | 2.80E-02 | 2.85E-02 | 2.86E-02 | 2.84E-02 | 2.79E-02 | 2.70E-02 | 2.58E-02 | 2.42E-02 | 2.24E-02 | 2.02E-02 | 1.80E-02 | 1.60E-02 |
| ZR 92 | 2.09E-02 | 2.22E-02 | 2.41E-02 | 2.60E-02 | 2.76E-02 | 2.88E-02 | 2.97E-02 | 3.02E-02 | 3.04E-02 | 3.02E-02 | 2.96E-02 | 2.86E-02 | 2.73E-02 | 2.56E-02 | 2.37E-02 | 2.14E-02 | 1.89E-02 | 1.68E-02 |
| ZR 93 | 2.29E-02 | 2.44E-02 | 2.65E-02 | 2.86E-02 | 3.03E-02 | 3.17E-02 | 3.27E-02 | 3.32E-02 | 3.34E-02 | 3.32E-02 | 3.25E-02 | 3.15E-02 | 3.00E-02 | 2.82E-02 | 2.60E-02 | 2.35E-02 | 2.08E-02 | 1.85E-02 |
| NB 93 | 8.49E-08 | 9.03E-08 | 9.82E-08 | 1.06E-07 | 1.12E-07 | 1.17E-07 | 1.21E-07 | 1.23E-07 | 1.24E-07 | 1.23E-07 | 1.20E-07 | 1.17E-07 | 1.11E-07 | 1.04E-07 | 9.62E-08 | 8.70E-08 | 7.70E-08 | 6.84E-08 |
| NB 93M | 1.24E-07 | 1.32E-07 | 1.44E-07 | 1.55E-07 | 1.64E-07 | 1.72E-07 | 1.77E-07 | 1.80E-07 | 1.81E-07 | 1.80E-07 | 1.76E-07 | 1.70E-07 | 1.63E-07 | 1.53E-07 | 1.41E-07 | 1.27E-07 | 1.13E-07 | 1.00E-07 |
| ZR 94 | 2.22E-02 | 2.36E-02 | 2.57E-02 | 2.78E-02 | 2.95E-02 | 3.08E-02 | 3.18E-02 | 3.23E-02 | 3.25E-02 | 3.23E-02 | 3.16E-02 | 3.06E-02 | 2.92E-02 | 2.74E-02 | 2.52E-02 | 2.28E-02 | 2.02E-02 | 1.79E-02 |
| ZR 95 | 4.34E-34 | 4.63E-34 | 5.01E-34 | 5.37E-34 | 5.66E-34 | 5.89E-34 | 6.05E-34 | 6.14E-34 | 6.18E-34 | 6.14E-34 | 6.04E-34 | 5.88E-34 | 5.65E-34 | 5.35E-34 | 4.97E-34 | 4.54E-34 | 4.05E-34 | 3.61E-34 |
| NB 95 | 2.44E-34 | 2.61E-34 | 2.82E-34 | 3.02E-34 | 3.19E-34 | 3.32E-34 | 3.41E-34 | 3.46E-34 | 3.48E-34 | 3.46E-34 | 3.40E-34 | 3.31E-34 | 3.18E-34 | 3.01E-34 | 2.80E-34 | 2.55E-34 | 2.28E-34 | 2.03E-34 |
| NB 95M | 1.72E-37 | 1.83E-37 | 1.98E-37 | 2.12E-37 | 2.24E-37 | 2.33E-37 | 2.39E-37 | 2.43E-37 | 2.44E-37 | 2.43E-37 | 2.39E-37 | 2.32E-37 | 2.23E-37 | 2.11E-37 | 1.97E-37 | 1.79E-37 | 1.60E-37 | 1.43E-37 |
| MO 95 | 2.35E-02 | 2.50E-02 | 2.72E-02 | 2.92E-02 | 3.10E-02 | 3.24E-02 | 3.34E-02 | 3.39E-02 | 3.41E-02 | 3.38E-02 | 3.32E-02 | 3.21E-02 | 3.07E-02 | 2.88E-02 | 2.66E-02 | 2.41E-02 | 2.14E-02 | 1.90E-02 |
| ZR 96 | 2.34E-02 | 2.50E-02 | 2.72E-02 | 2.93E-02 | 3.11E-02 | 3.26E-02 | 3.36E-02 | 3.41E-02 | 3.43E-02 | 3.41E-02 | 3.34E-02 | 3.23E-02 | 3.08E-02 | 2.89E-02 | 2.66E-02 | 2.41E-02 | 2.13E-02 | 1.89E-02 |
| MO 96 | 2.90E-04 | 3.57E-04 | 4.38E-04 | 5.18E-04 | 5.92E-04 | 6.54E-04 | 6.99E-04 | 7.27E-04 | 7.35E-04 | 7.23E-04 | 6.92E-04 | 6.44E-04 | 5.81E-04 | 5.06E-04 | 4.24E-04 | 3.39E-04 | 2.58E-04 | 1.88E-04 |

Position=Segment location (midpoint of 2-in. segment) from bottom of fuel (BOF); 2 in. of fuel ~14.2g.

Table A-1e. Composition (grams) in 2-inch fuel segment: ORIGEN calculation results for Pin195011, decayed to 3/11/2011.

| Position: | 1 | 3 | 5 | 7 | 9 | 11 | 13 | 15 | 17 | 19 | 21 | 23 | 25 | 27 | 29 | 31 | 33 | 35 |
|---|---|---|---|---|---|---|---|---|---|---|---|---|---|---|---|---|---|---|
| MO 97 | 2.26E-02 | 2.41E-02 | 2.62E-02 | 2.82E-02 | 2.99E-02 | 3.13E-02 | 3.22E-02 | 3.28E-02 | 3.29E-02 | 3.27E-02 | 3.21E-02 | 3.10E-02 | 2.96E-02 | 2.78E-02 | 2.57E-02 | 2.32E-02 | 2.06E-02 | 1.83E-02 |
| MO 98 | 2.34E-02 | 2.50E-02 | 2.72E-02 | 2.94E-02 | 3.13E-02 | 3.28E-02 | 3.38E-02 | 3.44E-02 | 3.46E-02 | 3.43E-02 | 3.36E-02 | 3.25E-02 | 3.10E-02 | 2.90E-02 | 2.67E-02 | 2.41E-02 | 2.12E-02 | 1.88E-02 |
| TC 98 | 4.83E-07 | 5.95E-07 | 7.32E-07 | 8.68E-07 | 9.92E-07 | 1.10E-06 | 1.17E-06 | 1.22E-06 | 1.23E-06 | 1.21E-06 | 1.16E-06 | 1.08E-06 | 9.73E-07 | 8.47E-07 | 7.09E-07 | 5.66E-07 | 4.29E-07 | 3.12E-07 |
| TC 99 | 2.24E-02 | 2.38E-02 | 2.59E-02 | 2.79E-02 | 2.96E-02 | 3.09E-02 | 3.18E-02 | 3.24E-02 | 3.25E-02 | 3.23E-02 | 3.17E-02 | 3.07E-02 | 2.93E-02 | 2.75E-02 | 2.54E-02 | 2.30E-02 | 2.04E-02 | 1.81E-02 |
| RU 99 | 1.46E-06 | 1.56E-06 | 1.69E-06 | 1.82E-06 | 1.93E-06 | 2.02E-06 | 2.08E-06 | 2.12E-06 | 2.13E-06 | 2.11E-06 | 2.07E-06 | 2.00E-06 | 1.91E-06 | 1.80E-06 | 1.66E-06 | 1.50E-06 | 1.33E-06 | 1.18E-06 |
| MO100 | 2.50E-02 | 2.67E-02 | 2.91E-02 | 3.14E-02 | 3.33E-02 | 3.48E-02 | 3.59E-02 | 3.66E-02 | 3.67E-02 | 3.65E-02 | 3.57E-02 | 3.46E-02 | 3.30E-02 | 3.09E-02 | 2.85E-02 | 2.57E-02 | 2.27E-02 | 2.01E-02 |
| RU100 | 5.32E-04 | 6.55E-04 | 8.05E-04 | 9.54E-04 | 1.09E-03 | 1.20E-03 | 1.29E-03 | 1.34E-03 | 1.35E-03 | 1.33E-03 | 1.27E-03 | 1.19E-03 | 1.07E-03 | 9.31E-04 | 7.80E-04 | 6.24E-04 | 4.73E-04 | 3.44E-04 |
| RU101 | 2.17E-02 | 2.31E-02 | 2.52E-02 | 2.71E-02 | 2.88E-02 | 3.01E-02 | 3.10E-02 | 3.15E-02 | 3.16E-02 | 3.14E-02 | 3.08E-02 | 2.98E-02 | 2.85E-02 | 2.67E-02 | 2.47E-02 | 2.23E-02 | 1.98E-02 | 1.75E-02 |
| RU102 | 1.98E-02 | 2.13E-02 | 2.33E-02 | 2.53E-02 | 2.70E-02 | 2.83E-02 | 2.92E-02 | 2.98E-02 | 2.99E-02 | 2.97E-02 | 2.91E-02 | 2.81E-02 | 2.67E-02 | 2.49E-02 | 2.29E-02 | 2.05E-02 | 1.80E-02 | 1.58E-02 |
| RH102 | 9.34E-10 | 1.16E-09 | 1.43E-09 | 1.70E-09 | 1.94E-09 | 2.15E-09 | 2.30E-09 | 2.39E-09 | 2.42E-09 | 2.38E-09 | 2.28E-09 | 2.12E-09 | 1.91E-09 | 1.66E-09 | 1.39E-09 | 1.11E-09 | 8.36E-10 | 6.04E-10 |
| RU103 | 0.00E+00 | 0.00E+00 | 0.00E+00 | 0.00E+00 | 0.00E+00 | 0.00E+00 | 0.00E+00 | 0.00E+00 | 0.00E+00 | 0.00E+00 | 0.00E+00 | 0.00E+00 | 0.00E+00 | 0.00E+00 | 0.00E+00 | 0.00E+00 | 0.00E+00 | 0.00E+00 |
| RH103 | 1.43E-02 | 1.54E-02 | 1.68E-02 | 1.81E-02 | 1.93E-02 | 2.02E-02 | 2.08E-02 | 2.12E-02 | 2.13E-02 | 2.11E-02 | 2.07E-02 | 2.00E-02 | 1.91E-02 | 1.79E-02 | 1.64E-02 | 1.48E-02 | 1.31E-02 | 1.15E-02 |
| RH103M | 0.00E+00 | 0.00E+00 | 0.00E+00 | 0.00E+00 | 0.00E+00 | 0.00E+00 | 0.00E+00 | 0.00E+00 | 0.00E+00 | 0.00E+00 | 0.00E+00 | 0.00E+00 | 0.00E+00 | 0.00E+00 | 0.00E+00 | 0.00E+00 | 0.00E+00 | 0.00E+00 |
| RU104 | 1.08E-02 | 1.17E-02 | 1.28E-02 | 1.39E-02 | 1.49E-02 | 1.56E-02 | 1.62E-02 | 1.65E-02 | 1.65E-02 | 1.64E-02 | 1.61E-02 | 1.55E-02 | 1.47E-02 | 1.37E-02 | 1.26E-02 | 1.13E-02 | 9.87E-03 | 8.58E-03 |
| PD104 | 5.13E-04 | 6.36E-04 | 7.84E-04 | 9.31E-04 | 1.06E-03 | 1.18E-03 | 1.26E-03 | 1.31E-03 | 1.32E-03 | 1.30E-03 | 1.25E-03 | 1.16E-03 | 1.04E-03 | 9.09E-04 | 7.60E-04 | 6.07E-04 | 4.59E-04 | 3.32E-04 |
| PD105 | 6.07E-03 | 6.62E-03 | 7.30E-03 | 7.93E-03 | 8.46E-03 | 8.89E-03 | 9.18E-03 | 9.36E-03 | 9.41E-03 | 9.34E-03 | 9.13E-03 | 8.81E-03 | 8.37E-03 | 7.82E-03 | 7.16E-03 | 6.41E-03 | 5.60E-03 | 4.84E-03 |
| RU106 | 4.25E-09 | 4.70E-09 | 5.25E-09 | 5.76E-09 | 6.21E-09 | 6.56E-09 | 6.81E-09 | 6.96E-09 | 7.01E-09 | 6.94E-09 | 6.78E-09 | 6.51E-09 | 6.15E-09 | 5.69E-09 | 5.16E-09 | 4.57E-09 | 3.94E-09 | 3.34E-09 |
| PD106 | 3.93E-03 | 4.39E-03 | 4.93E-03 | 5.45E-03 | 5.90E-03 | 6.26E-03 | 6.51E-03 | 6.67E-03 | 6.71E-03 | 6.65E-03 | 6.47E-03 | 6.19E-03 | 5.82E-03 | 5.36E-03 | 4.83E-03 | 4.24E-03 | 3.62E-03 | 3.05E-03 |
| PD107 | 2.39E-03 | 2.63E-03 | 2.92E-03 | 3.20E-03 | 3.44E-03 | 3.63E-03 | 3.76E-03 | 3.84E-03 | 3.86E-03 | 3.83E-03 | 3.74E-03 | 3.59E-03 | 3.40E-03 | 3.15E-03 | 2.86E-03 | 2.54E-03 | 2.20E-03 | 1.88E-03 |
| AG107 | 5.11E-09 | 5.61E-09 | 6.24E-09 | 6.82E-09 | 7.33E-09 | 7.74E-09 | 8.02E-09 | 8.19E-09 | 8.24E-09 | 8.17E-09 | 7.97E-09 | 7.66E-09 | 7.24E-09 | 6.72E-09 | 6.11E-09 | 5.42E-09 | 4.69E-09 | 4.01E-09 |
| PD108 | 1.62E-03 | 1.79E-03 | 2.01E-03 | 2.22E-03 | 2.40E-03 | 2.55E-03 | 2.65E-03 | 2.71E-03 | 2.73E-03 | 2.71E-03 | 2.63E-03 | 2.52E-03 | 2.37E-03 | 2.18E-03 | 1.97E-03 | 1.73E-03 | 1.48E-03 | 1.25E-03 |

| | | | | | | | | | | | | | | | | | | |
|---|---|---|---|---|---|---|---|---|---|---|---|---|---|---|---|---|---|---|
| CD108 | 1.83E-08 | 2.33E-08 | 2.92E-08 | 3.51E-08 | 4.05E-08 | 4.51E-08 | 4.85E-08 | 5.06E-08 | 5.12E-08 | 5.03E-08 | 4.80E-08 | 4.43E-08 | 3.97E-08 | 3.42E-08 | 2.82E-08 | 2.22E-08 | 1.65E-08 | 1.16E-08 |
| AG109 | 1.11E-03 | 1.23E-03 | 1.37E-03 | 1.50E-03 | 1.62E-03 | 1.71E-03 | 1.78E-03 | 1.82E-03 | 1.83E-03 | 1.81E-03 | 1.77E-03 | 1.70E-03 | 1.60E-03 | 1.48E-03 | 1.34E-03 | 1.18E-03 | 1.02E-03 | 8.66E-04 |
| PD110 | 7.83E-04 | 8.65E-04 | 9.60E-04 | 1.05E-03 | 1.12E-03 | 1.18E-03 | 1.22E-03 | 1.25E-03 | 1.26E-03 | 1.25E-03 | 1.22E-03 | 1.17E-03 | 1.11E-03 | 1.03E-03 | 9.42E-04 | 8.39E-04 | 7.28E-04 | 6.20E-04 |

Position=Segment location (midpoint of 2-in. segment) from bottom of fuel (BOF); 2 in. of fuel ~14.2g.

Table A-1f. Composition (grams) in 2-inch fuel segment: ORIGEN calculation results for Pin195011, decayed to 3/11/2011.

| Position: | 1 | 3 | 5 | 7 | 9 | 11 | 13 | 15 | 17 | 19 | 21 | 23 | 25 | 27 | 29 | 31 | 33 | 35 |
|---|---|---|---|---|---|---|---|---|---|---|---|---|---|---|---|---|---|---|
| AG110M | 1.59E-14 | 2.02E-14 | 2.54E-14 | 3.06E-14 | 3.54E-14 | 3.94E-14 | 4.24E-14 | 4.42E-14 | 4.48E-14 | 4.40E-14 | 4.20E-14 | 3.88E-14 | 3.48E-14 | 2.99E-14 | 2.47E-14 | 1.94E-14 | 1.44E-14 | 1.01E-14 |
| CD110 | 3.25E-05 | 4.14E-05 | 5.19E-05 | 6.24E-05 | 7.20E-05 | 8.02E-05 | 8.62E-05 | 8.99E-05 | 9.10E-05 | 8.94E-05 | 8.53E-05 | 7.88E-05 | 7.06E-05 | 6.08E-05 | 5.02E-05 | 3.95E-05 | 2.93E-05 | 2.06E-05 |
| AG111 | 0.00E+00 | 0.00E+00 | 0.00E+00 | 0.00E+00 | 0.00E+00 | 0.00E+00 | 0.00E+00 | 0.00E+00 | 0.00E+00 | 0.00E+00 | 0.00E+00 | 0.00E+00 | 0.00E+00 | 0.00E+00 | 0.00E+00 | 0.00E+00 | 0.00E+00 | 0.00E+00 |
| CD111 | 6.29E-04 | 6.96E-04 | 7.72E-04 | 8.39E-04 | 8.97E-04 | 9.42E-04 | 9.73E-04 | 9.92E-04 | 9.97E-04 | 9.89E-04 | 9.68E-04 | 9.34E-04 | 8.88E-04 | 8.29E-04 | 7.58E-04 | 6.79E-04 | 5.90E-04 | 5.03E-04 |
| CD112 | 5.58E-04 | 6.21E-04 | 6.89E-04 | 7.50E-04 | 8.01E-04 | 8.41E-04 | 8.69E-04 | 8.85E-04 | 8.90E-04 | 8.83E-04 | 8.64E-04 | 8.34E-04 | 7.93E-04 | 7.41E-04 | 6.78E-04 | 6.07E-04 | 5.27E-04 | 4.48E-04 |
| CD113 | 5.27E-04 | 5.83E-04 | 6.44E-04 | 6.98E-04 | 7.44E-04 | 7.79E-04 | 8.04E-04 | 8.18E-04 | 8.22E-04 | 8.16E-04 | 7.99E-04 | 7.73E-04 | 7.37E-04 | 6.90E-04 | 6.34E-04 | 5.70E-04 | 4.98E-04 | 4.25E-04 |
| CD113M | 3.61E-06 | 4.04E-06 | 4.51E-06 | 4.94E-06 | 5.30E-06 | 5.58E-06 | 5.79E-06 | 5.90E-06 | 5.94E-06 | 5.89E-06 | 5.75E-06 | 5.54E-06 | 5.25E-06 | 4.88E-06 | 4.44E-06 | 3.95E-06 | 3.41E-06 | 2.88E-06 |
| IN113 | 5.74E-06 | 6.41E-06 | 7.15E-06 | 7.82E-06 | 8.39E-06 | 8.84E-06 | 9.16E-06 | 9.34E-06 | 9.40E-06 | 9.32E-06 | 9.10E-06 | 8.76E-06 | 8.30E-06 | 7.72E-06 | 7.03E-06 | 6.26E-06 | 5.41E-06 | 4.57E-06 |
| CD114 | 5.03E-04 | 5.54E-04 | 6.11E-04 | 6.62E-04 | 7.05E-04 | 7.39E-04 | 7.62E-04 | 7.76E-04 | 7.80E-04 | 7.74E-04 | 7.58E-04 | 7.33E-04 | 6.99E-04 | 6.54E-04 | 6.01E-04 | 5.40E-04 | 4.72E-04 | 4.05E-04 |
| SN114 | 1.49E-08 | 1.92E-08 | 2.39E-08 | 2.86E-08 | 3.29E-08 | 3.65E-08 | 3.91E-08 | 4.07E-08 | 4.11E-08 | 4.05E-08 | 3.86E-08 | 3.59E-08 | 3.22E-08 | 2.80E-08 | 2.32E-08 | 1.84E-08 | 1.37E-08 | 9.60E-09 |
| CD115M | 0.00E+00 | 0.00E+00 | 0.00E+00 | 0.00E+00 | 0.00E+00 | 0.00E+00 | 0.00E+00 | 0.00E+00 | 0.00E+00 | 0.00E+00 | 0.00E+00 | 0.00E+00 | 0.00E+00 | 0.00E+00 | 0.00E+00 | 0.00E+00 | 0.00E+00 | 0.00E+00 |
| IN115 | 4.04E-04 | 4.35E-04 | 4.67E-04 | 4.93E-04 | 5.14E-04 | 5.30E-04 | 5.40E-04 | 5.46E-04 | 5.48E-04 | 5.45E-04 | 5.38E-04 | 5.27E-04 | 5.11E-04 | 4.89E-04 | 4.61E-04 | 4.27E-04 | 3.85E-04 | 3.40E-04 |
| SN115 | 1.76E-05 | 1.96E-05 | 2.17E-05 | 2.35E-05 | 2.51E-05 | 2.63E-05 | 2.71E-05 | 2.76E-05 | 2.78E-05 | 2.76E-05 | 2.70E-05 | 2.61E-05 | 2.48E-05 | 2.32E-05 | 2.13E-05 | 1.91E-05 | 1.67E-05 | 1.42E-05 |
| CD116 | 4.94E-04 | 5.42E-04 | 5.96E-04 | 6.45E-04 | 6.86E-04 | 7.17E-04 | 7.39E-04 | 7.52E-04 | 7.55E-04 | 7.50E-04 | 7.35E-04 | 7.11E-04 | 6.79E-04 | 6.37E-04 | 5.87E-04 | 5.29E-04 | 4.64E-04 | 4.00E-04 |
| SN116 | 1.02E-04 | 1.27E-04 | 1.56E-04 | 1.83E-04 | 2.06E-04 | 2.26E-04 | 2.40E-04 | 2.48E-04 | 2.51E-04 | 2.47E-04 | 2.38E-04 | 2.23E-04 | 2.03E-04 | 1.79E-04 | 1.52E-04 | 1.23E-04 | 9.41E-05 | 6.76E-05 |
| SN117 | 4.92E-04 | 5.41E-04 | 5.96E-04 | 6.44E-04 | 6.85E-04 | 7.17E-04 | 7.39E-04 | 7.52E-04 | 7.56E-04 | 7.50E-04 | 7.35E-04 | 7.11E-04 | 6.79E-04 | 6.37E-04 | 5.86E-04 | 5.28E-04 | 4.63E-04 | 3.98E-04 |
| SN118 | 5.12E-04 | 5.62E-04 | 6.18E-04 | 6.69E-04 | 7.12E-04 | 7.45E-04 | 7.68E-04 | 7.82E-04 | 7.86E-04 | 7.80E-04 | 7.64E-04 | 7.39E-04 | 7.05E-04 | 6.61E-04 | 6.08E-04 | 5.47E-04 | 4.80E-04 | 4.14E-04 |
| SN119 | 5.08E-04 | 5.58E-04 | 6.14E-04 | 6.65E-04 | 7.08E-04 | 7.41E-04 | 7.64E-04 | 7.77E-04 | 7.81E-04 | 7.76E-04 | 7.60E-04 | 7.35E-04 | 7.01E-04 | 6.57E-04 | 6.04E-04 | 5.44E-04 | 4.77E-04 | 4.11E-04 |
| SN119M | 9.42E-15 | 1.04E-14 | 1.15E-14 | 1.25E-14 | 1.34E-14 | 1.41E-14 | 1.45E-14 | 1.48E-14 | 1.49E-14 | 1.48E-14 | 1.45E-14 | 1.40E-14 | 1.33E-14 | 1.25E-14 | 1.14E-14 | 1.03E-14 | 8.94E-15 | 7.65E-15 |
| SN120 | 5.21E-04 | 5.72E-04 | 6.29E-04 | 6.80E-04 | 7.24E-04 | 7.57E-04 | 7.81E-04 | 7.94E-04 | 7.98E-04 | 7.93E-04 | 7.77E-04 | 7.51E-04 | 7.17E-04 | 6.72E-04 | 6.19E-04 | 5.57E-04 | 4.89E-04 | 4.22E-04 |
| SN121M | 1.69E-07 | 1.79E-07 | 1.95E-07 | 2.12E-07 | 2.26E-07 | 2.38E-07 | 2.46E-07 | 2.51E-07 | 2.52E-07 | 2.50E-07 | 2.45E-07 | 2.36E-07 | 2.24E-07 | 2.09E-07 | 1.91E-07 | 1.71E-07 | 1.51E-07 | 1.34E-07 |

| | | | | | | | | | | | | | | | | | | |
|---|---|---|---|---|---|---|---|---|---|---|---|---|---|---|---|---|---|---|
| SB121 | 5.10E-04 | 5.58E-04 | 6.12E-04 | 6.60E-04 | 7.01E-04 | 7.32E-04 | 7.54E-04 | 7.66E-04 | 7.70E-04 | 7.65E-04 | 7.50E-04 | 7.26E-04 | 6.94E-04 | 6.53E-04 | 6.02E-04 | 5.44E-04 | 4.79E-04 | 4.14E-04 |
| SN122 | 5.66E-04 | 6.21E-04 | 6.83E-04 | 7.39E-04 | 7.86E-04 | 8.23E-04 | 8.48E-04 | 8.63E-04 | 8.67E-04 | 8.61E-04 | 8.44E-04 | 8.16E-04 | 7.79E-04 | 7.30E-04 | 6.72E-04 | 6.05E-04 | 5.31E-04 | 4.58E-04 |
| TE122 | 1.23E-05 | 1.56E-05 | 1.93E-05 | 2.29E-05 | 2.61E-05 | 2.88E-05 | 3.08E-05 | 3.20E-05 | 3.23E-05 | 3.18E-05 | 3.05E-05 | 2.84E-05 | 2.56E-05 | 2.24E-05 | 1.87E-05 | 1.50E-05 | 1.13E-05 | 8.02E-06 |

Position=Segment location (midpoint of 2-in. segment) from bottom of fuel (BOF); 2 in. of fuel ~14.2g.

Table A-1g. Composition (grams) in 2-inch fuel segment: ORIGEN calculation results for Pin195011, decayed to 3/11/2011.

| Position: | 1 | 3 | 5 | 7 | 9 | 11 | 13 | 15 | 17 | 19 | 21 | 23 | 25 | 27 | 29 | 31 | 33 | 35 |
|---|---|---|---|---|---|---|---|---|---|---|---|---|---|---|---|---|---|---|
| SN123 | 2.13E-21 | 2.33E-21 | 2.55E-21 | 2.75E-21 | 2.92E-21 | 3.05E-21 | 3.14E-21 | 3.19E-21 | 3.21E-21 | 3.18E-21 | 3.13E-21 | 3.04E-21 | 2.91E-21 | 2.74E-21 | 2.54E-21 | 2.30E-21 | 2.03E-21 | 1.76E-21 |
| SB123 | 6.06E-04 | 6.63E-04 | 7.29E-04 | 7.88E-04 | 8.37E-04 | 8.76E-04 | 9.02E-04 | 9.18E-04 | 9.22E-04 | 9.16E-04 | 8.98E-04 | 8.69E-04 | 8.30E-04 | 7.79E-04 | 7.18E-04 | 6.47E-04 | 5.68E-04 | 4.90E-04 |
| TE123 | 1.61E-07 | 2.35E-07 | 3.27E-07 | 4.26E-07 | 5.24E-07 | 6.09E-07 | 6.75E-07 | 7.16E-07 | 7.28E-07 | 7.11E-07 | 6.65E-07 | 5.96E-07 | 5.10E-07 | 4.13E-07 | 3.15E-07 | 2.23E-07 | 1.44E-07 | 8.44E-08 |
| TE123M | 0.00E+00 | 0.00E+00 | 4.80E-24 | 7.02E-24 | 8.63E-24 | 0.00E+00 | 0.00E+00 | 0.00E+00 | 0.00E+00 | 0.00E+00 | 0.00E+00 | 0.00E+00 | 8.43E-24 | 6.83E-24 | 4.65E-24 | 0.00E+00 | 0.00E+00 | 0.00E+00 |
| SN124 | 7.25E-04 | 7.94E-04 | 8.74E-04 | 9.45E-04 | 1.01E-03 | 1.05E-03 | 1.09E-03 | 1.10E-03 | 1.11E-03 | 1.10E-03 | 1.08E-03 | 1.04E-03 | 9.96E-04 | 9.34E-04 | 8.59E-04 | 7.74E-04 | 6.79E-04 | 5.86E-04 |
| SB124 | 3.08E-39 | 3.88E-39 | 4.78E-39 | 5.66E-39 | 6.45E-39 | 7.10E-39 | 7.58E-39 | 7.87E-39 | 7.96E-39 | 7.84E-39 | 7.52E-39 | 7.02E-39 | 6.37E-39 | 5.57E-39 | 4.69E-39 | 3.77E-39 | 2.86E-39 | 2.05E-39 |
| TE124 | 8.25E-06 | 1.03E-05 | 1.27E-05 | 1.50E-05 | 1.71E-05 | 1.88E-05 | 2.00E-05 | 2.08E-05 | 2.10E-05 | 2.07E-05 | 1.98E-05 | 1.85E-05 | 1.67E-05 | 1.46E-05 | 1.23E-05 | 9.91E-06 | 7.55E-06 | 5.46E-06 |
| SN125 | 0.00E+00 | 0.00E+00 | 0.00E+00 | 0.00E+00 | 0.00E+00 | 0.00E+00 | 0.00E+00 | 0.00E+00 | 0.00E+00 | 0.00E+00 | 0.00E+00 | 0.00E+00 | 0.00E+00 | 0.00E+00 | 0.00E+00 | 0.00E+00 | 0.00E+00 | 0.00E+00 |
| SB125 | 5.75E-06 | 6.29E-06 | 6.92E-06 | 7.48E-06 | 7.95E-06 | 8.32E-06 | 8.57E-06 | 8.72E-06 | 8.77E-06 | 8.71E-06 | 8.54E-06 | 8.26E-06 | 7.88E-06 | 7.40E-06 | 6.82E-06 | 6.14E-06 | 5.39E-06 | 4.66E-06 |
| TE125 | 8.55E-04 | 9.35E-04 | 1.03E-03 | 1.11E-03 | 1.18E-03 | 1.24E-03 | 1.28E-03 | 1.30E-03 | 1.31E-03 | 1.30E-03 | 1.27E-03 | 1.23E-03 | 1.17E-03 | 1.10E-03 | 1.01E-03 | 9.11E-04 | 7.99E-04 | 6.90E-04 |
| TE125M | 8.04E-08 | 8.80E-08 | 9.68E-08 | 1.05E-07 | 1.11E-07 | 1.16E-07 | 1.20E-07 | 1.22E-07 | 1.23E-07 | 1.22E-07 | 1.19E-07 | 1.16E-07 | 1.10E-07 | 1.04E-07 | 9.53E-08 | 8.59E-08 | 7.54E-08 | 6.52E-08 |
| SN126 | 1.23E-03 | 1.34E-03 | 1.47E-03 | 1.59E-03 | 1.70E-03 | 1.78E-03 | 1.83E-03 | 1.87E-03 | 1.88E-03 | 1.86E-03 | 1.82E-03 | 1.76E-03 | 1.68E-03 | 1.57E-03 | 1.45E-03 | 1.30E-03 | 1.14E-03 | 9.94E-04 |
| SB126 | 5.86E-11 | 6.37E-11 | 7.00E-11 | 7.57E-11 | 8.06E-11 | 8.44E-11 | 8.71E-11 | 8.86E-11 | 8.91E-11 | 8.84E-11 | 8.66E-11 | 8.37E-11 | 7.98E-11 | 7.48E-11 | 6.87E-11 | 6.19E-11 | 5.43E-11 | 4.72E-11 |
| TE126 | 4.48E-05 | 5.03E-05 | 5.72E-05 | 6.40E-05 | 6.99E-05 | 7.47E-05 | 7.82E-05 | 8.03E-05 | 8.09E-05 | 8.00E-05 | 7.77E-05 | 7.39E-05 | 6.90E-05 | 6.29E-05 | 5.59E-05 | 4.84E-05 | 4.08E-05 | 3.41E-05 |
| TE127 | 1.74E-26 | 1.88E-26 | 3.22E-26 | 3.46E-26 | 3.67E-26 | 3.83E-26 | 3.94E-26 | 4.01E-26 | 4.03E-26 | 4.01E-26 | 3.94E-26 | 3.82E-26 | 3.66E-26 | 3.45E-26 | 3.19E-26 | 1.85E-26 | 1.64E-26 | 1.44E-26 |
| TE127M | 0.00E+00 | 0.00E+00 | 9.20E-24 | 9.91E-24 | 1.05E-23 | 1.10E-23 | 1.13E-23 | 1.15E-23 | 1.15E-23 | 1.15E-23 | 1.13E-23 | 1.09E-23 | 1.05E-23 | 9.86E-24 | 9.13E-24 | 0.00E+00 | 0.00E+00 | 0.00E+00 |
| I127 | 2.18E-03 | 2.34E-03 | 2.56E-03 | 2.76E-03 | 2.93E-03 | 3.06E-03 | 3.16E-03 | 3.21E-03 | 3.23E-03 | 3.20E-03 | 3.14E-03 | 3.04E-03 | 2.90E-03 | 2.73E-03 | 2.51E-03 | 2.27E-03 | 2.01E-03 | 1.76E-03 |
| TE128 | 4.04E-03 | 4.35E-03 | 4.75E-03 | 5.13E-03 | 5.46E-03 | 5.71E-03 | 5.89E-03 | 5.99E-03 | 6.02E-03 | 5.98E-03 | 5.86E-03 | 5.66E-03 | 5.40E-03 | 5.07E-03 | 4.66E-03 | 4.21E-03 | 3.71E-03 | 3.26E-03 |
| XE128 | 5.19E-05 | 6.46E-05 | 7.96E-05 | 9.45E-05 | 1.08E-04 | 1.19E-04 | 1.28E-04 | 1.33E-04 | 1.34E-04 | 1.32E-04 | 1.26E-04 | 1.18E-04 | 1.06E-04 | 9.23E-05 | 7.73E-05 | 6.17E-05 | 4.67E-05 | 3.36E-05 |
| TE129 | 0.00E+00 | 0.00E+00 | 0.00E+00 | 0.00E+00 | 0.00E+00 | 0.00E+00 | 0.00E+00 | 0.00E+00 | 0.00E+00 | 0.00E+00 | 0.00E+00 | 0.00E+00 | 0.00E+00 | 0.00E+00 | 0.00E+00 | 0.00E+00 | 0.00E+00 | 0.00E+00 |
| TE129M | 0.00E+00 | 0.00E+00 | 0.00E+00 | 0.00E+00 | 0.00E+00 | 0.00E+00 | 0.00E+00 | 0.00E+00 | 0.00E+00 | 0.00E+00 | 0.00E+00 | 0.00E+00 | 0.00E+00 | 0.00E+00 | 0.00E+00 | 0.00E+00 | 0.00E+00 | 0.00E+00 |

| | | | | | | | | | | | | | | | | | | |
|---|---|---|---|---|---|---|---|---|---|---|---|---|---|---|---|---|---|---|
| I129 | 5.93E-03 | 6.35E-03 | 6.93E-03 | 7.47E-03 | 7.93E-03 | 8.30E-03 | 8.55E-03 | 8.70E-03 | 8.74E-03 | 8.68E-03 | 8.51E-03 | 8.23E-03 | 7.85E-03 | 7.37E-03 | 6.80E-03 | 6.14E-03 | 5.42E-03 | 4.78E-03 |
| XE129 | 3.24E-07 | 4.56E-07 | 6.23E-07 | 8.05E-07 | 9.83E-07 | 1.14E-06 | 1.26E-06 | 1.34E-06 | 1.36E-06 | 1.33E-06 | 1.24E-06 | 1.12E-06 | 9.57E-07 | 7.79E-07 | 5.99E-07 | 4.31E-07 | 2.87E-07 | 1.78E-07 |
| TE130 | 1.05E-02 | 1.13E-02 | 1.23E-02 | 1.33E-02 | 1.42E-02 | 1.48E-02 | 1.53E-02 | 1.56E-02 | 1.56E-02 | 1.55E-02 | 1.52E-02 | 1.47E-02 | 1.40E-02 | 1.31E-02 | 1.21E-02 | 1.09E-02 | 9.61E-03 | 8.46E-03 |

Position=Segment location (midpoint of 2-in. segment) from bottom of fuel (BOF); 2 in. of fuel ~14.2g

Table A-1h. Composition (grams) in 2-inch fuel segment: ORIGEN calculation results for Pin195011, decayed to 3/11/2011.

| Position: | 1 | 3 | 5 | 7 | 9 | 11 | 13 | 15 | 17 | 19 | 21 | 23 | 25 | 27 | 29 | 31 | 33 | 35 |
|---|---|---|---|---|---|---|---|---|---|---|---|---|---|---|---|---|---|---|
| XE130 | 1.26E-04 | 1.56E-04 | 1.92E-04 | 2.27E-04 | 2.60E-04 | 2.86E-04 | 3.06E-04 | 3.18E-04 | 3.22E-04 | 3.17E-04 | 3.03E-04 | 2.82E-04 | 2.55E-04 | 2.22E-04 | 1.86E-04 | 1.49E-04 | 1.13E-04 | 8.20E-05 |
| I131 | 0.00E+00 | 0.00E+00 | 0.00E+00 | 0.00E+00 | 0.00E+00 | 0.00E+00 | 0.00E+00 | 0.00E+00 | 0.00E+00 | 0.00E+00 | 0.00E+00 | 0.00E+00 | 0.00E+00 | 0.00E+00 | 0.00E+00 | 0.00E+00 | 0.00E+00 | 0.00E+00 |
| XE131 | 1.73E-02 | 1.84E-02 | 2.01E-02 | 2.17E-02 | 2.30E-02 | 2.41E-02 | 2.48E-02 | 2.53E-02 | 2.54E-02 | 2.52E-02 | 2.47E-02 | 2.39E-02 | 2.28E-02 | 2.14E-02 | 1.97E-02 | 1.78E-02 | 1.57E-02 | 1.39E-02 |
| XE131M | 0.00E+00 | 0.00E+00 | 0.00E+00 | 0.00E+00 | 0.00E+00 | 0.00E+00 | 0.00E+00 | 0.00E+00 | 0.00E+00 | 0.00E+00 | 0.00E+00 | 0.00E+00 | 0.00E+00 | 0.00E+00 | 0.00E+00 | 0.00E+00 | 0.00E+00 | 0.00E+00 |
| XE132 | 2.50E-02 | 2.68E-02 | 2.93E-02 | 3.16E-02 | 3.36E-02 | 3.52E-02 | 3.63E-02 | 3.70E-02 | 3.72E-02 | 3.69E-02 | 3.61E-02 | 3.49E-02 | 3.33E-02 | 3.12E-02 | 2.87E-02 | 2.58E-02 | 2.28E-02 | 2.01E-02 |
| BA132 | 1.87E-08 | 2.31E-08 | 2.83E-08 | 3.36E-08 | 3.84E-08 | 4.24E-08 | 4.54E-08 | 4.71E-08 | 4.76E-08 | 4.69E-08 | 4.49E-08 | 4.17E-08 | 3.77E-08 | 3.28E-08 | 2.75E-08 | 2.20E-08 | 1.67E-08 | 1.21E-08 |
| XE133 | 0.00E+00 | 0.00E+00 | 0.00E+00 | 0.00E+00 | 0.00E+00 | 0.00E+00 | 0.00E+00 | 0.00E+00 | 0.00E+00 | 0.00E+00 | 0.00E+00 | 0.00E+00 | 0.00E+00 | 0.00E+00 | 0.00E+00 | 0.00E+00 | 0.00E+00 | 0.00E+00 |
| CS133 | 3.40E-02 | 3.62E-02 | 3.93E-02 | 4.23E-02 | 4.48E-02 | 4.68E-02 | 4.82E-02 | 4.90E-02 | 4.93E-02 | 4.89E-02 | 4.80E-02 | 4.65E-02 | 4.44E-02 | 4.17E-02 | 3.85E-02 | 3.49E-02 | 3.10E-02 | 2.75E-02 |
| XE134 | 4.08E-02 | 4.35E-02 | 4.74E-02 | 5.11E-02 | 5.43E-02 | 5.68E-02 | 5.86E-02 | 5.96E-02 | 5.99E-02 | 5.95E-02 | 5.83E-02 | 5.64E-02 | 5.37E-02 | 5.04E-02 | 4.65E-02 | 4.19E-02 | 3.71E-02 | 3.29E-02 |
| CS134 | 1.24E-06 | 1.52E-06 | 1.86E-06 | 2.20E-06 | 2.51E-06 | 2.76E-06 | 2.95E-06 | 3.06E-06 | 3.10E-06 | 3.05E-06 | 2.92E-06 | 2.72E-06 | 2.46E-06 | 2.15E-06 | 1.80E-06 | 1.45E-06 | 1.10E-06 | 8.04E-07 |
| BA134 | 9.04E-04 | 1.11E-03 | 1.36E-03 | 1.61E-03 | 1.84E-03 | 2.03E-03 | 2.16E-03 | 2.25E-03 | 2.27E-03 | 2.24E-03 | 2.14E-03 | 1.99E-03 | 1.80E-03 | 1.57E-03 | 1.32E-03 | 1.06E-03 | 8.04E-04 | 5.87E-04 |
| CS135 | 3.44E-02 | 3.67E-02 | 4.01E-02 | 4.32E-02 | 4.60E-02 | 4.81E-02 | 4.96E-02 | 5.05E-02 | 5.08E-02 | 5.04E-02 | 4.94E-02 | 4.77E-02 | 4.55E-02 | 4.26E-02 | 3.93E-02 | 3.54E-02 | 3.13E-02 | 2.76E-02 |
| BA135 | 8.31E-07 | 1.10E-06 | 1.45E-06 | 1.83E-06 | 2.20E-06 | 2.53E-06 | 2.78E-06 | 2.93E-06 | 2.98E-06 | 2.91E-06 | 2.73E-06 | 2.47E-06 | 2.14E-06 | 1.77E-06 | 1.39E-06 | 1.04E-06 | 7.29E-07 | 4.96E-07 |
| XE136 | 3.48E-02 | 3.72E-02 | 4.06E-02 | 4.38E-02 | 4.65E-02 | 4.87E-02 | 5.02E-02 | 5.11E-02 | 5.14E-02 | 5.10E-02 | 4.99E-02 | 4.83E-02 | 4.60E-02 | 4.32E-02 | 3.97E-02 | 3.58E-02 | 3.17E-02 | 2.80E-02 |
| CS136 | 0.00E+00 | 0.00E+00 | 0.00E+00 | 0.00E+00 | 0.00E+00 | 0.00E+00 | 0.00E+00 | 0.00E+00 | 0.00E+00 | 0.00E+00 | 0.00E+00 | 0.00E+00 | 0.00E+00 | 0.00E+00 | 0.00E+00 | 0.00E+00 | 0.00E+00 | 0.00E+00 |
| BA136 | 2.76E-04 | 3.14E-04 | 3.65E-04 | 4.15E-04 | 4.60E-04 | 4.97E-04 | 5.25E-04 | 5.41E-04 | 5.46E-04 | 5.39E-04 | 5.20E-04 | 4.91E-04 | 4.52E-04 | 4.06E-04 | 3.54E-04 | 3.00E-04 | 2.46E-04 | 2.01E-04 |
| CS137 | 2.08E-02 | 2.22E-02 | 2.42E-02 | 2.61E-02 | 2.77E-02 | 2.90E-02 | 2.99E-02 | 3.04E-02 | 3.06E-02 | 3.04E-02 | 2.98E-02 | 2.88E-02 | 2.74E-02 | 2.57E-02 | 2.37E-02 | 2.14E-02 | 1.89E-02 | 1.67E-02 |
| BA137 | 1.23E-02 | 1.31E-02 | 1.43E-02 | 1.54E-02 | 1.64E-02 | 1.71E-02 | 1.77E-02 | 1.80E-02 | 1.81E-02 | 1.80E-02 | 1.76E-02 | 1.70E-02 | 1.62E-02 | 1.52E-02 | 1.40E-02 | 1.26E-02 | 1.12E-02 | 9.87E-03 |
| BA138 | 3.58E-02 | 3.81E-02 | 4.16E-02 | 4.49E-02 | 4.77E-02 | 4.99E-02 | 5.14E-02 | 5.23E-02 | 5.26E-02 | 5.22E-02 | 5.12E-02 | 4.95E-02 | 4.72E-02 | 4.42E-02 | 4.08E-02 | 3.68E-02 | 3.25E-02 | 2.88E-02 |
| LA138 | 1.42E-07 | 1.49E-07 | 1.62E-07 | 1.74E-07 | 1.84E-07 | 1.92E-07 | 1.98E-07 | 2.01E-07 | 2.02E-07 | 2.01E-07 | 1.97E-07 | 1.91E-07 | 1.82E-07 | 1.71E-07 | 1.58E-07 | 1.43E-07 | 1.28E-07 | 1.14E-07 |
| LA139 | 3.49E-02 | 3.71E-02 | 4.05E-02 | 4.37E-02 | 4.64E-02 | 4.85E-02 | 5.00E-02 | 5.09E-02 | 5.11E-02 | 5.08E-02 | 4.98E-02 | 4.81E-02 | 4.59E-02 | 4.31E-02 | 3.97E-02 | 3.58E-02 | 3.17E-02 | 2.81E-02 |

| | | | | | | | | | | | | | | | | | | |
|---|---|---|---|---|---|---|---|---|---|---|---|---|---|---|---|---|---|---|
| BA140 | 0.00E+00 | 0.00E+00 | 0.00E+00 | 0.00E+00 | 0.00E+00 | 0.00E+00 | 0.00E+00 | 0.00E+00 | 0.00E+00 | 0.00E+00 | 0.00E+00 | 0.00E+00 | 0.00E+00 | 0.00E+00 | 0.00E+00 | 0.00E+00 | 0.00E+00 | 0.00E+00 |
| LA140 | 0.00E+00 | 0.00E+00 | 0.00E+00 | 0.00E+00 | 0.00E+00 | 0.00E+00 | 0.00E+00 | 0.00E+00 | 0.00E+00 | 0.00E+00 | 0.00E+00 | 0.00E+00 | 0.00E+00 | 0.00E+00 | 0.00E+00 | 0.00E+00 | 0.00E+00 | 0.00E+00 |
| CE140 | 3.40E-02 | 3.63E-02 | 3.95E-02 | 4.26E-02 | 4.53E-02 | 4.74E-02 | 4.88E-02 | 4.97E-02 | 4.99E-02 | 4.96E-02 | 4.86E-02 | 4.70E-02 | 4.48E-02 | 4.20E-02 | 3.87E-02 | 3.50E-02 | 3.09E-02 | 2.74E-02 |

Position=Segment location (midpoint of 2-in. segment) from bottom of fuel (BOF); 2 in. of fuel ~14.2g.

Table A-1i. Composition (grams) in 2-inch fuel segment: ORIGEN calculation results for Pin195011, decayed to 3/11/2011.

| Position: | 1 | 3 | 5 | 7 | 9 | 11 | 13 | 15 | 17 | 19 | 21 | 23 | 25 | 27 | 29 | 31 | 33 | 35 |
|---|---|---|---|---|---|---|---|---|---|---|---|---|---|---|---|---|---|---|
| CE141 | 0.00E+00 | 0.00E+00 | 0.00E+00 | 0.00E+00 | 0.00E+00 | 0.00E+00 | 0.00E+00 | 0.00E+00 | 0.00E+00 | 0.00E+00 | 0.00E+00 | 0.00E+00 | 0.00E+00 | 0.00E+00 | 0.00E+00 | 0.00E+00 | 0.00E+00 | 0.00E+00 |
| PR141 | 3.31E-02 | 3.52E-02 | 3.83E-02 | 4.13E-02 | 4.38E-02 | 4.58E-02 | 4.72E-02 | 4.81E-02 | 4.83E-02 | 4.80E-02 | 4.70E-02 | 4.55E-02 | 4.34E-02 | 4.07E-02 | 3.76E-02 | 3.39E-02 | 3.00E-02 | 2.67E-02 |
| CE142 | 3.12E-02 | 3.33E-02 | 3.62E-02 | 3.91E-02 | 4.15E-02 | 4.34E-02 | 4.47E-02 | 4.55E-02 | 4.58E-02 | 4.54E-02 | 4.45E-02 | 4.31E-02 | 4.11E-02 | 3.85E-02 | 3.55E-02 | 3.21E-02 | 2.84E-02 | 2.51E-02 |
| ND142 | 2.33E-04 | 2.87E-04 | 3.53E-04 | 4.18E-04 | 4.79E-04 | 5.29E-04 | 5.66E-04 | 5.88E-04 | 5.95E-04 | 5.85E-04 | 5.60E-04 | 5.21E-04 | 4.69E-04 | 4.08E-04 | 3.41E-04 | 2.73E-04 | 2.07E-04 | 1.51E-04 |
| PR143 | 0.00E+00 | 0.00E+00 | 0.00E+00 | 0.00E+00 | 0.00E+00 | 0.00E+00 | 0.00E+00 | 0.00E+00 | 0.00E+00 | 0.00E+00 | 0.00E+00 | 0.00E+00 | 0.00E+00 | 0.00E+00 | 0.00E+00 | 0.00E+00 | 0.00E+00 | 0.00E+00 |
| ND143 | 3.16E-02 | 3.35E-02 | 3.64E-02 | 3.92E-02 | 4.15E-02 | 4.34E-02 | 4.47E-02 | 4.55E-02 | 4.57E-02 | 4.54E-02 | 4.45E-02 | 4.31E-02 | 4.11E-02 | 3.87E-02 | 3.57E-02 | 3.23E-02 | 2.87E-02 | 2.55E-02 |
| CE144 | 5.93E-10 | 6.31E-10 | 6.85E-10 | 7.36E-10 | 7.79E-10 | 8.13E-10 | 8.37E-10 | 8.51E-10 | 8.55E-10 | 8.49E-10 | 8.34E-10 | 8.09E-10 | 7.74E-10 | 7.30E-10 | 6.76E-10 | 6.13E-10 | 5.45E-10 | 4.85E-10 |
| PR144 | 2.50E-14 | 2.66E-14 | 2.89E-14 | 3.11E-14 | 3.29E-14 | 3.43E-14 | 3.53E-14 | 3.59E-14 | 3.61E-14 | 3.59E-14 | 3.52E-14 | 3.42E-14 | 3.27E-14 | 3.08E-14 | 2.85E-14 | 2.59E-14 | 2.30E-14 | 2.05E-14 |
| ND144 | 2.99E-02 | 3.19E-02 | 3.48E-02 | 3.76E-02 | 3.99E-02 | 4.18E-02 | 4.31E-02 | 4.39E-02 | 4.41E-02 | 4.38E-02 | 4.29E-02 | 4.15E-02 | 3.95E-02 | 3.71E-02 | 3.41E-02 | 3.08E-02 | 2.72E-02 | 2.41E-02 |
| ND145 | 2.15E-02 | 2.29E-02 | 2.49E-02 | 2.68E-02 | 2.85E-02 | 2.97E-02 | 3.06E-02 | 3.12E-02 | 3.13E-02 | 3.11E-02 | 3.05E-02 | 2.95E-02 | 2.82E-02 | 2.65E-02 | 2.44E-02 | 2.21E-02 | 1.96E-02 | 1.74E-02 |
| ND146 | 1.73E-02 | 1.85E-02 | 2.03E-02 | 2.19E-02 | 2.33E-02 | 2.44E-02 | 2.52E-02 | 2.56E-02 | 2.58E-02 | 2.56E-02 | 2.50E-02 | 2.42E-02 | 2.31E-02 | 2.16E-02 | 1.99E-02 | 1.79E-02 | 1.58E-02 | 1.39E-02 |
| PM146 | 8.38E-08 | 1.02E-07 | 1.24E-07 | 1.46E-07 | 1.66E-07 | 1.82E-07 | 1.94E-07 | 2.01E-07 | 2.03E-07 | 2.00E-07 | 1.92E-07 | 1.80E-07 | 1.63E-07 | 1.43E-07 | 1.21E-07 | 9.75E-08 | 7.48E-08 | 5.51E-08 |
| SM146 | 8.13E-07 | 9.93E-07 | 1.21E-06 | 1.42E-06 | 1.62E-06 | 1.78E-06 | 1.89E-06 | 1.96E-06 | 1.98E-06 | 1.95E-06 | 1.87E-06 | 1.75E-06 | 1.59E-06 | 1.39E-06 | 1.17E-06 | 9.46E-07 | 7.24E-07 | 5.32E-07 |
| ND147 | 0.00E+00 | 0.00E+00 | 0.00E+00 | 0.00E+00 | 0.00E+00 | 0.00E+00 | 0.00E+00 | 0.00E+00 | 0.00E+00 | 0.00E+00 | 0.00E+00 | 0.00E+00 | 0.00E+00 | 0.00E+00 | 0.00E+00 | 0.00E+00 | 0.00E+00 | 0.00E+00 |
| PM147 | 6.26E-05 | 6.56E-05 | 7.04E-05 | 7.48E-05 | 7.85E-05 | 8.13E-05 | 8.32E-05 | 8.43E-05 | 8.47E-05 | 8.42E-05 | 8.29E-05 | 8.08E-05 | 7.79E-05 | 7.40E-05 | 6.93E-05 | 6.36E-05 | 5.73E-05 | 5.17E-05 |
| SM147 | 1.23E-02 | 1.29E-02 | 1.39E-02 | 1.47E-02 | 1.55E-02 | 1.60E-02 | 1.64E-02 | 1.67E-02 | 1.67E-02 | 1.66E-02 | 1.64E-02 | 1.59E-02 | 1.53E-02 | 1.46E-02 | 1.36E-02 | 1.25E-02 | 1.12E-02 | 1.01E-02 |
| ND148 | 1.01E-02 | 1.08E-02 | 1.17E-02 | 1.27E-02 | 1.34E-02 | 1.41E-02 | 1.45E-02 | 1.47E-02 | 1.48E-02 | 1.47E-02 | 1.44E-02 | 1.39E-02 | 1.33E-02 | 1.25E-02 | 1.15E-02 | 1.04E-02 | 9.19E-03 | 8.11E-03 |
| PM148 | 0.00E+00 | 0.00E+00 | 0.00E+00 | 0.00E+00 | 0.00E+00 | 0.00E+00 | 0.00E+00 | 0.00E+00 | 0.00E+00 | 0.00E+00 | 0.00E+00 | 0.00E+00 | 0.00E+00 | 0.00E+00 | 0.00E+00 | 0.00E+00 | 0.00E+00 | 0.00E+00 |
| PM148M | 0.00E+00 | 0.00E+00 | 0.00E+00 | 0.00E+00 | 0.00E+00 | 0.00E+00 | 0.00E+00 | 0.00E+00 | 0.00E+00 | 0.00E+00 | 0.00E+00 | 0.00E+00 | 0.00E+00 | 0.00E+00 | 0.00E+00 | 0.00E+00 | 0.00E+00 | 0.00E+00 |
| SM148 | 1.54E-03 | 1.88E-03 | 2.28E-03 | 2.67E-03 | 3.02E-03 | 3.31E-03 | 3.52E-03 | 3.65E-03 | 3.68E-03 | 3.63E-03 | 3.49E-03 | 3.26E-03 | 2.96E-03 | 2.61E-03 | 2.21E-03 | 1.79E-03 | 1.38E-03 | 1.02E-03 |
| SM149 | 6.40E-03 | 6.83E-03 | 7.42E-03 | 7.98E-03 | 8.45E-03 | 8.82E-03 | 9.08E-03 | 9.23E-03 | 9.28E-03 | 9.21E-03 | 9.04E-03 | 8.76E-03 | 8.37E-03 | 7.88E-03 | 7.28E-03 | 6.60E-03 | 5.86E-03 | 5.19E-03 |
| ND150 | 4.30E-03 | 4.63E-03 | 5.07E-03 | 5.48E-03 | 5.82E-03 | 6.09E-03 | 6.29E-03 | 6.40E-03 | 6.43E-03 | 6.38E-03 | 6.25E-03 | 6.05E-03 | 5.76E-03 | 5.40E-03 | 4.97E-03 | 4.48E-03 | 3.95E-03 | 3.46E-03 |
| SM150 | 4.63E-04 | 5.71E-04 | 7.00E-04 | 8.28E-04 | 9.44E-04 | 1.04E-03 | 1.11E-03 | 1.15E-03 | 1.17E-03 | 1.15E-03 | 1.10E-03 | 1.03E-03 | 9.26E-04 | 8.09E-04 | 6.79E-04 | 5.45E-04 | 4.14E-04 | 3.02E-04 |
| SM151 | 2.26E-03 | 2.41E-03 | 2.61E-03 | 2.80E-03 | 2.96E-03 | 3.09E-03 | 3.17E-03 | 3.22E-03 | 3.24E-03 | 3.22E-03 | 3.16E-03 | 3.06E-03 | 2.94E-03 | 2.77E-03 | 2.57E-03 | 2.33E-03 | 2.07E-03 | 1.84E-03 |

Position=Segment location (midpoint of 2-in. segment) from bottom of fuel (BOF); 2 in. of fuel ~14.2g

Table A-1j. Composition (grams) in 2-inch fuel segment: ORIGEN calculation results for Pin195011, decayed to 3/11/2011.

| Position: | 1 | 3 | 5 | 7 | 9 | 11 | 13 | 15 | 17 | 19 | 21 | 23 | 25 | 27 | 29 | 31 | 33 | 35 |
|---|---|---|---|---|---|---|---|---|---|---|---|---|---|---|---|---|---|---|
| EU151 | 3.74E-04 | 3.99E-04 | 4.32E-04 | 4.63E-04 | 4.89E-04 | 5.10E-04 | 5.24E-04 | 5.32E-04 | 5.34E-04 | 5.31E-04 | 5.21E-04 | 5.06E-04 | 4.85E-04 | 4.57E-04 | 4.24E-04 | 3.86E-04 | 3.44E-04 | 3.05E-04 |
| SM152 | 2.20E-03 | 2.42E-03 | 2.69E-03 | 2.95E-03 | 3.18E-03 | 3.36E-03 | 3.49E-03 | 3.56E-03 | 3.58E-03 | 3.55E-03 | 3.46E-03 | 3.33E-03 | 3.14E-03 | 2.91E-03 | 2.63E-03 | 2.33E-03 | 2.01E-03 | 1.73E-03 |
| EU152 | 8.79E-07 | 1.05E-06 | 1.26E-06 | 1.45E-06 | 1.61E-06 | 1.75E-06 | 1.84E-06 | 1.90E-06 | 1.92E-06 | 1.89E-06 | 1.83E-06 | 1.72E-06 | 1.58E-06 | 1.41E-06 | 1.22E-06 | 1.01E-06 | 7.91E-07 | 5.94E-07 |
| GD152 | 1.34E-06 | 1.60E-06 | 1.90E-06 | 2.19E-06 | 2.44E-06 | 2.64E-06 | 2.79E-06 | 2.87E-06 | 2.89E-06 | 2.86E-06 | 2.76E-06 | 2.61E-06 | 2.40E-06 | 2.14E-06 | 1.85E-06 | 1.53E-06 | 1.20E-06 | 9.06E-07 |
| EU153 | 1.24E-03 | 1.33E-03 | 1.45E-03 | 1.56E-03 | 1.65E-03 | 1.73E-03 | 1.78E-03 | 1.81E-03 | 1.81E-03 | 1.80E-03 | 1.77E-03 | 1.71E-03 | 1.64E-03 | 1.54E-03 | 1.42E-03 | 1.29E-03 | 1.14E-03 | 1.01E-03 |
| GD153 | 2.08E-16 | 2.89E-16 | 3.90E-16 | 4.96E-16 | 5.96E-16 | 6.83E-16 | 7.49E-16 | 7.88E-16 | 8.00E-16 | 7.84E-16 | 7.39E-16 | 6.70E-16 | 5.83E-16 | 4.82E-16 | 3.77E-16 | 2.75E-16 | 1.85E-16 | 1.13E-16 |
| SM154 | 6.41E-04 | 6.97E-04 | 7.69E-04 | 8.36E-04 | 8.93E-04 | 9.38E-04 | 9.70E-04 | 9.89E-04 | 9.94E-04 | 9.86E-04 | 9.65E-04 | 9.30E-04 | 8.83E-04 | 8.24E-04 | 7.54E-04 | 6.75E-04 | 5.90E-04 | 5.11E-04 |
| EU154 | 2.67E-05 | 3.27E-05 | 3.97E-05 | 4.66E-05 | 5.27E-05 | 5.78E-05 | 6.15E-05 | 6.37E-05 | 6.43E-05 | 6.34E-05 | 6.09E-05 | 5.70E-05 | 5.18E-05 | 4.56E-05 | 3.86E-05 | 3.13E-05 | 2.40E-05 | 1.76E-05 |
| GD154 | 1.03E-04 | 1.27E-04 | 1.54E-04 | 1.81E-04 | 2.05E-04 | 2.24E-04 | 2.39E-04 | 2.47E-04 | 2.50E-04 | 2.46E-04 | 2.36E-04 | 2.21E-04 | 2.01E-04 | 1.77E-04 | 1.50E-04 | 1.21E-04 | 9.30E-05 | 6.81E-05 |
| EU155 | 2.36E-05 | 2.56E-05 | 2.81E-05 | 3.06E-05 | 3.27E-05 | 3.43E-05 | 3.55E-05 | 3.62E-05 | 3.64E-05 | 3.61E-05 | 3.53E-05 | 3.40E-05 | 3.23E-05 | 3.02E-05 | 2.76E-05 | 2.48E-05 | 2.17E-05 | 1.89E-05 |
| GD155 | 3.62E-04 | 3.92E-04 | 4.30E-04 | 4.67E-04 | 4.98E-04 | 5.23E-04 | 5.41E-04 | 5.52E-04 | 5.55E-04 | 5.50E-04 | 5.38E-04 | 5.19E-04 | 4.93E-04 | 4.60E-04 | 4.22E-04 | 3.79E-04 | 3.32E-04 | 2.90E-04 |
| EU156 | 0.00E+00 | 0.00E+00 | 0.00E+00 | 0.00E+00 | 0.00E+00 | 0.00E+00 | 0.00E+00 | 0.00E+00 | 0.00E+00 | 0.00E+00 | 0.00E+00 | 0.00E+00 | 0.00E+00 | 0.00E+00 | 0.00E+00 | 0.00E+00 | 0.00E+00 | 0.00E+00 |
| GD156 | 2.57E-04 | 2.89E-04 | 3.27E-04 | 3.63E-04 | 3.95E-04 | 4.21E-04 | 4.40E-04 | 4.51E-04 | 4.54E-04 | 4.49E-04 | 4.37E-04 | 4.17E-04 | 3.90E-04 | 3.57E-04 | 3.20E-04 | 2.79E-04 | 2.36E-04 | 1.97E-04 |
| GD157 | 1.24E-04 | 1.34E-04 | 1.47E-04 | 1.60E-04 | 1.70E-04 | 1.78E-04 | 1.84E-04 | 1.87E-04 | 1.88E-04 | 1.87E-04 | 1.83E-04 | 1.77E-04 | 1.68E-04 | 1.57E-04 | 1.45E-04 | 1.30E-04 | 1.14E-04 | 9.91E-05 |
| GD158 | 9.37E-05 | 1.06E-04 | 1.20E-04 | 1.35E-04 | 1.47E-04 | 1.57E-04 | 1.65E-04 | 1.69E-04 | 1.70E-04 | 1.69E-04 | 1.63E-04 | 1.56E-04 | 1.45E-04 | 1.32E-04 | 1.18E-04 | 1.02E-04 | 8.54E-05 | 7.08E-05 |
| TB159 | 3.32E-05 | 3.68E-05 | 4.11E-05 | 4.53E-05 | 4.89E-05 | 5.17E-05 | 5.38E-05 | 5.50E-05 | 5.53E-05 | 5.48E-05 | 5.34E-05 | 5.12E-05 | 4.82E-05 | 4.45E-05 | 4.02E-05 | 3.55E-05 | 3.05E-05 | 2.58E-05 |
| GD160 | 1.77E-05 | 1.97E-05 | 2.21E-05 | 2.45E-05 | 2.65E-05 | 2.81E-05 | 2.93E-05 | 3.00E-05 | 3.02E-05 | 2.99E-05 | 2.91E-05 | 2.78E-05 | 2.61E-05 | 2.40E-05 | 2.16E-05 | 1.89E-05 | 1.61E-05 | 1.36E-05 |
| TB160 | 2.84E-34 | 3.64E-34 | 4.58E-34 | 5.53E-34 | 6.41E-34 | 7.15E-34 | 7.70E-34 | 8.04E-34 | 8.14E-34 | 8.00E-34 | 7.63E-34 | 7.05E-34 | 6.30E-34 | 5.42E-34 | 4.47E-34 | 3.51E-34 | 2.59E-34 | 1.80E-34 |
| DY160 | 1.96E-06 | 2.49E-06 | 3.10E-06 | 3.72E-06 | 4.29E-06 | 4.76E-06 | 5.11E-06 | 5.33E-06 | 5.39E-06 | 5.30E-06 | 5.06E-06 | 4.68E-06 | 4.20E-06 | 3.63E-06 | 3.01E-06 | 2.38E-06 | 1.77E-06 | 1.24E-06 |
| DY161 | 7.71E-06 | 8.62E-06 | 9.69E-06 | 1.07E-05 | 1.16E-05 | 1.23E-05 | 1.28E-05 | 1.30E-05 | 1.31E-05 | 1.30E-05 | 1.27E-05 | 1.21E-05 | 1.14E-05 | 1.05E-05 | 9.48E-06 | 8.34E-06 | 7.12E-06 | 5.96E-06 |
| DY162 | 5.44E-06 | 6.22E-06 | 7.10E-06 | 7.93E-06 | 8.66E-06 | 9.24E-06 | 9.67E-06 | 9.92E-06 | 9.99E-06 | 9.88E-06 | 9.59E-06 | 9.14E-06 | 8.54E-06 | 7.80E-06 | 6.94E-06 | 6.02E-06 | 5.05E-06 | 4.13E-06 |

| | | | | | | | | | | | | | | | | | | |
|---|---|---|---|---|---|---|---|---|---|---|---|---|---|---|---|---|---|---|
| DY163 | 2.29E-06 | 2.64E-06 | 3.02E-06 | 3.36E-06 | 3.67E-06 | 3.92E-06 | 4.09E-06 | 4.20E-06 | 4.23E-06 | 4.18E-06 | 4.06E-06 | 3.87E-06 | 3.62E-06 | 3.31E-06 | 2.95E-06 | 2.57E-06 | 2.15E-06 | 1.74E-06 |
| DY164 | 1.30E-06 | 1.50E-06 | 1.71E-06 | 1.91E-06 | 2.08E-06 | 2.22E-06 | 2.32E-06 | 2.38E-06 | 2.39E-06 | 2.37E-06 | 2.30E-06 | 2.19E-06 | 2.05E-06 | 1.88E-06 | 1.68E-06 | 1.46E-06 | 1.22E-06 | 9.87E-07 |
| HO165 | 6.58E-07 | 7.55E-07 | 8.58E-07 | 9.52E-07 | 1.03E-06 | 1.10E-06 | 1.14E-06 | 1.17E-06 | 1.18E-06 | 1.17E-06 | 1.14E-06 | 1.09E-06 | 1.02E-06 | 9.37E-07 | 8.41E-07 | 7.35E-07 | 6.20E-07 | 5.05E-07 |

Position=Segment location (midpoint of 2-in. segment) from bottom of fuel (BOF); 2 in. of fuel ~14.2g.

Table A-1k. Composition (grams) in 2-inch fuel segment: ORIGEN calculation results for Pin195011, decayed to 3/11/2011.

| Position: | 1 | 3 | 5 | 7 | 9 | 11 | 13 | 15 | 17 | 19 | 21 | 23 | 25 | 27 | 29 | 31 | 33 | 35 |
|---|---|---|---|---|---|---|---|---|---|---|---|---|---|---|---|---|---|---|
| ER166 | 4.14E-07 | 4.83E-07 | 5.58E-07 | 6.27E-07 | 6.88E-07 | 7.37E-07 | 7.73E-07 | 7.94E-07 | 8.00E-07 | 7.91E-07 | 7.67E-07 | 7.29E-07 | 6.78E-07 | 6.16E-07 | 5.46E-07 | 4.69E-07 | 3.89E-07 | 3.10E-07 |
| ER167 | 2.09E-07 | 2.40E-07 | 2.72E-07 | 3.01E-07 | 3.26E-07 | 3.46E-07 | 3.60E-07 | 3.68E-07 | 3.71E-07 | 3.67E-07 | 3.57E-07 | 3.42E-07 | 3.22E-07 | 2.97E-07 | 2.67E-07 | 2.34E-07 | 1.99E-07 | 1.62E-07 |
| ER168 | 1.32E-08 | 1.75E-08 | 2.23E-08 | 2.70E-08 | 3.13E-08 | 3.50E-08 | 3.77E-08 | 3.93E-08 | 3.98E-08 | 3.91E-08 | 3.72E-08 | 3.44E-08 | 3.07E-08 | 2.64E-08 | 2.17E-08 | 1.69E-08 | 1.24E-08 | 8.31E-09 |
| SUM FPs isotope | 9.50E-01 | 1.01E+00 | 1.11E+00 | 1.19E+00 | 1.27E+00 | 1.33E+00 | 1.37E+00 | 1.39E+00 | 1.40E+00 | 1.39E+00 | 1.36E+00 | 1.32E+00 | 1.26E+00 | 1.18E+00 | 1.08E+00 | 9.78E-01 | 8.65E-01 | 7.65E-01 |
| H | 7.93E-07 | 8.48E-07 | 9.25E-07 | 9.98E-07 | 1.06E-06 | 1.11E-06 | 1.14E-06 | 1.16E-06 | 1.17E-06 | 1.16E-06 | 1.14E-06 | 1.10E-06 | 1.05E-06 | 9.85E-07 | 9.07E-07 | 8.19E-07 | 7.24E-07 | 6.40E-07 |
| LI | 1.21E-08 | 1.29E-08 | 1.40E-08 | 1.50E-08 | 1.59E-08 | 1.66E-08 | 1.71E-08 | 1.74E-08 | 1.75E-08 | 1.74E-08 | 1.70E-08 | 1.65E-08 | 1.58E-08 | 1.48E-08 | 1.37E-08 | 1.24E-08 | 1.10E-08 | 9.81E-09 |
| GE | 5.03E-05 | 5.37E-05 | 5.85E-05 | 6.31E-05 | 6.69E-05 | 6.99E-05 | 7.21E-05 | 7.33E-05 | 7.37E-05 | 7.31E-05 | 7.17E-05 | 6.94E-05 | 6.63E-05 | 6.22E-05 | 5.74E-05 | 5.19E-05 | 4.59E-05 | 4.06E-05 |
| AS | 1.51E-05 | 1.61E-05 | 1.75E-05 | 1.88E-05 | 2.00E-05 | 2.08E-05 | 2.15E-05 | 2.18E-05 | 2.19E-05 | 2.18E-05 | 2.14E-05 | 2.07E-05 | 1.98E-05 | 1.86E-05 | 1.72E-05 | 1.56E-05 | 1.38E-05 | 1.22E-05 |
| SE | 1.96E-03 | 2.09E-03 | 2.27E-03 | 2.45E-03 | 2.60E-03 | 2.71E-03 | 2.80E-03 | 2.85E-03 | 2.86E-03 | 2.84E-03 | 2.78E-03 | 2.69E-03 | 2.57E-03 | 2.42E-03 | 2.23E-03 | 2.02E-03 | 1.79E-03 | 1.58E-03 |
| BR | 7.36E-04 | 7.82E-04 | 8.49E-04 | 9.12E-04 | 9.65E-04 | 1.01E-03 | 1.04E-03 | 1.05E-03 | 1.06E-03 | 1.05E-03 | 1.03E-03 | 9.99E-04 | 9.56E-04 | 9.00E-04 | 8.32E-04 | 7.55E-04 | 6.71E-04 | 5.97E-04 |
| KR | 1.23E-02 | 1.30E-02 | 1.42E-02 | 1.53E-02 | 1.62E-02 | 1.69E-02 | 1.74E-02 | 1.77E-02 | 1.78E-02 | 1.77E-02 | 1.74E-02 | 1.68E-02 | 1.60E-02 | 1.51E-02 | 1.39E-02 | 1.26E-02 | 1.11E-02 | 9.89E-03 |
| RB | 1.24E-02 | 1.32E-02 | 1.43E-02 | 1.54E-02 | 1.63E-02 | 1.70E-02 | 1.76E-02 | 1.79E-02 | 1.79E-02 | 1.78E-02 | 1.75E-02 | 1.69E-02 | 1.62E-02 | 1.52E-02 | 1.40E-02 | 1.27E-02 | 1.13E-02 | 1.00E-02 |
| SR | 2.41E-02 | 2.56E-02 | 2.78E-02 | 2.99E-02 | 3.17E-02 | 3.31E-02 | 3.42E-02 | 3.47E-02 | 3.49E-02 | 3.47E-02 | 3.40E-02 | 3.29E-02 | 3.14E-02 | 2.95E-02 | 2.72E-02 | 2.46E-02 | 2.19E-02 | 1.95E-02 |
| Y | 1.56E-02 | 1.66E-02 | 1.80E-02 | 1.94E-02 | 2.06E-02 | 2.15E-02 | 2.21E-02 | 2.25E-02 | 2.26E-02 | 2.25E-02 | 2.20E-02 | 2.13E-02 | 2.04E-02 | 1.91E-02 | 1.77E-02 | 1.60E-02 | 1.42E-02 | 1.26E-02 |
| ZR | 1.17E-01 | 1.24E-01 | 1.35E-01 | 1.45E-01 | 1.54E-01 | 1.61E-01 | 1.66E-01 | 1.69E-01 | 1.70E-01 | 1.69E-01 | 1.65E-01 | 1.60E-01 | 1.53E-01 | 1.43E-01 | 1.32E-01 | 1.20E-01 | 1.06E-01 | 9.41E-02 |
| NB | 2.14E-07 | 2.28E-07 | 2.48E-07 | 2.68E-07 | 2.84E-07 | 2.97E-07 | 3.07E-07 | 3.12E-07 | 3.14E-07 | 3.11E-07 | 3.05E-07 | 2.95E-07 | 2.81E-07 | 2.64E-07 | 2.43E-07 | 2.19E-07 | 1.94E-07 | 1.72E-07 |
| MO | 9.48E-02 | 1.01E-01 | 1.10E-01 | 1.19E-01 | 1.26E-01 | 1.32E-01 | 1.36E-01 | 1.38E-01 | 1.39E-01 | 1.38E-01 | 1.35E-01 | 1.31E-01 | 1.25E-01 | 1.17E-01 | 1.08E-01 | 9.74E-02 | 8.62E-02 | 7.63E-02 |
| TC | 2.24E-02 | 2.38E-02 | 2.59E-02 | 2.79E-02 | 2.96E-02 | 3.09E-02 | 3.18E-02 | 3.24E-02 | 3.25E-02 | 3.23E-02 | 3.17E-02 | 3.07E-02 | 2.93E-02 | 2.75E-02 | 2.54E-02 | 2.30E-02 | 2.04E-02 | 1.81E-02 |
| RU | 5.28E-02 | 5.67E-02 | 6.22E-02 | 6.73E-02 | 7.17E-02 | 7.52E-02 | 7.76E-02 | 7.91E-02 | 7.95E-02 | 7.89E-02 | 7.72E-02 | 7.46E-02 | 7.09E-02 | 6.64E-02 | 6.09E-02 | 5.47E-02 | 4.81E-02 | 4.22E-02 |
| RH | 1.43E-02 | 1.54E-02 | 1.68E-02 | 1.81E-02 | 1.93E-02 | 2.02E-02 | 2.08E-02 | 2.12E-02 | 2.13E-02 | 2.11E-02 | 2.07E-02 | 2.00E-02 | 1.91E-02 | 1.79E-02 | 1.64E-02 | 1.48E-02 | 1.31E-02 | 1.15E-02 |
| PD | 1.53E-02 | 1.69E-02 | 1.89E-02 | 2.08E-02 | 2.24E-02 | 2.37E-02 | 2.46E-02 | 2.51E-02 | 2.53E-02 | 2.51E-02 | 2.44E-02 | 2.35E-02 | 2.21E-02 | 2.05E-02 | 1.85E-02 | 1.64E-02 | 1.41E-02 | 1.20E-02 |
| AG | 1.11E-03 | 1.23E-03 | 1.37E-03 | 1.50E-03 | 1.62E-03 | 1.71E-03 | 1.78E-03 | 1.82E-03 | 1.83E-03 | 1.81E-03 | 1.77E-03 | 1.70E-03 | 1.60E-03 | 1.48E-03 | 1.34E-03 | 1.18E-03 | 1.02E-03 | 8.66E-04 |
| CD | 2.75E-03 | 3.04E-03 | 3.37E-03 | 3.66E-03 | 3.91E-03 | 4.10E-03 | 4.24E-03 | 4.32E-03 | 4.34E-03 | 4.31E-03 | 4.22E-03 | 4.07E-03 | 3.87E-03 | 3.62E-03 | 3.31E-03 | 2.97E-03 | 2.59E-03 | 2.21E-03 |
| IN | 4.10E-04 | 4.41E-04 | 4.74E-04 | 5.01E-04 | 5.23E-04 | 5.39E-04 | 5.49E-04 | 5.55E-04 | 5.57E-04 | 5.54E-04 | 5.47E-04 | 5.36E-04 | 5.19E-04 | 4.97E-04 | 4.68E-04 | 4.33E-04 | 3.90E-04 | 3.45E-04 |

Position=Segment location (midpoint of 2-in. segment) from bottom of fuel (BOF); 2 in. of fuel ~14.2g

Table A-11. Composition (grams) in 2-inch fuel segment: ORIGEN calculation results for Pin195011, decayed to 3/11/2011.

| Position: | 1 | 3 | 5 | 7 | 9 | 11 | 13 | 15 | 17 | 19 | 21 | 23 | 25 | 27 | 29 | 31 | 33 | 35 |
|---|---|---|---|---|---|---|---|---|---|---|---|---|---|---|---|---|---|---|
| SN | 4.68E-03 | 5.13E-03 | 5.66E-03 | 6.14E-03 | 6.55E-03 | 6.86E-03 | 7.08E-03 | 7.21E-03 | 7.25E-03 | 7.20E-03 | 7.05E-03 | 6.81E-03 | 6.48E-03 | 6.07E-03 | 5.57E-03 | 5.00E-03 | 4.37E-03 | 3.76E-03 |
| SB | 1.12E-03 | 1.23E-03 | 1.35E-03 | 1.46E-03 | 1.55E-03 | 1.62E-03 | 1.66E-03 | 1.69E-03 | 1.70E-03 | 1.69E-03 | 1.66E-03 | 1.60E-03 | 1.53E-03 | 1.44E-03 | 1.33E-03 | 1.20E-03 | 1.05E-03 | 9.09E-04 |
| TE | 1.55E-02 | 1.66E-02 | 1.82E-02 | 1.97E-02 | 2.09E-02 | 2.19E-02 | 2.26E-02 | 2.30E-02 | 2.31E-02 | 2.29E-02 | 2.25E-02 | 2.17E-02 | 2.07E-02 | 1.94E-02 | 1.78E-02 | 1.61E-02 | 1.42E-02 | 1.25E-02 |
| I | 8.11E-03 | 8.69E-03 | 9.49E-03 | 1.02E-02 | 1.09E-02 | 1.14E-02 | 1.17E-02 | 1.19E-02 | 1.20E-02 | 1.19E-02 | 1.17E-02 | 1.13E-02 | 1.08E-02 | 1.01E-02 | 9.31E-03 | 8.41E-03 | 7.43E-03 | 6.54E-03 |
| XE | 1.18E-01 | 1.26E-01 | 1.38E-01 | 1.49E-01 | 1.58E-01 | 1.65E-01 | 1.70E-01 | 1.73E-01 | 1.74E-01 | 1.73E-01 | 1.70E-01 | 1.64E-01 | 1.56E-01 | 1.47E-01 | 1.35E-01 | 1.22E-01 | 1.08E-01 | 9.50E-02 |
| CS | 8.92E-02 | 9.50E-02 | 1.04E-01 | 1.12E-01 | 1.19E-01 | 1.24E-01 | 1.28E-01 | 1.30E-01 | 1.31E-01 | 1.30E-01 | 1.27E-01 | 1.23E-01 | 1.17E-01 | 1.10E-01 | 1.02E-01 | 9.16E-02 | 8.11E-02 | 7.19E-02 |
| BA | 4.93E-02 | 5.27E-02 | 5.76E-02 | 6.23E-02 | 6.64E-02 | 6.95E-02 | 7.18E-02 | 7.31E-02 | 7.35E-02 | 7.29E-02 | 7.14E-02 | 6.90E-02 | 6.56E-02 | 6.14E-02 | 5.64E-02 | 5.08E-02 | 4.47E-02 | 3.95E-02 |
| LA | 3.49E-02 | 3.71E-02 | 4.05E-02 | 4.37E-02 | 4.64E-02 | 4.85E-02 | 5.00E-02 | 5.09E-02 | 5.11E-02 | 5.08E-02 | 4.98E-02 | 4.81E-02 | 4.59E-02 | 4.31E-02 | 3.97E-02 | 3.58E-02 | 3.17E-02 | 2.81E-02 |
| CE | 6.52E-02 | 6.95E-02 | 7.57E-02 | 8.17E-02 | 8.68E-02 | 9.08E-02 | 9.36E-02 | 9.52E-02 | 9.57E-02 | 9.50E-02 | 9.31E-02 | 9.00E-02 | 8.59E-02 | 8.06E-02 | 7.42E-02 | 6.70E-02 | 5.93E-02 | 5.25E-02 |
| PR | 3.31E-02 | 3.52E-02 | 3.83E-02 | 4.13E-02 | 4.38E-02 | 4.58E-02 | 4.72E-02 | 4.81E-02 | 4.83E-02 | 4.80E-02 | 4.70E-02 | 4.55E-02 | 4.34E-02 | 4.07E-02 | 3.76E-02 | 3.39E-02 | 3.00E-02 | 2.67E-02 |
| ND | 1.15E-01 | 1.23E-01 | 1.34E-01 | 1.44E-01 | 1.53E-01 | 1.60E-01 | 1.65E-01 | 1.68E-01 | 1.69E-01 | 1.68E-01 | 1.64E-01 | 1.59E-01 | 1.51E-01 | 1.42E-01 | 1.31E-01 | 1.18E-01 | 1.05E-01 | 9.26E-02 |
| PM | 6.26E-05 | 6.57E-05 | 7.05E-05 | 7.49E-05 | 7.86E-05 | 8.14E-05 | 8.34E-05 | 8.45E-05 | 8.49E-05 | 8.44E-05 | 8.31E-05 | 8.10E-05 | 7.80E-05 | 7.42E-05 | 6.94E-05 | 6.37E-05 | 5.74E-05 | 5.18E-05 |
| SM | 2.58E-02 | 2.77E-02 | 3.03E-02 | 3.28E-02 | 3.49E-02 | 3.66E-02 | 3.78E-02 | 3.85E-02 | 3.87E-02 | 3.84E-02 | 3.76E-02 | 3.63E-02 | 3.46E-02 | 3.24E-02 | 2.97E-02 | 2.67E-02 | 2.36E-02 | 2.07E-02 |
| EU | 1.67E-03 | 1.79E-03 | 1.95E-03 | 2.10E-03 | 2.23E-03 | 2.33E-03 | 2.40E-03 | 2.44E-03 | 2.45E-03 | 2.43E-03 | 2.39E-03 | 2.31E-03 | 2.21E-03 | 2.08E-03 | 1.92E-03 | 1.73E-03 | 1.53E-03 | 1.35E-03 |
| GD | 9.59E-04 | 1.07E-03 | 1.20E-03 | 1.33E-03 | 1.44E-03 | 1.54E-03 | 1.60E-03 | 1.64E-03 | 1.65E-03 | 1.63E-03 | 1.59E-03 | 1.52E-03 | 1.43E-03 | 1.31E-03 | 1.18E-03 | 1.03E-03 | 8.78E-04 | 7.39E-04 |
| TB | 3.32E-05 | 3.68E-05 | 4.11E-05 | 4.53E-05 | 4.89E-05 | 5.17E-05 | 5.38E-05 | 5.50E-05 | 5.53E-05 | 5.48E-05 | 5.34E-05 | 5.12E-05 | 4.82E-05 | 4.45E-05 | 4.02E-05 | 3.55E-05 | 3.05E-05 | 2.58E-05 |
| DY | 1.87E-05 | 2.15E-05 | 2.46E-05 | 2.76E-05 | 3.02E-05 | 3.24E-05 | 3.39E-05 | 3.49E-05 | 3.51E-05 | 3.47E-05 | 3.37E-05 | 3.20E-05 | 2.98E-05 | 2.71E-05 | 2.41E-05 | 2.08E-05 | 1.73E-05 | 1.41E-05 |
| HO | 6.60E-07 | 7.58E-07 | 8.62E-07 | 9.56E-07 | 1.04E-06 | 1.10E-06 | 1.15E-06 | 1.18E-06 | 1.19E-06 | 1.18E-06 | 1.14E-06 | 1.09E-06 | 1.03E-06 | 9.42E-07 | 8.45E-07 | 7.38E-07 | 6.23E-07 | 5.07E-07 |
| ER | 6.37E-07 | 7.41E-07 | 8.52E-07 | 9.55E-07 | 1.05E-06 | 1.12E-06 | 1.17E-06 | 1.20E-06 | 1.21E-06 | 1.20E-06 | 1.16E-06 | 1.11E-06 | 1.03E-06 | 9.39E-07 | 8.34E-07 | 7.21E-07 | 6.00E-07 | 4.81E-07 |
| SUM FPs elemental | 9.50E-01 | 1.01E+00 | 1.11E+00 | 1.19E+00 | 1.27E+00 | 1.33E+00 | 1.37E+00 | 1.39E+00 | 1.40E+00 | 1.39E+00 | 1.36E+00 | 1.32E+00 | 1.26E+00 | 1.18E+00 | 1.08E+00 | 9.78E-01 | 8.65E-01 | 7.65E-01 |

Position=Segment location (midpoint of 2-in. segment) from bottom of fuel (BOF); 2 in. of fuel ~14.2g

Table A-2a. Composition (grams) in 2-inch fuel segment: ORIGEN calculation results for Pin193045, decayed to 3/11/2011.

| Position: | 1 | 3 | 5 | 7 | 9 | 11 | 13 | 15 | 17 | 19 | 21 | 23 | 25 | 27 | 29 | 31 | 33 | 35 |
|---|---|---|---|---|---|---|---|---|---|---|---|---|---|---|---|---|---|---|
| HE 4 | 6.52E-06 | 7.29E-06 | 8.57E-06 | 9.95E-06 | 1.13E-05 | 1.24E-05 | 1.32E-05 | 1.37E-05 | 1.38E-05 | 1.35E-05 | 1.29E-05 | 1.20E-05 | 1.08E-05 | 9.47E-06 | 8.04E-06 | 6.62E-06 | 5.33E-06 | 4.40E-06 |
| TH230 | 4.98E-08 | 5.72E-08 | 6.37E-08 | 6.94E-08 | 7.41E-08 | 7.77E-08 | 8.02E-08 | 8.17E-08 | 8.21E-08 | 8.14E-08 | 7.95E-08 | 7.67E-08 | 7.28E-08 | 6.80E-08 | 6.24E-08 | 5.59E-08 | 0.00E+00 | 0.00E+00 |
| TH232 | 1.87E-07 | 1.80E-07 | 1.87E-07 | 1.97E-07 | 2.06E-07 | 2.13E-07 | 2.18E-07 | 2.21E-07 | 2.21E-07 | 2.20E-07 | 2.16E-07 | 2.10E-07 | 2.02E-07 | 1.91E-07 | 1.79E-07 | 1.65E-07 | 1.52E-07 | 1.49E-07 |
| PA231 | 6.90E-08 | 6.77E-08 | 6.51E-08 | 6.25E-08 | 6.03E-08 | 5.86E-08 | 5.74E-08 | 5.68E-08 | 5.66E-08 | 5.69E-08 | 5.78E-08 | 5.91E-08 | 6.10E-08 | 6.34E-08 | 6.62E-08 | 6.95E-08 | 7.30E-08 | 7.57E-08 |
| U233 | 0.00E+00 | 0.00E+00 | 0.00E+00 | 1.40E-07 | 1.65E-07 | 1.86E-07 | 2.02E-07 | 2.11E-07 | 2.13E-07 | 2.09E-07 | 1.97E-07 | 1.79E-07 | 1.57E-07 | 1.32E-07 | 0.00E+00 | 0.00E+00 | 0.00E+00 | 0.00E+00 |
| U234 | 1.84E-06 | 2.04E-06 | 2.20E-06 | 2.31E-06 | 2.40E-06 | 2.46E-06 | 2.50E-06 | 2.52E-06 | 2.52E-06 | 2.51E-06 | 2.49E-06 | 2.44E-06 | 2.38E-06 | 2.29E-06 | 2.17E-06 | 2.02E-06 | 1.83E-06 | 1.58E-06 |
| U235 | 9.42E-04 | 1.09E-03 | 1.23E-03 | 1.36E-03 | 1.47E-03 | 1.56E-03 | 1.63E-03 | 1.66E-03 | 1.67E-03 | 1.65E-03 | 1.61E-03 | 1.54E-03 | 1.44E-03 | 1.33E-03 | 1.20E-03 | 1.06E-03 | 9.06E-04 | 7.44E-04 |
| U236 | 3.07E+00 | 3.03E+00 | 2.92E+00 | 2.81E+00 | 2.72E+00 | 2.64E+00 | 2.59E+00 | 2.56E+00 | 2.56E+00 | 2.57E+00 | 2.61E+00 | 2.67E+00 | 2.75E+00 | 2.85E+00 | 2.97E+00 | 3.12E+00 | 3.26E+00 | 3.37E+00 |
| U237 | 3.11E-01 | 2.97E-01 | 3.10E-01 | 3.26E-01 | 3.40E-01 | 3.52E-01 | 3.60E-01 | 3.65E-01 | 3.66E-01 | 3.63E-01 | 3.57E-01 | 3.47E-01 | 3.34E-01 | 3.17E-01 | 2.97E-01 | 2.74E-01 | 2.53E-01 | 2.48E-01 |
| U238 | 4.04E-12 | 3.38E-12 | 3.89E-12 | 4.73E-12 | 5.60E-12 | 6.38E-12 | 7.01E-12 | 7.38E-12 | 7.46E-12 | 7.26E-12 | 6.78E-12 | 6.07E-12 | 5.18E-12 | 4.24E-12 | 3.31E-12 | 2.47E-12 | 1.87E-12 | 1.80E-12 |
| NP236 | 9.10E+00 | 9.06E+00 | 9.01E+00 | 8.97E+00 | 8.93E+00 | 8.89E+00 | 8.87E+00 | 8.86E+00 | 8.85E+00 | 8.86E+00 | 8.88E+00 | 8.90E+00 | 8.94E+00 | 8.98E+00 | 9.03E+00 | 9.09E+00 | 9.15E+00 | 9.20E+00 |
| NP237 | 1.79E-07 | 2.32E-07 | 3.02E-07 | 3.77E-07 | 4.48E-07 | 5.10E-07 | 5.57E-07 | 5.85E-07 | 5.92E-07 | 5.78E-07 | 5.43E-07 | 4.91E-07 | 4.26E-07 | 3.53E-07 | 2.79E-07 | 2.07E-07 | 1.45E-07 | 0.00E+00 |
| PU238 | 1.48E-02 | 1.64E-02 | 1.90E-02 | 2.16E-02 | 2.39E-02 | 2.58E-02 | 2.71E-02 | 2.79E-02 | 2.81E-02 | 2.77E-02 | 2.67E-02 | 2.52E-02 | 2.31E-02 | 2.07E-02 | 1.79E-02 | 1.50E-02 | 1.22E-02 | 9.97E-03 |
| PU239 | 9.65E-04 | 1.23E-03 | 1.59E-03 | 1.97E-03 | 2.33E-03 | 2.64E-03 | 2.87E-03 | 3.01E-03 | 3.04E-03 | 2.97E-03 | 2.80E-03 | 2.54E-03 | 2.22E-03 | 1.85E-03 | 1.47E-03 | 1.11E-03 | 7.80E-04 | 5.26E-04 |
| PU240 | 3.19E-01 | 3.25E-01 | 3.45E-01 | 3.66E-01 | 3.85E-01 | 3.99E-01 | 4.09E-01 | 4.15E-01 | 4.16E-01 | 4.13E-01 | 4.06E-01 | 3.94E-01 | 3.77E-01 | 3.57E-01 | 3.33E-01 | 3.05E-01 | 2.77E-01 | 2.57E-01 |
| PU241 | 1.37E-02 | 1.22E-02 | 1.34E-02 | 1.52E-02 | 1.70E-02 | 1.85E-02 | 1.97E-02 | 2.04E-02 | 2.05E-02 | 2.01E-02 | 1.93E-02 | 1.79E-02 | 1.61E-02 | 1.41E-02 | 1.20E-02 | 9.90E-03 | 8.24E-03 | 8.03E-03 |
| PU242 | 1.30E-04 | 1.09E-04 | 1.26E-04 | 1.53E-04 | 1.81E-04 | 2.06E-04 | 2.26E-04 | 2.38E-04 | 2.41E-04 | 2.34E-04 | 2.19E-04 | 1.96E-04 | 1.67E-04 | 1.37E-04 | 1.07E-04 | 7.98E-05 | 6.04E-05 | 5.82E-05 |
| AM241 | 5.37E-06 | 4.28E-06 | 5.25E-06 | 6.88E-06 | 8.70E-06 | 1.04E-05 | 1.19E-05 | 1.28E-05 | 1.30E-05 | 1.25E-05 | 1.14E-05 | 9.75E-06 | 7.83E-06 | 5.94E-06 | 4.22E-06 | 2.82E-06 | 1.91E-06 | 1.79E-06 |
| CM242 | 2.03E-04 | 1.70E-04 | 1.96E-04 | 2.38E-04 | 2.81E-04 | 3.20E-04 | 3.52E-04 | 3.70E-04 | 3.75E-04 | 3.64E-04 | 3.40E-04 | 3.05E-04 | 2.60E-04 | 2.13E-04 | 1.66E-04 | 1.24E-04 | 9.40E-05 | 9.05E-05 |
| SUM HM isotpes | 1.20E-07 | 0.00E+00 | 1.51E-07 | 1.99E-07 | 2.50E-07 | 2.99E-07 | 3.38E-07 | 3.61E-07 | 3.67E-07 | 3.53E-07 | 3.23E-07 | 2.80E-07 | 2.27E-07 | 1.74E-07 | 1.25E-07 | 0.00E+00 | 0.00E+00 | 0.00E+00 |

Position=Segment location (midpoint of 2-in. segment) from bottom of fuel (BOF); sample wgt. 14.2g

Table A-2b. Composition (grams) in 2-inch fuel segment: ORIGEN calculation results for Pin193045, decayed to 3/11/2011.

| Position: | 1 | 3 | 5 | 7 | 9 | 11 | 13 | 15 | 17 | 19 | 21 | 23 | 25 | 27 | 29 | 31 | 33 | 35 |
|---|---|---|---|---|---|---|---|---|---|---|---|---|---|---|---|---|---|---|
| HE | 6.52E-06 | 7.29E-06 | 8.57E-06 | 9.95E-06 | 1.13E-05 | 1.24E-05 | 1.32E-05 | 1.37E-05 | 1.38E-05 | 1.35E-05 | 1.29E-05 | 1.20E-05 | 1.08E-05 | 9.47E-06 | 8.04E-06 | 6.62E-06 | 5.33E-06 | 4.40E-06 |
| TH | 2.39E-07 | 2.39E-07 | 2.54E-07 | 2.70E-07 | 2.85E-07 | 2.96E-07 | 3.04E-07 | 3.08E-07 | 3.09E-07 | 3.07E-07 | 3.01E-07 | 2.92E-07 | 2.79E-07 | 2.63E-07 | 2.45E-07 | 2.24E-07 | 2.03E-07 | 1.91E-07 |
| PA | 6.95E-08 | 6.83E-08 | 6.57E-08 | 6.32E-08 | 6.11E-08 | 5.95E-08 | 5.84E-08 | 5.77E-08 | 5.76E-08 | 5.79E-08 | 5.87E-08 | 6.00E-08 | 6.18E-08 | 6.41E-08 | 6.68E-08 | 7.00E-08 | 7.34E-08 | 7.61E-08 |
| U | 1.25E+01 | 1.24E+01 | 1.22E+01 | 1.21E+01 | 1.20E+01 | 1.19E+01 | 1.18E+01 | 1.18E+01 | 1.18E+01 | 1.18E+01 | 1.18E+01 | 1.19E+01 | 1.20E+01 | 1.22E+01 | 1.23E+01 | 1.25E+01 | 1.27E+01 | 1.28E+01 |
| NP | 1.48E-02 | 1.64E-02 | 1.90E-02 | 2.16E-02 | 2.39E-02 | 2.58E-02 | 2.71E-02 | 2.79E-02 | 2.81E-02 | 2.77E-02 | 2.67E-02 | 2.52E-02 | 2.31E-02 | 2.07E-02 | 1.79E-02 | 1.50E-02 | 1.22E-02 | 9.97E-03 |
| PU | 3.34E-01 | 3.39E-01 | 3.60E-01 | 3.84E-01 | 4.04E-01 | 4.20E-01 | 4.32E-01 | 4.38E-01 | 4.40E-01 | 4.36E-01 | 4.28E-01 | 4.14E-01 | 3.96E-01 | 3.73E-01 | 3.46E-01 | 3.16E-01 | 2.86E-01 | 2.66E-01 |
| AM | 2.03E-04 | 1.70E-04 | 1.96E-04 | 2.38E-04 | 2.82E-04 | 3.21E-04 | 3.52E-04 | 3.71E-04 | 3.75E-04 | 3.65E-04 | 3.41E-04 | 3.05E-04 | 2.61E-04 | 2.13E-04 | 1.67E-04 | 1.24E-04 | 9.40E-05 | 9.05E-05 |
| CM | 2.12E-09 | 2.34E-09 | 3.46E-09 | 5.16E-09 | 7.18E-09 | 9.23E-09 | 1.10E-08 | 1.21E-08 | 1.24E-08 | 1.18E-08 | 1.04E-08 | 8.47E-09 | 6.35E-09 | 4.38E-09 | 2.76E-09 | 1.59E-09 | 0.00E+00 | 0.00E+00 |
| SUM HM elements | 1.28E+01 | 1.27E+01 | 1.26E+01 | 1.25E+01 | 1.24E+01 | 1.23E+01 | 1.23E+01 | 1.22E+01 | 1.22E+01 | 1.23E+01 | 1.23E+01 | 1.24E+01 | 1.24E+01 | 1.25E+01 | 1.27E+01 | 1.28E+01 | 1.30E+01 | 1.31E+01 |
| H 3 | 1.05E-06 | 1.11E-06 | 1.21E-06 | 1.30E-06 | 1.38E-06 | 1.44E-06 | 1.48E-06 | 1.51E-06 | 1.51E-06 | 1.50E-06 | 1.47E-06 | 1.42E-06 | 1.36E-06 | 1.27E-06 | 1.18E-06 | 1.06E-06 | 9.41E-07 | 8.36E-07 |
| LI 6 | 1.60E-08 | 1.69E-08 | 1.83E-08 | 1.96E-08 | 2.07E-08 | 2.15E-08 | 2.21E-08 | 2.24E-08 | 2.25E-08 | 2.23E-08 | 2.19E-08 | 2.12E-08 | 2.03E-08 | 1.92E-08 | 1.77E-08 | 1.61E-08 | 1.44E-08 | 1.29E-08 |
| GE 72 | 2.44E-06 | 2.64E-06 | 2.89E-06 | 3.11E-06 | 3.30E-06 | 3.45E-06 | 3.55E-06 | 3.61E-06 | 3.63E-06 | 3.60E-06 | 3.52E-06 | 3.41E-06 | 3.25E-06 | 3.04E-06 | 2.80E-06 | 2.53E-06 | 2.22E-06 | 1.94E-06 |
| GE 73 | 6.07E-06 | 6.47E-06 | 7.03E-06 | 7.55E-06 | 7.98E-06 | 8.31E-06 | 8.54E-06 | 8.66E-06 | 8.70E-06 | 8.63E-06 | 8.47E-06 | 8.20E-06 | 7.84E-06 | 7.38E-06 | 6.83E-06 | 6.20E-06 | 5.50E-06 | 4.87E-06 |
| GE 74 | 1.22E-05 | 1.30E-05 | 1.41E-05 | 1.52E-05 | 1.61E-05 | 1.68E-05 | 1.73E-05 | 1.76E-05 | 1.77E-05 | 1.75E-05 | 1.72E-05 | 1.66E-05 | 1.58E-05 | 1.49E-05 | 1.37E-05 | 1.24E-05 | 1.10E-05 | 9.70E-06 |
| AS 75 | 2.04E-05 | 2.16E-05 | 2.35E-05 | 2.51E-05 | 2.66E-05 | 2.76E-05 | 2.84E-05 | 2.88E-05 | 2.89E-05 | 2.87E-05 | 2.82E-05 | 2.73E-05 | 2.61E-05 | 2.46E-05 | 2.28E-05 | 2.07E-05 | 1.84E-05 | 1.64E-05 |
| GE 76 | 4.78E-05 | 5.06E-05 | 5.49E-05 | 5.90E-05 | 6.24E-05 | 6.50E-05 | 6.69E-05 | 6.79E-05 | 6.82E-05 | 6.76E-05 | 6.63E-05 | 6.42E-05 | 6.13E-05 | 5.77E-05 | 5.33E-05 | 4.83E-05 | 4.29E-05 | 3.82E-05 |
| SE 76 | 5.08E-07 | 6.26E-07 | 7.69E-07 | 9.09E-07 | 1.04E-06 | 1.14E-06 | 1.22E-06 | 1.26E-06 | 1.27E-06 | 1.25E-06 | 1.20E-06 | 1.11E-06 | 9.99E-07 | 8.69E-07 | 7.28E-07 | 5.82E-07 | 4.41E-07 | 3.20E-07 |
| SE 77 | 9.46E-05 | 9.96E-05 | 1.08E-04 | 1.15E-04 | 1.22E-04 | 1.26E-04 | 1.30E-04 | 1.32E-04 | 1.32E-04 | 1.31E-04 | 1.29E-04 | 1.25E-04 | 1.20E-04 | 1.13E-04 | 1.04E-04 | 9.49E-05 | 8.47E-05 | 7.60E-05 |
| SE 78 | 1.94E-04 | 2.04E-04 | 2.21E-04 | 2.38E-04 | 2.52E-04 | 2.63E-04 | 2.70E-04 | 2.75E-04 | 2.76E-04 | 2.73E-04 | 2.68E-04 | 2.59E-04 | 2.47E-04 | 2.32E-04 | 2.15E-04 | 1.94E-04 | 1.73E-04 | 1.54E-04 |
| SE 79 | 2.94E-04 | 3.13E-04 | 3.40E-04 | 3.66E-04 | 3.87E-04 | 4.04E-04 | 4.16E-04 | 4.23E-04 | 4.24E-04 | 4.21E-04 | 4.12E-04 | 3.99E-04 | 3.81E-04 | 3.57E-04 | 3.30E-04 | 2.98E-04 | 2.64E-04 | 2.35E-04 |
| BR 79 | 6.49E-08 | 6.90E-08 | 7.50E-08 | 8.07E-08 | 8.55E-08 | 8.92E-08 | 9.18E-08 | 9.32E-08 | 9.36E-08 | 9.28E-08 | 9.10E-08 | 8.80E-08 | 8.39E-08 | 7.88E-08 | 7.27E-08 | 6.58E-08 | 5.83E-08 | 5.17E-08 |

| | | | | | | | | | | | | | | | | | | |
|---|---|---|---|---|---|---|---|---|---|---|---|---|---|---|---|---|---|---|
| SE 80 | 6.29E-04 | 6.64E-04 | 7.19E-04 | 7.72E-04 | 8.16E-04 | 8.50E-04 | 8.74E-04 | 8.88E-04 | 8.91E-04 | 8.84E-04 | 8.67E-04 | 8.39E-04 | 8.02E-04 | 7.55E-04 | 6.98E-04 | 6.33E-04 | 5.63E-04 | 5.04E-04 |
| BR 81 | 9.94E-04 | 1.05E-03 | 1.13E-03 | 1.21E-03 | 1.28E-03 | 1.33E-03 | 1.37E-03 | 1.39E-03 | 1.39E-03 | 1.38E-03 | 1.35E-03 | 1.31E-03 | 1.26E-03 | 1.19E-03 | 1.10E-03 | 1.00E-03 | 8.93E-04 | 8.00E-04 |
| SE 82 | 1.46E-03 | 1.54E-03 | 1.68E-03 | 1.80E-03 | 1.91E-03 | 1.99E-03 | 2.04E-03 | 2.08E-03 | 2.08E-03 | 2.07E-03 | 2.03E-03 | 1.96E-03 | 1.87E-03 | 1.76E-03 | 1.63E-03 | 1.47E-03 | 1.31E-03 | 1.16E-03 |

Position=Segment location (midpoint of 2-in. segment) from bottom of fuel (BOF); 2-in of fuel ~14.2g

Table A-2c. Composition (grams) in 2-inch fuel segment: ORIGEN calculation results for Pin193045, decayed to 3/11/2011.

| Position: | 1 | 3 | 5 | 7 | 9 | 11 | 13 | 15 | 17 | 19 | 21 | 23 | 25 | 27 | 29 | 31 | 33 | 35 |
|---|---|---|---|---|---|---|---|---|---|---|---|---|---|---|---|---|---|---|
| KR 82 | 3.09E-05 | 3.76E-05 | 4.59E-05 | 5.41E-05 | 6.14E-05 | 6.75E-05 | 7.19E-05 | 7.45E-05 | 7.51E-05 | 7.38E-05 | 7.06E-05 | 6.57E-05 | 5.93E-05 | 5.17E-05 | 4.34E-05 | 3.49E-05 | 2.66E-05 | 1.96E-05 |
| KR 83 | 2.48E-03 | 2.62E-03 | 2.83E-03 | 3.02E-03 | 3.19E-03 | 3.32E-03 | 3.40E-03 | 3.45E-03 | 3.47E-03 | 3.44E-03 | 3.38E-03 | 3.28E-03 | 3.14E-03 | 2.96E-03 | 2.74E-03 | 2.50E-03 | 2.23E-03 | 2.00E-03 |
| KR 84 | 4.85E-03 | 5.14E-03 | 5.59E-03 | 6.01E-03 | 6.37E-03 | 6.65E-03 | 6.85E-03 | 6.96E-03 | 6.99E-03 | 6.93E-03 | 6.79E-03 | 6.57E-03 | 6.26E-03 | 5.87E-03 | 5.42E-03 | 4.89E-03 | 4.34E-03 | 3.86E-03 |
| KR 85 | 3.28E-04 | 3.46E-04 | 3.76E-04 | 4.04E-04 | 4.28E-04 | 4.46E-04 | 4.59E-04 | 4.66E-04 | 4.68E-04 | 4.64E-04 | 4.55E-04 | 4.40E-04 | 4.20E-04 | 3.95E-04 | 3.65E-04 | 3.30E-04 | 2.93E-04 | 2.62E-04 |
| RB 85 | 5.43E-03 | 5.72E-03 | 6.19E-03 | 6.64E-03 | 7.01E-03 | 7.30E-03 | 7.51E-03 | 7.62E-03 | 7.65E-03 | 7.59E-03 | 7.45E-03 | 7.21E-03 | 6.89E-03 | 6.49E-03 | 6.01E-03 | 5.45E-03 | 4.85E-03 | 4.35E-03 |
| KR 86 | 8.99E-03 | 9.48E-03 | 1.03E-02 | 1.10E-02 | 1.17E-02 | 1.22E-02 | 1.25E-02 | 1.27E-02 | 1.28E-02 | 1.27E-02 | 1.24E-02 | 1.20E-02 | 1.15E-02 | 1.08E-02 | 9.97E-03 | 9.03E-03 | 8.03E-03 | 7.19E-03 |
| RB 86 | 0.00E+00 | 0.00E+00 | 0.00E+00 | 0.00E+00 | 0.00E+00 | 0.00E+00 | 0.00E+00 | 0.00E+00 | 0.00E+00 | 0.00E+00 | 0.00E+00 | 0.00E+00 | 0.00E+00 | 0.00E+00 | 0.00E+00 | 0.00E+00 | 0.00E+00 | 0.00E+00 |
| SR 86 | 6.90E-05 | 8.43E-05 | 1.03E-04 | 1.22E-04 | 1.39E-04 | 1.53E-04 | 1.63E-04 | 1.69E-04 | 1.71E-04 | 1.68E-04 | 1.60E-04 | 1.49E-04 | 1.34E-04 | 1.17E-04 | 9.75E-05 | 7.80E-05 | 5.93E-05 | 4.34E-05 |
| RB 87 | 1.14E-02 | 1.21E-02 | 1.31E-02 | 1.40E-02 | 1.48E-02 | 1.55E-02 | 1.59E-02 | 1.62E-02 | 1.62E-02 | 1.61E-02 | 1.58E-02 | 1.53E-02 | 1.46E-02 | 1.37E-02 | 1.27E-02 | 1.15E-02 | 1.02E-02 | 9.15E-03 |
| SR 87 | 3.45E-07 | 4.43E-07 | 5.74E-07 | 7.16E-07 | 8.53E-07 | 9.73E-07 | 1.06E-06 | 1.12E-06 | 1.13E-06 | 1.11E-06 | 1.04E-06 | 9.37E-07 | 8.13E-07 | 6.75E-07 | 5.36E-07 | 4.05E-07 | 2.92E-07 | 2.08E-07 |
| SR 88 | 1.68E-02 | 1.78E-02 | 1.92E-02 | 2.06E-02 | 2.18E-02 | 2.27E-02 | 2.34E-02 | 2.38E-02 | 2.38E-02 | 2.37E-02 | 2.32E-02 | 2.25E-02 | 2.14E-02 | 2.02E-02 | 1.87E-02 | 1.69E-02 | 1.50E-02 | 1.35E-02 |
| SR 89 | 1.12E-42 | 1.25E-42 | 1.37E-42 | 1.37E-42 | 1.50E-42 | 1.50E-42 | 1.50E-42 | 1.50E-42 | 1.50E-42 | 1.50E-42 | 1.50E-42 | 1.50E-42 | 1.50E-42 | 1.37E-42 | 1.25E-42 | 1.25E-42 | 1.12E-42 | 9.98E-43 |
| Y 89 | 2.12E-02 | 2.24E-02 | 2.43E-02 | 2.60E-02 | 2.75E-02 | 2.87E-02 | 2.95E-02 | 2.99E-02 | 3.01E-02 | 2.98E-02 | 2.92E-02 | 2.83E-02 | 2.71E-02 | 2.55E-02 | 2.35E-02 | 2.13E-02 | 1.90E-02 | 1.70E-02 |
| SR 90 | 1.57E-02 | 1.65E-02 | 1.79E-02 | 1.92E-02 | 2.03E-02 | 2.11E-02 | 2.17E-02 | 2.20E-02 | 2.21E-02 | 2.20E-02 | 2.15E-02 | 2.09E-02 | 1.99E-02 | 1.87E-02 | 1.73E-02 | 1.57E-02 | 1.40E-02 | 1.25E-02 |
| Y 90 | 3.93E-06 | 4.14E-06 | 4.48E-06 | 4.81E-06 | 5.08E-06 | 5.30E-06 | 5.44E-06 | 5.53E-06 | 5.55E-06 | 5.51E-06 | 5.40E-06 | 5.23E-06 | 5.00E-06 | 4.70E-06 | 4.35E-06 | 3.94E-06 | 3.51E-06 | 3.15E-06 |
| ZR 90 | 1.03E-02 | 1.08E-02 | 1.17E-02 | 1.26E-02 | 1.33E-02 | 1.39E-02 | 1.43E-02 | 1.45E-02 | 1.46E-02 | 1.45E-02 | 1.42E-02 | 1.37E-02 | 1.31E-02 | 1.23E-02 | 1.14E-02 | 1.03E-02 | 9.16E-03 | 8.20E-03 |
| Y 91 | 3.80E-37 | 3.97E-37 | 4.24E-37 | 4.49E-37 | 4.70E-37 | 4.85E-37 | 4.95E-37 | 5.02E-37 | 5.03E-37 | 5.01E-37 | 4.94E-37 | 4.83E-37 | 4.67E-37 | 4.45E-37 | 4.18E-37 | 3.86E-37 | 3.49E-37 | 3.18E-37 |
| ZR 91 | 2.69E-02 | 2.84E-02 | 3.07E-02 | 3.30E-02 | 3.49E-02 | 3.63E-02 | 3.73E-02 | 3.79E-02 | 3.81E-02 | 3.78E-02 | 3.70E-02 | 3.59E-02 | 3.43E-02 | 3.22E-02 | 2.98E-02 | 2.70E-02 | 2.41E-02 | 2.15E-02 |
| ZR 92 | 2.84E-02 | 3.00E-02 | 3.26E-02 | 3.50E-02 | 3.71E-02 | 3.86E-02 | 3.98E-02 | 4.04E-02 | 4.05E-02 | 4.02E-02 | 3.94E-02 | 3.81E-02 | 3.64E-02 | 3.42E-02 | 3.16E-02 | 2.86E-02 | 2.54E-02 | 2.27E-02 |
| ZR 93 | 3.13E-02 | 3.30E-02 | 3.58E-02 | 3.85E-02 | 4.07E-02 | 4.24E-02 | 4.36E-02 | 4.43E-02 | 4.45E-02 | 4.41E-02 | 4.33E-02 | 4.19E-02 | 4.00E-02 | 3.76E-02 | 3.47E-02 | 3.15E-02 | 2.80E-02 | 2.50E-02 |
| NB 93 | 1.22E-07 | 1.29E-07 | 1.40E-07 | 1.50E-07 | 1.59E-07 | 1.66E-07 | 1.70E-07 | 1.73E-07 | 1.74E-07 | 1.72E-07 | 1.69E-07 | 1.63E-07 | 1.56E-07 | 1.46E-07 | 1.35E-07 | 1.22E-07 | 1.09E-07 | 9.68E-08 |
| NB 93M | 1.72E-07 | 1.82E-07 | 1.97E-07 | 2.12E-07 | 2.24E-07 | 2.34E-07 | 2.41E-07 | 2.44E-07 | 2.45E-07 | 2.43E-07 | 2.39E-07 | 2.31E-07 | 2.20E-07 | 2.07E-07 | 1.91E-07 | 1.73E-07 | 1.54E-07 | 1.37E-07 |

| | | | | | | | | | | | | | | | | | |
|---|---|---|---|---|---|---|---|---|---|---|---|---|---|---|---|---|---|
| ZR 94 | 3.04E-02 | 3.21E-02 | 3.49E-02 | 3.75E-02 | 3.97E-02 | 4.14E-02 | 4.27E-02 | 4.33E-02 | 4.35E-02 | 4.32E-02 | 4.23E-02 | 4.09E-02 | 3.90E-02 | 3.66E-02 | 3.38E-02 | 3.06E-02 | 2.71E-02 | 2.42E-02 |

Position=Segment location (midpoint of 2-in. segment) from bottom of fuel (BOF); 2 in. of fuel ~14.2g

Table A-2d. Composition (grams) in 2-inch fuel segment: ORIGEN calculation results for Pin193045, decayed to 3/11/2011.

| Position: | 1 | 3 | 5 | 7 | 9 | 11 | 13 | 15 | 17 | 19 | 21 | 23 | 25 | 27 | 29 | 31 | 33 | 35 |
|---|---|---|---|---|---|---|---|---|---|---|---|---|---|---|---|---|---|---|
| ZR 95 | 3.83E-34 | 4.01E-34 | 4.30E-34 | 4.57E-34 | 4.79E-34 | 4.96E-34 | 5.08E-34 | 5.14E-34 | 5.17E-34 | 5.14E-34 | 5.06E-34 | 4.94E-34 | 4.76E-34 | 4.53E-34 | 4.24E-34 | 3.89E-34 | 3.51E-34 | 3.17E-34 |
| NB 95 | 2.16E-34 | 2.26E-34 | 2.42E-34 | 2.57E-34 | 2.70E-34 | 2.79E-34 | 2.86E-34 | 2.90E-34 | 2.91E-34 | 2.89E-34 | 2.85E-34 | 2.78E-34 | 2.68E-34 | 2.55E-34 | 2.39E-34 | 2.19E-34 | 1.98E-34 | 1.79E-34 |
| NB 95M | 1.51E-37 | 1.59E-37 | 1.70E-37 | 1.81E-37 | 1.89E-37 | 1.96E-37 | 2.01E-37 | 2.03E-37 | 2.04E-37 | 2.03E-37 | 2.00E-37 | 1.95E-37 | 1.88E-37 | 1.79E-37 | 1.67E-37 | 1.54E-37 | 1.39E-37 | 1.25E-37 |
| MO 95 | 3.19E-02 | 3.37E-02 | 3.65E-02 | 3.92E-02 | 4.14E-02 | 4.31E-02 | 4.43E-02 | 4.50E-02 | 4.52E-02 | 4.48E-02 | 4.40E-02 | 4.26E-02 | 4.07E-02 | 3.83E-02 | 3.54E-02 | 3.21E-02 | 2.86E-02 | 2.56E-02 |
| ZR 96 | 3.20E-02 | 3.39E-02 | 3.68E-02 | 3.95E-02 | 4.19E-02 | 4.37E-02 | 4.50E-02 | 4.57E-02 | 4.59E-02 | 4.55E-02 | 4.46E-02 | 4.31E-02 | 4.11E-02 | 3.86E-02 | 3.56E-02 | 3.22E-02 | 2.86E-02 | 2.55E-02 |
| MO 96 | 5.71E-04 | 7.00E-04 | 8.59E-04 | 1.02E-03 | 1.16E-03 | 1.28E-03 | 1.37E-03 | 1.42E-03 | 1.43E-03 | 1.40E-03 | 1.34E-03 | 1.24E-03 | 1.12E-03 | 9.71E-04 | 8.12E-04 | 6.48E-04 | 4.91E-04 | 3.58E-04 |
| MO 97 | 3.08E-02 | 3.26E-02 | 3.53E-02 | 3.79E-02 | 4.01E-02 | 4.18E-02 | 4.30E-02 | 4.37E-02 | 4.38E-02 | 4.35E-02 | 4.26E-02 | 4.13E-02 | 3.94E-02 | 3.70E-02 | 3.42E-02 | 3.10E-02 | 2.76E-02 | 2.46E-02 |
| MO 98 | 3.20E-02 | 3.40E-02 | 3.71E-02 | 4.00E-02 | 4.24E-02 | 4.43E-02 | 4.57E-02 | 4.64E-02 | 4.66E-02 | 4.62E-02 | 4.53E-02 | 4.37E-02 | 4.16E-02 | 3.90E-02 | 3.59E-02 | 3.24E-02 | 2.87E-02 | 2.54E-02 |
| TC 98 | 8.98E-07 | 1.10E-06 | 1.36E-06 | 1.61E-06 | 1.83E-06 | 2.02E-06 | 2.16E-06 | 2.24E-06 | 2.26E-06 | 2.22E-06 | 2.12E-06 | 1.97E-06 | 1.77E-06 | 1.54E-06 | 1.28E-06 | 1.02E-06 | 7.73E-07 | 5.62E-07 |
| TC 99 | 3.04E-02 | 3.22E-02 | 3.49E-02 | 3.74E-02 | 3.96E-02 | 4.12E-02 | 4.24E-02 | 4.31E-02 | 4.32E-02 | 4.29E-02 | 4.21E-02 | 4.07E-02 | 3.89E-02 | 3.66E-02 | 3.38E-02 | 3.07E-02 | 2.73E-02 | 2.43E-02 |
| RU 99 | 2.05E-06 | 2.17E-06 | 2.35E-06 | 2.52E-06 | 2.67E-06 | 2.78E-06 | 2.86E-06 | 2.90E-06 | 2.91E-06 | 2.89E-06 | 2.83E-06 | 2.74E-06 | 2.62E-06 | 2.46E-06 | 2.28E-06 | 2.06E-06 | 1.83E-06 | 1.64E-06 |
| MO100 | 3.42E-02 | 3.62E-02 | 3.94E-02 | 4.24E-02 | 4.49E-02 | 4.69E-02 | 4.82E-02 | 4.90E-02 | 4.92E-02 | 4.88E-02 | 4.78E-02 | 4.62E-02 | 4.41E-02 | 4.14E-02 | 3.82E-02 | 3.45E-02 | 3.06E-02 | 2.72E-02 |
| RU100 | 9.87E-04 | 1.21E-03 | 1.49E-03 | 1.76E-03 | 2.01E-03 | 2.21E-03 | 2.36E-03 | 2.45E-03 | 2.47E-03 | 2.43E-03 | 2.32E-03 | 2.15E-03 | 1.94E-03 | 1.68E-03 | 1.41E-03 | 1.12E-03 | 8.51E-04 | 6.19E-04 |
| RU101 | 2.95E-02 | 3.12E-02 | 3.39E-02 | 3.64E-02 | 3.84E-02 | 4.01E-02 | 4.12E-02 | 4.18E-02 | 4.20E-02 | 4.17E-02 | 4.09E-02 | 3.96E-02 | 3.78E-02 | 3.55E-02 | 3.29E-02 | 2.98E-02 | 2.64E-02 | 2.36E-02 |
| RU102 | 2.73E-02 | 2.93E-02 | 3.21E-02 | 3.47E-02 | 3.70E-02 | 3.88E-02 | 4.00E-02 | 4.07E-02 | 4.09E-02 | 4.05E-02 | 3.96E-02 | 3.82E-02 | 3.63E-02 | 3.39E-02 | 3.11E-02 | 2.79E-02 | 2.45E-02 | 2.15E-02 |
| RH102 | 1.67E-09 | 2.07E-09 | 2.55E-09 | 3.02E-09 | 3.45E-09 | 3.81E-09 | 4.07E-09 | 4.22E-09 | 4.26E-09 | 4.19E-09 | 4.00E-09 | 3.71E-09 | 3.33E-09 | 2.89E-09 | 2.41E-09 | 1.92E-09 | 1.45E-09 | 1.04E-09 |
| RU103 | 0.00E+00 | 0.00E+00 | 0.00E+00 | 0.00E+00 | 0.00E+00 | 0.00E+00 | 0.00E+00 | 0.00E+00 | 0.00E+00 | 0.00E+00 | 0.00E+00 | 0.00E+00 | 0.00E+00 | 0.00E+00 | 0.00E+00 | 0.00E+00 | 0.00E+00 | 0.00E+00 |
| RH103 | 1.95E-02 | 2.08E-02 | 2.27E-02 | 2.44E-02 | 2.59E-02 | 2.70E-02 | 2.78E-02 | 2.83E-02 | 2.84E-02 | 2.82E-02 | 2.76E-02 | 2.67E-02 | 2.54E-02 | 2.39E-02 | 2.20E-02 | 1.98E-02 | 1.76E-02 | 1.55E-02 |
| RH103M | 0.00E+00 | 0.00E+00 | 0.00E+00 | 0.00E+00 | 0.00E+00 | 0.00E+00 | 0.00E+00 | 0.00E+00 | 0.00E+00 | 0.00E+00 | 0.00E+00 | 0.00E+00 | 0.00E+00 | 0.00E+00 | 0.00E+00 | 0.00E+00 | 0.00E+00 | 0.00E+00 |
| RU104 | 1.49E-02 | 1.60E-02 | 1.76E-02 | 1.91E-02 | 2.04E-02 | 2.14E-02 | 2.21E-02 | 2.25E-02 | 2.26E-02 | 2.24E-02 | 2.19E-02 | 2.11E-02 | 2.00E-02 | 1.86E-02 | 1.71E-02 | 1.53E-02 | 1.34E-02 | 1.17E-02 |
| PD104 | 9.96E-04 | 1.23E-03 | 1.52E-03 | 1.80E-03 | 2.05E-03 | 2.26E-03 | 2.42E-03 | 2.51E-03 | 2.53E-03 | 2.49E-03 | 2.37E-03 | 2.20E-03 | 1.98E-03 | 1.72E-03 | 1.43E-03 | 1.14E-03 | 8.63E-04 | 6.23E-04 |

| | | | | | | | | | | | | | | | | | | |
|---|---|---|---|---|---|---|---|---|---|---|---|---|---|---|---|---|---|---|
| PD105 | 8.40E-03 | 9.11E-03 | 1.00E-02 | 1.09E-02 | 1.16E-02 | 1.22E-02 | 1.26E-02 | 1.28E-02 | 1.28E-02 | 1.27E-02 | 1.24E-02 | 1.20E-02 | 1.14E-02 | 1.06E-02 | 9.71E-03 | 8.69E-03 | 7.60E-03 | 6.59E-03 |
| RU106 | 4.64E-09 | 5.08E-09 | 5.67E-09 | 6.22E-09 | 6.70E-09 | 7.09E-09 | 7.36E-09 | 7.52E-09 | 7.56E-09 | 7.49E-09 | 7.29E-09 | 6.99E-09 | 6.58E-09 | 6.07E-09 | 5.49E-09 | 4.85E-09 | 4.17E-09 | 3.56E-09 |

Position=Segment location (midpoint of 2-in. segment) from bottom of fuel (BOF); 2 in. of fuel ~14.2g

Table A-2e. Composition (grams) in 2-inch fuel segment: ORIGEN calculation results for Pin193045, decayed to 3/11/2011.

| Position: | 1 | 3 | 5 | 7 | 9 | 11 | 13 | 15 | 17 | 19 | 21 | 23 | 25 | 27 | 29 | 31 | 33 | 35 |
|---|---|---|---|---|---|---|---|---|---|---|---|---|---|---|---|---|---|---|
| PD106 | 5.68E-03 | 6.32E-03 | 7.13E-03 | 7.89E-03 | 8.55E-03 | 9.09E-03 | 9.46E-03 | 9.68E-03 | 9.74E-03 | 9.63E-03 | 9.35E-03 | 8.92E-03 | 8.35E-03 | 7.66E-03 | 6.86E-03 | 6.00E-03 | 5.10E-03 | 4.29E-03 |
| PD107 | 3.39E-03 | 3.70E-03 | 4.11E-03 | 4.50E-03 | 4.84E-03 | 5.10E-03 | 5.29E-03 | 5.40E-03 | 5.42E-03 | 5.37E-03 | 5.23E-03 | 5.02E-03 | 4.73E-03 | 4.38E-03 | 3.97E-03 | 3.51E-03 | 3.03E-03 | 2.60E-03 |
| AG107 | 7.43E-09 | 8.11E-09 | 9.01E-09 | 9.86E-09 | 1.06E-08 | 1.12E-08 | 1.16E-08 | 1.18E-08 | 1.19E-08 | 1.18E-08 | 1.15E-08 | 1.10E-08 | 1.04E-08 | 9.59E-09 | 8.69E-09 | 7.70E-09 | 6.65E-09 | 5.71E-09 |
| PD108 | 2.34E-03 | 2.59E-03 | 2.91E-03 | 3.22E-03 | 3.48E-03 | 3.70E-03 | 3.85E-03 | 3.94E-03 | 3.96E-03 | 3.92E-03 | 3.81E-03 | 3.63E-03 | 3.40E-03 | 3.12E-03 | 2.80E-03 | 2.45E-03 | 2.09E-03 | 1.76E-03 |
| CD108 | 3.49E-08 | 4.43E-08 | 5.57E-08 | 6.71E-08 | 7.76E-08 | 8.63E-08 | 9.28E-08 | 9.66E-08 | 9.76E-08 | 9.57E-08 | 9.09E-08 | 8.37E-08 | 7.45E-08 | 6.38E-08 | 5.25E-08 | 4.11E-08 | 3.03E-08 | 2.12E-08 |
| AG109 | 1.59E-03 | 1.74E-03 | 1.94E-03 | 2.13E-03 | 2.30E-03 | 2.43E-03 | 2.52E-03 | 2.58E-03 | 2.59E-03 | 2.56E-03 | 2.50E-03 | 2.39E-03 | 2.25E-03 | 2.07E-03 | 1.87E-03 | 1.65E-03 | 1.42E-03 | 1.21E-03 |
| PD110 | 1.09E-03 | 1.20E-03 | 1.33E-03 | 1.46E-03 | 1.56E-03 | 1.64E-03 | 1.70E-03 | 1.73E-03 | 1.74E-03 | 1.72E-03 | 1.68E-03 | 1.62E-03 | 1.53E-03 | 1.42E-03 | 1.29E-03 | 1.15E-03 | 9.95E-04 | 8.51E-04 |
| AG110M | 2.39E-14 | 3.04E-14 | 3.81E-14 | 4.60E-14 | 5.32E-14 | 5.93E-14 | 6.38E-14 | 6.65E-14 | 6.72E-14 | 6.59E-14 | 6.26E-14 | 5.77E-14 | 5.13E-14 | 4.39E-14 | 3.61E-14 | 2.82E-14 | 2.08E-14 | 1.46E-14 |
| CD110 | 6.21E-05 | 7.88E-05 | 9.90E-05 | 1.19E-04 | 1.38E-04 | 1.53E-04 | 1.65E-04 | 1.72E-04 | 1.73E-04 | 1.70E-04 | 1.62E-04 | 1.49E-04 | 1.32E-04 | 1.13E-04 | 9.32E-05 | 7.30E-05 | 5.39E-05 | 3.77E-05 |
| AG111 | 0.00E+00 | 0.00E+00 | 0.00E+00 | 0.00E+00 | 0.00E+00 | 0.00E+00 | 0.00E+00 | 0.00E+00 | 0.00E+00 | 0.00E+00 | 0.00E+00 | 0.00E+00 | 0.00E+00 | 0.00E+00 | 0.00E+00 | 0.00E+00 | 0.00E+00 | 0.00E+00 |
| CD111 | 8.67E-04 | 9.56E-04 | 1.06E-03 | 1.15E-03 | 1.23E-03 | 1.29E-03 | 1.33E-03 | 1.35E-03 | 1.36E-03 | 1.35E-03 | 1.32E-03 | 1.27E-03 | 1.20E-03 | 1.12E-03 | 1.03E-03 | 9.19E-04 | 7.99E-04 | 6.83E-04 |
| CD112 | 7.69E-04 | 8.53E-04 | 9.45E-04 | 1.03E-03 | 1.10E-03 | 1.15E-03 | 1.19E-03 | 1.21E-03 | 1.22E-03 | 1.20E-03 | 1.18E-03 | 1.13E-03 | 1.08E-03 | 1.00E-03 | 9.19E-04 | 8.21E-04 | 7.14E-04 | 6.07E-04 |
| CD113 | 7.19E-04 | 7.92E-04 | 8.73E-04 | 9.45E-04 | 1.01E-03 | 1.05E-03 | 1.08E-03 | 1.10E-03 | 1.11E-03 | 1.10E-03 | 1.07E-03 | 1.04E-03 | 9.87E-04 | 9.25E-04 | 8.50E-04 | 7.64E-04 | 6.68E-04 | 5.73E-04 |
| CD113M | 4.92E-06 | 5.50E-06 | 6.16E-06 | 6.74E-06 | 7.25E-06 | 7.64E-06 | 7.91E-06 | 8.07E-06 | 8.11E-06 | 8.03E-06 | 7.83E-06 | 7.52E-06 | 7.10E-06 | 6.58E-06 | 5.97E-06 | 5.30E-06 | 4.56E-06 | 3.85E-06 |
| IN113 | 8.14E-06 | 9.09E-06 | 1.02E-05 | 1.11E-05 | 1.19E-05 | 1.26E-05 | 1.30E-05 | 1.33E-05 | 1.34E-05 | 1.32E-05 | 1.29E-05 | 1.24E-05 | 1.17E-05 | 1.09E-05 | 9.85E-06 | 8.74E-06 | 7.53E-06 | 6.36E-06 |
| CD114 | 6.87E-04 | 7.54E-04 | 8.30E-04 | 8.98E-04 | 9.55E-04 | 9.99E-04 | 1.03E-03 | 1.05E-03 | 1.05E-03 | 1.04E-03 | 1.02E-03 | 9.86E-04 | 9.39E-04 | 8.79E-04 | 8.07E-04 | 7.26E-04 | 6.35E-04 | 5.47E-04 |
| SN114 | 4.11E-08 | 5.27E-08 | 6.60E-08 | 7.90E-08 | 9.08E-08 | 1.01E-07 | 1.08E-07 | 1.12E-07 | 1.13E-07 | 1.11E-07 | 1.06E-07 | 9.76E-08 | 8.74E-08 | 7.54E-08 | 6.25E-08 | 4.93E-08 | 3.66E-08 | 2.55E-08 |
| CD115M | 0.00E+00 | 0.00E+00 | 0.00E+00 | 0.00E+00 | 0.00E+00 | 0.00E+00 | 0.00E+00 | 0.00E+00 | 0.00E+00 | 0.00E+00 | 0.00E+00 | 0.00E+00 | 0.00E+00 | 0.00E+00 | 0.00E+00 | 0.00E+00 | 0.00E+00 | 0.00E+00 |
| IN115 | 5.12E-04 | 5.43E-04 | 5.76E-04 | 6.02E-04 | 6.22E-04 | 6.37E-04 | 6.46E-04 | 6.51E-04 | 6.52E-04 | 6.49E-04 | 6.43E-04 | 6.32E-04 | 6.16E-04 | 5.94E-04 | 5.65E-04 | 5.29E-04 | 4.83E-04 | 4.33E-04 |
| SN115 | 2.41E-05 | 2.67E-05 | 2.95E-05 | 3.20E-05 | 3.41E-05 | 3.57E-05 | 3.68E-05 | 3.74E-05 | 3.76E-05 | 3.73E-05 | 3.65E-05 | 3.52E-05 | 3.35E-05 | 3.13E-05 | 2.87E-05 | 2.58E-05 | 2.25E-05 | 1.92E-05 |
| CD116 | 6.71E-04 | 7.33E-04 | 8.04E-04 | 8.67E-04 | 9.20E-04 | 9.60E-04 | 9.88E-04 | 1.00E-03 | 1.01E-03 | 9.99E-04 | 9.79E-04 | 9.47E-04 | 9.04E-04 | 8.49E-04 | 7.82E-04 | 7.06E-04 | 6.21E-04 | 5.37E-04 |

| | | | | | | | | | | | | | | | | | | |
|---|---|---|---|---|---|---|---|---|---|---|---|---|---|---|---|---|---|---|
| SN116 | 1.81E-04 | 2.25E-04 | 2.73E-04 | 3.19E-04 | 3.58E-04 | 3.90E-04 | 4.13E-04 | 4.26E-04 | 4.30E-04 | 4.23E-04 | 4.06E-04 | 3.81E-04 | 3.47E-04 | 3.07E-04 | 2.61E-04 | 2.12E-04 | 1.63E-04 | 1.18E-04 |
| SN117 | 6.69E-04 | 7.32E-04 | 8.04E-04 | 8.68E-04 | 9.21E-04 | 9.62E-04 | 9.90E-04 | 1.01E-03 | 1.01E-03 | 1.00E-03 | 9.82E-04 | 9.49E-04 | 9.06E-04 | 8.50E-04 | 7.83E-04 | 7.06E-04 | 6.19E-04 | 5.35E-04 |
| SN118 | 6.97E-04 | 7.62E-04 | 8.37E-04 | 9.04E-04 | 9.60E-04 | 1.00E-03 | 1.03E-03 | 1.05E-03 | 1.05E-03 | 1.05E-03 | 1.02E-03 | 9.90E-04 | 9.43E-04 | 8.85E-04 | 8.14E-04 | 7.33E-04 | 6.44E-04 | 5.57E-04 |
| SN119 | 6.93E-04 | 7.57E-04 | 8.32E-04 | 8.99E-04 | 9.55E-04 | 9.98E-04 | 1.03E-03 | 1.04E-03 | 1.05E-03 | 1.04E-03 | 1.02E-03 | 9.84E-04 | 9.38E-04 | 8.80E-04 | 8.09E-04 | 7.29E-04 | 6.40E-04 | 5.53E-04 |

Table A-2f. Composition (grams) in 2-inch fuel segment: ORIGEN calculation results for Pin193045, decayed to 3/11/2011.

| Position: | 1 | 3 | 5 | 7 | 9 | 11 | 13 | 15 | 17 | 19 | 21 | 23 | 25 | 27 | 29 | 31 | 33 | 35 |
|---|---|---|---|---|---|---|---|---|---|---|---|---|---|---|---|---|---|---|
| SN119M | 9.15E-15 | 1.01E-14 | 1.11E-14 | 1.21E-14 | 1.29E-14 | 1.35E-14 | 1.39E-14 | 1.42E-14 | 1.42E-14 | 1.41E-14 | 1.38E-14 | 1.33E-14 | 1.27E-14 | 1.19E-14 | 1.09E-14 | 9.78E-15 | 8.54E-15 | 7.35E-15 |
| SN120 | 7.09E-04 | 7.74E-04 | 8.50E-04 | 9.18E-04 | 9.74E-04 | 1.02E-03 | 1.05E-03 | 1.06E-03 | 1.07E-03 | 1.06E-03 | 1.04E-03 | 1.00E-03 | 9.58E-04 | 8.98E-04 | 8.27E-04 | 7.46E-04 | 6.55E-04 | 5.67E-04 |
| SN121M | 2.33E-07 | 2.46E-07 | 2.68E-07 | 2.91E-07 | 3.10E-07 | 3.25E-07 | 3.36E-07 | 3.43E-07 | 3.44E-07 | 3.41E-07 | 3.33E-07 | 3.21E-07 | 3.04E-07 | 2.83E-07 | 2.59E-07 | 2.32E-07 | 2.04E-07 | 1.82E-07 |
| SB121 | 6.88E-04 | 7.49E-04 | 8.19E-04 | 8.81E-04 | 9.32E-04 | 9.71E-04 | 9.97E-04 | 1.01E-03 | 1.02E-03 | 1.01E-03 | 9.89E-04 | 9.58E-04 | 9.16E-04 | 8.63E-04 | 7.97E-04 | 7.22E-04 | 6.37E-04 | 5.53E-04 |
| SN122 | 7.70E-04 | 8.41E-04 | 9.23E-04 | 9.97E-04 | 1.06E-03 | 1.11E-03 | 1.14E-03 | 1.16E-03 | 1.16E-03 | 1.15E-03 | 1.13E-03 | 1.09E-03 | 1.04E-03 | 9.75E-04 | 8.98E-04 | 8.10E-04 | 7.11E-04 | 6.15E-04 |
| TE122 | 2.26E-05 | 2.84E-05 | 3.52E-05 | 4.17E-05 | 4.75E-05 | 5.23E-05 | 5.57E-05 | 5.78E-05 | 5.83E-05 | 5.73E-05 | 5.47E-05 | 5.08E-05 | 4.58E-05 | 3.99E-05 | 3.34E-05 | 2.66E-05 | 2.01E-05 | 1.43E-05 |
| SN123 | 1.90E-21 | 2.06E-21 | 2.23E-21 | 2.40E-21 | 2.53E-21 | 2.63E-21 | 2.70E-21 | 2.74E-21 | 2.75E-21 | 2.74E-21 | 2.69E-21 | 2.61E-21 | 2.51E-21 | 2.37E-21 | 2.20E-21 | 2.00E-21 | 1.78E-21 | 1.56E-21 |
| SB123 | 8.21E-04 | 8.95E-04 | 9.81E-04 | 1.06E-03 | 1.12E-03 | 1.17E-03 | 1.20E-03 | 1.22E-03 | 1.23E-03 | 1.22E-03 | 1.19E-03 | 1.15E-03 | 1.10E-03 | 1.04E-03 | 9.55E-04 | 8.62E-04 | 7.59E-04 | 6.58E-04 |
| TE123 | 4.01E-07 | 5.84E-07 | 8.15E-07 | 1.06E-06 | 1.30E-06 | 1.51E-06 | 1.67E-06 | 1.77E-06 | 1.79E-06 | 1.74E-06 | 1.63E-06 | 1.45E-06 | 1.23E-06 | 9.94E-07 | 7.54E-07 | 5.32E-07 | 3.43E-07 | 2.00E-07 |
| TE123M | 0.00E+00 | 7.20E-24 | 0.00E+00 | 0.00E+00 | 0.00E+00 | 0.00E+00 | 0.00E+00 | 0.00E+00 | 0.00E+00 | 0.00E+00 | 0.00E+00 | 0.00E+00 | 0.00E+00 | 0.00E+00 | 0.00E+00 | 6.61E-24 | 0.00E+00 | 0.00E+00 |
| SN124 | 9.88E-04 | 1.08E-03 | 1.18E-03 | 1.28E-03 | 1.35E-03 | 1.42E-03 | 1.46E-03 | 1.48E-03 | 1.49E-03 | 1.47E-03 | 1.44E-03 | 1.40E-03 | 1.33E-03 | 1.25E-03 | 1.15E-03 | 1.04E-03 | 9.10E-04 | 7.89E-04 |
| SB124 | 3.92E-39 | 4.90E-39 | 6.03E-39 | 7.12E-39 | 8.10E-39 | 8.91E-39 | 9.49E-39 | 9.83E-39 | 9.93E-39 | 9.77E-39 | 9.36E-39 | 8.71E-39 | 7.88E-39 | 6.88E-39 | 5.78E-39 | 4.64E-39 | 3.52E-39 | 2.53E-39 |
| TE124 | 1.52E-05 | 1.90E-05 | 2.34E-05 | 2.77E-05 | 3.15E-05 | 3.46E-05 | 3.69E-05 | 3.83E-05 | 3.86E-05 | 3.79E-05 | 3.63E-05 | 3.37E-05 | 3.04E-05 | 2.65E-05 | 2.22E-05 | 1.78E-05 | 1.35E-05 | 9.71E-06 |
| SN125 | 0.00E+00 | 0.00E+00 | 0.00E+00 | 0.00E+00 | 0.00E+00 | 0.00E+00 | 0.00E+00 | 0.00E+00 | 0.00E+00 | 0.00E+00 | 0.00E+00 | 0.00E+00 | 0.00E+00 | 0.00E+00 | 0.00E+00 | 0.00E+00 | 0.00E+00 | 0.00E+00 |
| SB125 | 6.85E-06 | 7.45E-06 | 8.16E-06 | 8.79E-06 | 9.32E-06 | 9.73E-06 | 1.00E-05 | 1.02E-05 | 1.02E-05 | 1.01E-05 | 9.93E-06 | 9.61E-06 | 9.18E-06 | 8.62E-06 | 7.95E-06 | 7.18E-06 | 6.32E-06 | 5.50E-06 |
| TE125 | 1.16E-03 | 1.27E-03 | 1.39E-03 | 1.50E-03 | 1.59E-03 | 1.66E-03 | 1.71E-03 | 1.74E-03 | 1.74E-03 | 1.73E-03 | 1.70E-03 | 1.64E-03 | 1.56E-03 | 1.47E-03 | 1.35E-03 | 1.22E-03 | 1.07E-03 | 9.30E-04 |
| TE125M | 9.58E-08 | 1.04E-07 | 1.14E-07 | 1.23E-07 | 1.30E-07 | 1.36E-07 | 1.40E-07 | 1.42E-07 | 1.43E-07 | 1.42E-07 | 1.39E-07 | 1.34E-07 | 1.28E-07 | 1.21E-07 | 1.11E-07 | 1.00E-07 | 8.85E-08 | 7.69E-08 |
| SN126 | 1.69E-03 | 1.83E-03 | 2.00E-03 | 2.16E-03 | 2.30E-03 | 2.40E-03 | 2.47E-03 | 2.51E-03 | 2.52E-03 | 2.50E-03 | 2.45E-03 | 2.37E-03 | 2.25E-03 | 2.11E-03 | 1.94E-03 | 1.75E-03 | 1.54E-03 | 1.34E-03 |
| SB126 | 8.02E-11 | 8.67E-11 | 9.50E-11 | 1.03E-10 | 1.09E-10 | 1.14E-10 | 1.17E-10 | 1.19E-10 | 1.20E-10 | 1.19E-10 | 1.16E-10 | 1.12E-10 | 1.07E-10 | 1.00E-10 | 9.23E-11 | 8.31E-11 | 7.31E-11 | 6.38E-11 |
| TE126 | 6.78E-05 | 7.66E-05 | 8.78E-05 | 9.87E-05 | 1.08E-04 | 1.16E-04 | 1.22E-04 | 1.25E-04 | 1.26E-04 | 1.24E-04 | 1.20E-04 | 1.14E-04 | 1.06E-04 | 9.55E-05 | 8.43E-05 | 7.23E-05 | 6.03E-05 | 4.99E-05 |
| TE127 | 1.56E-26 | 1.66E-26 | 1.80E-26 | 1.93E-26 | 3.17E-26 | 3.30E-26 | 3.39E-26 | 3.44E-26 | 3.45E-26 | 3.43E-26 | 3.37E-26 | 3.28E-26 | 3.15E-26 | 1.90E-26 | 1.77E-26 | 1.61E-26 | 1.44E-26 | 1.28E-26 |

| | | | | | | | | | | | | | | | | | | |
|---|---|---|---|---|---|---|---|---|---|---|---|---|---|---|---|---|---|---|
| TE127M | 0.00E+00 | 0.00E+00 | 0.00E+00 | 0.00E+00 | 9.07E-24 | 9.43E-24 | 9.68E-24 | 9.83E-24 | 9.87E-24 | 9.81E-24 | 9.65E-24 | 9.37E-24 | 9.00E-24 | 0.00E+00 | 0.00E+00 | 0.00E+00 | 0.00E+00 | 0.00E+00 |
| I127 | 2.96E-03 | 3.16E-03 | 3.44E-03 | 3.70E-03 | 3.92E-03 | 4.08E-03 | 4.20E-03 | 4.26E-03 | 4.28E-03 | 4.25E-03 | 4.16E-03 | 4.03E-03 | 3.85E-03 | 3.62E-03 | 3.34E-03 | 3.03E-03 | 2.68E-03 | 2.37E-03 |
| TE128 | 5.52E-03 | 5.90E-03 | 6.44E-03 | 6.94E-03 | 7.35E-03 | 7.68E-03 | 7.91E-03 | 8.03E-03 | 8.07E-03 | 8.00E-03 | 7.84E-03 | 7.58E-03 | 7.22E-03 | 6.78E-03 | 6.25E-03 | 5.64E-03 | 4.98E-03 | 4.40E-03 |

Position=Segment location (midpoint of 2-in. segment) from bottom of fuel (BOF); 2 in. of fuel ~14.2g

Table A-2g. Composition (grams) in 2-inch fuel segment: ORIGEN calculation results for Pin193045, decayed to 3/11/2011.

| Position: | 1 | 3 | 5 | 7 | 9 | 11 | 13 | 15 | 17 | 19 | 21 | 23 | 25 | 27 | 29 | 31 | 33 | 35 |
|---|---|---|---|---|---|---|---|---|---|---|---|---|---|---|---|---|---|---|
| XE128 | 9.75E-05 | 1.21E-04 | 1.49E-04 | 1.77E-04 | 2.02E-04 | 2.22E-04 | 2.37E-04 | 2.46E-04 | 2.48E-04 | 2.44E-04 | 2.33E-04 | 2.16E-04 | 1.94E-04 | 1.69E-04 | 1.41E-04 | 1.13E-04 | 8.50E-05 | 6.11E-05 |
| TE129 | 0.00E+00 | 0.00E+00 | 0.00E+00 | 0.00E+00 | 0.00E+00 | 0.00E+00 | 0.00E+00 | 0.00E+00 | 0.00E+00 | 0.00E+00 | 0.00E+00 | 0.00E+00 | 0.00E+00 | 0.00E+00 | 0.00E+00 | 0.00E+00 | 0.00E+00 | 0.00E+00 |
| TE129M | 0.00E+00 | 0.00E+00 | 0.00E+00 | 0.00E+00 | 0.00E+00 | 0.00E+00 | 0.00E+00 | 0.00E+00 | 0.00E+00 | 0.00E+00 | 0.00E+00 | 0.00E+00 | 0.00E+00 | 0.00E+00 | 0.00E+00 | 0.00E+00 | 0.00E+00 | 0.00E+00 |
| I129 | 8.08E-03 | 8.60E-03 | 9.35E-03 | 1.01E-02 | 1.06E-02 | 1.11E-02 | 1.14E-02 | 1.16E-02 | 1.17E-02 | 1.16E-02 | 1.13E-02 | 1.10E-02 | 1.05E-02 | 9.82E-03 | 9.07E-03 | 8.20E-03 | 7.27E-03 | 6.45E-03 |
| XE129 | 7.93E-07 | 1.13E-06 | 1.55E-06 | 2.01E-06 | 2.46E-06 | 2.85E-06 | 3.16E-06 | 3.34E-06 | 3.38E-06 | 3.29E-06 | 3.07E-06 | 2.74E-06 | 2.33E-06 | 1.88E-06 | 1.43E-06 | 1.02E-06 | 6.69E-07 | 4.05E-07 |
| TE130 | 1.44E-02 | 1.54E-02 | 1.67E-02 | 1.80E-02 | 1.91E-02 | 2.00E-02 | 2.06E-02 | 2.09E-02 | 2.10E-02 | 2.08E-02 | 2.04E-02 | 1.97E-02 | 1.88E-02 | 1.76E-02 | 1.62E-02 | 1.46E-02 | 1.29E-02 | 1.15E-02 |
| XE130 | 2.34E-04 | 2.88E-04 | 3.54E-04 | 4.20E-04 | 4.79E-04 | 5.28E-04 | 5.63E-04 | 5.84E-04 | 5.90E-04 | 5.79E-04 | 5.53E-04 | 5.13E-04 | 4.62E-04 | 4.01E-04 | 3.35E-04 | 2.67E-04 | 2.02E-04 | 1.47E-04 |
| I131 | 0.00E+00 | 0.00E+00 | 0.00E+00 | 0.00E+00 | 0.00E+00 | 0.00E+00 | 0.00E+00 | 0.00E+00 | 0.00E+00 | 0.00E+00 | 0.00E+00 | 0.00E+00 | 0.00E+00 | 0.00E+00 | 0.00E+00 | 0.00E+00 | 0.00E+00 | 0.00E+00 |
| XE131 | 2.36E-02 | 2.50E-02 | 2.72E-02 | 2.92E-02 | 3.10E-02 | 3.23E-02 | 3.33E-02 | 3.38E-02 | 3.39E-02 | 3.37E-02 | 3.30E-02 | 3.19E-02 | 3.04E-02 | 2.86E-02 | 2.64E-02 | 2.38E-02 | 2.11E-02 | 1.88E-02 |
| XE131M | 0.00E+00 | 0.00E+00 | 0.00E+00 | 0.00E+00 | 0.00E+00 | 0.00E+00 | 0.00E+00 | 0.00E+00 | 0.00E+00 | 0.00E+00 | 0.00E+00 | 0.00E+00 | 0.00E+00 | 0.00E+00 | 0.00E+00 | 0.00E+00 | 0.00E+00 | 0.00E+00 |
| XE132 | 3.44E-02 | 3.66E-02 | 3.98E-02 | 4.30E-02 | 4.56E-02 | 4.77E-02 | 4.91E-02 | 4.99E-02 | 5.01E-02 | 4.97E-02 | 4.87E-02 | 4.70E-02 | 4.48E-02 | 4.20E-02 | 3.86E-02 | 3.48E-02 | 3.08E-02 | 2.73E-02 |
| BA132 | 3.48E-08 | 4.27E-08 | 5.25E-08 | 6.21E-08 | 7.09E-08 | 7.81E-08 | 8.34E-08 | 8.65E-08 | 8.73E-08 | 8.57E-08 | 8.19E-08 | 7.59E-08 | 6.83E-08 | 5.93E-08 | 4.96E-08 | 3.96E-08 | 3.00E-08 | 2.18E-08 |
| XE133 | 0.00E+00 | 0.00E+00 | 0.00E+00 | 0.00E+00 | 0.00E+00 | 0.00E+00 | 0.00E+00 | 0.00E+00 | 0.00E+00 | 0.00E+00 | 0.00E+00 | 0.00E+00 | 0.00E+00 | 0.00E+00 | 0.00E+00 | 0.00E+00 | 0.00E+00 | 0.00E+00 |
| CS133 | 4.62E-02 | 4.87E-02 | 5.28E-02 | 5.66E-02 | 5.98E-02 | 6.22E-02 | 6.39E-02 | 6.49E-02 | 6.52E-02 | 6.47E-02 | 6.34E-02 | 6.14E-02 | 5.87E-02 | 5.53E-02 | 5.12E-02 | 4.64E-02 | 4.14E-02 | 3.70E-02 |
| XE134 | 5.57E-02 | 5.91E-02 | 6.42E-02 | 6.91E-02 | 7.32E-02 | 7.64E-02 | 7.86E-02 | 7.99E-02 | 8.02E-02 | 7.96E-02 | 7.80E-02 | 7.54E-02 | 7.19E-02 | 6.75E-02 | 6.22E-02 | 5.62E-02 | 4.99E-02 | 4.44E-02 |
| CS134 | 2.04E-06 | 2.50E-06 | 3.05E-06 | 3.60E-06 | 4.09E-06 | 4.50E-06 | 4.79E-06 | 4.97E-06 | 5.01E-06 | 4.93E-06 | 4.71E-06 | 4.38E-06 | 3.95E-06 | 3.45E-06 | 2.89E-06 | 2.32E-06 | 1.77E-06 | 1.29E-06 |
| BA134 | 1.68E-03 | 2.05E-03 | 2.51E-03 | 2.97E-03 | 3.38E-03 | 3.72E-03 | 3.96E-03 | 4.11E-03 | 4.14E-03 | 4.07E-03 | 3.89E-03 | 3.62E-03 | 3.26E-03 | 2.84E-03 | 2.38E-03 | 1.90E-03 | 1.45E-03 | 1.06E-03 |
| CS135 | 4.71E-02 | 5.00E-02 | 5.44E-02 | 5.86E-02 | 6.22E-02 | 6.50E-02 | 6.69E-02 | 6.80E-02 | 6.83E-02 | 6.77E-02 | 6.63E-02 | 6.41E-02 | 6.11E-02 | 5.72E-02 | 5.27E-02 | 4.76E-02 | 4.21E-02 | 3.74E-02 |
| BA135 | 2.42E-06 | 3.33E-06 | 4.51E-06 | 5.78E-06 | 7.03E-06 | 8.12E-06 | 8.95E-06 | 9.45E-06 | 9.58E-06 | 9.32E-06 | 8.70E-06 | 7.78E-06 | 6.65E-06 | 5.41E-06 | 4.16E-06 | 3.01E-06 | 2.03E-06 | 1.29E-06 |
| XE136 | 4.77E-02 | 5.06E-02 | 5.50E-02 | 5.93E-02 | 6.29E-02 | 6.56E-02 | 6.76E-02 | 6.87E-02 | 6.90E-02 | 6.84E-02 | 6.70E-02 | 6.48E-02 | 6.17E-02 | 5.79E-02 | 5.33E-02 | 4.82E-02 | 4.27E-02 | 3.79E-02 |
| CS136 | 0.00E+00 | 0.00E+00 | 0.00E+00 | 0.00E+00 | 0.00E+00 | 0.00E+00 | 0.00E+00 | 0.00E+00 | 0.00E+00 | 0.00E+00 | 0.00E+00 | 0.00E+00 | 0.00E+00 | 0.00E+00 | 0.00E+00 | 0.00E+00 | 0.00E+00 | 0.00E+00 |

| | | | | | | | | | | | | | | | | | | |
|---|---|---|---|---|---|---|---|---|---|---|---|---|---|---|---|---|---|---|
| BA136 | 4.42E-04 | 5.05E-04 | 5.90E-04 | 6.75E-04 | 7.52E-04 | 8.14E-04 | 8.60E-04 | 8.87E-04 | 8.93E-04 | 8.80E-04 | 8.47E-04 | 7.95E-04 | 7.29E-04 | 6.50E-04 | 5.62E-04 | 4.71E-04 | 3.82E-04 | 3.08E-04 |
| CS137 | 2.80E-02 | 2.97E-02 | 3.23E-02 | 3.48E-02 | 3.69E-02 | 3.85E-02 | 3.97E-02 | 4.03E-02 | 4.05E-02 | 4.01E-02 | 3.93E-02 | 3.80E-02 | 3.62E-02 | 3.40E-02 | 3.13E-02 | 2.83E-02 | 2.51E-02 | 2.23E-02 |
| BA137 | 1.72E-02 | 1.82E-02 | 1.98E-02 | 2.14E-02 | 2.27E-02 | 2.37E-02 | 2.44E-02 | 2.48E-02 | 2.49E-02 | 2.47E-02 | 2.42E-02 | 2.34E-02 | 2.23E-02 | 2.09E-02 | 1.92E-02 | 1.74E-02 | 1.54E-02 | 1.37E-02 |

Position=Segment location (midpoint of 2-in. segment) from bottom of fuel (BOF); 2 in. of fuel ~14.2g

Table A-2h. Composition (grams) in 2-inch fuel segment: ORIGEN calculation results for Pin193045, decayed to 3/11/2011.

| | | | | | | | | | | | | | | | | | | |
|---|---|---|---|---|---|---|---|---|---|---|---|---|---|---|---|---|---|---|
| BA138 | 4.90E-02 | 5.19E-02 | 5.64E-02 | 6.07E-02 | 6.43E-02 | 6.72E-02 | 6.92E-02 | 7.03E-02 | 7.06E-02 | 7.00E-02 | 6.86E-02 | 6.63E-02 | 6.32E-02 | 5.93E-02 | 5.47E-02 | 4.94E-02 | 4.38E-02 | 3.90E-02 |
| LA138 | 1.93E-07 | 2.02E-07 | 2.18E-07 | 2.34E-07 | 2.47E-07 | 2.57E-07 | 2.65E-07 | 2.69E-07 | 2.70E-07 | 2.68E-07 | 2.62E-07 | 2.54E-07 | 2.43E-07 | 2.28E-07 | 2.11E-07 | 1.92E-07 | 1.71E-07 | 1.54E-07 |
| LA139 | 4.76E-02 | 5.05E-02 | 5.48E-02 | 5.90E-02 | 6.25E-02 | 6.52E-02 | 6.71E-02 | 6.82E-02 | 6.85E-02 | 6.79E-02 | 6.66E-02 | 6.44E-02 | 6.14E-02 | 5.76E-02 | 5.32E-02 | 4.80E-02 | 4.26E-02 | 3.79E-02 |
| BA140 | 0.00E+00 | 0.00E+00 | 0.00E+00 | 0.00E+00 | 0.00E+00 | 0.00E+00 | 0.00E+00 | 0.00E+00 | 0.00E+00 | 0.00E+00 | 0.00E+00 | 0.00E+00 | 0.00E+00 | 0.00E+00 | 0.00E+00 | 0.00E+00 | 0.00E+00 | 0.00E+00 |
| LA140 | 0.00E+00 | 0.00E+00 | 0.00E+00 | 0.00E+00 | 0.00E+00 | 0.00E+00 | 0.00E+00 | 0.00E+00 | 0.00E+00 | 0.00E+00 | 0.00E+00 | 0.00E+00 | 0.00E+00 | 0.00E+00 | 0.00E+00 | 0.00E+00 | 0.00E+00 | 0.00E+00 |
| CE140 | 4.66E-02 | 4.93E-02 | 5.36E-02 | 5.77E-02 | 6.12E-02 | 6.38E-02 | 6.57E-02 | 6.68E-02 | 6.71E-02 | 6.65E-02 | 6.52E-02 | 6.30E-02 | 6.01E-02 | 5.64E-02 | 5.20E-02 | 4.70E-02 | 4.16E-02 | 3.71E-02 |
| CE141 | 0.00E+00 | 0.00E+00 | 0.00E+00 | 0.00E+00 | 0.00E+00 | 0.00E+00 | 0.00E+00 | 0.00E+00 | 0.00E+00 | 0.00E+00 | 0.00E+00 | 0.00E+00 | 0.00E+00 | 0.00E+00 | 0.00E+00 | 0.00E+00 | 0.00E+00 | 0.00E+00 |
| PR141 | 4.51E-02 | 4.77E-02 | 5.18E-02 | 5.57E-02 | 5.89E-02 | 6.15E-02 | 6.32E-02 | 6.42E-02 | 6.45E-02 | 6.40E-02 | 6.27E-02 | 6.07E-02 | 5.79E-02 | 5.44E-02 | 5.02E-02 | 4.54E-02 | 4.03E-02 | 3.60E-02 |
| CE142 | 4.26E-02 | 4.51E-02 | 4.90E-02 | 5.27E-02 | 5.59E-02 | 5.83E-02 | 6.00E-02 | 6.10E-02 | 6.12E-02 | 6.07E-02 | 5.95E-02 | 5.75E-02 | 5.49E-02 | 5.15E-02 | 4.75E-02 | 4.30E-02 | 3.81E-02 | 3.40E-02 |
| ND142 | 4.49E-04 | 5.52E-04 | 6.78E-04 | 8.04E-04 | 9.18E-04 | 1.01E-03 | 1.08E-03 | 1.12E-03 | 1.13E-03 | 1.11E-03 | 1.06E-03 | 9.85E-04 | 8.85E-04 | 7.68E-04 | 6.40E-04 | 5.10E-04 | 3.86E-04 | 2.81E-04 |
| PR143 | 0.00E+00 | 0.00E+00 | 0.00E+00 | 0.00E+00 | 0.00E+00 | 0.00E+00 | 0.00E+00 | 0.00E+00 | 0.00E+00 | 0.00E+00 | 0.00E+00 | 0.00E+00 | 0.00E+00 | 0.00E+00 | 0.00E+00 | 0.00E+00 | 0.00E+00 | 0.00E+00 |
| ND143 | 4.29E-02 | 4.52E-02 | 4.89E-02 | 5.25E-02 | 5.55E-02 | 5.78E-02 | 5.94E-02 | 6.03E-02 | 6.06E-02 | 6.01E-02 | 5.89E-02 | 5.71E-02 | 5.45E-02 | 5.13E-02 | 4.75E-02 | 4.31E-02 | 3.83E-02 | 3.43E-02 |
| CE144 | 5.76E-10 | 6.04E-10 | 6.51E-10 | 6.95E-10 | 7.32E-10 | 7.60E-10 | 7.79E-10 | 7.91E-10 | 7.94E-10 | 7.89E-10 | 7.76E-10 | 7.54E-10 | 7.23E-10 | 6.84E-10 | 6.37E-10 | 5.81E-10 | 5.21E-10 | 4.69E-10 |
| PR144 | 2.43E-14 | 2.55E-14 | 2.75E-14 | 2.93E-14 | 3.09E-14 | 3.21E-14 | 3.29E-14 | 3.34E-14 | 3.35E-14 | 3.33E-14 | 3.28E-14 | 3.18E-14 | 3.05E-14 | 2.89E-14 | 2.69E-14 | 2.45E-14 | 2.20E-14 | 1.98E-14 |
| ND144 | 4.10E-02 | 4.35E-02 | 4.73E-02 | 5.10E-02 | 5.41E-02 | 5.65E-02 | 5.82E-02 | 5.91E-02 | 5.94E-02 | 5.89E-02 | 5.77E-02 | 5.57E-02 | 5.31E-02 | 4.98E-02 | 4.59E-02 | 4.14E-02 | 3.66E-02 | 3.26E-02 |
| ND145 | 2.93E-02 | 3.10E-02 | 3.36E-02 | 3.61E-02 | 3.81E-02 | 3.97E-02 | 4.09E-02 | 4.15E-02 | 4.17E-02 | 4.13E-02 | 4.05E-02 | 3.92E-02 | 3.75E-02 | 3.52E-02 | 3.26E-02 | 2.95E-02 | 2.62E-02 | 2.34E-02 |
| ND146 | 2.38E-02 | 2.53E-02 | 2.76E-02 | 2.98E-02 | 3.16E-02 | 3.31E-02 | 3.41E-02 | 3.47E-02 | 3.48E-02 | 3.45E-02 | 3.38E-02 | 3.26E-02 | 3.11E-02 | 2.91E-02 | 2.68E-02 | 2.41E-02 | 2.13E-02 | 1.89E-02 |
| PM146 | 1.34E-07 | 1.62E-07 | 1.96E-07 | 2.30E-07 | 2.59E-07 | 2.84E-07 | 3.01E-07 | 3.12E-07 | 3.14E-07 | 3.09E-07 | 2.96E-07 | 2.77E-07 | 2.51E-07 | 2.20E-07 | 1.86E-07 | 1.50E-07 | 1.16E-07 | 8.54E-08 |
| SM146 | 1.79E-06 | 2.17E-06 | 2.64E-06 | 3.10E-06 | 3.50E-06 | 3.84E-06 | 4.08E-06 | 4.22E-06 | 4.26E-06 | 4.18E-06 | 4.01E-06 | 3.74E-06 | 3.38E-06 | 2.96E-06 | 2.50E-06 | 2.02E-06 | 1.55E-06 | 1.14E-06 |
| ND147 | 0.00E+00 | 0.00E+00 | 0.00E+00 | 0.00E+00 | 0.00E+00 | 0.00E+00 | 0.00E+00 | 0.00E+00 | 0.00E+00 | 0.00E+00 | 0.00E+00 | 0.00E+00 | 0.00E+00 | 0.00E+00 | 0.00E+00 | 0.00E+00 | 0.00E+00 | 0.00E+00 |
| PM147 | 7.19E-05 | 7.44E-05 | 7.91E-05 | 8.34E-05 | 8.69E-05 | 8.95E-05 | 9.13E-05 | 9.23E-05 | 9.26E-05 | 9.21E-05 | 9.08E-05 | 8.88E-05 | 8.59E-05 | 8.20E-05 | 7.73E-05 | 7.15E-05 | 6.50E-05 | 5.94E-05 |
| SM147 | 1.63E-02 | 1.69E-02 | 1.80E-02 | 1.91E-02 | 1.99E-02 | 2.05E-02 | 2.10E-02 | 2.12E-02 | 2.13E-02 | 2.11E-02 | 2.08E-02 | 2.03E-02 | 1.96E-02 | 1.87E-02 | 1.76E-02 | 1.62E-02 | 1.47E-02 | 1.34E-02 |
| ND148 | 1.37E-02 | 1.46E-02 | 1.58E-02 | 1.70E-02 | 1.80E-02 | 1.88E-02 | 1.94E-02 | 1.97E-02 | 1.98E-02 | 1.96E-02 | 1.92E-02 | 1.86E-02 | 1.77E-02 | 1.67E-02 | 1.54E-02 | 1.39E-02 | 1.23E-02 | 1.09E-02 |
| PM148 | 0.00E+00 | 0.00E+00 | 0.00E+00 | 0.00E+00 | 0.00E+00 | 0.00E+00 | 0.00E+00 | 0.00E+00 | 0.00E+00 | 0.00E+00 | 0.00E+00 | 0.00E+00 | 0.00E+00 | 0.00E+00 | 0.00E+00 | 0.00E+00 | 0.00E+00 | 0.00E+00 |

Position=Segment location (midpoint of 2-in. segment) from bottom of fuel (BOF); 2 in. of fuel ~14.2g

Table A-2i. Composition (grams) in 2-inch fuel segment: ORIGEN calculation results for Pin193045, decayed to 3/11/2011.

| Position: | 1 | 3 | 5 | 7 | 9 | 11 | 13 | 15 | 17 | 19 | 21 | 23 | 25 | 27 | 29 | 31 | 33 | 35 |
|---|---|---|---|---|---|---|---|---|---|---|---|---|---|---|---|---|---|---|
| PM148M | 0.00E+00 | 0.00E+00 | 0.00E+00 | 0.00E+00 | 0.00E+00 | 0.00E+00 | 0.00E+00 | 0.00E+00 | 0.00E+00 | 0.00E+00 | 0.00E+00 | 0.00E+00 | 0.00E+00 | 0.00E+00 | 0.00E+00 | 0.00E+00 | 0.00E+00 | 0.00E+00 |
| SM148 | 2.66E-03 | 3.22E-03 | 3.88E-03 | 4.54E-03 | 5.11E-03 | 5.58E-03 | 5.92E-03 | 6.12E-03 | 6.17E-03 | 6.07E-03 | 5.82E-03 | 5.44E-03 | 4.94E-03 | 4.35E-03 | 3.69E-03 | 2.99E-03 | 2.31E-03 | 1.71E-03 |
| SM149 | 8.63E-03 | 9.13E-03 | 9.89E-03 | 1.06E-02 | 1.12E-02 | 1.16E-02 | 1.20E-02 | 1.21E-02 | 1.22E-02 | 1.21E-02 | 1.19E-02 | 1.15E-02 | 1.10E-02 | 1.04E-02 | 9.60E-03 | 8.73E-03 | 7.78E-03 | 6.94E-03 |
| ND150 | 5.88E-03 | 6.29E-03 | 6.87E-03 | 7.40E-03 | 7.85E-03 | 8.20E-03 | 8.45E-03 | 8.58E-03 | 8.62E-03 | 8.55E-03 | 8.37E-03 | 8.09E-03 | 7.71E-03 | 7.23E-03 | 6.66E-03 | 6.01E-03 | 5.31E-03 | 4.68E-03 |
| SM150 | 8.43E-04 | 1.03E-03 | 1.27E-03 | 1.49E-03 | 1.70E-03 | 1.87E-03 | 1.99E-03 | 2.06E-03 | 2.08E-03 | 2.05E-03 | 1.96E-03 | 1.82E-03 | 1.64E-03 | 1.43E-03 | 1.20E-03 | 9.61E-04 | 7.31E-04 | 5.32E-04 |
| SM151 | 3.01E-03 | 3.18E-03 | 3.43E-03 | 3.67E-03 | 3.86E-03 | 4.01E-03 | 4.11E-03 | 4.17E-03 | 4.18E-03 | 4.15E-03 | 4.08E-03 | 3.96E-03 | 3.80E-03 | 3.59E-03 | 3.34E-03 | 3.04E-03 | 2.72E-03 | 2.43E-03 |
| EU151 | 5.11E-04 | 5.39E-04 | 5.81E-04 | 6.19E-04 | 6.51E-04 | 6.75E-04 | 6.92E-04 | 7.01E-04 | 7.04E-04 | 6.99E-04 | 6.87E-04 | 6.67E-04 | 6.40E-04 | 6.06E-04 | 5.65E-04 | 5.16E-04 | 4.62E-04 | 4.14E-04 |
| SM152 | 3.14E-03 | 3.44E-03 | 3.84E-03 | 4.22E-03 | 4.54E-03 | 4.80E-03 | 4.98E-03 | 5.09E-03 | 5.12E-03 | 5.06E-03 | 4.93E-03 | 4.72E-03 | 4.44E-03 | 4.10E-03 | 3.71E-03 | 3.27E-03 | 2.82E-03 | 2.41E-03 |
| EU152 | 2.16E-06 | 2.56E-06 | 3.01E-06 | 3.43E-06 | 3.78E-06 | 4.06E-06 | 4.26E-06 | 4.37E-06 | 4.40E-06 | 4.34E-06 | 4.20E-06 | 3.97E-06 | 3.67E-06 | 3.30E-06 | 2.87E-06 | 2.39E-06 | 1.90E-06 | 1.45E-06 |
| GD152 | 3.36E-06 | 3.96E-06 | 4.65E-06 | 5.29E-06 | 5.83E-06 | 6.25E-06 | 6.55E-06 | 6.72E-06 | 6.76E-06 | 6.67E-06 | 6.46E-06 | 6.12E-06 | 5.66E-06 | 5.09E-06 | 4.44E-06 | 3.71E-06 | 2.95E-06 | 2.25E-06 |
| EU153 | 1.68E-03 | 1.78E-03 | 1.93E-03 | 2.07E-03 | 2.19E-03 | 2.28E-03 | 2.34E-03 | 2.37E-03 | 2.38E-03 | 2.37E-03 | 2.32E-03 | 2.25E-03 | 2.15E-03 | 2.03E-03 | 1.88E-03 | 1.71E-03 | 1.52E-03 | 1.35E-03 |
| GD153 | 6.05E-16 | 8.30E-16 | 1.11E-15 | 1.39E-15 | 1.65E-15 | 1.88E-15 | 2.05E-15 | 2.15E-15 | 2.17E-15 | 2.12E-15 | 2.00E-15 | 1.82E-15 | 1.58E-15 | 1.32E-15 | 1.03E-15 | 7.61E-16 | 5.16E-16 | 3.20E-16 |
| SM154 | 8.89E-04 | 9.62E-04 | 1.06E-03 | 1.15E-03 | 1.23E-03 | 1.29E-03 | 1.33E-03 | 1.36E-03 | 1.36E-03 | 1.35E-03 | 1.32E-03 | 1.27E-03 | 1.20E-03 | 1.12E-03 | 1.03E-03 | 9.17E-04 | 8.02E-04 | 6.97E-04 |
| EU154 | 4.63E-05 | 5.63E-05 | 6.81E-05 | 7.94E-05 | 8.95E-05 | 9.76E-05 | 1.04E-04 | 1.07E-04 | 1.08E-04 | 1.06E-04 | 1.02E-04 | 9.52E-05 | 8.66E-05 | 7.62E-05 | 6.47E-05 | 5.25E-05 | 4.05E-05 | 2.98E-05 |
| GD154 | 1.87E-04 | 2.27E-04 | 2.75E-04 | 3.21E-04 | 3.61E-04 | 3.94E-04 | 4.18E-04 | 4.32E-04 | 4.35E-04 | 4.28E-04 | 4.11E-04 | 3.84E-04 | 3.49E-04 | 3.08E-04 | 2.61E-04 | 2.12E-04 | 1.63E-04 | 1.20E-04 |
| EU155 | 3.04E-05 | 3.28E-05 | 3.62E-05 | 3.94E-05 | 4.22E-05 | 4.44E-05 | 4.60E-05 | 4.69E-05 | 4.71E-05 | 4.67E-05 | 4.55E-05 | 4.38E-05 | 4.14E-05 | 3.84E-05 | 3.50E-05 | 3.13E-05 | 2.74E-05 | 2.39E-05 |
| GD155 | 5.01E-04 | 5.40E-04 | 5.94E-04 | 6.46E-04 | 6.90E-04 | 7.26E-04 | 7.51E-04 | 7.65E-04 | 7.69E-04 | 7.61E-04 | 7.43E-04 | 7.14E-04 | 6.76E-04 | 6.30E-04 | 5.75E-04 | 5.15E-04 | 4.51E-04 | 3.95E-04 |
| EU156 | 0.00E+00 | 0.00E+00 | 0.00E+00 | 0.00E+00 | 0.00E+00 | 0.00E+00 | 0.00E+00 | 0.00E+00 | 0.00E+00 | 0.00E+00 | 0.00E+00 | 0.00E+00 | 0.00E+00 | 0.00E+00 | 0.00E+00 | 0.00E+00 | 0.00E+00 | 0.00E+00 |
| GD156 | 3.80E-04 | 4.26E-04 | 4.85E-04 | 5.41E-04 | 5.91E-04 | 6.31E-04 | 6.59E-04 | 6.76E-04 | 6.80E-04 | 6.72E-04 | 6.51E-04 | 6.18E-04 | 5.76E-04 | 5.24E-04 | 4.66E-04 | 4.03E-04 | 3.39E-04 | 2.82E-04 |
| GD157 | 1.70E-04 | 1.82E-04 | 1.99E-04 | 2.15E-04 | 2.29E-04 | 2.40E-04 | 2.47E-04 | 2.51E-04 | 2.52E-04 | 2.50E-04 | 2.45E-04 | 2.36E-04 | 2.25E-04 | 2.10E-04 | 1.93E-04 | 1.74E-04 | 1.53E-04 | 1.34E-04 |
| GD158 | 1.41E-04 | 1.59E-04 | 1.82E-04 | 2.05E-04 | 2.25E-04 | 2.41E-04 | 2.52E-04 | 2.59E-04 | 2.60E-04 | 2.57E-04 | 2.49E-04 | 2.36E-04 | 2.19E-04 | 1.98E-04 | 1.75E-04 | 1.50E-04 | 1.25E-04 | 1.03E-04 |

| | | | | | | | | | | | | | | | | | | |
|---|---|---|---|---|---|---|---|---|---|---|---|---|---|---|---|---|---|---|
| TB159 | 0.00E+00 | 0.00E+00 | 0.00E+00 | 0.00E+00 | 0.00E+00 | 0.00E+00 | 0.00E+00 | 0.00E+00 | 0.00E+00 | 0.00E+00 | 0.00E+00 | 0.00E+00 | 0.00E+00 | 0.00E+00 | 0.00E+00 | 0.00E+00 | 0.00E+00 | 0.00E+00 |
| GD160 | 2.58E-05 | 2.85E-05 | 3.20E-05 | 3.55E-05 | 3.85E-05 | 4.09E-05 | 4.26E-05 | 4.36E-05 | 4.39E-05 | 4.33E-05 | 4.21E-05 | 4.01E-05 | 3.75E-05 | 3.44E-05 | 3.08E-05 | 2.69E-05 | 2.28E-05 | 1.92E-05 |
| TB160 | 3.83E-34 | 4.87E-34 | 6.14E-34 | 7.42E-34 | 8.60E-34 | 9.60E-34 | 1.03E-33 | 1.08E-33 | 1.09E-33 | 1.07E-33 | 1.02E-33 | 9.35E-34 | 8.31E-34 | 7.10E-34 | 5.82E-34 | 4.54E-34 | 3.34E-34 | 2.33E-34 |

Table A-2j. Composition (grams) in 2-inch fuel segment: ORIGEN calculation results for Pin193045, decayed to 3/11/2011.

| Position: | 1 | 3 | 5 | 7 | 9 | 11 | 13 | 15 | 17 | 19 | 21 | 23 | 25 | 27 | 29 | 31 | 33 | 35 |
|---|---|---|---|---|---|---|---|---|---|---|---|---|---|---|---|---|---|---|
| DY160 | 3.68E-06 | 4.65E-06 | 5.80E-06 | 6.95E-06 | 8.01E-06 | 8.88E-06 | 9.53E-06 | 9.91E-06 | 1.00E-05 | 9.81E-06 | 9.34E-06 | 8.62E-06 | 7.70E-06 | 6.63E-06 | 5.47E-06 | 4.31E-06 | 3.20E-06 | 2.25E-06 |
| DY161 | 1.11E-05 | 1.23E-05 | 1.39E-05 | 1.54E-05 | 1.66E-05 | 1.77E-05 | 1.84E-05 | 1.88E-05 | 1.89E-05 | 1.87E-05 | 1.82E-05 | 1.73E-05 | 1.62E-05 | 1.49E-05 | 1.34E-05 | 1.17E-05 | 9.95E-06 | 8.35E-06 |
| DY162 | 8.12E-06 | 9.26E-06 | 1.06E-05 | 1.19E-05 | 1.31E-05 | 1.40E-05 | 1.46E-05 | 1.50E-05 | 1.51E-05 | 1.49E-05 | 1.44E-05 | 1.37E-05 | 1.27E-05 | 1.15E-05 | 1.02E-05 | 8.77E-06 | 7.30E-06 | 5.95E-06 |
| DY163 | 3.38E-06 | 3.89E-06 | 4.47E-06 | 5.01E-06 | 5.49E-06 | 5.87E-06 | 6.15E-06 | 6.31E-06 | 6.35E-06 | 6.27E-06 | 6.06E-06 | 5.75E-06 | 5.35E-06 | 4.86E-06 | 4.30E-06 | 3.71E-06 | 3.09E-06 | 2.49E-06 |
| DY164 | 1.92E-06 | 2.20E-06 | 2.53E-06 | 2.83E-06 | 3.10E-06 | 3.31E-06 | 3.46E-06 | 3.55E-06 | 3.58E-06 | 3.53E-06 | 3.42E-06 | 3.24E-06 | 3.02E-06 | 2.74E-06 | 2.43E-06 | 2.10E-06 | 1.75E-06 | 1.41E-06 |
| HO165 | 9.59E-07 | 1.09E-06 | 1.24E-06 | 1.38E-06 | 1.51E-06 | 1.60E-06 | 1.67E-06 | 1.71E-06 | 1.72E-06 | 1.70E-06 | 1.65E-06 | 1.57E-06 | 1.47E-06 | 1.34E-06 | 1.20E-06 | 1.04E-06 | 8.76E-07 | 7.14E-07 |
| ER166 | 6.27E-07 | 7.28E-07 | 8.45E-07 | 9.54E-07 | 1.05E-06 | 1.13E-06 | 1.19E-06 | 1.22E-06 | 1.23E-06 | 1.21E-06 | 1.17E-06 | 1.10E-06 | 1.02E-06 | 9.22E-07 | 8.10E-07 | 6.91E-07 | 5.68E-07 | 4.52E-07 |
| ER167 | 3.02E-07 | 3.44E-07 | 3.90E-07 | 4.33E-07 | 4.69E-07 | 4.99E-07 | 5.19E-07 | 5.31E-07 | 5.34E-07 | 5.28E-07 | 5.13E-07 | 4.89E-07 | 4.58E-07 | 4.20E-07 | 3.77E-07 | 3.29E-07 | 2.78E-07 | 2.27E-07 |
| ER168 | 2.54E-08 | 3.37E-08 | 4.30E-08 | 5.22E-08 | 6.07E-08 | 6.78E-08 | 7.31E-08 | 7.62E-08 | 7.70E-08 | 7.54E-08 | 7.15E-08 | 6.57E-08 | 5.83E-08 | 4.97E-08 | 4.06E-08 | 3.15E-08 | 2.29E-08 | 1.53E-08 |
| SUM FPs isotopes | 1.30E+00 | 1.38E+00 | 1.50E+00 | 1.62E+00 | 1.71E+00 | 1.79E+00 | 1.84E+00 | 1.87E+00 | 1.88E+00 | 1.86E+00 | 1.83E+00 | 1.77E+00 | 1.68E+00 | 1.58E+00 | 1.46E+00 | 1.31E+00 | 1.16E+00 | 1.03E+00 |
| H | 1.05E-06 | 1.11E-06 | 1.21E-06 | 1.30E-06 | 1.38E-06 | 1.44E-06 | 1.48E-06 | 1.51E-06 | 1.51E-06 | 1.50E-06 | 1.47E-06 | 1.42E-06 | 1.36E-06 | 1.27E-06 | 1.18E-06 | 1.06E-06 | 9.41E-07 | 8.36E-07 |
| LI | 1.64E-08 | 1.73E-08 | 1.87E-08 | 2.01E-08 | 2.12E-08 | 2.20E-08 | 2.26E-08 | 2.30E-08 | 2.31E-08 | 2.29E-08 | 2.25E-08 | 2.18E-08 | 2.08E-08 | 1.96E-08 | 1.82E-08 | 1.65E-08 | 1.47E-08 | 1.32E-08 |
| GE | 6.84E-05 | 7.27E-05 | 7.89E-05 | 8.48E-05 | 8.98E-05 | 9.36E-05 | 9.63E-05 | 9.78E-05 | 9.82E-05 | 9.74E-05 | 9.55E-05 | 9.24E-05 | 8.82E-05 | 8.29E-05 | 7.66E-05 | 6.94E-05 | 6.16E-05 | 5.47E-05 |
| AS | 2.04E-05 | 2.16E-05 | 2.35E-05 | 2.51E-05 | 2.66E-05 | 2.76E-05 | 2.84E-05 | 2.88E-05 | 2.89E-05 | 2.87E-05 | 2.82E-05 | 2.73E-05 | 2.61E-05 | 2.46E-05 | 2.28E-05 | 2.07E-05 | 1.84E-05 | 1.64E-05 |
| SE | 2.67E-03 | 2.83E-03 | 3.07E-03 | 3.29E-03 | 3.48E-03 | 3.63E-03 | 3.73E-03 | 3.79E-03 | 3.81E-03 | 3.78E-03 | 3.70E-03 | 3.58E-03 | 3.42E-03 | 3.22E-03 | 2.97E-03 | 2.69E-03 | 2.39E-03 | 2.13E-03 |
| BR | 9.94E-04 | 1.05E-03 | 1.13E-03 | 1.21E-03 | 1.28E-03 | 1.33E-03 | 1.37E-03 | 1.39E-03 | 1.39E-03 | 1.38E-03 | 1.35E-03 | 1.31E-03 | 1.26E-03 | 1.19E-03 | 1.10E-03 | 1.00E-03 | 8.93E-04 | 8.00E-04 |
| KR | 1.67E-02 | 1.76E-02 | 1.91E-02 | 2.05E-02 | 2.17E-02 | 2.26E-02 | 2.33E-02 | 2.37E-02 | 2.38E-02 | 2.36E-02 | 2.31E-02 | 2.24E-02 | 2.13E-02 | 2.01E-02 | 1.85E-02 | 1.68E-02 | 1.49E-02 | 1.33E-02 |
| RB | 1.69E-02 | 1.78E-02 | 1.93E-02 | 2.07E-02 | 2.19E-02 | 2.28E-02 | 2.34E-02 | 2.38E-02 | 2.39E-02 | 2.37E-02 | 2.32E-02 | 2.25E-02 | 2.15E-02 | 2.02E-02 | 1.87E-02 | 1.69E-02 | 1.51E-02 | 1.35E-02 |
| SR | 3.26E-02 | 3.43E-02 | 3.72E-02 | 3.99E-02 | 4.22E-02 | 4.40E-02 | 4.53E-02 | 4.60E-02 | 4.61E-02 | 4.58E-02 | 4.49E-02 | 4.35E-02 | 4.15E-02 | 3.90E-02 | 3.61E-02 | 3.27E-02 | 2.91E-02 | 2.60E-02 |
| Y | 2.12E-02 | 2.24E-02 | 2.43E-02 | 2.60E-02 | 2.75E-02 | 2.87E-02 | 2.95E-02 | 3.00E-02 | 3.01E-02 | 2.98E-02 | 2.93E-02 | 2.83E-02 | 2.71E-02 | 2.55E-02 | 2.35E-02 | 2.13E-02 | 1.90E-02 | 1.70E-02 |
| ZR | 1.59E-01 | 1.68E-01 | 1.83E-01 | 1.96E-01 | 2.08E-01 | 2.16E-01 | 2.23E-01 | 2.26E-01 | 2.27E-01 | 2.25E-01 | 2.21E-01 | 2.14E-01 | 2.04E-01 | 1.92E-01 | 1.77E-01 | 1.60E-01 | 1.42E-01 | 1.27E-01 |

| | | | | | | | | | | | | | | | | | | |
|---|---|---|---|---|---|---|---|---|---|---|---|---|---|---|---|---|---|---|
| NB | 3.01E-07 | 3.19E-07 | 3.46E-07 | 3.73E-07 | 3.95E-07 | 4.12E-07 | 4.25E-07 | 4.32E-07 | 4.33E-07 | 4.30E-07 | 4.21E-07 | 4.07E-07 | 3.88E-07 | 3.64E-07 | 3.36E-07 | 3.03E-07 | 2.69E-07 | 2.40E-07 |
| MO | 1.30E-01 | 1.37E-01 | 1.49E-01 | 1.60E-01 | 1.70E-01 | 1.77E-01 | 1.83E-01 | 1.86E-01 | 1.86E-01 | 1.85E-01 | 1.81E-01 | 1.75E-01 | 1.67E-01 | 1.57E-01 | 1.45E-01 | 1.31E-01 | 1.16E-01 | 1.03E-01 |
| TC | 3.04E-02 | 3.22E-02 | 3.49E-02 | 3.74E-02 | 3.96E-02 | 4.13E-02 | 4.24E-02 | 4.31E-02 | 4.32E-02 | 4.29E-02 | 4.21E-02 | 4.07E-02 | 3.89E-02 | 3.66E-02 | 3.38E-02 | 3.07E-02 | 2.73E-02 | 2.43E-02 |
| RU | 7.27E-02 | 7.77E-02 | 8.50E-02 | 9.20E-02 | 9.78E-02 | 1.02E-01 | 1.06E-01 | 1.07E-01 | 1.08E-01 | 1.07E-01 | 1.05E-01 | 1.01E-01 | 9.60E-02 | 8.97E-02 | 8.24E-02 | 7.40E-02 | 6.52E-02 | 5.74E-02 |

Table A-2k. Composition (grams) in 2-inch fuel segment: ORIGEN calculation results for Pin193045, decayed to 3/11/2011.

| Position: | 1 | 3 | 5 | 7 | 9 | 11 | 13 | 15 | 17 | 19 | 21 | 23 | 25 | 27 | 29 | 31 | 33 | 35 |
|---|---|---|---|---|---|---|---|---|---|---|---|---|---|---|---|---|---|---|
| RH | 1.95E-02 | 2.08E-02 | 2.27E-02 | 2.44E-02 | 2.59E-02 | 2.70E-02 | 2.78E-02 | 2.83E-02 | 2.84E-02 | 2.82E-02 | 2.76E-02 | 2.67E-02 | 2.54E-02 | 2.39E-02 | 2.20E-02 | 1.98E-02 | 1.76E-02 | 1.55E-02 |
| PD | 2.19E-02 | 2.41E-02 | 2.70E-02 | 2.97E-02 | 3.21E-02 | 3.40E-02 | 3.53E-02 | 3.60E-02 | 3.62E-02 | 3.58E-02 | 3.49E-02 | 3.34E-02 | 3.14E-02 | 2.89E-02 | 2.61E-02 | 2.29E-02 | 1.97E-02 | 1.67E-02 |
| AG | 1.59E-03 | 1.74E-03 | 1.94E-03 | 2.13E-03 | 2.30E-03 | 2.43E-03 | 2.52E-03 | 2.58E-03 | 2.59E-03 | 2.56E-03 | 2.50E-03 | 2.39E-03 | 2.25E-03 | 2.07E-03 | 1.87E-03 | 1.65E-03 | 1.42E-03 | 1.21E-03 |
| CD | 3.78E-03 | 4.17E-03 | 4.62E-03 | 5.01E-03 | 5.35E-03 | 5.61E-03 | 5.79E-03 | 5.89E-03 | 5.92E-03 | 5.87E-03 | 5.74E-03 | 5.53E-03 | 5.25E-03 | 4.90E-03 | 4.48E-03 | 4.01E-03 | 3.50E-03 | 2.99E-03 |
| IN | 5.20E-04 | 5.52E-04 | 5.86E-04 | 6.13E-04 | 6.34E-04 | 6.49E-04 | 6.59E-04 | 6.64E-04 | 6.65E-04 | 6.63E-04 | 6.56E-04 | 6.44E-04 | 6.28E-04 | 6.05E-04 | 5.75E-04 | 5.38E-04 | 4.91E-04 | 4.40E-04 |
| SN | 6.42E-03 | 7.02E-03 | 7.73E-03 | 8.37E-03 | 8.91E-03 | 9.33E-03 | 9.61E-03 | 9.78E-03 | 9.82E-03 | 9.73E-03 | 9.53E-03 | 9.20E-03 | 8.75E-03 | 8.19E-03 | 7.51E-03 | 6.75E-03 | 5.90E-03 | 5.10E-03 |
| SB | 1.52E-03 | 1.65E-03 | 1.81E-03 | 1.95E-03 | 2.06E-03 | 2.15E-03 | 2.21E-03 | 2.24E-03 | 2.25E-03 | 2.24E-03 | 2.19E-03 | 2.12E-03 | 2.03E-03 | 1.91E-03 | 1.76E-03 | 1.59E-03 | 1.40E-03 | 1.22E-03 |
| TE | 2.12E-02 | 2.27E-02 | 2.47E-02 | 2.66E-02 | 2.83E-02 | 2.95E-02 | 3.04E-02 | 3.09E-02 | 3.11E-02 | 3.08E-02 | 3.02E-02 | 2.91E-02 | 2.78E-02 | 2.60E-02 | 2.40E-02 | 2.16E-02 | 1.91E-02 | 1.69E-02 |
| I | 1.10E-02 | 1.18E-02 | 1.28E-02 | 1.38E-02 | 1.46E-02 | 1.52E-02 | 1.56E-02 | 1.59E-02 | 1.59E-02 | 1.58E-02 | 1.55E-02 | 1.50E-02 | 1.43E-02 | 1.34E-02 | 1.24E-02 | 1.12E-02 | 9.95E-03 | 8.81E-03 |
| XE | 1.62E-01 | 1.72E-01 | 1.87E-01 | 2.01E-01 | 2.13E-01 | 2.23E-01 | 2.29E-01 | 2.33E-01 | 2.34E-01 | 2.32E-01 | 2.27E-01 | 2.20E-01 | 2.09E-01 | 1.96E-01 | 1.81E-01 | 1.63E-01 | 1.45E-01 | 1.29E-01 |
| CS | 1.21E-01 | 1.28E-01 | 1.40E-01 | 1.50E-01 | 1.59E-01 | 1.66E-01 | 1.71E-01 | 1.73E-01 | 1.74E-01 | 1.73E-01 | 1.69E-01 | 1.64E-01 | 1.56E-01 | 1.47E-01 | 1.35E-01 | 1.22E-01 | 1.09E-01 | 9.67E-02 |
| BA | 6.83E-02 | 7.27E-02 | 7.93E-02 | 8.57E-02 | 9.11E-02 | 9.54E-02 | 9.84E-02 | 1.00E-01 | 1.01E-01 | 9.96E-02 | 9.75E-02 | 9.41E-02 | 8.94E-02 | 8.36E-02 | 7.68E-02 | 6.91E-02 | 6.10E-02 | 5.40E-02 |
| LA | 4.76E-02 | 5.05E-02 | 5.48E-02 | 5.90E-02 | 6.25E-02 | 6.52E-02 | 6.71E-02 | 6.82E-02 | 6.85E-02 | 6.79E-02 | 6.66E-02 | 6.44E-02 | 6.14E-02 | 5.76E-02 | 5.32E-02 | 4.80E-02 | 4.26E-02 | 3.79E-02 |
| CE | 8.92E-02 | 9.45E-02 | 1.03E-01 | 1.10E-01 | 1.17E-01 | 1.22E-01 | 1.26E-01 | 1.28E-01 | 1.28E-01 | 1.27E-01 | 1.25E-01 | 1.21E-01 | 1.15E-01 | 1.08E-01 | 9.95E-02 | 8.99E-02 | 7.98E-02 | 7.10E-02 |
| PR | 4.51E-02 | 4.77E-02 | 5.18E-02 | 5.57E-02 | 5.89E-02 | 6.15E-02 | 6.32E-02 | 6.42E-02 | 6.45E-02 | 6.40E-02 | 6.27E-02 | 6.07E-02 | 5.79E-02 | 5.44E-02 | 5.02E-02 | 4.54E-02 | 4.03E-02 | 3.60E-02 |
| ND | 1.57E-01 | 1.66E-01 | 1.81E-01 | 1.95E-01 | 2.06E-01 | 2.15E-01 | 2.21E-01 | 2.25E-01 | 2.26E-01 | 2.24E-01 | 2.20E-01 | 2.12E-01 | 2.03E-01 | 1.90E-01 | 1.75E-01 | 1.59E-01 | 1.41E-01 | 1.25E-01 |
| PM | 7.20E-05 | 7.46E-05 | 7.93E-05 | 8.36E-05 | 8.72E-05 | 8.98E-05 | 9.16E-05 | 9.26E-05 | 9.29E-05 | 9.24E-05 | 9.11E-05 | 8.91E-05 | 8.61E-05 | 8.23E-05 | 7.74E-05 | 7.16E-05 | 6.51E-05 | 5.95E-05 |
| SM | 3.55E-02 | 3.79E-02 | 4.14E-02 | 4.47E-02 | 4.75E-02 | 4.97E-02 | 5.13E-02 | 5.21E-02 | 5.23E-02 | 5.19E-02 | 5.08E-02 | 4.90E-02 | 4.66E-02 | 4.37E-02 | 4.01E-02 | 3.61E-02 | 3.18E-02 | 2.81E-02 |
| EU | 2.27E-03 | 2.41E-03 | 2.62E-03 | 2.81E-03 | 2.97E-03 | 3.10E-03 | 3.19E-03 | 3.23E-03 | 3.25E-03 | 3.22E-03 | 3.16E-03 | 3.06E-03 | 2.92E-03 | 2.75E-03 | 2.54E-03 | 2.31E-03 | 2.05E-03 | 1.82E-03 |
| GD | 1.41E-03 | 1.57E-03 | 1.77E-03 | 1.97E-03 | 2.14E-03 | 2.28E-03 | 2.38E-03 | 2.43E-03 | 2.45E-03 | 2.42E-03 | 2.35E-03 | 2.24E-03 | 2.09E-03 | 1.91E-03 | 1.71E-03 | 1.48E-03 | 1.26E-03 | 1.06E-03 |
| TB | 4.76E-05 | 5.24E-05 | 5.87E-05 | 6.46E-05 | 6.98E-05 | 7.40E-05 | 7.69E-05 | 7.86E-05 | 7.90E-05 | 7.82E-05 | 7.60E-05 | 7.27E-05 | 6.82E-05 | 6.28E-05 | 5.65E-05 | 4.96E-05 | 4.25E-05 | 3.60E-05 |

| | | | | | | | | | | | | | | | | | | |
|---|---|---|---|---|---|---|---|---|---|---|---|---|---|---|---|---|---|---|
| DY | 2.82E-05 | 3.23E-05 | 3.73E-05 | 4.21E-05 | 4.63E-05 | 4.97E-05 | 5.22E-05 | 5.36E-05 | 5.40E-05 | 5.32E-05 | 5.14E-05 | 4.86E-05 | 4.50E-05 | 4.06E-05 | 3.58E-05 | 3.06E-05 | 2.53E-05 | 2.05E-05 |
| HO | 9.63E-07 | 1.10E-06 | 1.25E-06 | 1.39E-06 | 1.51E-06 | 1.61E-06 | 1.68E-06 | 1.72E-06 | 1.73E-06 | 1.71E-06 | 1.66E-06 | 1.58E-06 | 1.48E-06 | 1.35E-06 | 1.21E-06 | 1.05E-06 | 8.80E-07 | 7.17E-07 |
| ER | 9.54E-07 | 1.11E-06 | 1.28E-06 | 1.44E-06 | 1.58E-06 | 1.70E-06 | 1.78E-06 | 1.83E-06 | 1.84E-06 | 1.81E-06 | 1.75E-06 | 1.66E-06 | 1.54E-06 | 1.39E-06 | 1.23E-06 | 1.05E-06 | 8.69E-07 | 6.94E-07 |
| SUM FPs elemental | 1.30E+00 | 1.38E+00 | 1.50E+00 | 1.62E+00 | 1.71E+00 | 1.79E+00 | 1.84E+00 | 1.87E+00 | 1.88E+00 | 1.86E+00 | 1.83E+00 | 1.77E+00 | 1.68E+00 | 1.58E+00 | 1.45E+00 | 1.31E+00 | 1.16E+00 | 1.03E+00 |

c

# Appendix B

# Neutron Radiography

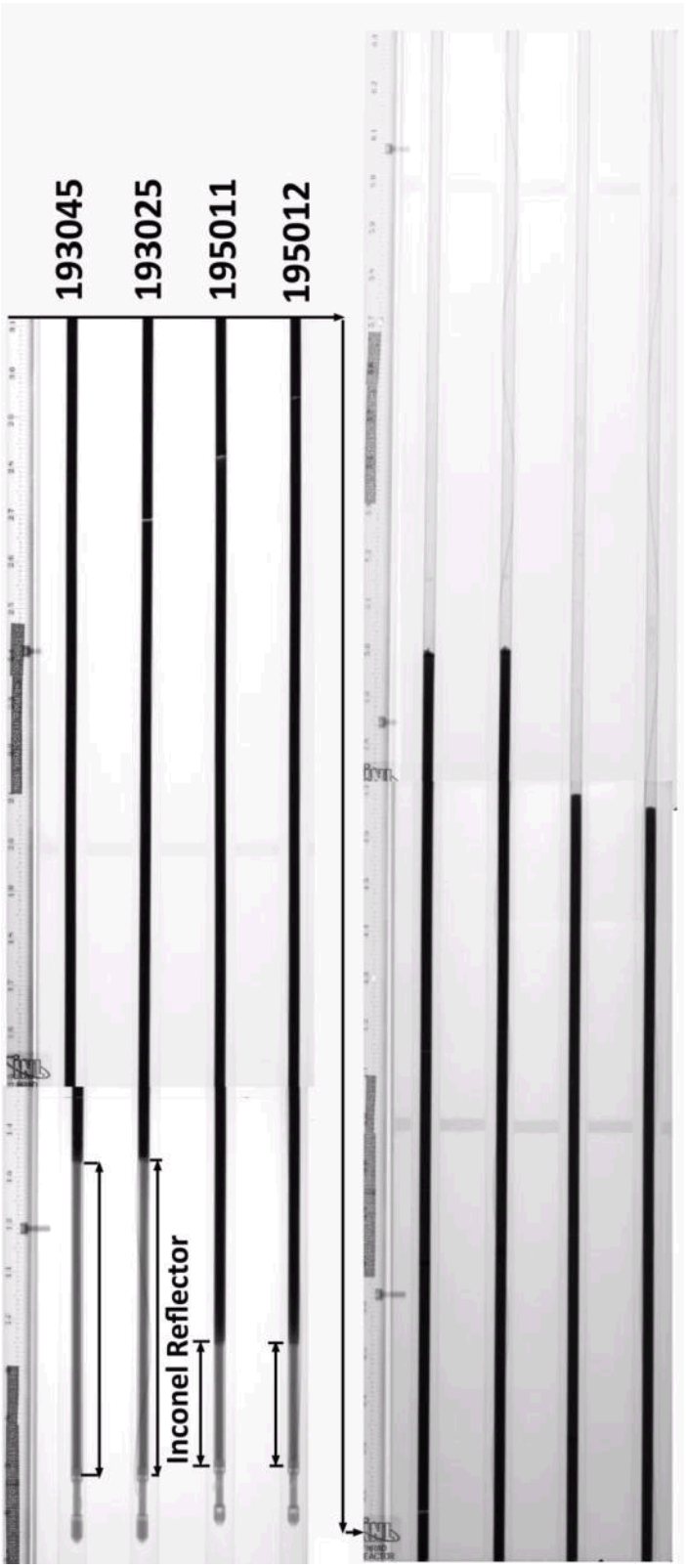
193045
193025
195011
195012
Inconel Reflector

Figure B-1. Thermal neutron radiograph of MFF3 Pins 193065 and 193025 and MFF-5 Pins 195011 and 195012. Note that Pin 193065 shifted between the first and second shots.

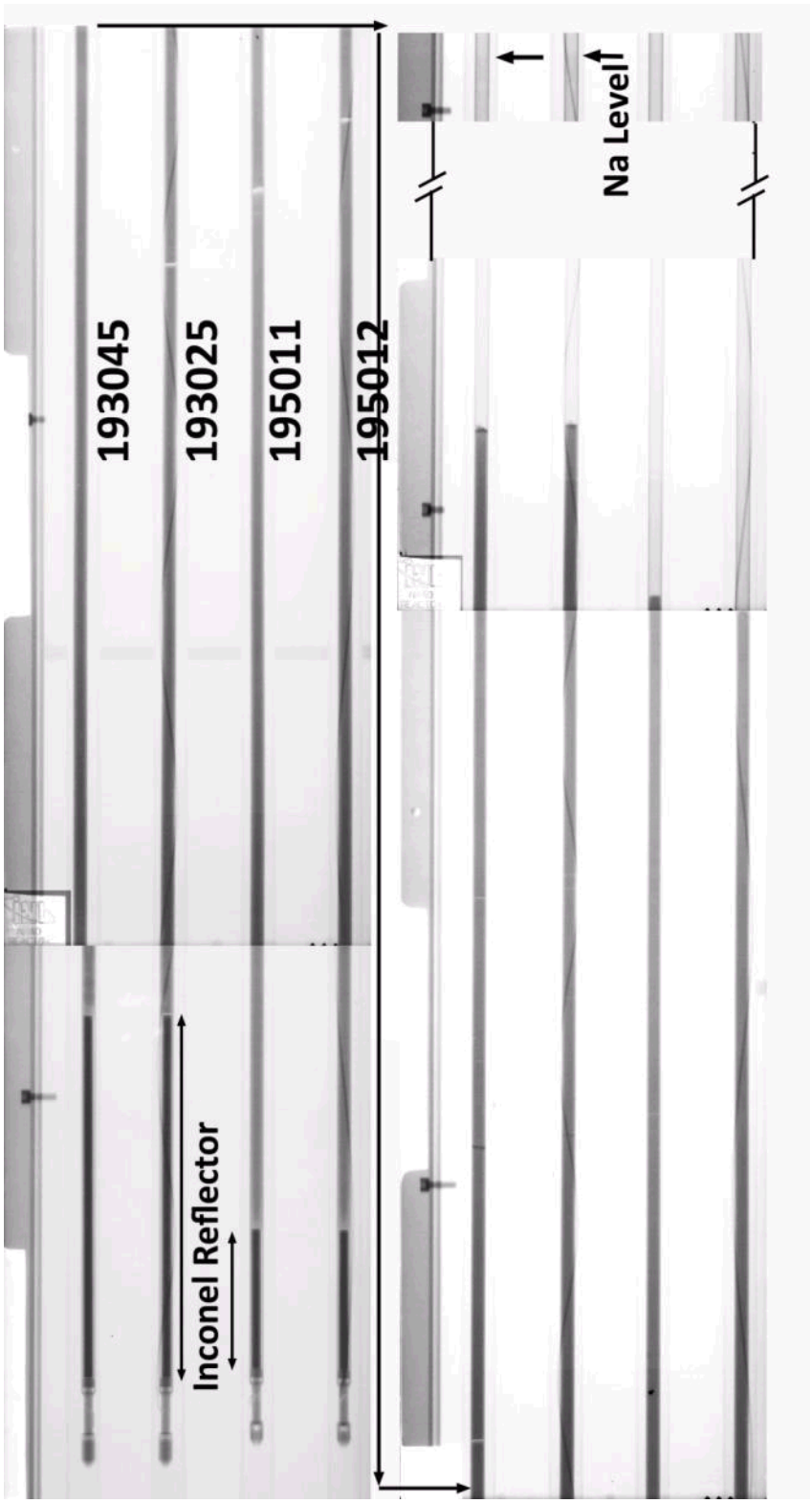


Figure B-2. Epithermal neutron radiograph of MFF3 Pins 193065 and 193025 and MFF-5 Pins 195011

and 195012. Note that Pin 193065 shifted between the first and second shots. Note that Na level is best seen in epithermal images.

Figure B -3. Thermal neutron radiograph of MFF3 Pins 193020 and 193062 and MFF-5 Pins 195051 and 195052.


Figure B-4. Thermal neutron radiograph of MFF3 Pins 193020 and 193062 and MFF-5 Pins 195051 and 195052.

# Appendix C

# Precision Gamma Scanning

# Appendix C

# Precision Gamma Scanning

## MFF-3 Gamma Scans

Four MFF-3 pins were scanned for gamma activity and specifically Co-60, Cs-134, and Eu-154 were noted. The scans are shown in Figures C-1 through C-4.

Note that the top of the element is actually at the lower Z-position, on the left-hand-side of the graphs. The Co-60 peaks in the Inconel reflector as expected. In some of the scans the Co-60 seems also to peak above the fuel column. The reason for this is not clear, unless shielding is also responsible, or if there is an interference with the Cs activity.

Usually, the Cs-134 peaks just above the fuel column, in the bond sodium which has been pushed above the fuel as the fuel swelled. It is also a stronger signal there as there is no shielding from the fuel.

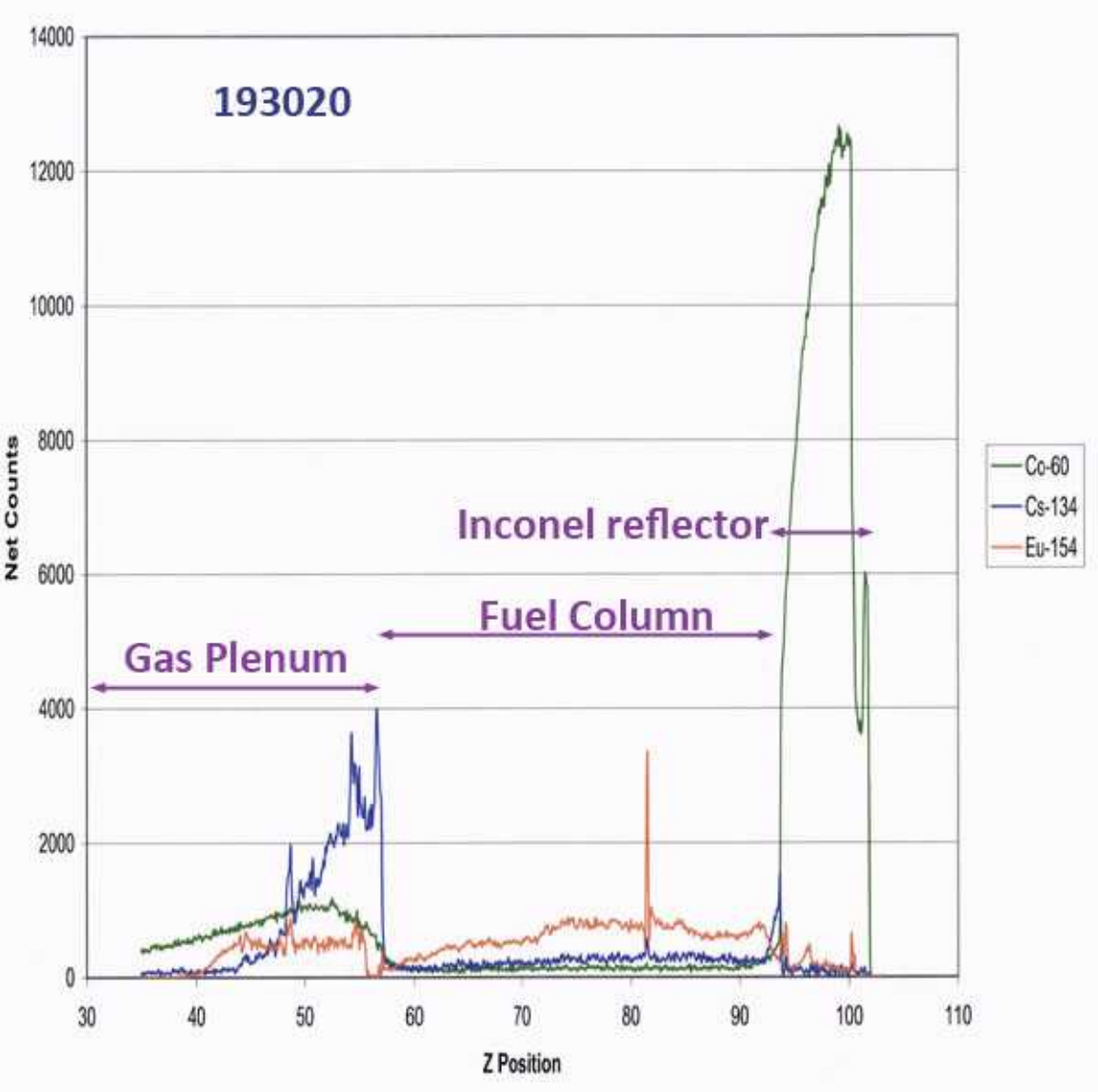

Figure C-1. Gamma scan traces for MFF-3 Pin 193020. Co-60 peaks in Inconel reflector, Cs-134 peaks just above fuel column (lower Z-position is top of pin).

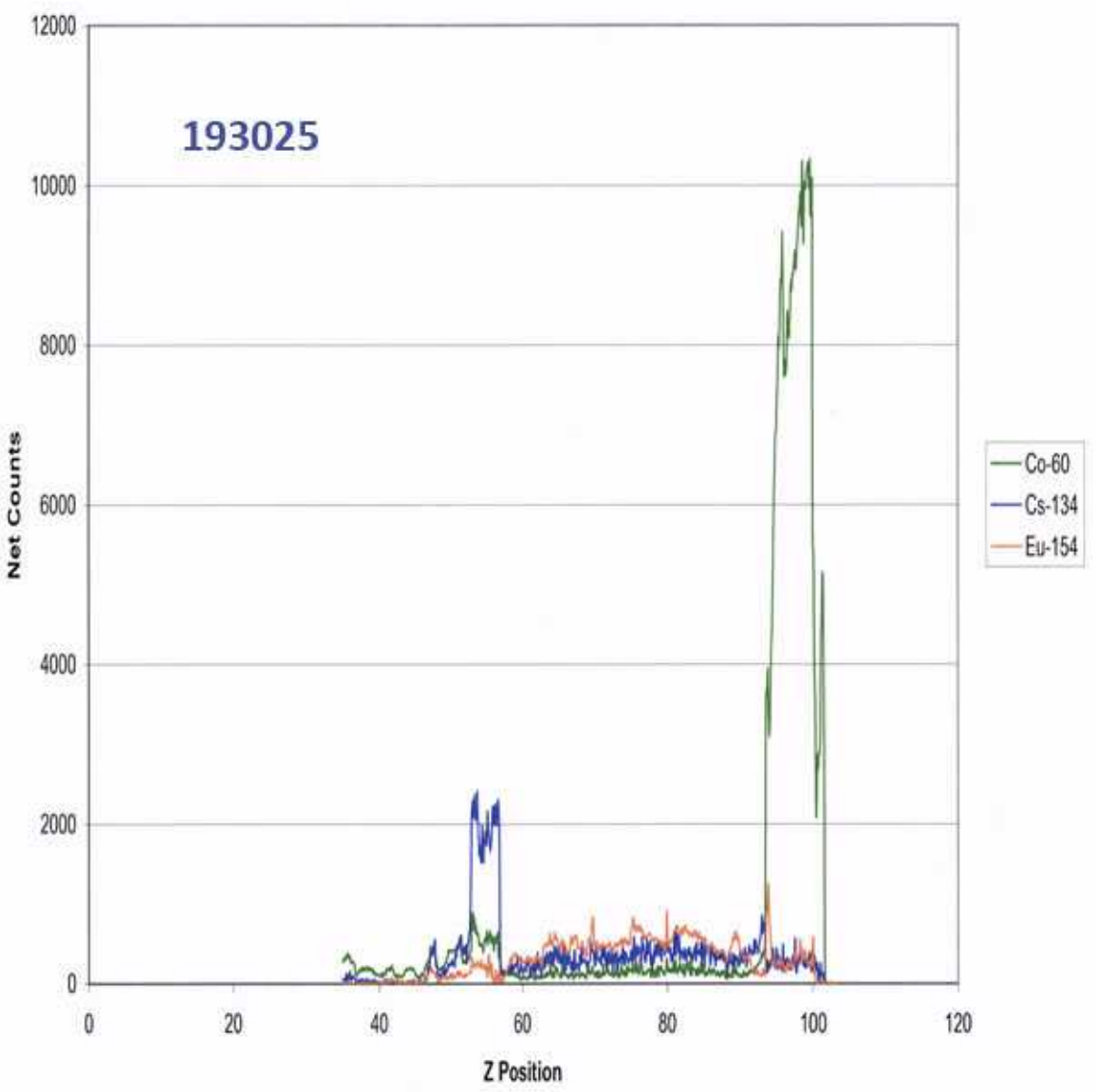


Figure C-2. Gamma scan traces for MFF-3 Pin 193025. Co-60 peaks in Inconel reflector, Cs-134 peaks just above fuel column (lower Z-position is top of pin).

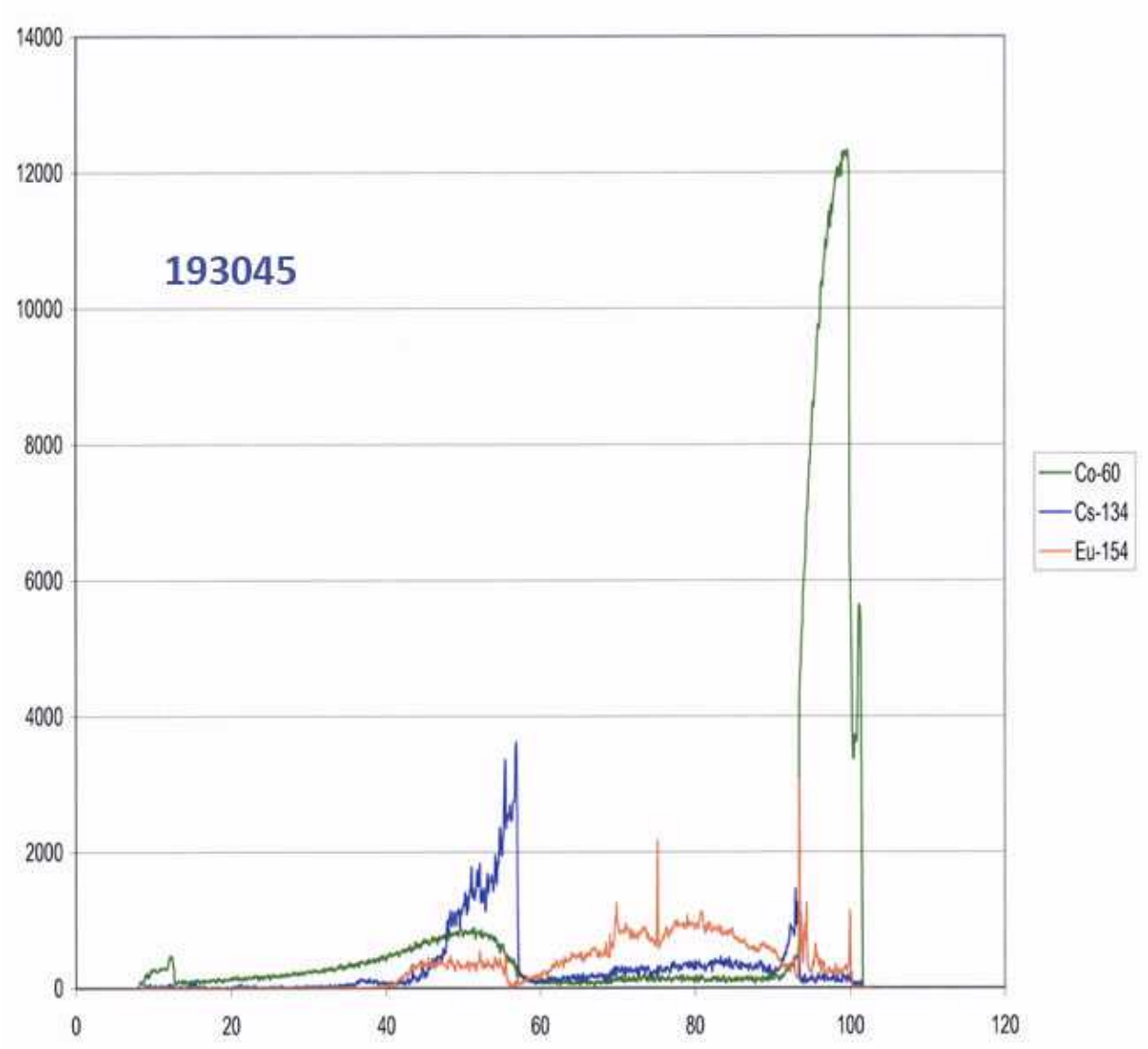


Figure C-3. Gamma scan traces for MFF-3 Pin 193045. Co-60 peaks in Inconel reflector, Cs-134 peaks just above fuel column (lower Z-position is top of pin).

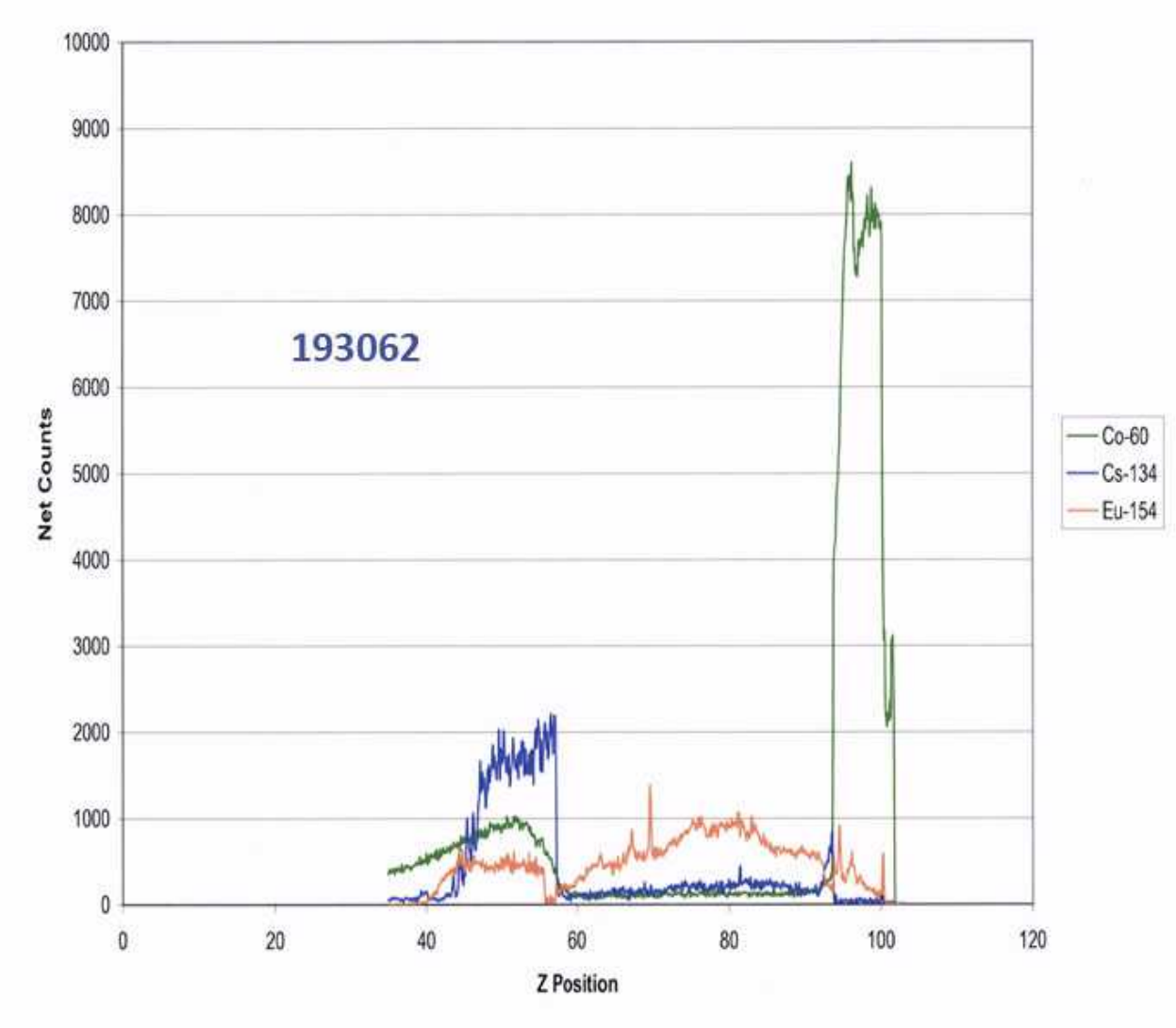


Figure C-4. Gamma scan traces for MFF-3 Pin 193062. Co-60 peaks in Inconel reflector, Cs-134 peaks just above fuel column (lower Z-position is top of pin).

## MFF-5 Gamma Scans

Four MFF-5 pins were scanned for gamma activity and specifically Co-60, Cs-134, and Eu-154 were noted. The scans are shown in Figures C-5 through C-8.

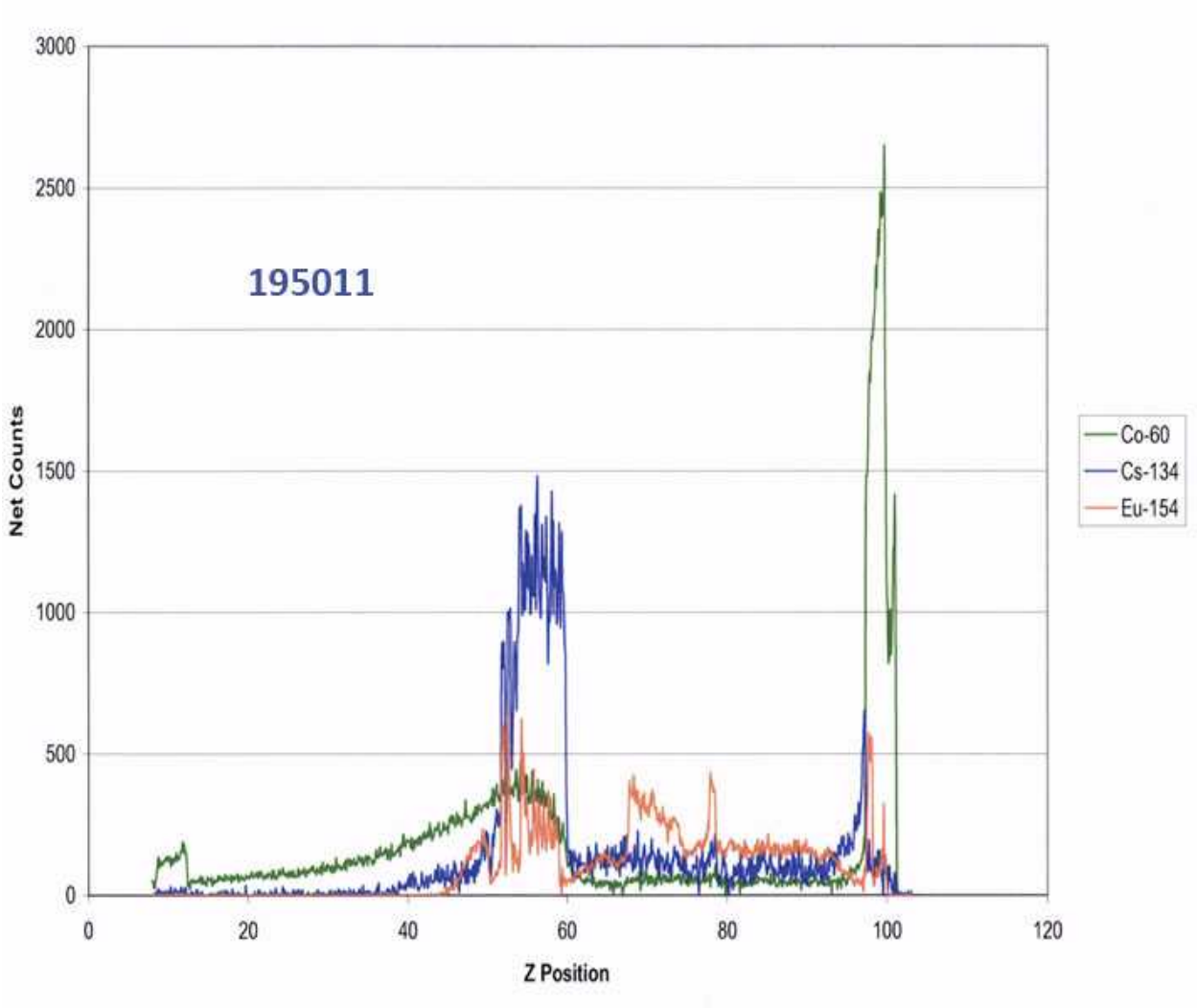


Figure C-5. Gamma scan traces for MFF-5 Pin 195011. Co-60 peaks in Inconel reflector, Cs-134 peaks just above fuel column (lower Z-position is top of pin).

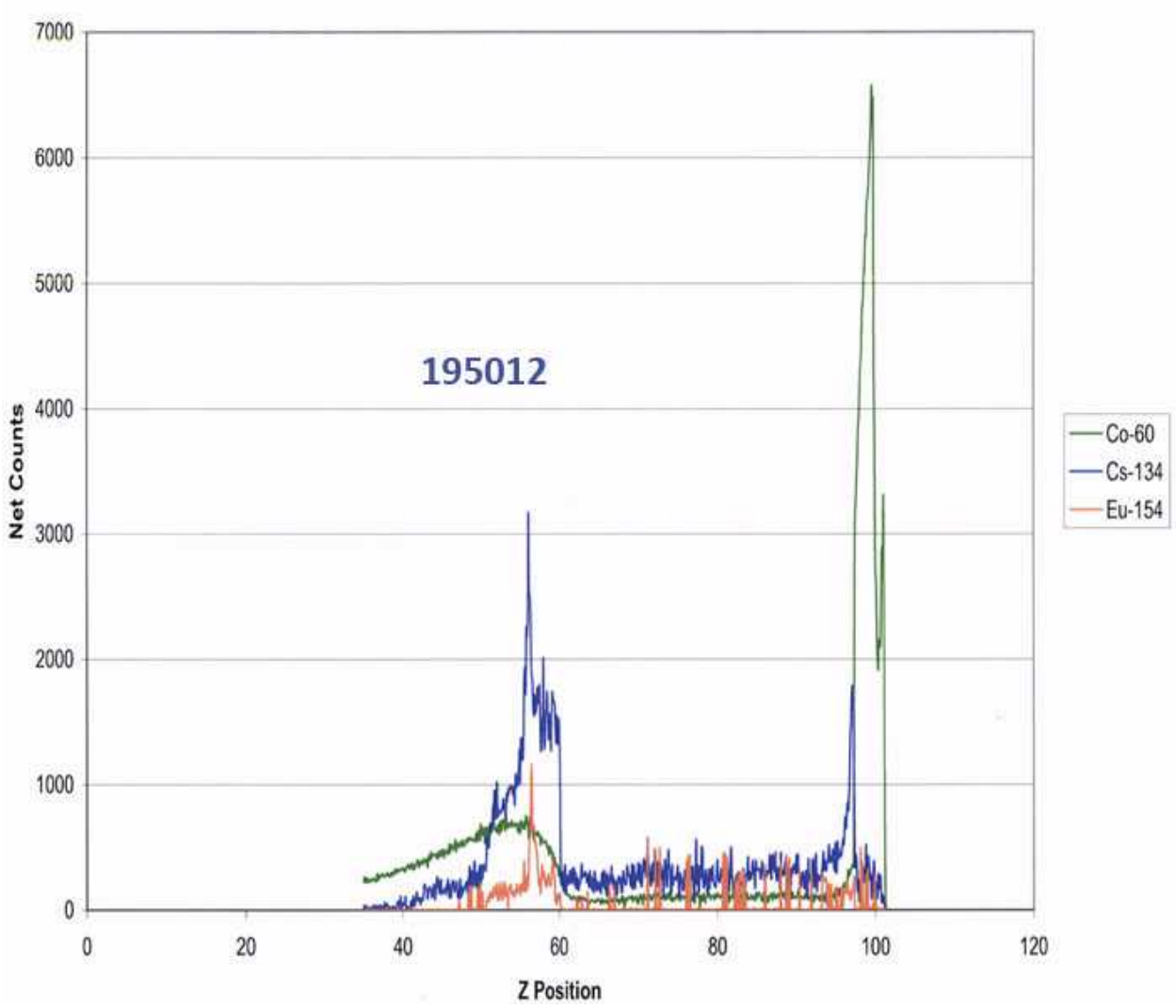


Figure C-6. Gamma scan traces for MFF-5 Pin 195012. Co-60 peaks in Inconel reflector, Cs-134 peaks just above fuel column (lower Z-position is top of pin).

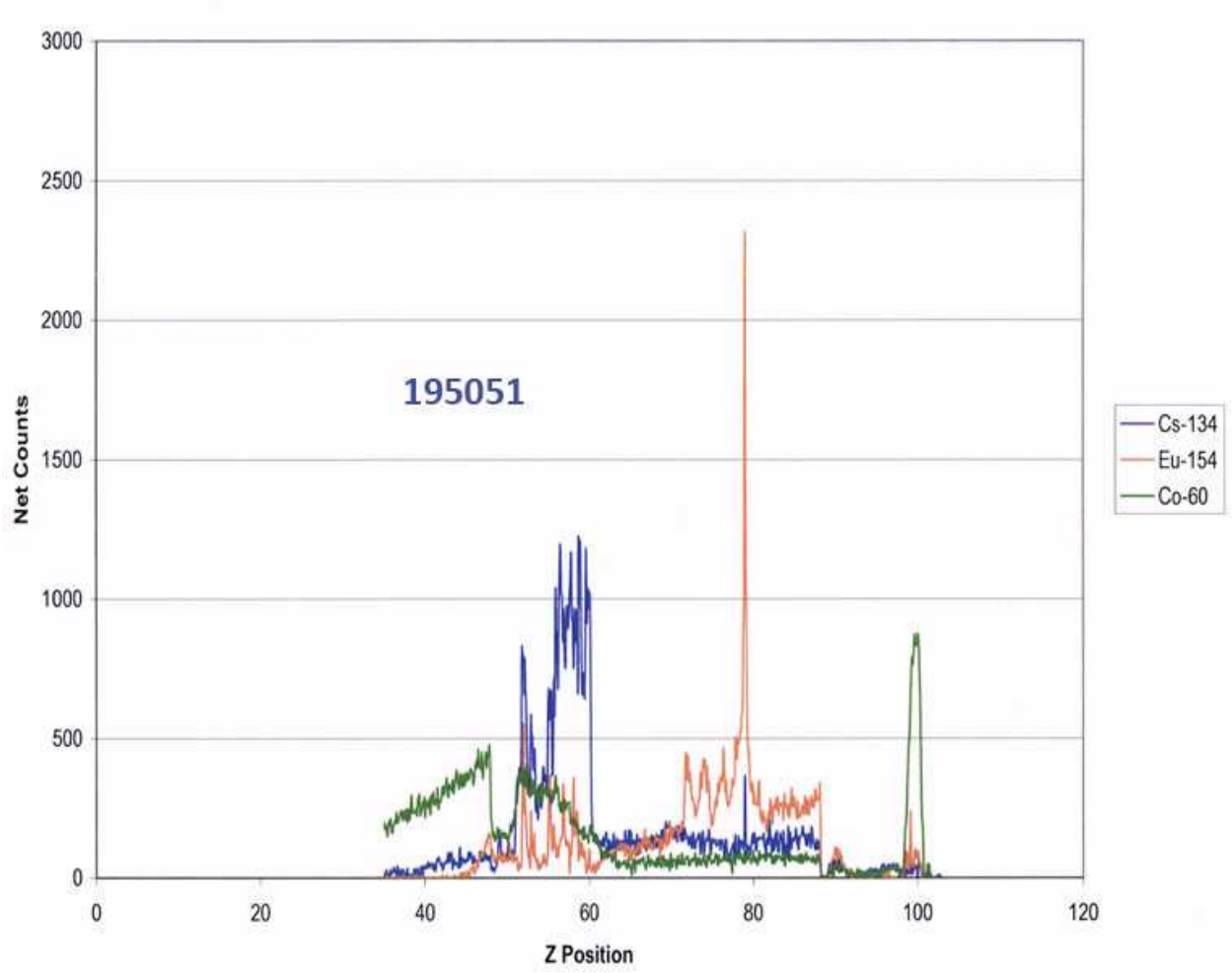


Figure C-7. Gamma scan traces for MFF-5 Pin 195051. Co-60 peaks in Inconel reflector, Cs-134 peaks just above fuel column (lower Z-position is top of pin).

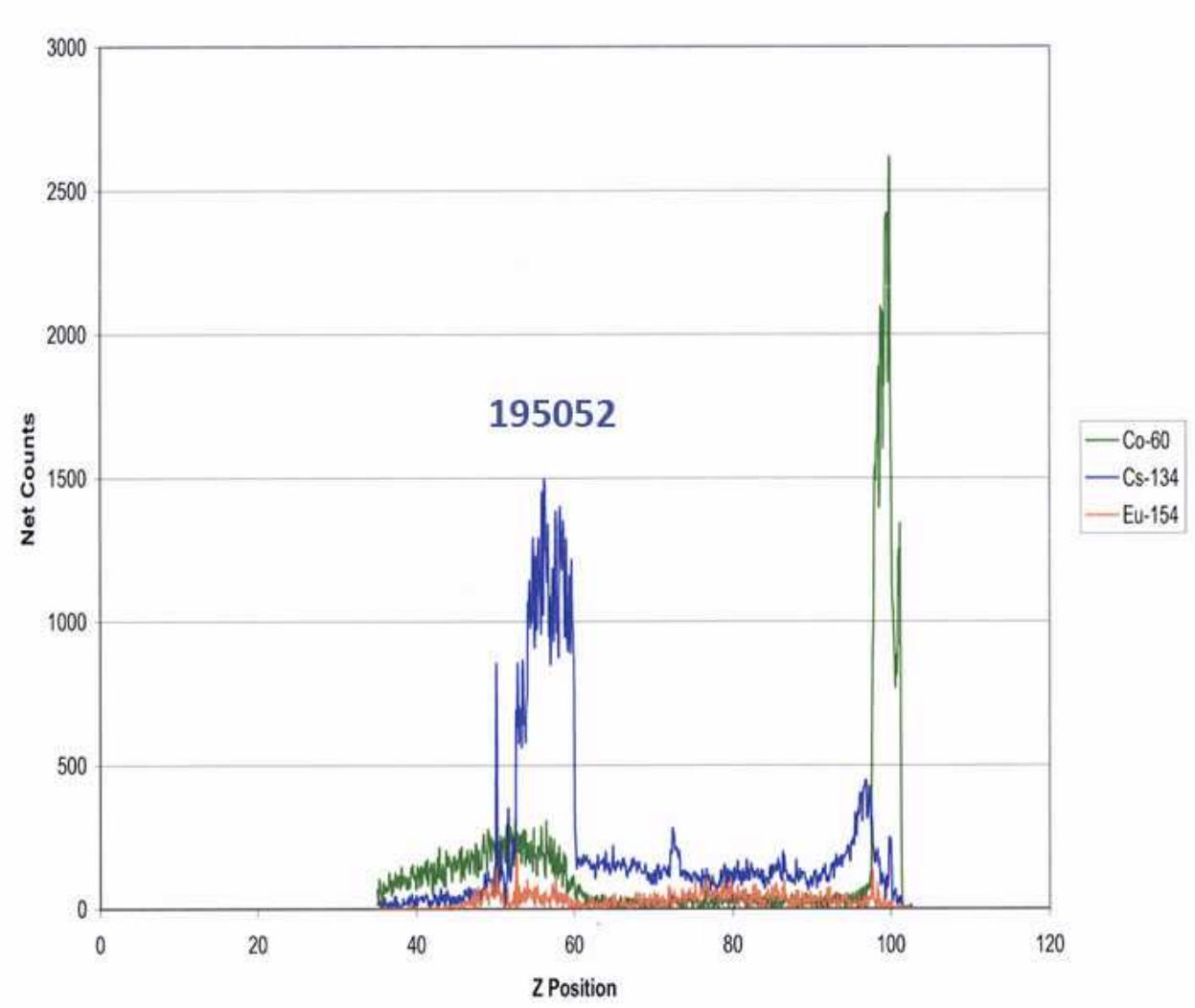


Figure C-8. Gamma scan traces for MFF-5 Pin 195052. Co-60 peaks in Inconel reflector, Cs-134 peaks just above fuel column (lower Z-position is top of pin).


1. Till, C. E. and Y. I. Chang, "PLENTIFUL ENERGY – The Story of the Integral Fast Reactor," ISBN:978-1466384606 (2012).
2. Crawford, D. C., D. L. Porter, and S. L. Hayes, 2007, "Fuels for Sodium-cooled Fast Reactors: U.S. Perspective," *Journal of Nuclear Materials*, Vol. 371, pp. 202–231.
3. Porter, D. L. and H. Tsai, "Full-length U–xPu–10Zr (x = 0, 8, 19 wt.%) Fast Reactor Fuel Test in FFTF," *Journal of Nuclear Materials*, Vol. 427 (2012), pp. 46–57
4. Pitner, A. L. and R. B. Baker, "Metal Fuel Test Program in FFTF," *Journal of Nuclear Materials*, Vol. 204 (1993), pp. 124-130.
5. Pahl, R. G., C. E. Lahm and S. L. Hayes, "Performance of HT9 Clad Metallic Fuel at High Temperature," *Journal of Nuclear Materials*, Vol. 204 (1993) pp. 141-147.
6. Wootan, D. W. and J. V. Nelson, "Irradiation Data for the MFF-3 and MFF-5 Tests in the FFTF," PNNL-20249, March, 2011.
7. Nelson, J. V., *3DBF User's Manual*, WHC-SD-FF-SWD-037, Rev. 0, Westinghouse Hanford

Company, Richland, Washington.

8. Bennett, R. A., et. al., 1994, *FFTF Core Management Methods*, WHC-SD-FF-CMMD-001, Rev. 0E, Westinghouse Hanford Company, Richland, Washington. [Applied Technology].
9. Cramer, E. R. and A. L. Pitner, *Transactions of the American Nuclear Society* (San Francisco, California 1989) p. 306.
10. Hayes, S. L., *SAFE: a computer code for the steady-state and transient thermal analysis of LMR fuel elements*, ANL-IFR-221 (1993).
11. Hofman, G. L., R. G. Pahl, C. E. Lahm, and D. L. Porter, 1990, "Swelling Behavior of U-Pu-Zr Fuel," *Metallurgical Transactions A*, Vol. 21A, pp. 518–528.
12. Unpublished work.
13. Ethridge, J. L. to B. R. Seidel, personnel communication, "MFF-2 Axial Fuel Growth to Account for Power Decrease," September 12, 1988.
14. Hofman, G. L., S. L. Hayes, and M. C. Petri, "Temperature Gradient Driven Constituent Redistribution in U-Zr Alloys," *Journal of Nuclear Materials*, Vol. 227 (1996) pp. 277-286.
15. Pahl, R. G., D. L. Porter, C. E. Lahm, and G. L. Hofman, "Experimental Studies of U-Pu-Zr Fast Reactor Fuel Pins in the Experimental Breeder reactor-II," Metallurgical Transactions A, Vol. 21A (1990) pp. 1863-1870.
16. Keiser, D. D., *Fuel-Cladding Interaction Layers in Irradiated U-Zr and U-Pu-Zr Fuel Elements*, ANL-NT-240 (2006).
17. Carmack, W. J., *Temperature and Burnup Correlated FCCI in U-10Zr Metallic Fuel,* A Dissertation Presented in Partial Fulfillment of the Requirements for the Degree of Doctor of Philosophy with a Major in Nuclear Engineering in the College of Engineering, University of Idaho (May 2012).
18 Hofman, G. L. and L. C. Walters, *Metallic Fast Reactor Fuels from Nuclear Materials*, Part I Vol 10 A, Materials Science and Technology, A comprehensive Treatment, B. R. T. Frost, R. W. Cahn, P. Haasen, and E. J. Kramer editors, VCH Verlagsgesellschaft mbH.